

BOARD OF DIRECTORS, 1955
 J. D. Ryder, President
 Franz Tank, Vice-President
 W. R. G. Baker, Treasurer
 Haradan Pratt, Secretary
 John R. Pierce, Editor
 J. W. McRae, Senior Past President
 W. R. Hewlett, Junior Past President

1955

S. L. Bailey
 A. N. Goldsmith
 A. V. Loughren
 C. J. Marshall (R5)
 L. E. Packard (R1)
 J. M. Pettit (R7)
 B. E. Shackelford
 C. H. Vollum
 H. W. Wells (R3)

1955-1956

E. M. Boone (R4)
 J. N. Dyer (R2)
 J. T. Henderson (R8)
 A. G. Jensen
 George Rappaport
 D. J. Tucker (R6)

1955-1957

J. F. Byrne
 Ernst Weber

George W. Bailey
 Executive Secretary

John B. Buckley, Chief Accountant
 Laurence G. Cumming,
 Technical Secretary
 Evelyn Davis, Assistant to the
 Executive Secretary
 Emily Sirjane, Office Manager

EDITORIAL DEPARTMENT

Alfred N. Goldsmith
 Editor Emeritus
 John R. Pierce, Editor
 E. K. Gannett,
 Managing Editor
 Marita D. Sands,
 Production Manager

ADVERTISING DEPARTMENT

William C. Copp,
 Advertising Manager
 Lillian Petranek,
 Assistant Advertising Manager

EDITORIAL BOARD

John R. Pierce, Chairman
 D. G. Fink
 E. K. Gannett
 T. A. Hunter
 W. R. Hewlett
 J. A. Stratton
 W. N. Tuttle



Responsibility for the contents of papers published in the PROCEEDINGS of the IRE rests upon the authors. Statements made in papers are not binding on the IRE or its members.



Change of address (with 15 days advance notice) and letters regarding subscriptions and payments should be mailed to the Secretary of the IRE, 1 East 79 Street, New York 21, N. Y. All rights of publication, including foreign language translations, are reserved by the IRE. Abstracts of papers with mention of their source may be printed. Requests for republication should be addressed to The Institute of Radio Engineers.

PROCEEDINGS OF THE IRE

Published Monthly by

The Institute of Radio Engineers, Inc.

VOLUME 44

January, 1956

NUMBER 1

CONTENTS

Arthur V. Loughren, President, 1956.....	2
The State of Radio and Electronics in Egypt..... Professor H. M. Mahmoud	3
5598. A Survey of Application of Ferrites to Inductor Design R. S. Duncan, H. A. Stone, Jr.	4
5599. Electromechanical Filters for 100-Kc Carrier and Sideband Selection... R. W. George	14
5600. New Microwave Repeater System Using Traveling-Wave Tubes..... N. Sawazaki and T. Honma	19
5601. Geophysical Prospection of Underground Water in the Desert by Means of Electromagnetic Interference Fringes..... M. A. H. El-Said	24
5602. A Transmission Line Taper of Improved Design..... R. W. Klopfenstein	31
5603. A Precision Resonance Method for Measuring Dielectric Properties of Low-Loss Solid Materials in the Microwave Region..... S. Saito and K. Kurokawa	35
5604. Transistor Amplifiers for Use in a Digital Computer.. Q. W. Simkins, J. H. Vogelsong	43
5605. A Developmental Wide-Band, 100-Watt, 20 DB, S-Band Traveling-Wave Amplifier Utilizing Periodic Permanent Magnets..... W. W. Siekanowicz and F. Sterzer	55
5606. Spurious Modulation of Electron Beams..... C. C. Cutler	61
5607. Negative Resistance Regions in the Collector Characteristics of the Point-Contact Transistor..... L. E. Miller	65
5608. The Dependence of Transistor Parameters on the Distribution of Base Layer Resistivity..... J. L. Moll and I. M. Ross	72
5609. Surface Resistance and Reactance of Metals at Infrared Frequencies..... J. R. Beattie and G. K. T. Conn	78
5610. Transverse-Field Traveling-Wave Tubes with Periodic Electrostatic Focusing..... R. Adler, O. M. Kromhout, and P. A. Clavier	82
5611. A Simplified Method of Solving Linear and Nonlinear Systems... R. Boxer, S. Thaler	89
5612. Multi-Beam Velocity-Type Frequency Multiplier..... Yukito Matsuo	101
5613. IRE Standards on Terminology for Feedback Control Systems.....	107
Correction to "Temperature Coefficient of AT Cut Quartz Crystals," by E. A. Gerber.....	109
Correspondence:	
5614. Scattering Matrix Measurements on Nonreciprocal Microwave Devices... J. E. Pippin	110
5615. A New Treatment for Parabolic Reflector Problems..... B. Chatterjee	110
5616. A Method of Launching Surface Waves..... J. D. Lawson	111
5617. Noise Reduction in CW Magnetrons..... R. L. Kruele and J. A. Mullen	111
5618. Russian Vacuum-Tube Terminology..... G. F. Schultz	112
Contributors	
IRE News and Radio Notes..... 115-126	
5619. Abstracts of IRE Transactions.....	130
5620. Abstracts and References.....	134
Annual Index to Convention Record of the IRE.....	Follows Page 148

ADVERTISING SECTION

Meetings with Exhibits	6A	Notes.....	32A	Membership.....	72A
News—New Products	16A	IRE People.....	44A	Positions Open.....	140A
Section Meetings....	22A	Professional Group		Positions Wanted.....	152A
Industrial Engineering		Meetings.....	68A	Advertising Index.....	197A



THE COVER—If a suspension of tiny iron-oxide particles is poured over the polished surface of a magnetic material and examined through a microscope, an unusual pattern similar to that depicted on this month's cover will be observed. The accumulation of the iron powder along well-defined boundary lines indicates the existence of small magnetic "domains" running in various directions within the material. Each domain is magnetized to saturation, but the material as a whole will not reach saturation until all the domains are pointing in the same direction.

Interest in magnetic materials has been greatly stimulated by the widespread application of ferrites in such devices as the control coil shown on the cover. An excellent survey of the use of ferrites in inductors appears in the first paper in this issue.

Photo—Bell Telephone Laboratories, Inc.



Arthur V. Loughren

PRESIDENT, 1956

Arthur V. Loughren was born in Rensselaer, New York, on September 15, 1902. He received the B.A. and the E.E. degrees from Columbia University in 1923 and 1925, respectively.

Upon graduation, Mr. Loughren spent two years at the Research Laboratory of the General Electric Company concerned with problems arising from the adaptation of vacuum tubes to circuits. Then followed two and a half years in the Radio Engineering Department. In 1930 he transferred to the RCA Manufacturing Company at Camden, New Jersey, where, successively, he became responsible for the design of tuned radio-frequency receivers, loudspeakers and phonograph pickups, as well as all factory tests and inspections. In 1934, he rejoined the General Electric Company at Bridgeport, Connecticut, to work on the design of radio receivers.

In 1936 Mr. Loughren joined the laboratories of Hazeltine Corporation. He then rose to become, successively, engineer in charge of television development, design supervisor for military equipment programs, and director of research. He is currently vice-president in charge of research for Hazeltine Corporation and executive vice-president of Hazeltine Research Inc., a subsidiary of Hazeltine Corporation.

During World War II Mr. Loughren received the U. S. Navy, Bureau of Ships, Certificate of Commendation for Outstanding Service to the Navy for contributions to electronic development. During his long career Mr. Loughren has been

awarded thirty U. S. electronics patents. He is a member of Phi Beta Kappa, Sigma Xi, and Tau Beta Pi.

His professional and industrial activities have included membership in Panels 7 and 9 of the first National Television System Committee and Panel 6 of the Radio Technical Planning Board, the chairmanship of the Joint Advisory Committee, and service on RETMA committees. He is currently vice-chairman of the present National Television System Committee and chairman of its Panels 7 and 13. He was awarded the David Sarnoff Gold Medal in 1953 by the Society of Motion Picture and Television Engineers for "meritorious achievement in television engineering," and the 1954 Plaque of the RETMA-IRE Radio Fall Meeting with the citation, "for his contributions to color television circuitry." His outstanding contributions in the formulation of the signal specifications for compatible color television won him the coveted IRE Morris Liebmann Memorial Prize in 1955.

Mr. Loughren joined the IRE as an Associate in 1924. He became a Member in 1929, a Senior Member in 1943 and a Fellow in 1944. He has served on the Papers Procurement, Membership, Finance, Executive, and Editorial Review committees, and as Chairman of the Awards and Policy Advisory Committees. He has also been a member of Radio Receivers, Standards, Television, and Vacuum Tubes committees. He served as Director from 1952-1955.

The State of Radio and Electronics in Egypt

PROFESSOR H. M. MAHMOUD, CAIRO UNIVERSITY

In view of the recent formation of an IRE Section in Egypt, the following report on the recent growth of radio engineering there is of special timeliness and interest.—*The Editor.*

Egypt's unique geographical juxtaposition to the Mediterranean and Red Seas, and the African and Asian continents has since the days of the Pharaohs made Egypt a center of culture, trade and communications—a melting pot where eastern and western ideas meet and mingle. In recent years Egypt has shown a strong determination to improve her standard of living and develop the land through modern methods. This editorial aims to show this determination in the particular fields of radio and electronics by outlining the history of the development of radio and electronics in Egypt during the past two decades, the present situation, and future plans.

Regular Egyptian broadcasting, which is government-controlled, was started in 1933 as a single program from a 20-kw transmitter. From the beginning it was realized that such service was inadequate, but the advent of World War II inevitably delayed normal expansion. After the war's end, the situation was rectified to such an extent that today Egypt has in operation three medium-wave high-power transmitters with ratings up to 100 kw, six low-power regional transmitters, and three high-power short-wave transmitters with powers of 100 kw, 120 kw and 140 kw. The antenna system serving these transmitters occupies a 250-acre area, and the switching of short-wave antennas is carried out by a novel remotely-controlled mechanical switch. As a result, Cairo is now able to broadcast programs in twelve different languages over a total broadcasting time of 100 hours per day. The broadcasting station itself, even though it has undergone two major expansions since 1933, is still inadequate. A new station, therefore, is now being erected, including modern programming facilities and television studios, which will embody the most up-to-date architectural and acoustical designs.

Television broadcasting has not yet begun in Egypt, but the potentialities and value of this medium have not been overlooked. A committee was formed to draft a scheme defining the lines along which television would be introduced to the country. This committee has submitted its report, and steps are now being taken to realize this scheme. In the meantime occasional experimental transmissions are being carried out by the Electronics Laboratory of the Faculty of Engineering, Cairo University.

Wireless telecommunication services are run by a division of the State Telegraph & Telephone. They include maritime, meteorological, and press agencies' teleprinter services.

Public security and police radio services are used now only in the big cities, but a country-wide network will soon be put into operation.

Public radiotelephone and telegraph services have been in operation for a long time. These services are owned and operated by a private company whose contract expires in 1958; at that date the government will assume control. Meanwhile, to meet the increasing demand for radiotelephone and telegraph services a large transmitting station is being constructed in the vicinity of Cairo. The antenna system of this station will occupy nine hundred acres. A receiving station, with an antenna system covering two hundred acres, is also being built.

A tremendous expansion in military electronics has occurred in the last decade. The Signal Corps, Artillery, and Air Force now use modern electronic equipment in communications, early warning and fire control radar.

Egyptian radio and electronic industry has just started radio receiver production on an assembly-line basis.

Since 1930 the need for competent engineers to man these projects has been met by giving courses in basic radio, communications and electronics to electrical engineers. About a hundred such engineers graduate annually from Cairo, Alexandria, and Ein Shams Universities. To meet the need for more specialized radio engineers, a more advanced course in radio and electronics was started by the University of Alexandria in 1947, and by the University of Cairo in 1948. The number of graduates each year started at thirty, but it has doubled since. These two universities also offer postgraduate courses which include advanced studies in mathematical communications theories, pulse, television, radar techniques, and microwave theories. A third of the time spent in postgraduate study is allotted to experimental work.

In the past the universities have been responsible for all of the research effort in Egypt. Recently, however, a National Research Council was created, and the nucleus of an Electronics Institute, concerned with problems of research and development, has been formed. This organization, which has a modern, properly-equipped laboratory operated by a group of qualified scientists and engineers, is presently investigating the possibility of underground water prospecting by radio methods.

At one time the progress of a nation was measured in terms of the means of communications it possessed; today, however, we feel the state of its radio and electronics is a better criterion.

A Survey of the Application of Ferrites to Inductor Design*

R. S. DUNCAN†, ASSOCIATE, IRE, AND H. A. STONE, JR.†

The following paper is one of a planned series of invited papers, in which men of recognized standing will review recent developments in, and the present status of, various fields in which noteworthy progress has been made.—*The Editor*

Summary—Within the last ten years, due to the advent of ferrites important new possibilities in inductor design have materialized. Higher Q 's, smaller sizes, and lower costs are among the advantages these new magnetic materials offer. This paper discusses the properties of ferrites and reviews the progress that has been made thus far in their application to inductors.

INTRODUCTION

IN THE EARLY 1940's the design of high Q magnetic core inductors might be said to have been in a state of uninspired stability. The molybdenum permalloy powders [1] had become established as the outstanding core materials for coil usage at frequencies up to at least 100 kc. Silicon iron in laminar form continued to dominate powder applications, but where precision, stability, and high Q were required the "moly" toroids were almost invariably called for. These were available in several sizes and permeabilities and their properties were well characterized; which is to say that the limitations in coil design were well defined.

During the war, as the need developed for electronic gear of improved performance and smaller size, the shortcomings of the available magnetic materials began to become oppressive. Shortly after the war the birth of the transistor added impetus to the clamor for more compact equipment. The need for high quality coils of small size clearly would not be met with molybdenum permalloy or other known metallic alloys.

It was into this sort of situation that the high permeability ferrites were introduced. As we review their adaptability to present-day coil needs it will not be surprising that they have so rapidly assumed major importance.

This survey is concerned primarily with the application of ferrites to inductors. Most of the emphasis is on linear or current-stable coils, such as are used in conventional filters, equalizers, tuners, etc. Brief attention is also given to a few special nonlinear coil applications. The important contributions of ferrites to other devices such as pulse transformers, antenna rods, gyrators, etc., lie beyond the scope of this paper.

In metallurgical circles the word ferrite has other connotations, but in the electronic field it refers simply to iron oxides, or magnetic mixtures of iron oxides with oxides of other metals. The use of ferrites as core materials for inductors is generally considered a recent development and, in a practical sense, this is justified since extensive use is based on the work done by the Philips Company in Holland, and announced in 1946 [2]. As a matter of historical interest, however, ferrites were used in coils, at least as far back as 1935. These first ferrite cores were made from naturally occurring magnetite, Fe_3O_4 . The ore was ground and impurities removed by magnetic separation [3]. Synthetic magnetite has also been used. Although inexpensive, magnetite cores are extremely limited by their low permeability, between 2 and 4. Their principal use has been as slugs for high frequency coils and even in this application they have now been largely replaced by carbonyl iron and permalloy powders.

The importance of the Philips' research was in the establishment on a practicable basis of mixed ferrites with permeabilities in excess of 1,000. High permeability combined with the high resistivity of semiconductors has opened the door to achievements in inductors which, only a few years ago, would have been considered fantastic.

FERRITE PROPERTIES

Foremost among the desirable characteristics of a core material is permeability, commonly symbolized by μ . The improvement in an inductor due to use of a magnetic core whose permeability is significantly greater than unity is effected in two distinct ways. First, the physical size of the coil can be reduced since a winding of fewer turns of smaller wire in a high μ core will give performance equivalent to a larger winding used without a core. Second, the high permeability core tends to reduce leakage of magnetic flux, thus obviating the need for bulky shielding enclosures frequently required with air core inductor designs. From this one might assume that the highest possible permeability would always be the best. However, in ferromagnetic materials the increase of μ without limit is not desirable

* Original manuscript received by the IRE, September 9, 1955.
† Bell Telephone Labs., Inc., Murray Hill, N. J.

because it entails a sacrifice with respect to core losses which relates to the second important core property, Q .

The quality factor, Q , of an inductor is defined as the ratio of reactance to resistance. It is of major importance as a measure of the purity of the inductance or its relative freedom from the degrading effect of losses which appear as series resistance in the equivalent circuit. For example, since the value of Q of the components in a filter determines the maximum amount of frequency discrimination which that filter can exhibit, in this large field of inductor application high Q is invariably a desideratum.

As is well-known, alternating current losses in magnetic materials are a function of permeability, flux density (B_m) and frequency (f) as expressed in Legg's equation for equivalent series resistance [4]:

$$R_m = e\mu f^2 L + a\mu B_m L + c\mu f L,$$

in which e , a , and c are constants and L is inductance. It is seen that an increase in μ will inevitably result in increased ac core losses and therefore lower Q . Due to the presence of direct current resistance in addition to core losses, at any given frequency an optimum value of μ can be determined for which total coil losses are a minimum (and therefore Q a maximum).

It has been shown [5] that the product $\mu_m Q_m$ is a very useful parameter for characterizing ferrite core materials. Here Q_m is the "material Q " and μ_m the permeability measured on a closed core. The introduction of air gaps in the core structure changes the relative values of μ and Q in the product $\mu_m Q_e$ where now the subscripts refer to effective values of the two factors in the gapped structure. However, so long as average flux density is maintained constant and if leakage is not excessive, $\mu_m Q_e$ will be approximately equal to $\mu_m Q_m$. A more important and useful property of the μQ product is that with a given core structure into which various amounts of air gap are introduced, the maximum Q obtainable at the frequency of interest with a given core material and the corresponding value of effective μ are each directly proportional to $\sqrt{\mu Q}$ of that material. Thus the μQ product is a sort of synthetic parameter of special utility in evaluation of the magnetic ferrites as core materials.

A third magnetic core property of importance is the saturation flux density. This value is related to the upper bend of the $B-H$ magnetization characteristic of the material. In this region increases in the magnetizing force produce relatively small increases in flux density. Magnetic nonlinearity sets an upper limit to the current level which can be used in ferromagnetic core inductors for applications requiring a high degree of inductance stability.

The mechanical properties of a core material affect to a large extent its scope of usefulness. Among the qualities desired are high tensile and compressive

strength, good resistance to impact, ability to function unimpaired over a wide range of ambient conditions of temperature and humidity, good dimensional stability, and ability to be formed into complex core shapes at low cost.

The above properties will now be considered with specific reference to modern ferrites. Table I shows

μ	Composition	Application Frequency Range	μQ
4,000	NiZn	up to 100 kc	50,000 at 10 kc
1,500	MnZn	5 kc to 500 kc	300,000 at 10 kc
500	NiZn	100 kc to 2 mc	20,000 at 500 kc
100	NiZn	1 mc to 15 mc	5,000 at 2 mc
50	NiZn	5 mc to 25 mc	5,000 at 10 mc
15	Ni	above 25 mc	500 at 50 mc

permeability and μQ values for a few typical ferrite compositions. It is seen that values of μ up to about 4,000 are available which is ample to permit effective inductor miniaturization. The situation with regard to μQ is shown in Fig. 1, a chronological step chart of values available in various materials including ferrite. It is in μQ that ferrite most significantly outperforms previously available materials.

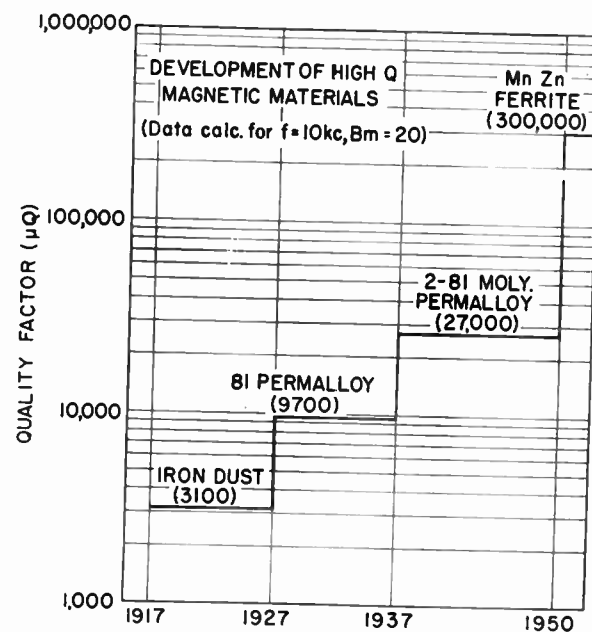


Fig. 1—Improvement in μQ related to time of introduction of various magnetic materials.

The saturation flux density of typical ferrite ranges from about 2,000 to 4,000 gauss. This value is relatively low and it is this property which definitely limits the applicability of ferrites for high-current level inductor cores.

In mechanical properties the ferrites are not far from ideal. Strength, dimensional stability, and producibility

in complex shapes are all satisfactory. However, one area of relative weakness is that of temperature behavior, where the Curie temperature ranging from 70 to 300°C sets a top limit to operating temperature ranges. The great hardness of the ferrites, while generally advantageous, imposes one restriction on the coil designer. Precise core dimensions can be produced only by grinding operations which tend to be expensive and therefore must be held to a minimum for economical core designs.

COIL DESIGN CONSIDERATIONS

As a way to a useful, if arbitrary, kind of order in discussing coil design we can divide all inductors into two categories—"air core" and "magnetic core." The quotations belong in both places because solenoidal or duotateral coils with magnetic slugs are considered by coil designers to be in the air core class, and almost all magnetic core coils have air gaps in one form or another.

Ferrites have some importance as tuning slugs for air core inductors especially where it is important to provide a long range of adjustment. Their chief use, however, is in magnetic core coils. These can again be divided into two categories: the "ring" type as exemplified by the toroidal and rectangular core coils, and the "pot" type in which the winding is substantially surrounded by the core. Generally speaking, the rectangular type coil using simple ferrite pieces such as "C's" and "I's" represents the simplest and most economical structure. Air gaps as required can be included at the butted joints in the core. Adjustment of inductance by removal of turns is possible but the structure is not generally suitable where such adjustments must be made outside of the coil assembly shop. The rectangular structure does not show up well where extreme miniaturization is important, for although its displacement volume may be small, its shape is inefficient from the standpoint of usable equipment space. The toroidal type ferrite coil, except for those restricted applications where a one-piece closed core is indicated, has little to recommend it. Toroidal windings are inherently expensive since the winding machines cannot compete in speed with simple solenoidal winders and they must be reloaded for each coil. The toroids have the same limitation in adjustment as the rectangular types and, to a somewhat lesser extent, the same shape disadvantage.

The pot type structures lend themselves handily to various kinds of adjustment schemes; they are self-shielding, they embody implicit protection for fine wire windings, and their cylindrical shape is efficient from the standpoint of equipment miniaturization. For these reasons they have been favored for most of the more exacting ferrite coil work.

ADJUSTABLE INDUCTORS

In the field of dc chokes and brute force filters inductance requirements may be quite wide, consisting in

some cases only of a minimum limit. With a few exceptions of this sort almost any inductor can be said to be or to have been adjustable, at least at some time in its existence. Even if it is eventually sold as a fixed inductor, somewhere along the line of manufacture the design has allowed for an adjusting procedure. As a general thing, it is not economical to hold tolerances on parts and processes tightly enough to obviate the need for supplemental adjustment.

In some kinds of designs this adjustment may be accomplished simply, such as, for example, by removing turns from a toroidal coil. In others, notably pot types, special design features must be provided to permit factory adjustment. In either case, having in hand a fixed coil for a precision application, the coil user has presumably already paid for adjustment. Often, in spite of this, he will still have to provide further adjustment. In a filter circuit, for instance, he may have to add trimming capacitance, or he may have to select and match his components. Admittedly, the latter is not exactly adjustment, but it is an awkward way of accomplishing the same thing.

The advantages of an adjustable coil, then, are two-fold. One, it does not normally have to be adjusted in the factory; and two, it provides the means by which the circuit in which it is used can be lined up.

In general, when we talk of adjustable inductors we have this sort of application in mind. The adjustment range may be from a few per cent to, perhaps, 40 or 50 per cent on either side of the mean. Mechanically the design need only allow for a small number of operations of the adjustment mechanism during the life of the apparatus. The inductor must be capable of being locked after adjustment, or the mechanism must be stiff enough to hold its adjustment under service conditions of shock and vibration. Calibration is not normally required.

An entirely different concept of adjustment relates to what, for distinction, we shall term tuners, for applications such as tuning a radio set. The requirements for these are entirely different than for ordinary adjustable inductors. The ratio of maximum to minimum inductance may have to be 20 or 30 to 1. The design must allow for many thousands of operations during service life. Locking devices are not usually required but calibration may very likely be. Tuners will be considered separately because their peculiar requirements call for entirely different design approaches.

Adjustable magnetic core inductors are not new, but for filters and networks they were not generally practicable before the advent of ferrites. Although some attempts had been made to adapt adjusting devices to powder toroids, these had tended to be expensive both in dollars and *Q*.

The first high quality adjustable ferrite core inductor is believed to be a design introduced by the Philips Company [6]. This was a pot type coil made up of manganese zinc core parts. The principle of its adjust-

ment is shown in Fig. 2. The length of the main gap is controlled by grinding the center post and outside ring to prescribed differential dimensions. Final adjustment is then accomplished by the use of a plastic strip coated with ferrite powder. As shown in the figure, this strip, which is about 0.15 inch wide and 7 or 8 inches long, is threaded through slots in the ring so that it passes through the main air gap. The coating of ferrite on the strip is graded from about 0.001-inch thick at one end

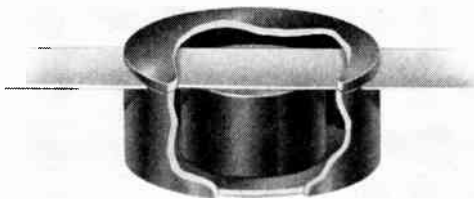


Fig. 2—Inductor using ferrite-coated plastic strip within the air gap for adjustment of inductance.

to anywhere from 0.003- to 0.008-inch at the other. The effective length of the main gap is thus, to a first approximation, reduced in proportion to the thickness of ferrite on the strip and this in turn is a function of the lengthwise position of the strip in the core. After locating the strip so that the required inductance is met it can be cemented in place and the excess cut off. The range of control of inductance by use of this strip is in the order of 10 per cent.

Both of the coils described above permit accurate adjustment, and this means that several conditions have been met:

1. The ratio of inductance change to mechanical displacement is low. It is accomplished in the Philips' coil by the very gradual taper of the thickness of core material on the plastic strip, and in the Bell Laboratories' coil by a fine thread screw. In the latter about seven revolutions of the adjusting screw are required to cover the adjustment range.
2. This ratio always has the same sign. "Waviness" in the adjustment characteristic is always undesirable and if it exists to such a degree that the inductance goes through successive maxima and minima as the coil is being adjusted by null methods, spurious balances will result.
3. Backlash and other phenomena of mechanical looseness have been kept to a minimum.
4. Locking can be accomplished and the hand or adjusting tools removed without changing the adjustment.

In both of these designs the approach is to provide a mechanically stable main air gap modified by an extra magnetic detail; in the one case the ferrite coated plastic and in the other a ferrite slug. This approach appeals because it provides rigidity in those core members that have the greatest effect on inductance. Since in adjusting these coils the differential dimensions involved may be fractions of a thousandth of an inch, there is a measure of security in allowing motion only in the relatively small and light supplementary parts.

This security, however, carries economic penalties in two ways. First, directly, since the provision and the assembly of the extra parts cost money. Second, as a result of inflexibility. The range of frequency best served by the two inductors so far described is determined by the mean air gap, which is a fixed parameter of the structure. To adapt them to a different frequency range would involve more changes than are at once apparent. Suppose, for instance, in the design shown in Fig. 3 it were desired to change the coil so that the best *Q*'s would be realized at 10 kc instead of 100 kc. The length of the main air gap would have to be materially reduced and this could be accomplished simply by specifying a longer center post or a shorter outside ring. But then it would be found that the slug was far less effective in shunting the shortened air gap and the range of adjustment would be reduced. To restore this range the diameter of the slug might be increased. This, however, would introduce a new trouble. Reduced clearance between the slug and the walls of the main core would aggravate spurious cyclic changes of inductance, or "waviness," superimposed on the normal adjustment characteristic.

Where the need for very precise setting of the inductance is not a factor, it becomes possible to use designs

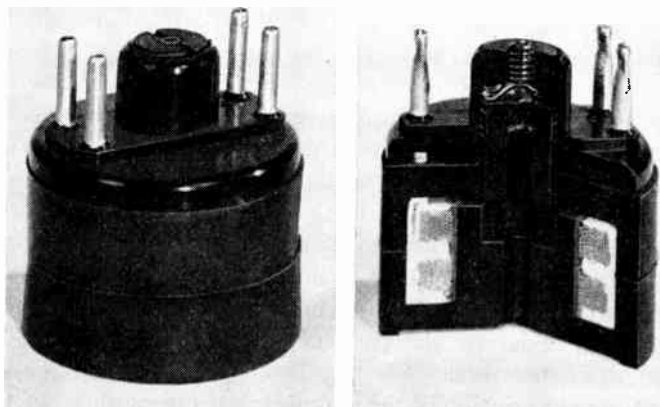


Fig. 3—Adjustable inductor using auxiliary ferrite slug. (1509 type adjustable ferrite core coil for type 0 carrier system.)

In this country there was also early interest in pot type coils with provisions for adjustment. Fig. 3 shows a design created at Bell Laboratories and now in wide use in carrier telephone system filters [7]. This design features a slug which can be inserted, by rotating a screw, into a depression in the center post, providing an essentially linear inductance adjustment range of about ± 20 per cent. It is mechanically capable of positioning to a precision of about 0.01 per cent and can be locked after adjustment. This coil meets unusually high *Q* requirements; from 500 to 600, depending on inductance value and frequency.

in which the effective mechanical motion can be restricted to 180° . This is important because it permits the use of very simple structures of the type exemplified by Fig. 4, where one of the cores is rotated with respect to the other. The required air gap spacing can be provided by insertion of a physical spacer or it can be achieved by differential grinding, as illustrated in the figure. The latter has the disadvantage of a more difficult grinding operation but it avoids the problems of strength and dimensional stability that apply to paper or plastic separators. The change in inductance in this type of coil results, not from a change in effective air gap length but from a change in effective cross section of the gap. This is accomplished either by irregularity in the shape of the post, as shown, or by cutaway sections in the periphery of the shell. Both versions have been used and each has its advantages. A somewhat higher Q for a given size structure can be obtained if the shell is cut away because in cores of practical dimensions there tends to be more area in the rim than in the center post. Proportionately more of it can be sacrificed without degrading the coil's performance. On the other hand, this method reduces the effective self-shielding of the coil. If the post is shaped, it can be done in such a way as to achieve a variety of desired characteristics of rotation vs. inductance, such as, for instance, an approximation of a straight-line frequency characteristic.

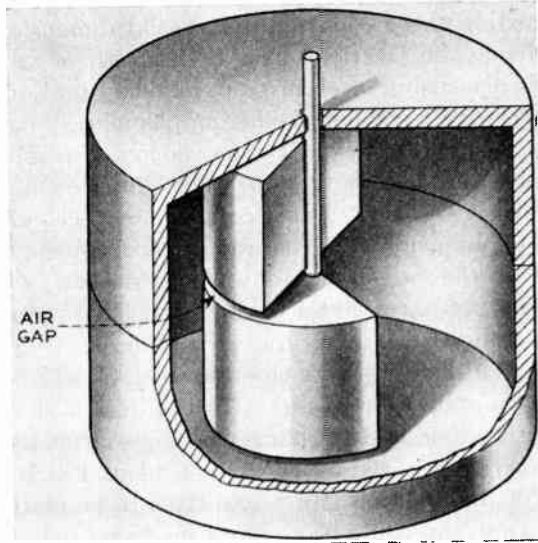


Fig. 4—Inductance adjustment by rotation of core to produce variation in air gap area.

All of the adjustment mechanisms described above have been based on manipulation, in one way or another, of the air gap. While this seems to have been the most popular approach, it is not the only one. For example, Fig. 5 shows a pot type coil in which continuous adjustment of turns is possible [7].

Adjustment by magnetization of the core with permanent magnets has been used in connection with permalloy powder toroids [8], but so far as the authors

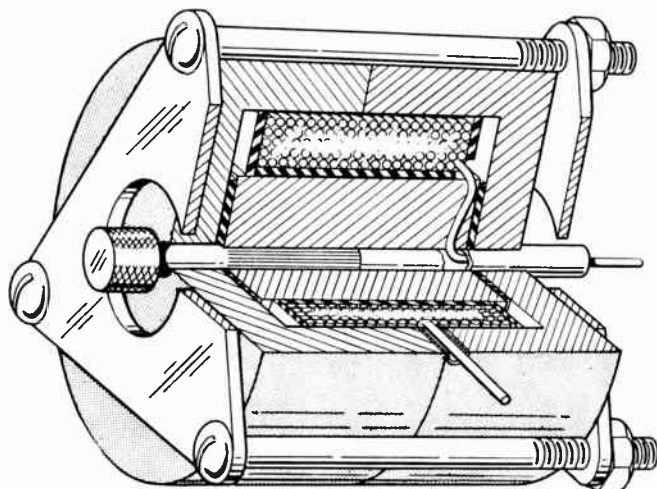


Fig. 5—Adjustment of inductance based on addition or removal of turns.

are aware, not with ferrites. In using such a method it is necessary to consider modulation and other distortion effects, as well as loss of Q .

TUNERS

The chief distinction between tuners and other adjustable inductors is in the requirement for long range of adjustment. Since, using a fixed capacitor, resonance frequency is proportional to the square root of inductance, it requires a 9 to 1 inductance adjustment range just to cover the 0.5 to 1.5 mc broadcast band. This contrasts with the $1\frac{1}{4}$ or $1\frac{1}{2}$ to 1 kind of performance that we have considered so far.

Success in handling this long range has been achieved by use of a magnetic variometer. Fig. 6 illustrates the principle. The windings on the two cores are so poled that during rotation they pass from a series aiding to a series opposing condition. With a coupling of 90 per cent between cores, which is easily achieved, almost a 20 to 1 variation of inductance is implied. Even though the Q tends to suffer when the windings are directly in opposition, existing designs have permitted practical ranges of this order.

A novel variation of the magnetic variometer has been devised to fill a need for double tuning. This device, illustrated in Fig. 7 has been descriptively dubbed the "twinductor." Electrically, it can be considered as two variometers, the opposite windings on each core being connected in the same manner as in the single variometer. Since the flux patterns in each core due to the two pairs of windings are at right angles to each other, there is no mutual interaction between them. Thus the windings are electrically independent while, at the same time, they are controlled by one simple mechanical motion. Once the coil has been initially balanced, no problem in tracking can occur.

The chief weakness of variometer type tuners has been that the long range of adjustment must be effected in a 180° turning of the cores. This makes them too

sensitive to be usable for some of the more exacting applications. Gear reduction schemes have been partially successful in overcoming this disadvantage but the problem of backlash, as well as expense, limits their practical use.

Where the frequency range of interest is high enough so that Q 's obtainable with slug tuned coils are adequate, say above a megacycle, the ferrites can contribute to long range tuning. The two conditions that are needed are high permeability in the core, which the ferrites can provide, and close proximity of the core and the winding, which must be provided by design. In one instance the need for a thin wall between the ferrite core and the winding was met in the following way. In order to

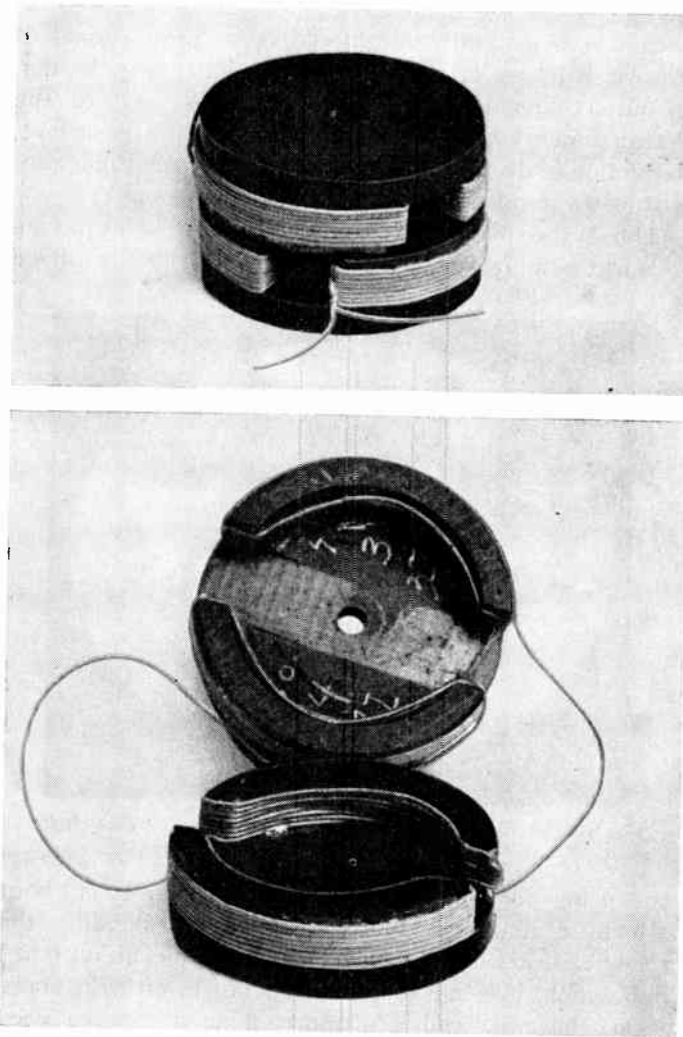


Fig. 6—Ferrite core variometer.

realize a 10 to 1 range it was determined that the wall thickness should not exceed 0.004 inch. Tubes of this thickness were too fragile to be handled so the inductor was wound on a solid rod of epoxy casting resin. The rod was then recast to envelop and protect the winding, and finally the inside was drilled out leaving the required thin wall. Slug tuned coils can be designed for very sensitive control by use of a fine thread lead screw for the tuning slug.

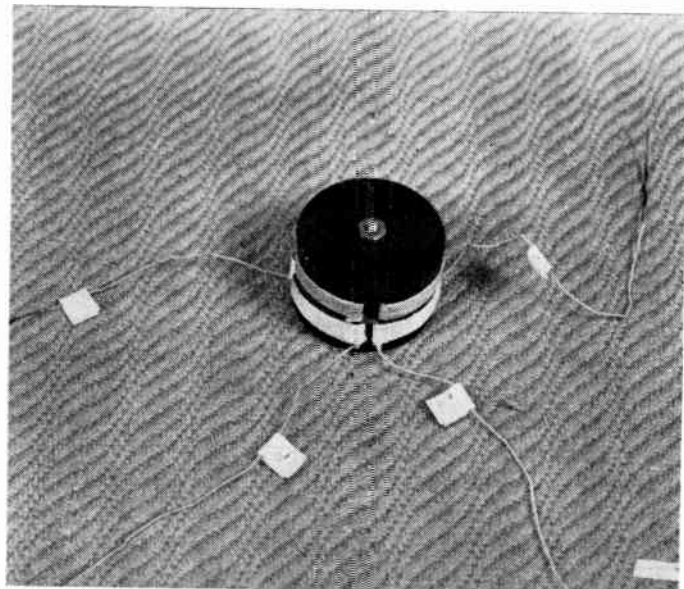


Fig. 7—The "twinductor." Two electrically independent variometers using common core parts.

MINIATURIZATION

In recent years there has been a growing demand for miniaturized apparatus. The use of improbable numbers of electronic components in aircraft, the need for light and compact equipment for soldiers in the field, the public interest in portable radios and smaller deaf sets, are factors in this trend toward small size. Until recently practical miniaturization was limited by the size and power requirements of electron tubes but new orders in size are now being paced by the transistor. The transistor demands passive components of a size comparable with itself so that its own potentials for equipment miniaturization can be realized, and at the same time it provides the possibility of such miniaturization by its very modest demands for power.

Coil designers have been finding in the ferrites the answer to their part of the responsibility for equipment size reduction. The possibility of using high and controllable permeabilities and the ability to let the coil parameters determine the form of core rather than designing the coil to meet restrictive requirements for core shape have resulted in impressive accomplishments in miniaturization.

The permalloy powder cores are not only limited to such simple forms as the toroid, but they are also restricted to a few discrete permeabilities. Since this characteristic is a function of the fineness of the powder and the amount of insulation it is commercially impractical to manufacture cores having a great variety of permeabilities. Another restriction is that the highest value of permeability obtainable is only about 125.

Unlike the permalloys, the ferrites are used in bulk form and the effective permeability may be tailored, by inclusion of appropriate air gaps, to fit the individual needs of different coil designs. Effective permeabilities as high as 1,500 can be realized.

Some of the ramifications of coil miniaturization might best be reviewed by considering first an inductor, which may be of any shape or size, but whose permeability is such as to insure the highest possible Q for the inductance and frequency of interest. It will be assumed that the power level is low enough so that the core loss is not current sensitive. It will also be assumed, for the moment, that ac losses in the wire and losses due to distributed capacitance are small. The remaining losses, then, consist of the dc resistance in the winding, the "residual" loss in the core and the eddy current loss in the core [4]. It is of interest that neither of these core losses are dependent on volume, *per se*. They are, however, directly proportional to permeability.

If the inductor under consideration is reduced in size in such a way that none of the proportions are altered, it will be found that the inductance is reduced directly as the linear dimensions. To make a meaningful comparison between the reduced size coil and the original it is necessary, then, to restore the inductance. This can be done either by increasing the number of turns, increasing the permeability, or both. It can be shown that increasing the permeability and leaving the turns alone will result in the highest Q , and, in fact, that the optimum permeability is inversely proportional to the linear dimensions of the coil. Thus, to maintain as high a Q as possible when size is reduced, it is important to have materials, such as the ferrites, where intrinsic permeability is high and can be controlled by simple means.

The value of Q under the conditions described will turn out to be proportional to the cube root of the volume; that is, directly proportional to any of the linear dimensions of the coil. Limits to miniaturization by proportional reduction of dimensions, and readjustment of coil permeability, may be of four kinds:

1. Q becomes too low to be practicable for the circuit need. If the required size is such that the Q cannot even theoretically be met, the problem reverts back to the circuit designer.
2. The intrinsic permeability of the core material is too low to permit adjustment as size is further reduced. With ferrites this is unlikely to be a problem except at voice frequencies. In such cases, where the permeability can no longer be adjusted upward, the deterioration of Q begins to approach the $\frac{2}{3}$ instead of the $\frac{1}{3}$ power of coil volume.
3. The solution of the mechanical problems attendant on putting smaller pieces together and maintaining closer tolerances becomes economically impractical.
4. Temperature stability of the coil, due to the higher working permeability, fails to meet requirements.

Item (3), obviously, and (4), a little less obviously, are problems for the coil designer. With regard to (4), substantially all of today's ferrites give decided positive

temperature coefficients of inductance. The effect of this instability is approximately in proportion to the effective permeability of the inductor in which the ferrite is used. The inductor designer has, however, the possibility of designing temperature compensation into his coils. One simple approach is to have the air gap expand with temperature at such a rate as to maintain constant effective coil permeability as the material permeability increases. This requires careful choice of materials and of design proportions.

Referring to temporary assumptions above, that the ac wire losses and distributed capacitance effects were small, most often such is the case. Where it is not, and these losses are significant, they tend to become less significant as the size of the coil is decreased. The ac wire loss is generally considered to be proportional to the sixth power of the wire diameter [9] and the distributed capacitance is roughly proportional to the linear dimensions of the structure. As a matter of fact, reduction of distributed capacitance can sometimes constitute an important bonus in miniaturization.

One of the smallest ferrite core inductors so far having reached manufacture is shown in Fig. 8. This is a fixed

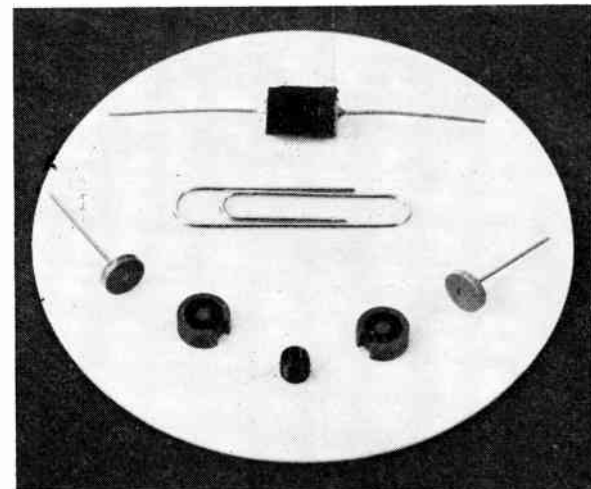


Fig. 8—Details of construction of miniature ferrite core choke.

coil using pot type manganese zinc cores. It is about $\frac{1}{4}$ -inch in diameter and $\frac{5}{16}$ -inch long, excluding the terminal leads. In spite of its small volume, about 0.015 cubic inch, it is suitable for inductances of up to more than 100 mh, and Q 's approaching 100 have been realized. These characteristics, as is generally the case with the smallest coils, are dependent on low level operation. Thus, they are particularly suitable for transistor circuitry.

While fixed miniature coils such as the above have their field of use, adjustability of inductors tends to become more important as size is reduced. This is because adjustable air capacitors, or even fixed trimmers, take up an amount of space that is out of all proportion with

the volume of the more miniature assemblies. The inductors, then, must assume the burden of adjustability that capacitors could have carried in larger equipments.

Some of the same principles of adjustment that have been described for larger coils are applicable for the miniature ones, even though tolerances become progressively harder to meet as designs are scaled down. The principle illustrated in Fig. 3 has been successfully used for an inductor only $\frac{3}{8}$ -inch in diameter and about $\frac{3}{8}$ -inch long. A screw type adjustment was used for a coil of about the same volume and a working Q of almost 300 was realized [10]. A novel scheme of adjustment adapted to a miniature solenoidal coil consisted of a traveling contact that effectively shorted out turns as it was rotated [11]. Adjustment was limited to a few end turns so that the Q of the coil would not be excessively degraded. Miniature tuners both of the variometer and slug tuned types have been successfully used.

LOADING COILS

One of the largest fields of use for high Q inductors is in the loading of telephone cables. This use differs from many of the filter and network applications in several important respects. First, it is usually required that loading coils carry appreciable direct current for signaling. This may, in some cases, approach 100 milliamperes. Second, modulation requirements are particularly severe, especially for carrier telephone circuits where there is danger of modulation products appearing in adjacent talking channels. Third, crosstalk must be kept to a very low level. Crosstalk is a function of balance, leakage, external shielding and relative positioning of adjacent coils.

Toroidal coils of molybdenum permalloy powder, which was originally developed expressly for this application, are used almost exclusively for low frequency loading in this country. Permalloy powder cores are ideally suited to this use by their ability to carry appreciable direct current and their very low leakage. Although present ferrites could be used, this is one field where they would not offer outstanding advantages. Their dc carrying characteristics are marginal and the use of discrete air gaps with attendant local leakage aggravates the crosstalk problem.

In spite of these facts, and because the main constituent of permalloy is nickel, which is a strategic material, some attention has been given to ferrites for loading. Work has been aimed toward creating a ferrite which would be, for all practical purposes, a direct substitute for molybdenum permalloy powder. Such a material, formed into standard sizes of toroidal cores, could be put into use without the delay and expense involved in modification of manufacturing plant facilities. So far, experimental work has produced some promising materials but, as of this writing, none suitable for use as a direct replacement for permalloy.

The story in Europe is quite different. There ferrites are used for both voice and carrier frequency loading. Circuit requirements, the state of raw material supply, present investment in manufacturing equipment, etc., have been just different enough in some cases to have tipped the balance in favor of ferrites. The pot type coils have been generally favored, and ingenious schemes have been devised to insure the required balances. For example, one such scheme, introduced by the Philips Company, involves a mechanism for moving the windings axially within the pot structure, thus modifying the leakage pattern and the resultant self inductances [12, 13].

NONLINEAR COIL APPLICATIONS

It has previously been mentioned that the value of ferrites as stable magnetic materials depends on using them at relatively low flux density. Lately there has been an increasing number of applications where the value of the ferrites depends on their instability at higher flux density, and, in fact, increasing attention is being given to development of the so-called square loop ferrites whose permeability is a critical function of their magnetization [14, 15]. These materials are used for modulators, magnetic amplifiers, memory devices, etc. which are generically, but only incidentally, inductors, as well as for control coils, whose design lies directly in the inductor field.

Control coils are simply adjustable inductors whose adjustment is effected by electrical rather than mechanical means [16], usually as a function of variations in applied direct current. Magnetic amplifiers represent a specialized use for such coils, but the application of more immediate interest is in frequency control.

In essence a control coil consists of two windings, a signal winding and a control winding, on a common core structure. The signal winding, circuitwise, is to be considered as an inductor, having inductance, inductance range, and Q requirements. It is usually part of a network intended for frequency control, as in an oscillator, or for frequency discrimination, as in a filter. The control winding carries a current whose instantaneous magnitude determines the permeability of the core structure, and hence the inductance of the signal winding. As in a magnetic amplifier the variations in the control current must be at a low rate compared to the signal frequency.

Direct transfer of energy between the control and signal windings must be avoided. This sometimes can be done, although somewhat inefficiently, by the use of low pass filtering in the control winding circuit and high pass filtering in the circuit of the signal winding. More commonly, however, it is done by use of suitable core configurations, three of which are shown in Fig. 9. In 9(a), two cores are used and the windings poled so that the net inductive coupling is zero. This sort of structure has

the advantage of simplicity and can be balanced easily by turns adjustment. Control coils of this type have been on the market for several years. Design parameters can be adjusted for use at audio frequencies or up to 10 mc and higher. At the lower frequencies inductance variations of several hundred to one are possible.

Coils depending on mutually orthogonal flux paths, as shown in Fig. 9(b), have been used experimentally but so far as is known to the authors they have not found commercial application. They tend to be inflexible from the design point of view because of the interdependence between core and winding dimensions.

The style of control coil shown in Fig. 9(c), in which separate structures are used for the control and signal windings, provides the greatest design flexibility. It is possible to choose core materials, and, to some extent, their size and shape independently for the signal and control windings.

The basic requirement for the signal winding core is that its permeability be sensitive to flux level. This property, and the need for a favorable μQ in the frequency range of interest, will be factors in determining which ferrite to use. Size and proportions of the signal coil will be dependent on impedance and frequency requirements. The desire, in general, will be to keep the core structure as small as possible so as to increase its sensitivity to the control flux. At higher frequencies small size in the signal coil may also be advantageous in reducing parasitic capacitance.

The requirements for the control winding core are entirely different. Usually it will operate essentially under dc conditions. For sensitive control many ampere turns may be required, necessitating large structures. In the control winding there is little interest in the variation of permeability with flux level, providing the core does not saturate. In some instances the control winding core is a ferrite which may or may not be the same as that in the signal winding. In other instances it has been made up of silicon iron laminations.

The chief difficulty in the design of these coils has been in insuring a high degree of balance of the control winding flux in the signal winding core. This is done by maintaining close symmetry in the latter and locating it with care within the air gap.

The long range of inductance adjustment possible in control coils may be taken advantage of directly for some applications, or the control coil may be used in series with a fixed coil where precise control is essential but the range is not extensive. One such use is in the regeneration of carrier frequency in a carrier telephone television terminal. In this application a ferrite control coil as part of a feedback system keeps a 4 mc carrier generator synchronized with carrier frequency information derived from the received signal [17].

Experimental control coils have been used at frequencies up to 200 mc. With present ferrites, however, both Q and adjustment range become restricted at frequencies much over 10 mc.

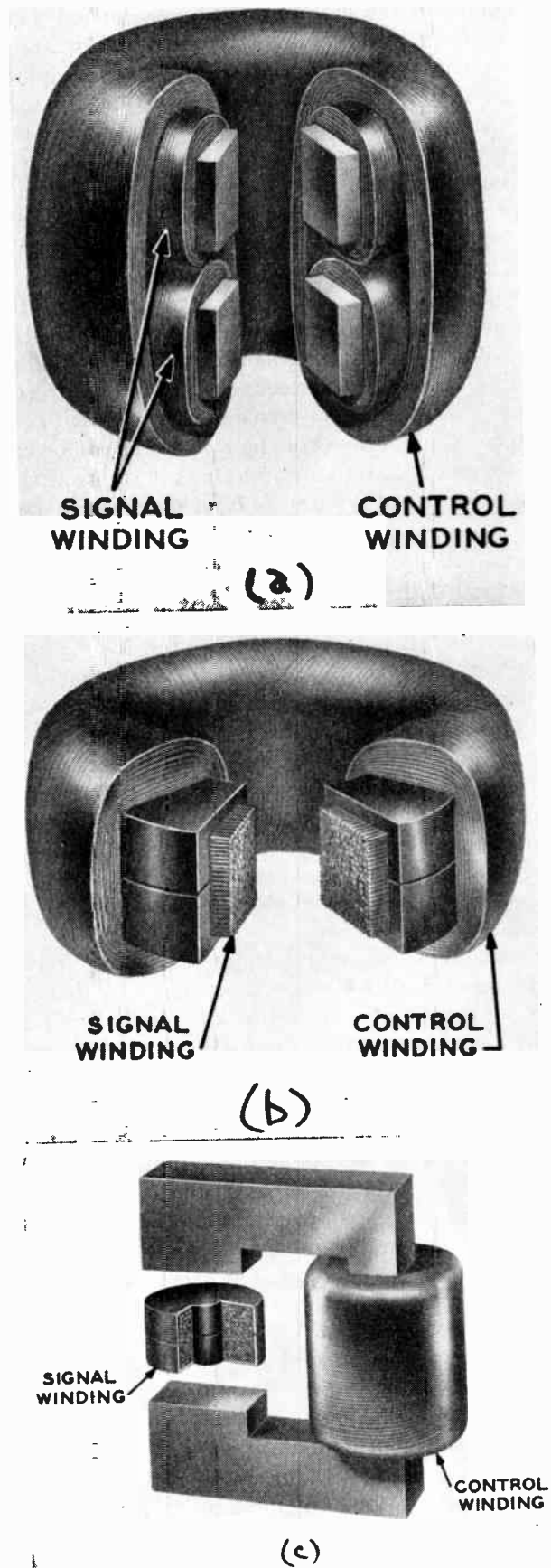


Fig. 9—Control coil design. Methods of avoiding coupling between control and signal windings. (a) Balanced windings on two cores. (b) Mutually perpendicular flux paths in common core. (c) Use of separate core structures.

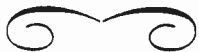
CONCLUSION

In the not quite ten years since high permeability ferrites were announced they have largely usurped the position of permalloy powders as the leading core materials for transmission type inductors. Designers have been quick to take advantage of their structural adaptability and the possibilities they offer for mechanical control of permeability. Currently manufactured inductors attest to the improved performance that these new dimensions in design can offer.

It is not unreasonable to suppose that the continuing application of research to improvement of ferrites will result in higher μQ at all frequencies and higher frequencies of practical use. Nor should it be assumed that the ultimate in coil design or ingenuity in coil application has yet been observed. It is not reasonable to predict ferrites for power applications in the near future but in the transmission inductor field, for which they are inherently suited, it is safe to expect a continuing and profitable increase in their use.

BIBLIOGRAPHY

- [1] Legg, V. E., and Given, F. J., "Compressed Powdered Molybdenum Permalloy." *Bell System Technical Journal*, Vol. 19 (July, 1940), p. 385.
- [2] Snoek, J. L., "Non-Metallic Magnetic Materials for High Frequencies." *Philips Technical Review*, Vol. 8 (December, 1946), p. 353.
- [3] Shea, H. G., "Magnetic Powders." *Electronic Industries*, Vol. 4 (August, 1945), p. 86.
- [4] Legg, V. E., "Survey of Magnetic Materials and Applications in the Telephone System." *Bell System Technical Journal*, Vol. 18 (July, 1939), p. 438.
- [5] Owens, C. D., "Analysis of Measurements on Magnetic Ferrites." *PROCEEDINGS OF THE IRE*, Vol. 41 (March, 1953), p. 359.
- [6] Latimer, K. E., and MacDonald, H. B., "A Survey of the Possible Applications of Ferrites." *Proceedings of the IRE*, Vol. 97 (April, 1950), p. 257.
- [7] Stone, Jr., H. A., "Ferrite Core Inductors." *Bell System Technical Journal*, Vol. 32 (March, 1953), p. 265.
- [8] Burnell, L. G., "Variable Toroidal Inductors—New Electronic Components." *Tele-Tech.* Vol. 13 (October, 1954), p. 68.
- [9] Wien, M., "On the Transmission of High Frequency Alternating Currents in Stranded Wire." (German) *Annalen der Physik* (4), Vol. 14 (1904), p. 1.
- [10] Darnell, P. S., "Miniaturized Components for Transistor Applications." *Telegraph and Telephone Age* (August, 1952), p. 8.
- [11] Eng, J. W., "Microminiature Variable Inductors for Transistorization." *Tele-Tech.*, Vol. 12 (August, 1953), p. 74.
- [12] Hering, H., and Leichseuring, F., "Modern Loading Coils with Siferrit Pot-cores." (German) *Siemens-Zeitschrift*, Vol. 27 (September, 1953), p. 124.
- [13] Six, W., "Some Applications of Ferroxcube." *Philips Technical Review*, Vol. 13 (May, 1952), p. 301.
- [14] Williams, H. J., Sherwood, R. C., Goertz, M., and Schnettler, F. J., "Stressed Ferrites Having Rectangular Hysteresis Loops." *Transactions of the AIEE*, Vol. 72, Part I (November, 1953), p. 531.
- [15] Wijn, H. P. J., Gorter, E. W., Esvaldt, C. J., and Gildermans, P., "Conditions for Square Hysteresis Loops in Ferrites." *Philips Technical Review*, Vol. 16 (August, 1954), p. 49.
- [16] Weis, Von A., "Variometers Controlled by Magnetic Fields." (German) *Entwicklungs-Berichte der Siemens & Halske Aktiengesellschaft*, Vol. 17, (November, 1954), p. 251.
- [17] Rieke, J. W., and Graham, R. S., "The L3 Coaxial System—Television Terminals." *Bell System Technical Journal*, Vol. 32 (July, 1953), p. 915.
- [18] Weis, A., "High Frequency Magnetic Cores of Ferrites." (German) *Funk u Ton*, Vol. 11 (November, 1948), p. 564.
- [19] Landon, V. D., "Use of Ferrite Coated Coils as Converters, Amplifiers and Oscillators." *Radio Corporation of America Review*, Vol. 10 (September, 1949), p. 387.
- [20] Polder, D., "Ferrite Materials." *Proceedings of the IRE*, Vol. 97 (April, 1950), p. 246.
- [21] Kornetzki, M., "Ferrite Cores for High Frequency Coils." (German) *Siemens-Zeitschrift*, Vol. 25 (April, 1951), p. 94.
- [22] Legg, V. E., "Ferrites: New Magnetic Materials for Communication Engineering." *Bell Telephone Laboratories Record*, Vol. 29 (May, 1951), p. 203.
- [23] Vanderschmitt, B. V., Obert, M. J., and Stott, H. B., "Ferrite Applications in Electronic Components." *Electronics*, Vol. 25 (March, 1952), p. 138.
- [24] Both, E., "Development and Utilization of Magnetic Ferrites." *Ceramic Age*, Vol. 59 (April, 1952), p. 39.
- [25] Emmerich, E., and Klaus Jr., S. C., "Evaluation of Electrical Properties of Ferrite Materials for Specific Applications." *Ceramic Age*, Vol. 59 (May, 1952), p. 26.
- [26] Gelbard, E., "Magnetic Properties of Ferrite Materials." *Tele-Tech.* Vol. 11 (May, 1952), p. 50.
- [27] Newhall, E., Gomard, P., and Ainlay, A., "Saturable Reactors as R. F. Tuning Elements." *Electronics*, Vol. 25 (September, 1952), p. 112.
- [28] "Ferrite Core Loading Coil, 80MH." *Rundschau*, F. and G., (German) No. 35, (October, 1952), p. 123.
- [29] Kornetzki, M., Brackmann, J., Frey, J., and Gieseke, W., "Measurements on High Permeability Ferrite Cores." (German) *Zeitschrift für Angewandte Physik*, Vol. 4 (October, 1952), p. 371.
- [30] Salpeter, J. L., "Developments in Sintered Magnetic Materials." *PROCEEDINGS OF THE IRE*, (Australia), Vol. 14 (May, 1953), p. 105, and *PROCEEDINGS OF THE IRE*, Vol. 42 (March, 1954), p. 514.
- [31] Kornetzki, M., "Ferrite Cores for Communication Engineering." (German) *Siemens Zeitschrift*, Vol. 27 (June, 1953), p. 212.
- [32] Roberts, W. Van B., "Magnetostriction Devices and Mechanical Filters for Radio Frequencies." *Q.S.T.*, Vol. 37 (June, 1953), p. 24; (July, 1953), p. 28; and (August, 1953), p. 32.
- [33] Kornetzki, M., "Magnetic Constants of Ferrite Cores." (German) *Siemens Entwicklungs Berichte*, Vol. 16 (July, 1953), p. 135.
- [34] Stiber, S., "Remote Tuning Receiver Has No Moving Parts." *Electronics*, Vol. 26 (July, 1953), p. 186.
- [35] Harvey, R. L., "Ferrites and their Properties at Radio Frequencies." *Proceedings of the National Electronics Conference* Vol. 9 (September, 1953), p. 287.
- [36] Hoh, S. R., "Evaluation of High Performance Magnetic Core Materials." *Tele-Tech.*, Vol. 12 (October, 1953), p. 86, and (November, 1953), p. 92.
- [37] Geroulo, M., Peck, D. B., and Cushman, N., "Improved Components Based on Ferrite Materials." *Proceedings of the Electronics Components Symposium*, (May, 1954), p. 141.
- [38] Legg, V. E., and Owens, C. D., "Magnetic Ferrites: New Materials for Modern Applications." *Electrical Engineering*, Vol. 73 (August, 1954), p. 726.



Electromechanical Filters for 100-Kc Carrier and Sideband Selection*

R. W. GEORGE†, SENIOR MEMBER, IRE

Summary—A general discussion of a torsional type mechanical filter and its termination by mechanical and electrical means is followed by a detailed description of two 100-kc filters, one 50 cycles wide and the other 3.1 kc wide.

The design, fabrication, and frequency adjustment of one-piece multiple section filters is described. Frequency stability better than 2 parts per million per degree centigrade is obtained with filters constructed of the metal alloy Ni-Span-C.

Magnetostrictive ferrite and Ni-Span-C transducers resonant in the longitudinal mode of vibration are attached tangentially to the end resonators of the torsion filter. The filter is terminated by converting the electrical resistance in low-*Q* input and output circuits to mechanical damping. Responses due to spurious modes of vibration in the filter are reduced by the use of a pair of transducers in a balanced arrangement at each end of the filter, and by mechanical damping in the end supports.

INTRODUCTION

THE electromechanical filter, employing a series of mechanically resonant elements mechanically coupled together, is of particular interest in the communications field because of the greatly increased use of single sideband systems. Communications filters must be accurately tuned and must have stable operating characteristics over a wide temperature range. Such filters are rather difficult to make by the commonly used method of assembling pretuned resonators and couplers because of the consequent detuning of the resonators and the mechanical imperfections in the resonator to coupler joints. The one-piece neck type torsional filter with quarter-wave couplers is not only free of these difficulties but is mechanically rugged and easy to tune.

The principles of electromechanical filters have been fairly well established.¹⁻⁵ References mentioned here are intended to furnish only a modest background for the described filters. Many articles and books on the related subject are available.

It is convenient to think of electromechanical filters in terms of the component parts and their functions. The mechanical filter determines the frequency response characteristic. It is designed to have the required

number of high-*Q* mechanical resonators and suitable mechanical coupling elements between the resonators. The design of the mechanical filter also determines the amount of mechanical damping required in the end resonators to properly terminate the filter.

Termination is a matter of introducing the required mechanical loss, or damping, in the end resonators. This is accomplished by the use of mechanically lossy materials, and/or by conversion of electrical damping to mechanical damping in the electromechanical coupling system.

The electromechanical coupling system provides the means for electrical input and output of the mechanical filter. It can also be made to supply all of the required mechanical termination damping when the electro-mechanical coupling coefficient is sufficiently high. In this case, the output/input voltage ratio approaches unity for equal input and output impedances.

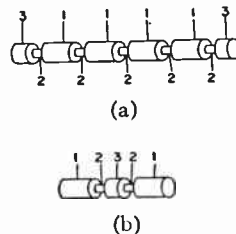


Fig. 1—(a) A neck type mechanical filter using half-wave cylindrical resonators, 1, coupled together by quarter-wave necks, 2. The quarter-wave neck extensions and slugs, 3, are for support of the filter. (b) Two resonators coupled together by a multiple coupler to give a very small coupling coefficient.

THE TORSIONAL MECHANICAL FILTER

The neck type mechanical filter shown in Fig. 1(a) is the type used in the carrier and sideband filters. It is most practical when operated in the torsional mode. A brief description including some physical characteristics which contribute to mechanical simplicity, strength, stability, and accurate tuning follows. Each large cylinder is a half-wave long resonator tuned to the midband frequency of the filter. Resonator vibration is such that at resonance, one end vibrates in rotation about the axis in the opposite direction to the vibration of the other end. The smaller diameter quarter-wave long sections are the couplers or coupling necks.

The coupler length, and the ratio of the coupler neck diameter to the resonator diameter, determine the fractional bandwidth or coefficient of coupling between resonators. A quarter-wave coupler in a given filter has the largest diameter which can be used to obtain the desired coupling coefficient. The length of the quarter-

* Original manuscript received by the IRE, June 28, 1955; revised manuscript received September 9, 1955.

† David Sarnoff Research Center, RCA Labs., Princeton, N. J.

¹ R. Adler, "Compact electromechanical filter," *Electronics*, vol. 20, pp. 100-105; April, 1947.

² W. van B. Roberts and L. L. Burns, "Mechanical filters for radio frequencies," *RCA Rev.*, vol. 10, pp. 348-365; September, 1949.

³ L. L. Burns, "A band-pass mechanical filter for 100 kilocycles," *RCA Rev.*, vol. 13, pp. 34-46; March, 1952.

⁴ M. L. Doelz and J. C. Hathaway, "How to use mechanical filters," *Electronics*, vol. 26, pp. 138-142; March, 1953.

⁵ W. van B. Roberts, "Some applications of permanently magnetized ferrite magnetostrictive resonators," *RCA Rev.*, vol. 14, pp. 3-16; March, 1953.

wave coupler is not too critical and therefore requires no adjustment. The coupling coefficient between resonators is nearly proportional to the 4th power of the ratio of neck diameter to resonator diameter.

It is a relatively simple matter to tune a resonator to a desired frequency when its resonant frequency can be measured. The frequency is raised by removing material from the ends of the resonator cylinder, and lowered by removing material from a narrow band around the center of the cylinder. The resonator should be resonant at the midband frequency of the filter when it is supported by quarter-wave necks anchored at their far ends. Torsional resonators can be effectively anchored or detuned by clamps. This makes it possible to isolate any resonator in the filter and accurately measure its resonant frequency after clamping the adjacent resonators. One-piece construction of a series of torsional resonators and couplers is thus feasible because the resonators can be accurately tuned after fabrication.

Very small coupling coefficients, such as are required in the carrier filter, can be obtained by the use of the multiple coupler without making the coupling necks impractically small in diameter. The multiple coupler Fig. 1(b), in its simplest form, uses two quarter-wave necks separated by a quarter-wave slug.

The mechanical filter is made with quarter-wave neck extensions and end slugs for mounting. The mounting anchors the extreme ends of the necks, thus isolating the filter from its supports.

MECHANICAL FILTER MATERIAL

The iron-nickel-chromium-titanium alloy known as Ni-Span-C⁶ appears to be one of the most practical materials available⁷ for use in mechanical filters. It can be processed by heat treatment to have a nearly zero thermoelastic coefficient which imparts an equally low frequency-temperature coefficient to the filter. The most satisfactory results have been obtained by solution-annealing the material before heat treating. The material is sensitive to cold working and this must be avoided after the solution anneal. Heat treatment time and temperature must be determined experimentally for each batch.

Ni-Span-C has good mechanical properties including a mechanical Q of about 16,000. As usual with nickel alloys, Ni-Span-C is so difficult to machine that grinding is usually preferred to cutting.

Resonators made of Ni-Span-C, can be magnetostrictively excited. This provides a very convenient aid in measuring the resonant frequency.

ELECTROMECHANICAL TRANSDUCERS

The electromechanical transducers should preferably be the end resonators of the filter and therefore should have good frequency stability. End resonators of Ni-

Span-C may be used as the magnetostrictive transducers but in general their high eddy current loss results in a low electromechanical coupling coefficient which usually prohibits the use of electrical termination.

A composite end-resonator can be made which includes the original high Q end resonator and an attached electromechanical transducer. One method of doing this is to tune a half-wave longitudinal mode transducer to the midband frequency, and attach one end tangentially to one end of a torsional resonator. Mechanical damping which the transducer derives from the terminal electrical circuits is shared by the composite resonator. Damping to terminate the filter can be obtained in this manner if the electromechanical coupling coefficient is sufficiently high. The tuned input and output circuits have relatively low Q and therefore provide a wide-band electrical termination.

The magnetostrictive ferrites⁸ have negligible eddy current loss and can have an electromechanical coupling coefficient, K_{em} , of 15 per cent to 20 per cent with suitable coils. These ferrites can be made to have substantially constant K_{em} over a wide temperature range, and a mechanical frequency-temperature coefficient of 20 parts per million per degree centigrade or less. Such ferrites are practical for use as resonant transducers in a wide-band termination system.

The manner in which the transducers are applied to the filter should be such as to minimize the possible excitation of undesired modes of mechanical vibration in the filter. The excitation of bending modes, which are likely to be the most objectionable ones in a torsion filter, can be reduced by the use of a pair of transducers in a balanced arrangement.

MECHANICAL FILTER DESIGN

Methods of calculating the required coupling coefficients to obtain maximum band-edge attenuation for a given amplitude of ripple in the pass band have been greatly simplified^{9,10} and are applicable to the design of a mechanical filter. The coupling coefficients are all different from an end to the center of a symmetrical filter and the differences become smaller near the center. In practice it is necessary to make some compromise of the exact coupling coefficients because of the difficulty and cost of making the coupling neck diameters different and to very close dimensional tolerances.

The simplest filter design, sometimes called the Campbell type, has uniform coupling coefficients except at the ends. It is used here because of its mechanical simplicity. One objection to this type of filter is that it is difficult to obtain the proper characteristics in the termination which are required to give flat response in the pass

⁶ R. L. Harvey, "Ferrites and their properties at radio frequencies," Proc. NEC, vol. 9, pp. 287-298; February, 1954.

⁷ M. Dishal, "Design of band-pass filters producing desired exact amplitude-frequency characteristics," Proc. IRE, vol. 37, pp. 1050-1069; September, 1949.

⁸ M. Dishal, "Two new equations for the design of filters," Elec. Commun., vol. 30, pp. 324-337; December, 1953.

⁹ Ni-Span-C, reg. trade mark of the International Nickel Co.

⁷ Ni-Span-C can be obtained from The H. A. Wilson Company, Union, N. J.

band. A compromise termination is practical, however, and can give as little as 10 or 15 per cent output variation in pass band with excellent band-edge attenuation.

A series of 9 coupled resonators is depicted in Fig. 2.

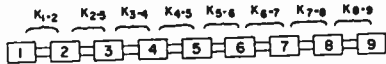


Fig. 2.—The general case of a filter having a number of very high-Q resonant elements all tuned to the same frequency and having coupling coefficients, K , between adjacent resonant elements.

The fractional-bandwidth, B , of the filter is equal to twice the coupling coefficient, K , between a pair of interior resonators.

$$\frac{B}{2} = K_{2-3} \cdots K_{7-8} \quad (1)$$

$$K_{1-2} = K_{8-9} = \frac{B}{\sqrt{2}}. \quad (2)$$

The mechanical design of the filter is based on work done at RCA Laboratories.² The following simplified formulas have been found satisfactory for general use.

The mechanical design to obtain the desired coupling coefficients using quarter-wave couplers is based on

$$K = \frac{2}{\pi} \phi \left(1 - \frac{\phi}{2}\right) \quad (3)$$

When the resonators are a half-wave long and of equal diameter, made of the same material as the coupling necks, and are operating in torsion, the value of ϕ is simply related to the resonator and neck diameters.

$$\phi = \frac{d_c^4}{D^4}.$$

d_c = diameter of coupler

D = diameter of resonator. (4)

A more general expression which can be reduced to the above is

$$\phi = \frac{W_e}{\sqrt{W_1 W_2}}. \quad (5)$$

W_e = Kinetic energy of a quarter-wave coupling neck calculated as if rigid.

W_1 and W_2 = respective kinetic energies of the coupled resonators.

The simple multiple coupler which uses two quarter-wave necks separated by a quarter-wave slug having the same diameter as the resonators, Fig. 1(b), is designed from the above equations with the exception of (3), which is replaced by

$$K_d = \frac{2}{\pi} \phi^2 \left(1 - \frac{\phi}{2}\right). \quad (6)$$

K_d = Coupling coefficient for double coupler.

The damping, d , required in the end resonators for termination of the Campbell type filter is not a constant value over the pass band. A practical compromise is used here.

$$d \cong K_{1-2} \cong .7B \quad (7)$$

$$\frac{1}{d} = Q \text{ of end resonator.} \quad (8)$$

ELECTRICAL TERMINATION

The mechanical damping required in the end resonator of the filter is obtained from the damping in the attached transducer. The transducer in turn receives its damping from the electrical tuned circuit to which it is coupled. The transducer should be large enough so that the required damping can be obtained. The inherent mechanical damping in the original end resonator is so small that it can be neglected.

The damping, d_t , required in the transducer, is calculated as though the transducer were isolated from the filter.

$$dt = \left(\frac{W_r}{W_t} + 1 \right) d. \quad (9)$$

d = Damping in the original end resonator to terminate the filter

W_r = Kinetic energy of original end resonator

W_t = Kinetic energy of transducer.

The mechanical damping in the transducer, which is obtained from the coupled electrical circuit, is given approximately by

$$dt \cong K_{em}^2 Q \quad (10)$$

K_{em} = Electromechanical coupling coefficient

Q = Q of the input and output circuits.

The most uniform value of damping is had in the pass band when

$$K_{em} Q \cong 1. \quad (11)$$

THE NARROW-BAND 100-KC CARRIER FILTER

An example of a 100-kc carrier filter is shown in Fig. 3. This uses 5 half-wave torsion resonators with double-couplers of quarter-wave elements. The mechanical filter was made from a rod of Ni-Span-C on which the coupling necks were ground to the desired diameter. The grinding wheel was dressed in width to cut the required $\lambda/4$ neck length.

The coupling design is of the Campbell type with B taken as 0.0005. The measured bandwidth shown in the frequency response curve, Fig. 4, is in good agreement with the design. A bandwidth of less than 25 cycles is equally practical and has been obtained in other experimental models.

The following dimensions of the resonators and couplers will be of interest:

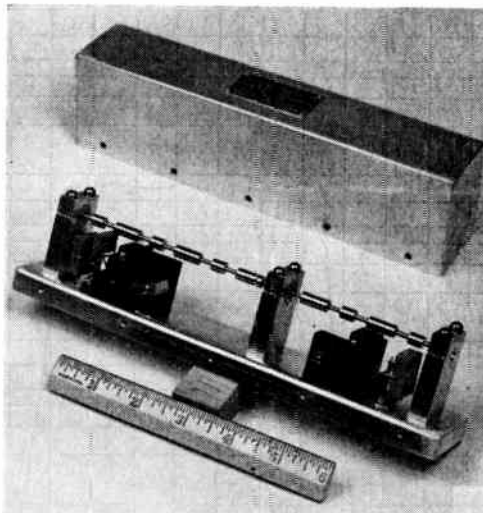


Fig. 3—100-kc carrier filter.

Resonator and coupler slug diameter	0.240 inch ± 0.0002 inch
Resonator length, $\lambda/2$	0.570 inch ± 0.001 inch
Coupler neck diameter for $K=B/2$	0.090 inch ± 0.0005 inch
Coupler neck diameter for $K=B/\sqrt{2}$	0.094 inch ± 0.0005 inch
Coupler neck and slug length, $\lambda/4$	0.285 inch ± 0.001 inch

A small fillet between coupler neck and resonator is not objectionable.

The resonators were tuned to 100-kc plus or minus one cycle. This accuracy is not difficult to achieve but of course does take some care. The resonant frequency of a resonator can be measured accurately with a suitable signal generator, bridge circuit, and events-per-unit-time counter. The resonator is excited magnetostriictively in torsion when placed in a coil in one arm of the bridge. Satisfactory residual magnetic bias is had by passing a few amperes axially through the filter for an instant. The resonant frequency is increased 15 to 20 cycles with maximum residual magnetic bias; therefore, it is necessary to use uniform bias when making frequency measurements. The residual circular bias is subject to partial loss during the tuning operation or when subjected to a strong rf field. Satisfactory results have been had by using the minimum bias which will give a suitable output of the bridge. One way to get this weak bias is to first magnetize with dc, then partially demagnetize by passing filter through an ac coil.

The small coupling coefficient in the filter makes it easy to detune the adjacent resonators by clamps in order to isolate the resonator under test. All resonators are tuned before attaching the transducers.

The magnetostrictive transducers, which are shown in the schematic diagram, Fig. 5, were made of 0.015-inch diameter Ni-Span-C wire. The result as shown in Fig. 4 was less electromechanical coupling than required for the best termination of the filter; however, this response characteristic is considered suitable for carrier separation. The transducers were tuned to within about 50 cycles of 100 kc before being spot-welded to the end resonators of the filter. Final frequency check and tuning of end resonators was made after adding transducers.

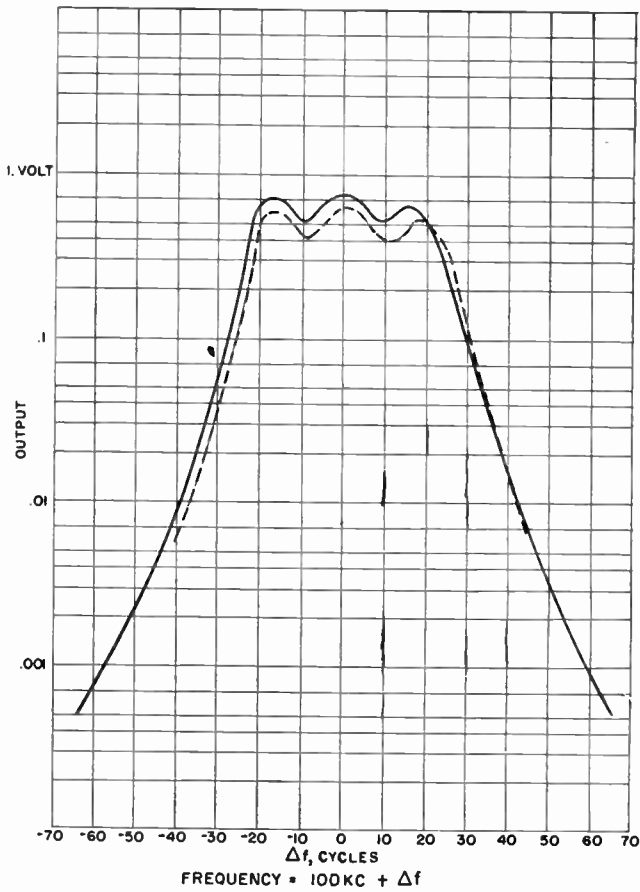


Fig. 4—100-kc carrier filter, output vs frequency for 1 volt input. Dashed curve shows response at 22°C, above room temperature.

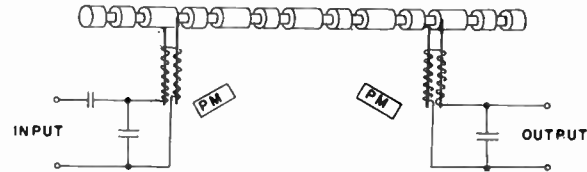


Fig. 5—Schematic diagram of carrier filter using multiple couplers and balanced magnetostrictive longitudinal transducers.

The input and output circuits, Fig. 5, are tuned for maximum output at 100 kc. The two coils coupled to a pair of transducers are connected to produce opposing fields so that with common magnetic bias from the nearby permanent magnet, one transducer becomes longer while the other becomes shorter, thus energizing the torsion resonator with minimum bending. The stray field of a pair of coils connected in this manner is so small that no special shielding is required to keep the the stray input-output coupling to a very low value. The position of the small alnico bias magnet was adjusted for maximum output. The input circuit is arranged to give some voltage step-up from a 500-ohm source such as a cathode follower.

The filter is securely clamped in the end supports with one end grounded. One or both of these clamps may include a plastic bushing to give some damping of bending modes if necessary. Spurious responses in this filter are few and usually not objectionable.

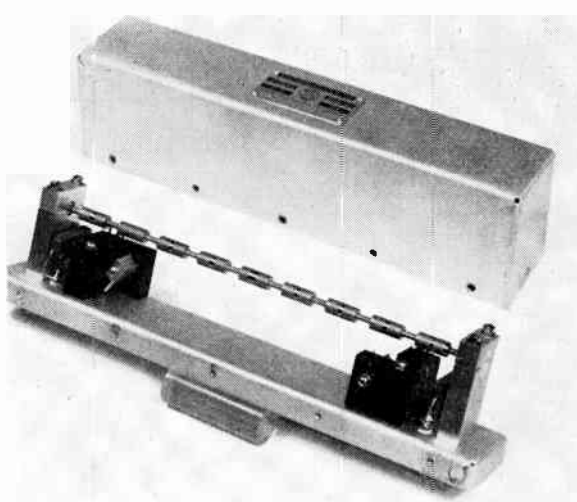


Fig. 6—100-kc upper sideband filter.

The support near the center (Fig. 3) makes the assembly better able to withstand shock. It has a nylon bushing with an inner ridge about $1/32$ inch wide in close contact with one of the coupler slugs. Coupler slugs can be touched without detuning the filter but a heavily damped slug adds appreciable mechanical transmission loss.

These filters have an output impedance of approximately 5,000 ohms. With an equal input impedance, the input/output voltage ratio is approximately 3. A 500-ohm input source to the circuit shown in Fig. 5 gives an input/output voltage ratio of 1.4. The peak to valley ratio is 1.4 at 28°C . and 1.5 at 50°C . The shape factor is approximately 2.6.

THE SIDEBAND FILTER

One of the sideband filters, electrically terminated with broad-band tuned circuits is shown in Fig. 6. This has 9 torsional resonators with Campbell type coupling coefficients. The filter was designed using a value of 0.031 for B which gave the corresponding bandwidth shown in Fig. 7. A pair of magnetostrictive ferrite transducers is used on each end resonator. The resonators were tuned to the midband frequency of 101,800 cycles plus or minus 10 cycles.

Damping is obtained from the end tuned circuits which, with the added resistors, have a Q of about 5. The electromechanical coupling coefficient to the ferrites is about 0.19. The pair of transducers has about $\frac{1}{8}$ the kinetic energy of the end resonator and therefore requires a mechanical damping, d_t , of about 9 times the damping required in the composite end resonator.

Two of these filters were made and found to have substantially identical characteristics. The frequency tem-

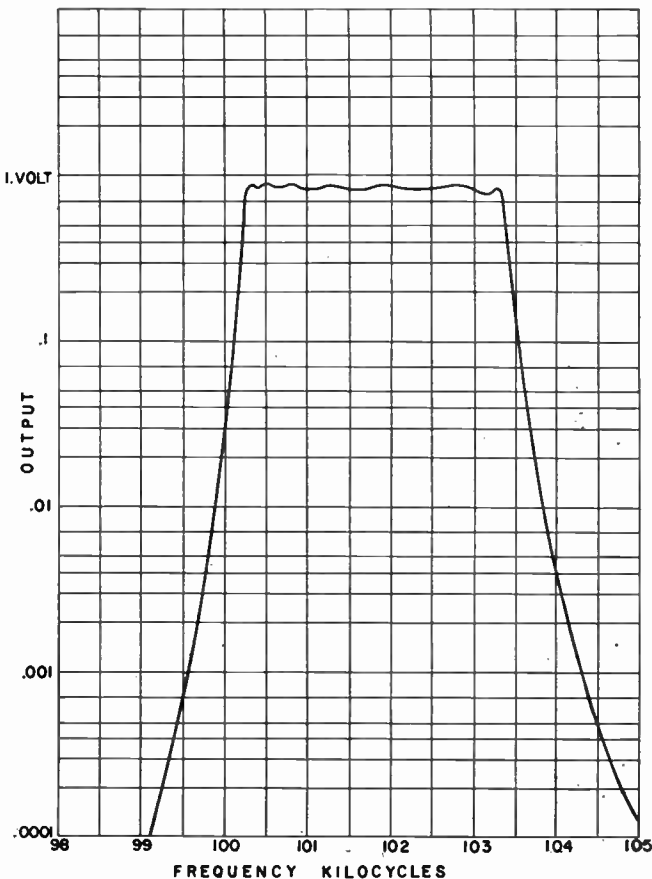


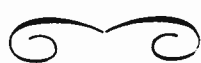
Fig. 7—100-kc sideband filter output vs frequency for 1 volt input.

perature coefficient was less than 2 parts per million per degree centigrade. The input, and output, impedance of these filters was approximately 4,500 ohms. The input/output voltage ratio was 1.14 at 24°C . and 1.19 at 74°C . At both temperatures, the maximum to minimum amplitude variation in the passband was 1.14 and the shape factor was 1.55. The frequency shift of the band edges was less than 10 cycles.

The excellent stability of the electrical termination at different temperatures was due to the favorable characteristics of the magnetostrictive ferrites which were made especially for this purpose. During the development of these ferrites which were of the equimolar iron-nickel type,⁸ it was found necessary to reduce the cobalt impurity content to 0.003 per cent or less in order to obtain the desired stability with varying temperature.

ACKNOWLEDGMENT

The author wishes to express his appreciation to Mr. R. L. Harvey, who made the special magnetostrictive ferrites, and to Mr. J. J. Murphy, who provided the sideband filter elements.



New Microwave Repeater System Using Traveling-Wave Tubes*

N. SAWAZAKI†, ASSOCIATE MEMBER, IRE, AND T. HONMA†

Summary—This paper describes a new microwave relaying system using traveling-wave tubes (TWT), and utilizing its large inherent frequency bandwidth. In this system, the increased gain is obtained by amplifying the input signal through the TWT Amplifier, and reamplifying it in the same TWTA after heterodyning the frequency to the second frequency. The signal received could be amplified in the same TWTA more than once simultaneously, and the gain of the TWTA would be increased in proportion to the amplifying times.

A 4,000-mc band television repeater using three TWT's, and its measured results are also described; we obtain the results that the over-all gain is above 100 db and is steady within ± 0.5 db with the frequency bandwidth of 20 mc, and also, the noise figure is below 15 db. The actual test was carried out by putting the equipment in the TV long-distance relay line as a repeater. From this test it was proved that there is no defect of the operation of the amplifier in using TWT as a reflex amplifier. In this new system, the number of TWT's can be reduced one-half to one-third and the cost of a repeater with increased reliability can be lowered.

INTRODUCTION

FOR a microwave relay system, the heterodyne type which uses intermediate amplifiers, such as the TD-2 system in the United States, has chiefly been used up to the present. In Japan, the development of such repeaters has been conducted actively in several places. The authors continued the research of the all-traveling-wave-tubes amplifier-type repeater in cooperation with the engineers of the Broadcasting Corporation of Japan (N.H.K.) from 1951 to 1953, after the completion of the heterodyne-type TV relay system, and obtained satisfactory results during practical use at the Hakone TV relay station. This system has many superior characteristics compared with the heterodyne type system: simplification of equipment by decreasing the number of tubes, improved S/N characteristics owing to the progress of the low-noise traveling-wave tube, and ease of maintenance due to eliminating such complicated parts as IF amplifiers, microwave oscillators, and AFC circuits.

It is possible to obtain another relaying system by taking advantage of the wide-band characteristic of the traveling-wave tube (TWT). The authors obtained satisfactory results in experiments applying this principle. One method is to relay not only one radio channel as conventionally used, but several channels simultaneously with the same TWT amplifier, and by this principle a TWT is used commonly for a local oscillator tube and an amplifier tube in a heterodyne type repeater.

In these applications, the repeater which amplifies the east-bound and west-bound channels with the same repeater has been completed by the joint research of

Tokyo Shibaura Electric Co. and N.H.K., for the use of TV relay equipment at the Hakone Relay Station. The testing of this set could not be performed because of the frequency allocation, though the remarkable results of this two-direction repeater were obtained in the room test. This repeater has practical use as a one-direction repeater.

The system mentioned in this paper is a new system designed for a one-direction, one-channel repeater by applying the wide-band characteristic of the TWT, and reducing the number of TWT's. In previous TWT repeaters, [1] seven stages of TWT's were used in series; in this new system the number of TWT's can be reduced one-half to one-third, which lowers the cost of a repeater, at the same time giving increased reliability. An improved version of this new system is also described in this paper.

BASIC PRINCIPLE OF THE NEW SYSTEM [2]

This new system can be called a reflex system which is applied to TWT amplifiers. Its principle is similar to the reflex-type receiver in broadcasting band because the same tubes are commonly used for radio frequency and audio frequency amplifiers. This reflex system utilizes certain special features: the TWT amplifier has a much wider frequency band compared with other types of amplifiers; in microwave systems the sending and receiving carriers are different in frequencies, and signals are frequency-modulated waves.

The increased gain is obtained by passing the received signal through the TWT amplifier, heterodyned by the crystal mixer to the second frequency, and reamplifying by the same TWT amplifier. If more gain is necessary, the output signal is heterodyned by the second mixer to the third frequency and reapplied to the input of the same TWT amplifier. Thus the signal is amplified three times by the same TWT amplifier. By using this method, multiplied gain will be two or three times more than that of the straight amplifier with the same TWT's. In Fig. 1, the schematic diagram of the 4,000-mc band reflex-type repeater with three-times amplification by the same TWT amplifier and its equivalent circuit is shown.

This repeater was designed on the following basis:

Frequency of the input signal	4,045 mc
Frequency of the output signal	4,000 mc
Frequency bandwidth	20 mc
Total gain	100 db.

In Fig. 1, the received 4,045 mc signal is applied through the 4,045-mc band-pass filter, BPF (1), located at the input side of the amplifier through the TWT's No. 1, No. 2, and No. 3. Amplified 4,045-mc signal from

* Original manuscript received by the IRE, June 7, 1955.

† Matsuda Research Lab., Tokyo Shibaura Elec. Co., Ltd., Kawasaki, Japan.

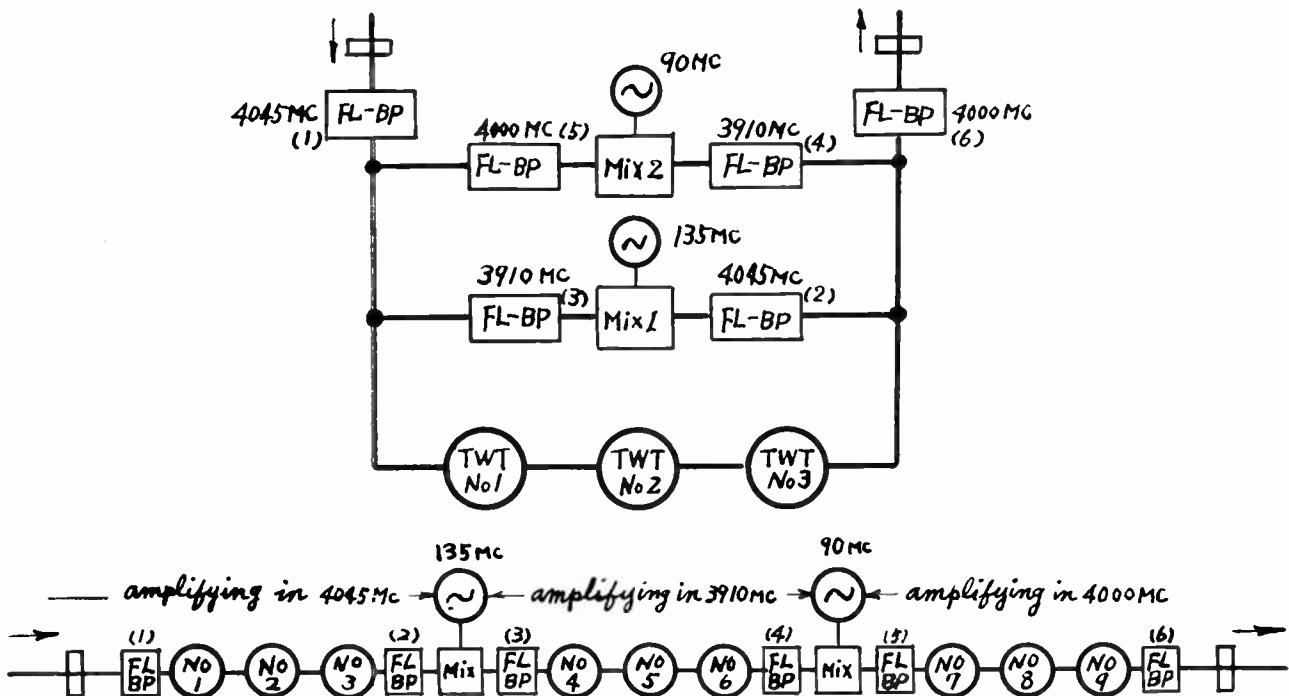


Fig. 1—Sematic and equivalent circuit of the reflex amplifier.

the output circuit is applied through the 4,045 mc BPF (2) to the crystal mixer (1), where the signal is converted to 3,910-mc signal using 135-mc local oscillator, and the 4,000-mc signal is also applied through the BPF (5) to the input of the TWT amplifier. Then the final amplified 4,000-mc signal by the same TWT's is transmitted through the 4,000-mc BPF (6) located at the output side. TWT amplifies the signal three times at three different frequencies; therefore, a total gain proportional to the multiple of the amplified times is obtained. The over-all gain G in the equivalent circuit may be written as

$$G = 3(g_1 + g_2 + g_3) - (L_{M_1} + L_{M_2}) - (L_{F_1} + L_{F_2} + \dots + L_{F_9})(\text{db}),$$

where g_1, g_2, g_3 are gains of TWT's No. 1, No. 2, and No. 3, L_{M_1}, L_{M_2} are conversion losses of crystal mixers No. 1 and No. 2. $L_{F_1}, L_{F_2}, \dots, L_{F_9}$ are insertion losses of the BPF (1), (2) \dots (6).

In the case of practical design, conversion loss of a crystal mixer and insertion loss of a band-pass filter composed of three sections are below 15 db. Additional loss in the reflex system as compared with the straight-amplifier system is shown by the sum of the losses of the additional parts for reflex use; these parts are one mixer and three band-pass filters. This loss will be below 20 db, and there are other decreasing factors of gain G caused by the saturation effect of the tubes in high-level input, so that G is nearly equal to that loss of the seven-stages straight amplifier; however, in this three-times reflex system three tubes are used.

Using this technique, many other applications requiring high-gain microwave amplifiers can also be made. The case of Fig. 1 is a relay of 100-km span at 4,000 mc. In the case of 50-km span with 80-db over-all gain, for

example, the TD-2 link which is shown in Fig. 2 can be used. Those are examples of a one-time reflex using three tubes and a two-times reflex using two TWT's.

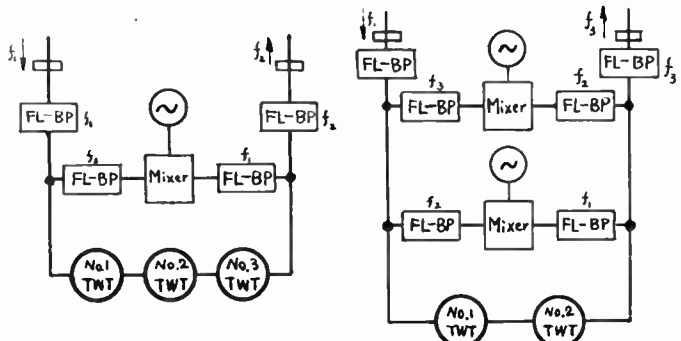


Fig. 2—Examples of the other type reflex amplifier.

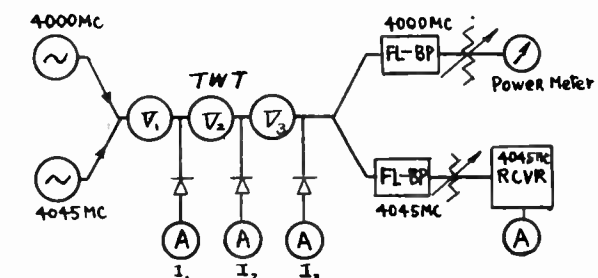
THE PRELIMINARY EXPERIMENTS OF THE REFLEX-TYPE AMPLIFIER

The characteristic of very large inherent bandwidth of the TWT is well-known, but the problems of stability, noise, distortion, gain, etc., when two or three signals are applied together to a TWT amplifier simultaneously, have not been clarified. The characteristics of TWT's cannot be calculated simply, so preliminary experiments have been carried out to learn the characteristics.

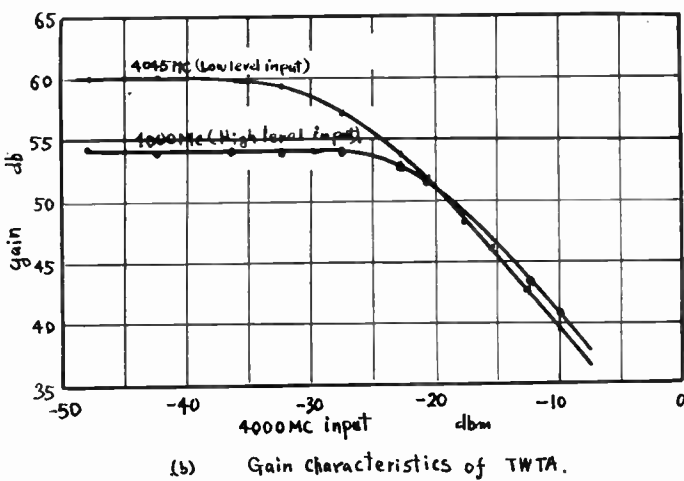
Examination of Problems on the TWT Amplifier When Two Signals Are Applied Simultaneously

When reflex amplifying, the signals are applied to the TWT amplifiers in different frequency ranges, are delayed by turns each time, and at the last time are at highest level. On the other hand, the TWT amplifier decreases its gain at high input level, so that output power

is constant to some certain input level; then power output decreases when input gets too high. The influences of the last-time high-level signal over gain of first- and second-time signal amplification are considered.



(a) Measuring circuit.



(b) Gain characteristics of TWTA.

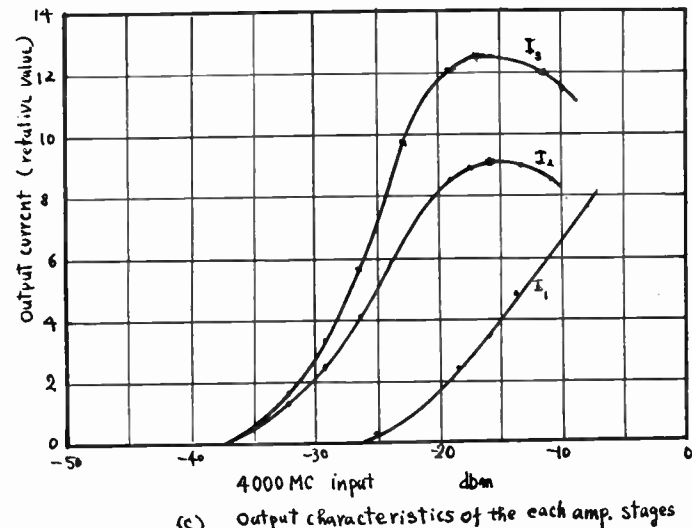


Fig. 3—Gain characteristics of TWTA when two signals are applied simultaneously. (a) Measuring circuit, (b) Gain characteristics of TWTA, (c) Output characteristics of each ampere stage.

Fig. 3 shows the gain characteristics of the three-stage TWT amplifier when two signals, differing in amplitude levels, are applied simultaneously. These characteristics are obtained by keeping the low-level 4,045-mc input at -50 dbm constant and by varying the 4,000-mc input signal from -50 dbm to -10 dbm. In these results, gain limitations of the TWT by saturation

begin to appear when the 4,000-mc signal level is about -30 to -20 dbm, and when the 4,000-mc signal level is more increased, the output power becomes nearly constant; then, the gain of the tubes decreases, as shown in Fig. 3. It also shows that the gain of the 4,045-mc signal varies equally as much as the gain of the 4,000-mc signal. These results prove the wide-range gain-control action in reflex amplifier, due to their power saturation, but, on the other hand, it shows that there is a possibility of oscillation or distortion if the amplifier is used under conditions of heavy saturation.

Crosstalk and Noise Due to Amplifying Two Signals Simultaneously

The experimental results of the crosstalk and noise due to amplifying the high-level fm signal and low-level fm signal simultaneously are shown in Fig. 4. This experiment has also been done, as similarly described above; that is, the 4,045-mc fm signal was kept constant at -40 dbm and the added 4,000-mc signal was varied from -50 to 0 dbm. It seems, as a result, that there were no interactions between signals in the range of weak signal input below -20 dbm, where there is no saturation; however, when the input became above -10 dbm, both S/N and crosstalk became worse according to the conspicuous tube saturation. In reflex amplification, this crosstalk change is due to signal distortion.

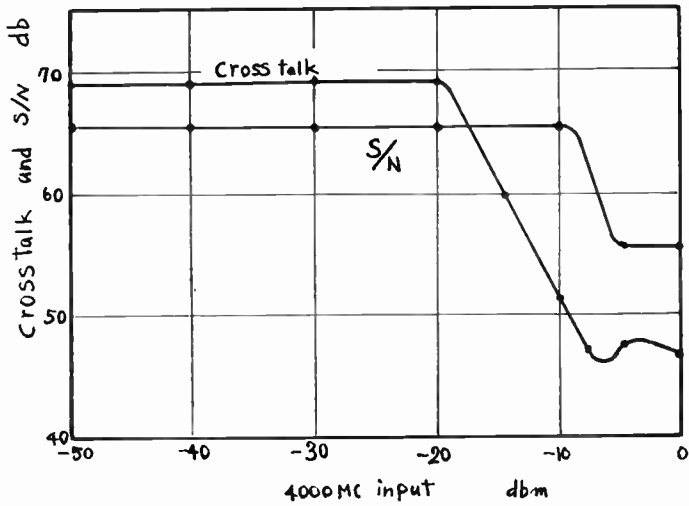


Fig. 4—Crosstalk and S/N when two signals are applied to the TWTA.

From these results with the reflex system, a good S/N ratio and small distortion like this in the cascade TWT repeater system can be expected, as far as the reflex amplifier works in the unsaturated region.

REFLEX-TYPE ALL-TWT REPEATER

After preliminary experiments above, reflex-type trial repeater was planned for use of television relay.

Specifications

Characteristic requirements for trial repeater were the same as of television repeaters stationed in span length of 100 km with 40-db gain paraboloids in Tokyo-Nagoya-Osaka links by N.H.K., and specifications were:

Input carrier frequency	4,045 mc
Output carrier frequency	4,000 mc
Output power	above 3 watts (within the input level -60 to -30 dbm)
Over-all gain	above 90 db
Frequency bandwidth	± 10 mc (3 db down)
Noise figure	below 15 db.

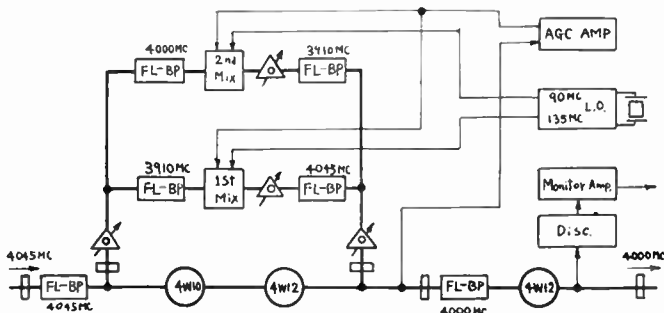


Fig. 5—Block diagram of the reflex-type trial repeater.

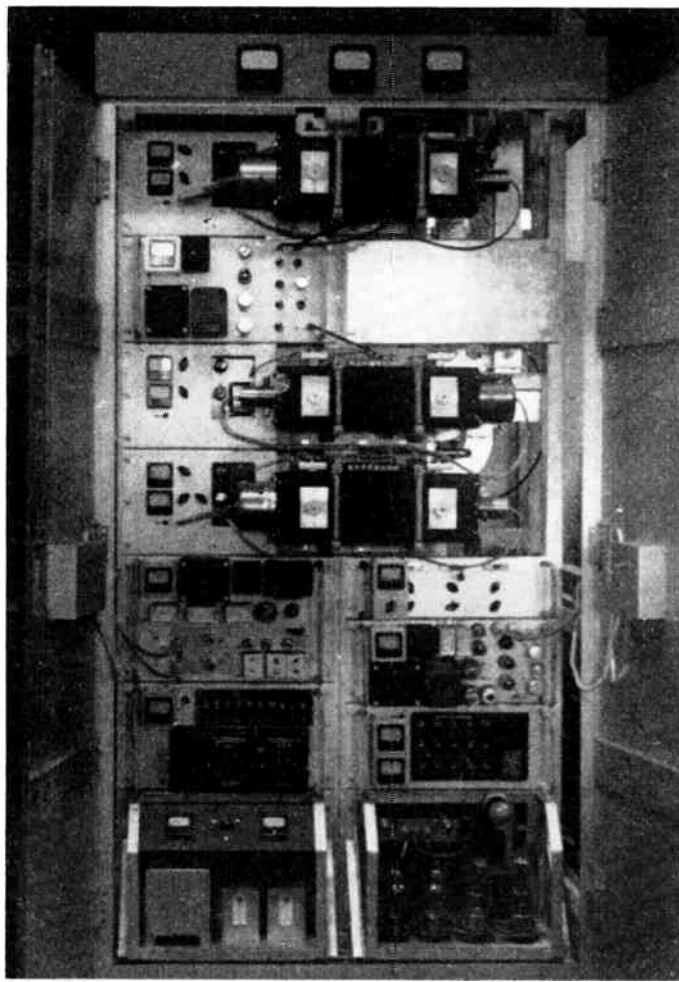


Fig. 6—Outside view of the reflex-type repeater.

Outline of the Repeater

As shown in the block diagram, Fig. 5, and photograph, Fig. 6, this repeater provides three traveling-wave tubes and the first two tubes V_1 and V_2 act as a

two-time reflex-type amplifier; the last tube, V_3 , is driven by this reflex output. 4W10, especially designed for low-noise TWT, is used for V_1 , and 4W12, designed for power tubes, is used for V_2 and V_3 . The scheme works as follows.

Input 4,045-mc signal is applied to input side 4,045-mc BPF, and the signal amplified in V_1 and V_2 is applied through a branching circuit and 4,045-mc BPF to the mixer, where the signal is mixed with 135-mc local oscillator output. The 3,910-mc signal output from this mixer is reapplied through the 3,910-mc BPF, and the branching circuit to the same TWT amplifiers. The signal is amplified again, and the same process is repeated; then, the 3,910-mc signal frequency is shifted to 4,000 mc by mixing with the output of the 90-mc local oscillator. Finally the 4,000-mc signal amplified with V_1 and V_2 is applied through BPF to last tube V_2 (4W12).

The agc action-reflex amplifier with TWT's has a good characteristic, but to avoid distortion due to its strong saturation, agc circuit is provided with constant output power for -60 to -30 dbm input level range.

135-mc and 90-mc local frequencies are those multiplied from the main crystal oscillator of 5,625 mc.

For a microwave circuit in the reflex section, waveguide-type band-pass filters ($Q \approx 100$), Y-type branching waveguides, and phase shifters are used in Fig. 5.

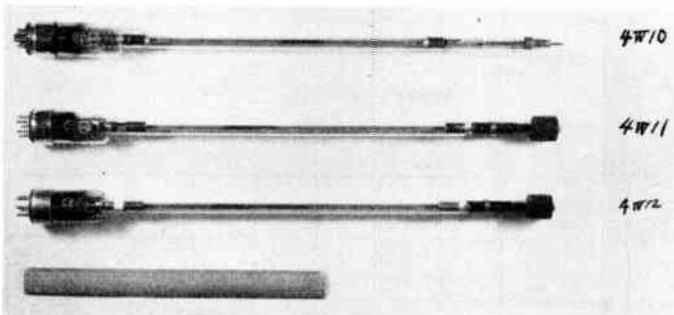


Fig. 7—Used traveling-wave tubes.

Traveling-Wave Tubes

Traveling-wave tubes used in this system, and their characteristics, are in Fig. 7 and Table I, p. 23. At the beginning, this system had been designed to use voltage-amplifier tube 4W11 for the second stage of the reflex section, but the design was changed to use power-amplifier tube 4W12 in order to decrease a variety of tubes and distortion due to the saturation effect in the reflex section.

Over-all Characteristics

Gain Characteristics: Fig. 8 shows the results of the gain measurements of the TWT amplifier acting as a straight-through amplifier, one-time reflex amplifier, and two-times reflex amplifier. For the gain measurements of the straight amplifier, two local oscillators and input side 4,045-mc BPF were removed, and 4,000-mc signal applied to the input. For the gain measurements of the one-time reflex amplifier, 135-mc local oscillator

TABLE I
TWT'S FOR 4,000-Mc BAND

	Heater		Max. dimension		Base	Freq. range (Mc.)	1st anode (V)	2nd anode (V)	Helix		Collector		Out-put (W)	Gain (db)	Noise Fig. (db)	Cool- ing	Mag. field (gauss)
	V	A	length mm.	diam. mm.					V	mA	V	mA					
4W10 (7810)	6.3	0.6	555	38	Octal	3500-4300	100-	150-250	1000	—	1000	0.5	—	15	15		400
4W11 (7811)	6.3	0.35	555	38	UY	3500-4300	—	—	1500	0.5	1500	4.0	0.36	26	—	forced air	400
4W12 (7812)	6.3	0.6	555	38	UY	3500-4300	—	—	2150	5.0	2150	28.0	3.5	17	—	foreal air	400

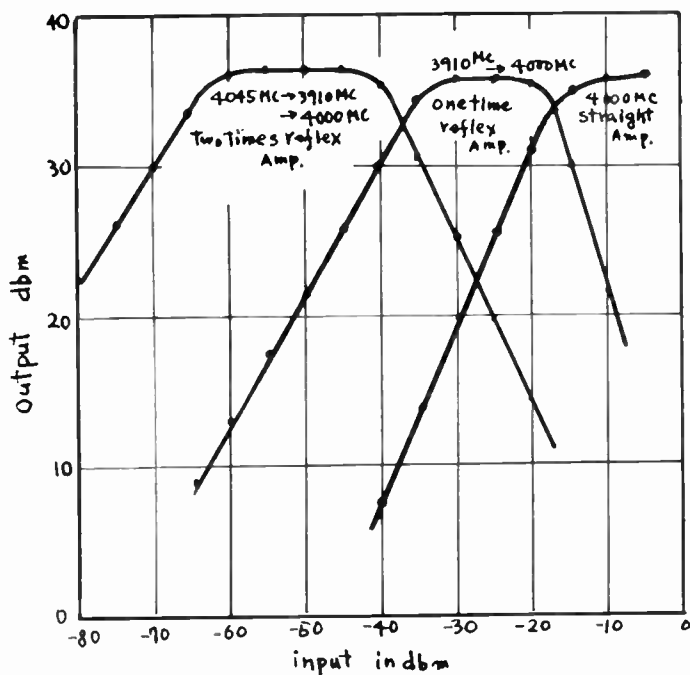
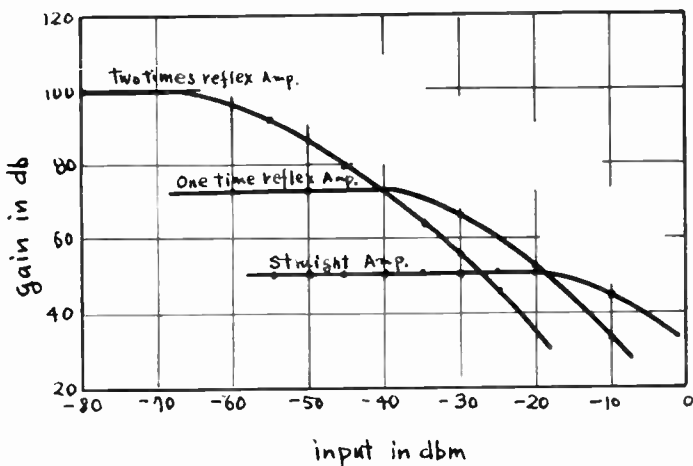


Fig. 8—Over-all gain characteristics of the reflex amplifiers.

and input side 4,045 mc BPF were removed, and 3,910-mc signal was applied to the input. For the two-times reflex amplifier, the system worked as shown in Fig. 5, and the gain measured in the last case was the repeater.

Measured Loss in a Feedback Circuit. From the output circuit of the TWT amplifier to the input circuit of the

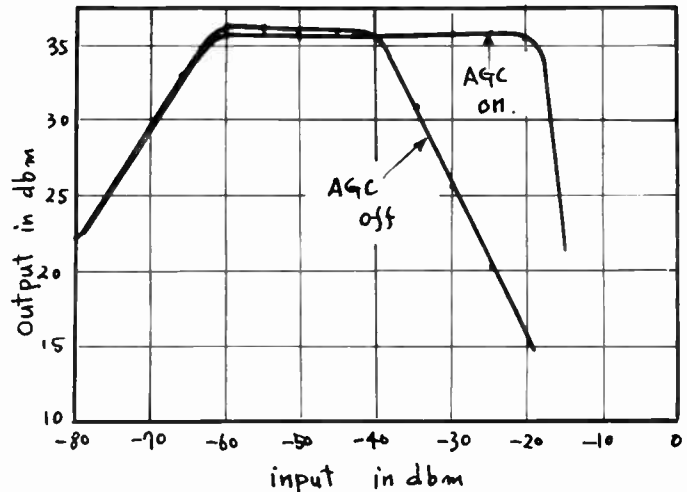


Fig. 9—Input power to output power characteristics.

TWT amplifier, there were four Y-type branching waveguides, two mixers and four BPFs in this circuit, and the total loss of one return was about 16 db. The results obtained by experiments above were 51 db, 74 db, and 100 db respectively, as shown in the figure, and these data were very close to what we expected.

AGC: Fig. 9 shows the input power to output power characteristics, when input level was increased gradually in the condition of agc off. The power output began to decrease from -40 dbm input level. With the agc circuit on, the output power was kept constant above 3 watts over the -60 to -20 dbm input range.

Automatic gain control was achieved in the following manner. First, part of the power output from the reflex section was rectified by a crystal detector, and the rectified direct current was applied to a magnetic dc amplifier. The conversion loss of the crystal mixer, and accordingly the gain of the amplifier, were varied by the output voltage of the magnetic amplifier, which varied the local oscillator strength.

Noise Figure. Over-all noise figure of about 14-5 db was obtained with a noise generator or microwave signal generator method. Comparing this value with that of straight amplifier in using the same tube, the same value was obtained, considering the loss of the input side bandpass filter and branching circuit. Therefore, it seems there was no worse effect in either reflexing method.

Over-all Frequency Characteristic and the Transient Characteristics: Over-all frequency characteristic may be affected by the characteristics of the branching circuits, band-pass filters, crystal mixers and coupling systems of traveling-wave tubes. But the power gain obtained from the actual equipment was steady within ± 0.5 db with the frequency band of 20 mc, as shown in Fig. 10.

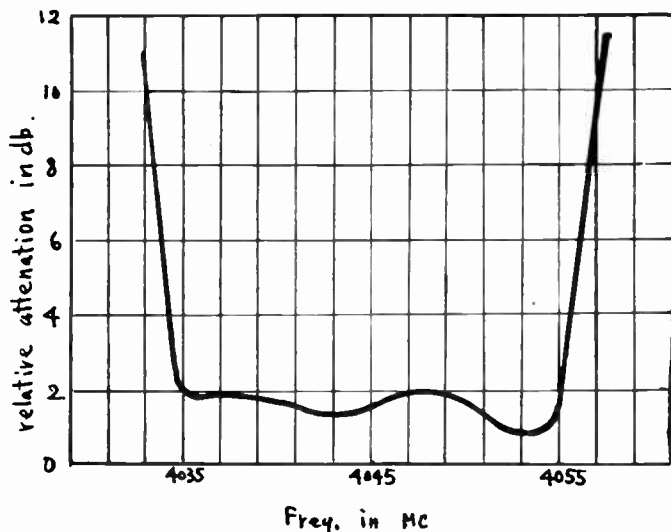


Fig. 10—Over-all frequency characteristic.

Concerning the distortion by phase delay, transient response characteristics were tested for signals of rectangular frequency-modulated wave with build-up times of about 0.05 microsecond, and there was no perceptible difference in the waveform between the input and the

output of the equipment. Also an actual test was carried out by putting the equipment in the television long-distance relay line as a repeater. The television pictures relayed by it were good and stable.

From these experiments, we can conclude that, as for distortions owing to reflex amplifying, they do not affect the operation of amplifiers to the use of traveling-wave tubes as reflex amplifiers.

CONCLUSION

The main purpose of using traveling-wave tubes as reflex amplifiers is to simplify the construction of repeaters and, as a result, to decrease maintenance expense without sacrificing operating characteristics of repeaters.

ACKNOWLEDGMENT

The television relay equipment explained herewith was completed by the joint research of the engineers of the Broadcasting Corporation of Japan (N.H.K.), and Tokyo Shibaura Electric Company.

The authors wish to express many thanks to T. Nomura and Dr. K. Suzuki of N.H.K., who made researches concerning the possibility of trial repeaters, and M. Mita of the Matsuda Research Laboratory for his advice and suggestions.

BIBLIOGRAPHY

1. Sawazaki, N., "Traveling Wave Tube Television Relaying Equipment." *Toshiba Review*, vol. 9 (January, 1954), pp. 22-31.
2. Sawazaki, N., and Honma, T., "Reflex Type All TWT Relay System." *Convention Record of the E.E. of Japan*, Part 3 (October, 1954), p. 503.
3. Suzuki, K., Sawazaki, N., and Honma, T., "4,000-Mc Reflex-Amplifier Type TV Relay Equipment." *Convention Record of the E.E. of Japan*, Part 5 (May, 1955), p. 846.

Geophysical Prospection of Underground Water in the Desert by Means of Electromagnetic Interference Fringes*

M. A. H. EL-SAID†, SENIOR MEMBER, IRE

Summary—This paper introduces the principles and techniques of underground water prospection in the desert by means of electromagnetic interference fringes.

Part I formulates the "Variable Frequency Interference Method" while Part II deals with the "Variable Distance Interference Method." Samples of interference patterns obtained at two places in the Egyptian deserts are shown. The water table at one of these places is known from actual boring.

Interpretation of the interference patterns and the proposed method of calculation of the water table depend upon a knowledge of the average dielectric constant of the propagational medium to-

gether with a single interference pattern determined by either of the methods in Part I or Part II. A good degree of agreement existed between the derived results and the actual water table.

INTRODUCTION

THE METHOD of electromagnetic interference fringes has long been known and was used in the early measurements for the determination of the height of the ionosphere.¹ It was proposed² to the National Research Council of Egypt for the geophysical prospection of underground water in the Egyptian deserts.

* Original manuscript received by the IRE, January 14, 1955; revised manuscript received, July 18, 1955.

† Assistant Professor of Radio Engineering, Faculty of Engineering, Cairo University, Egypt.

¹ E. V. Appleton and M. A. S. Barnett, *Nature*, vol. 115, p. 333; 1925.

² See Acknowledgments.

The method consists principally of diffusing electromagnetic energy into the underground medium and the surface by means of a continuous wave transmitter having its antenna laid on the ground surface. A suitable radio receiver is placed at a known distance from the transmitter and has its antenna similarly laid on the ground surface for the measurement of field strength. In the presence of an underground reflecting medium such as a water layer, the wave that has traveled into the ground will be reflected back to the surface. The field strength at any point on the surface will therefore be the resultant of at least two components: one caused by the surface wave, and the other by the underground reflected wave. Owing to the fact that the two waves may travel with different velocities but on the same path length, or on different path lengths but with the same velocities, or a combination of both effects, they arrive at the receiver with a phase retardation difference. Choosing conditions such that the two waves are of the same order of intensity, and the frequency at the transmitter is varied slowly through a suitable range, the resultant field strength will undergo maxima and minima at a regular period as shown in Fig. 1(a). Also, if the transmitter frequency is kept fixed while the distance from the transmitter is varied over a suitable range, the resultant field strength at the moving receiver will diminish with increasing distance but will also undergo maxima and minima as shown in Fig. 1(b). In both cases, the maxima and minima will always be present and correspond to the two waves becoming in-phase and out-of-phase. The only question is the useful operating range which makes the two waves of the same order of magnitude, enabling easier detection of interference fringes. These fringes are hereby utilized first, to indicate existence of an underground water layer; and second, to determine its depth from ground surface.

THE VARIABLE FREQUENCY METHOD

Referring to Fig. 1(c), let *T* be a transmitter and *R* a receiver, both situated on the ground at a distance *d* apart. Also, let there be an underground water layer at a depth *h* from the surface. Assuming that:

1. The receiver and the underground water layer are both in the so-called "far zone" of the transmitter.
2. The ratio of the intensities of the surface wave to the underground reflected wave is independent of frequency over some applicable frequency range.
3. The underground medium is homogeneous and the dielectric constant the same throughout.
4. The angle of incidence is greater than the angle of total reflection for various rock couples so that partial reflections from any layer other than the desired one are largely suppressed.
5. The underground water surface acts as a perfect reflector and the path length is independent of frequency over some applicable frequency range.
6. There are no multiple reflections; i.e., more than one hop.

Considering Fig. 1(c), and noting that the underground reflected ray undergoes a 180-degree phase shift

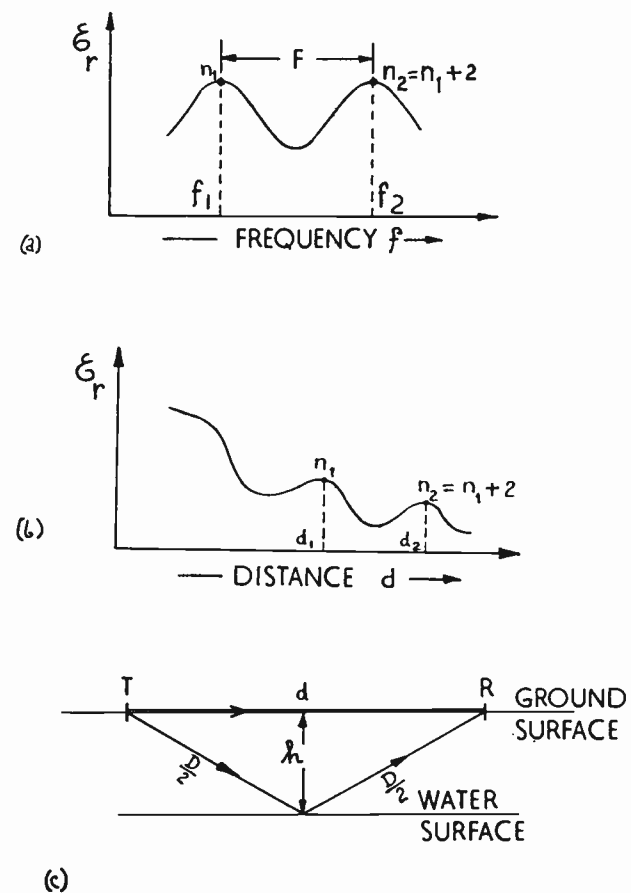


Fig. 1—Simplified interference patterns: (a) field strength vs frequency; (b) field strength vs distance; (c) dimensions in the plane of incidence.

at reflecting surface, interference fringes are given:

$$\frac{D}{v_g} - \frac{d}{v_s} = \frac{n}{2f} \quad (1)$$

where

$$\begin{aligned} n &= 0, 2, 4, \dots, \text{for minima} \\ &= 1, 3, 5, \dots, \text{for maxima.} \end{aligned}$$

D = $\sqrt{d^2 + 4h^2}$ is the distance traveled by the underground wave

v_g = the velocity of the underground wave
 $= c/\sqrt{\mu\epsilon} = c/\sqrt{\epsilon}$ for a nonmagnetic medium

c = velocity of light

ϵ = relative dielectric constant of the underground medium

v_s = velocity of surface wave = αc where α is a fraction
 f = the operating frequency of the transmitter.

From Fig. 1(a), when $f = f_1$, $n = n_1$ and when $f = f_2$, we have $n = n_2 = n_1 + 2$. The frequencies f_1 and f_2 are the frequencies for which consecutive maxima (or minima) will occur. Then, using (1) we find that

$$F = f_2 - f_1 = \frac{c}{\left(D\sqrt{\epsilon} - \frac{d}{\alpha}\right)} \quad (2)$$

where *F* has the dimension of frequency and is called *delay frequency*.

Eq. (2) shows that *F* depends only on the geometry and dielectric constant and is independent of frequency

in as much as ϵ , D , and α are independent of it. Eq. (2) may also be rewritten as:

$$D = \frac{1}{\sqrt{\epsilon}} \left(\frac{c}{F} + \frac{d}{\alpha} \right)$$

from which:

$$h = \frac{1}{2} \sqrt{\frac{1}{\epsilon} \left(\frac{c}{F} + \frac{d}{\alpha} \right)^2 - d^2} \quad (3)$$

Eq. (3) shows that in order to determine the depth h , the values of ϵ , F , d and α must be known. The normal procedure is to perform a variable frequency field experiment at an appropriate distance, from which F is obtained. Also, the dielectric constant ϵ is either measured on site³ or estimated from laboratory measurements on the various types of rock samples that are known to form the site. However, although a knowledge of ϵ is essential for determining h , latter is not critically dependent upon it. Value of α may either be assumed from experience or determined by actual measurement on site. But dependence of h on α may be diminished by proper choice of distance d in comparison with h .

For best utilization of the variable frequency field experiment, (2) is further investigated. Values of h are assumed and F is calculated for presumed values of ϵ and α . Fig. 2 shows the $F-d-h$ chart calculated

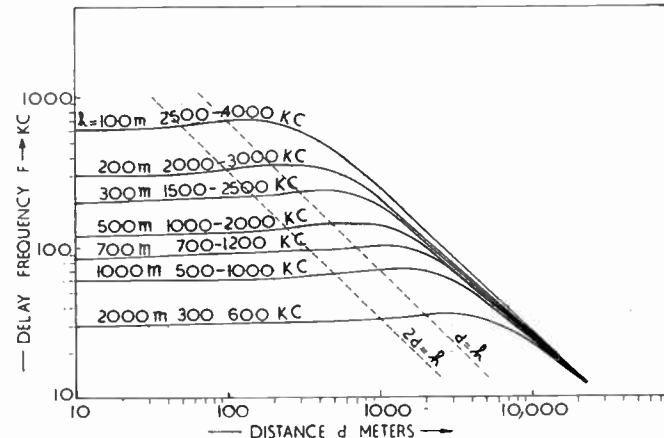


Fig. 2—Calculated chart relating delay frequency, distance and depth for $\sqrt{\epsilon}=2.5$ and $\alpha=0.75$; the appropriate frequency range is indicated.

from (2) for $\sqrt{\epsilon}=2.5$ and $\alpha=0.75$. These curves show that at relatively small distances, the delay frequency is a good identification of depth and becomes reasonably independent of α . On the other hand, at relatively large distances, the curves become asymptotic and F is almost independent of h . This far-distance condition, in which $d \gg h$ is given by:

$$F_0 = \frac{c}{d \left(\sqrt{\epsilon} - \frac{1}{\alpha} \right)} \quad (4)$$

³ The method of measurement of ϵ on site will be dealt with in a separate paper pending more field work.

In general, the choice of the appropriate distance for field tests depends on several factors, the most important of which are:

Far-Zone Condition

In order to apply the simple laws of propagation, both the receiver and the underground reflecting surface must be in the far zone of the transmitter. This implies a condition on the minimum value of the distance d relative to the longest wavelength used in the field test. In the far-zone, the field strength is entirely the radiation component E_0 . However, in the near far-zone the total tangential component of field strength E_θ is the resultant⁴ of three components such that:

$$E_\theta = E_0 (m^2 + Jm - 1)$$

where $m = \lambda / 2\pi d$, from which:

$$|E_\theta| = |E_0| [(m^2 - 1)^2 + m^2]^{1/2} = |E_0| [1 - m^2 + m^4]^{1/2}$$

If the distance d is so chosen that $m \ll 1$, then:

$$|E_\theta| \cong |E_0| (1 - \frac{1}{2}m^2) \quad (5)$$

Considering the surface ray, the value of λ to be used in (5) should be replaced by the surface wavelength $\lambda_s = \alpha \lambda_{air}$, and if the minimum distance is greater than half the longest surface wavelength, then the total tangential component is less than 5 per cent smaller than the radiation component. Similarly, for the underground reflected ray, a small discrepancy occurs if the depth h is greater than the longest surface wavelength.

Refraction and Total Reflection

In order to ensure the minimum amount of refraction and to avoid total reflection from the various underground strata, the incidence of the underground wave should be as near to normal as possible. This is satisfied practically if $d < h$.

Received Field Strength

To minimize effects of noise and interfering signals, the received field strength should be as high as possible. This calls for the use of the smallest value of d .

From these considerations, the appropriate distance for field tests is the smallest possible value that falls into the far zone. Thus, the practical relation is:

$$\frac{1}{2} \lambda_{air} \leq d \leq h \quad (6)$$

The appropriate frequency range is indicated on the curves of Fig. 2 for constant depth. Further, the lines $d = h$ and $2d = h$ are shown. The longest wavelength is deliberately made shorter than that obtained from (6) in order to minimize effects of anomalous dispersion.

In general, effects of anomalous dispersion cause resistivity to change with frequency. This causes degree with which weaker ray reinforces or weakens the other ray to vary with frequency; net result being a change in F with frequency. This effect is overcome largely if

⁴ J. G. Brainard, "Ultra High Frequency Techniques," D. Van Nostrand Co., Inc., New York, p. 397.

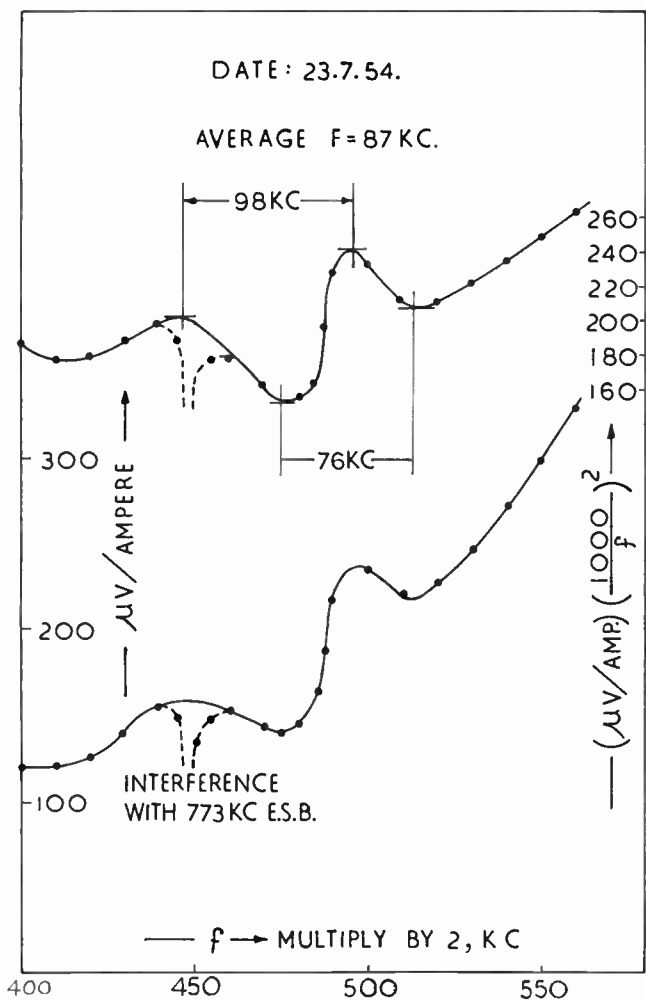


Fig. 3—Observed and transformed frequency-interference patterns at Baharya Road for $d=1,300$ meters.

we choose the frequency range such that F is only a small fraction of lowest frequency. Naturally, shorter wavelengths are reserved for smaller depths.

Further, it is found that with a reasonable value of the transmitted power, the received field strength at the appropriate distance is so small that broadcast transmitters often cause a serious amount of interference. The task of the engineer who performs this type of field test consist of employing a specially-built, highly-selective, self-calibrated field strength set, and of utilizing the vacant points of the frequency spectrum. It is particularly important that the radio frequency stage of the field strength set be so designed as to ensure the least possible amount of tube nonlinearity.

ACTUAL FIELD EXPERIMENTS

The field experiments presented here were made at two places in the Egyptian desert; namely, at Baharya Road, some 20 kilometers from the Pyramids, and at Abu Aweigla, Senai. The experiments at Baharya Road were the first attempt towards obtaining interference patterns which proved the phenomenon. Acquiring the proper style and technique of the field work was the major objective rather than the determination of the

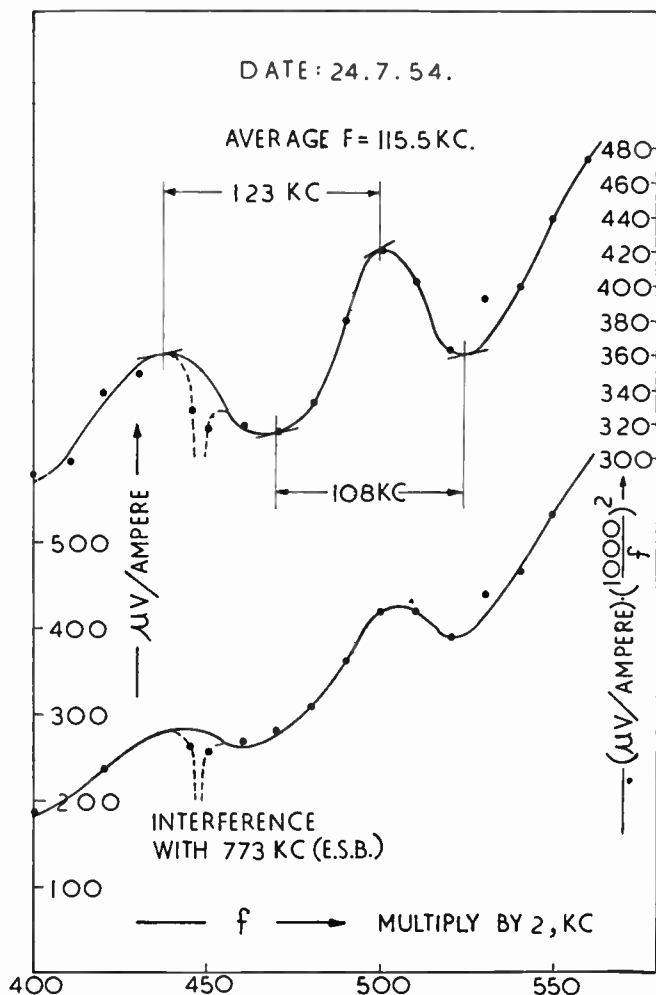


Fig. 4—Observed and transformed frequency-interference patterns at Baharya Road for $d=1,035$ meters.

water table which is unknown there. The experiments made at Abu Aweigla were primarily intended for checking the efficacy of the method for the determination of the water table which is known from a nearby boring. In all the tests, both transmitting and receiving antennas were parallel and perpendicular to the plane of incidence.

Experiments at Baharya Road

Figs. 3 and 4 show observed values of the voltage E_r induced in the receiving antenna at various frequencies at two different distances. The lower curves are calculated in terms of microvolts induced in the receiving antenna per ampere into the center of the transmitting antenna. The general tendency of these curves indicates that E_r increases almost with the square of frequency.

The upper curves are merely the lower ones multiplied by $(1,000/f)^2$. This graphical transformation is made only to enable more accurate determination of the maxima and minima. The curves indicate that the delay frequency is not constant. This illustrates clearly effects of anomalous dispersion. Curves also show serious interference caused by the beating action of the relatively strong field strength of the Egyptian State Broadcast

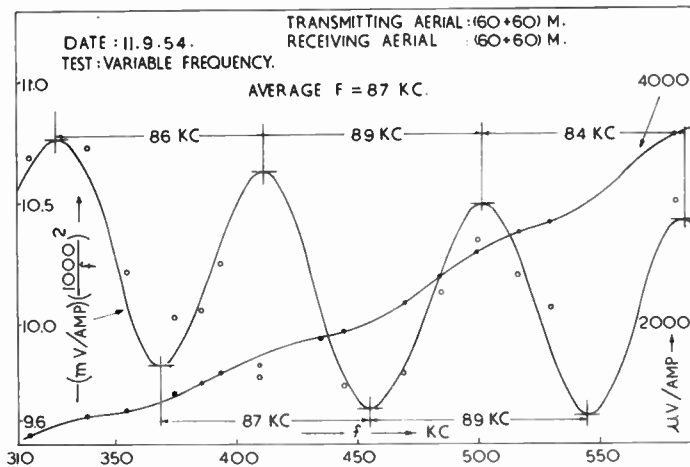


Fig. 5—Observed and transformed frequency-interference patterns at Abu Aweigla for $d=550$ meters.

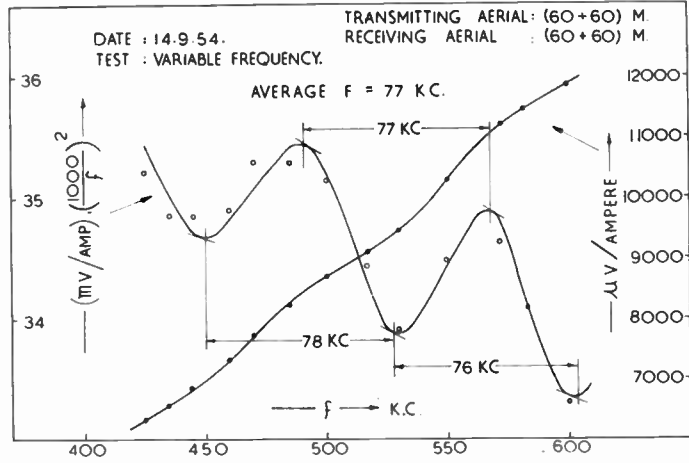


Fig. 6—Observed and transformed frequency-interference patterns at Abu Aweigla for $d=270$ meters.

Station at 773 kc with the local signal. Reduction in the output as a result of beat is due to an inherent characteristic of converter stage of receiving set.

Considering the average value of the delay frequency F , and using the results of measurements $\sqrt{\epsilon_0} = 2.75$ at Baharya Road, and assuming $\alpha = 0.75$ we get:

At $d = 1,035$ meters: observed $F = 115.5$ kc,
calculated $h = 507$ meters.

At $d = 1,300$ meters: observed $F = 87$ kc,
calculated $h = 682$ meters.

Average value of h is 594 meters. This value could not be checked definitely on water table at this place. Further, it is not advisable to depend much on these results because of large difference between two values of h , and because of serious variation of F with frequency. More reliable results could have been obtained with $d = 300$ meters and f ranging from 1,000 to 1,500 kc.

Experiments at Abu Aweigla

Figs. 5 and 6 give the resulting interference patterns. In these tests, the distances chosen were 550 and 270 meters which are small compared to the expected depth of the water layer. Further, the smaller of these distances is just about half the longest wavelength. It is interesting to note the constancy of the observed delay frequency and the relatively strong field strength. These conditions are favorable for field work.

Using the results of measurements of $\sqrt{\epsilon_0} = 2.38$ and with $\alpha = 0.75$, we get:

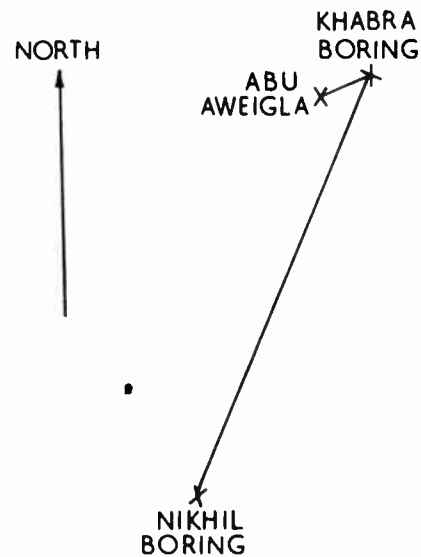
At $d = 550$ meters: observed $F = 87$ kc,
calculated $h = 835$ meters.

At $d = 270$ meters: observed $F = 77$ kc,
calculated $h = 885$ meters.

Average is $h = 861$ meters. This result agrees with water table borings made by Standard Oil Company at Khabra and Nikhil. Trusted reports of these borings gave depth at which water was first observed as follows:

Khabra Boring: 2,594 ft. or 790 meters
Nikhil Boring: 2,872 ft. or 875 meters

The test place at Abu Aweigla is indicated on the drawing of Fig. 7 relative to Khabra and Nikhil borings.



DATA:

KHABRA BORING: $h = 790$ m, 192 m. ABOVE S.L.

NIKHIL BORING: $h = 875$ " 206 " "

ABU AWEIGLA: $h = 861$ " 125 " "

SCALE: 1 Cm. = 10 KILOMETERS.

Fig. 7—Position of Abu Aweigla relative to Khabra and Nikhil borings.

THE VARIABLE DISTANCE INTERFERENCE METHOD

Referring to Fig. 1(c), the transmitter T is fixed while the receiver R is moved, the distance d being varied while the frequency f is constant. In addition to the assumptions made in the previous section, the variable distance method assumes no change in the surface levels or the water level throughout the test area. Under these conditions, the interference fringes are given by (1).

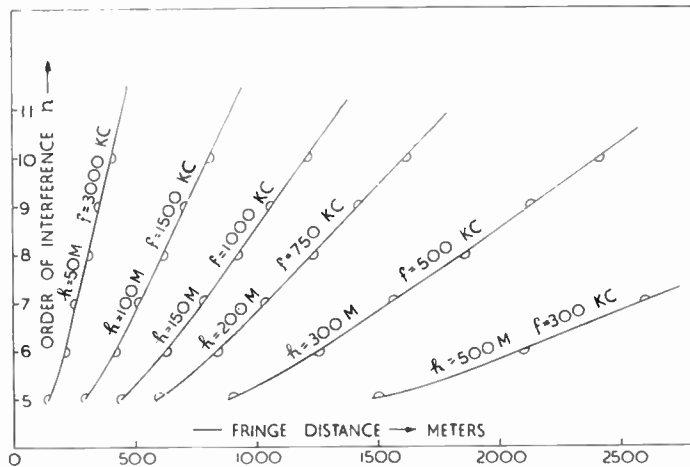


Fig. 8—Calculated chart relating fringe distance and depth for $\sqrt{\epsilon} = 2.5$ and $\alpha = 0.75$; the appropriate frequency range is indicated.

From Fig. 1(b) when $d = d_1$, $n = n_1$ and when $d = d_2$, we have $n = n_2 = n_1 + 2$. The distances d_1 and d_2 are the distances for which consecutive maxima (or minima) will occur. Then, using (1), we find that:

$$h = \frac{1}{4A} \sqrt{(B - 2d_1d_2)(B + 2d_1d_2)} \quad (7)$$

where

$$A = \frac{1}{\sqrt{\epsilon}} \left[\frac{c}{f} + \frac{1}{\alpha} (d_2 - d_1) \right] \quad (8)$$

$$B = d_2^2 + d_1^2 - A^2 \quad (9)$$

If in Fig. 1(b), d_1 and d_2 are any two points of successive maxima and minima, (7) would still hold but:

$$A = \frac{1}{\sqrt{\epsilon}} \left[\frac{c}{2f} + \frac{1}{\alpha} (d_2 - d_1) \right]. \quad (10)$$

For best utilization of a variable distance field experiment, (1) is further investigated by assuming the order of interference n and calculating the distance d at which maxima or minima occur for a given value of h . Values of $\sqrt{\epsilon}$, α and the appropriate frequency are presumed. Fig. 8 shows fringe distances vs n , for given values of h . These curves are calculated from the relation:

$$d = nh \left[0.3 + \sqrt{\left(0.314 - \frac{5.6}{n^2} \right)} \right] \quad (11)$$

which is derived from (1), for $\sqrt{\epsilon} = 2.5$, $\alpha = 0.75$, and $h = \frac{1}{2}\lambda$ air (see (6)). These curves show that the separation between any two consecutive maxima or minima decreases rapidly as the order of interference is increased until the separation becomes almost constant when $d \gg h$. This far distance condition is given by:

$$(d_2 - d_1) = \frac{c}{f \left(\sqrt{\epsilon} - \frac{1}{\alpha} \right)} = d_0. \quad (12)$$

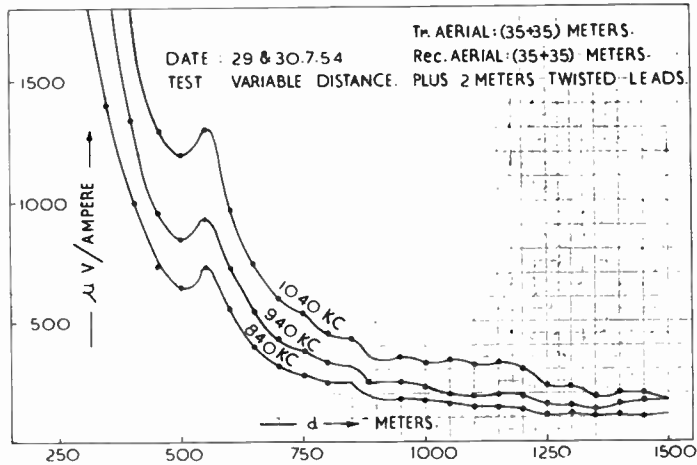


Fig. 9—Observed distance-interference patterns at Baharya Road for the frequencies 840, 940 and 1,040 kc.

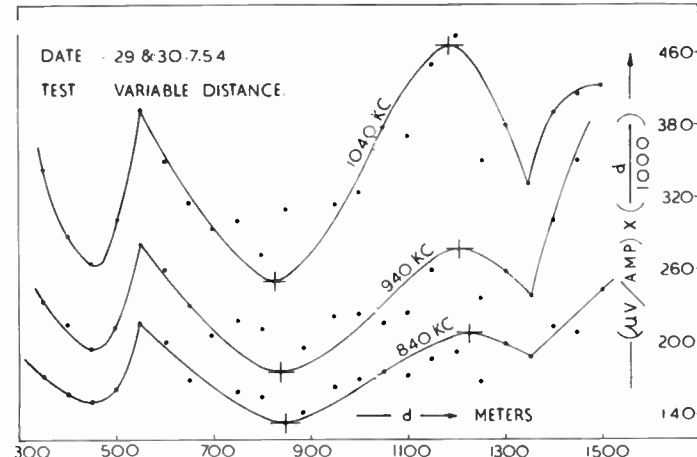


Fig. 10—Transformed patterns of Fig. 9.

In general, although the transmitting antenna is laid on the ground surface, a relatively strong vertical component of the electric field has been observed at the receiver. This makes the variable distance method sensitive to small changes in the antenna orientation in the vertical plane. With rough ground the measurement of the electric field is therefore subject to errors. The best utilization of this method is obtained only in fairly level ground for depths less than 500 meters. Greater depths require large fringe distances and these suggest many field problems.

ACTUAL FIELD EXPERIMENTS

Figs. 9 and 10 show interference patterns obtained at Baharya Road. The curves of Fig. 9 express the received microvolts per ampere at three fixed transmitter frequencies; namely, 840, 940, and 1,040 kilocycles. The general tendency of the curves indicates that the induced voltage decreases inversely with the square of the distance. The curves of Fig. 10 are those of Fig. 9 transformed to $(d/1000)^2$ for accurate graphical determination of the maxima and minima.

The curves of Fig. 10 illustrate the errors produced by variations in the antenna orientations in the vertical plane as the receiver is moved from place to place. This effect is most pronounced at distances from 700 to 1,000 meters where the ground surface was rough. The curves also illustrate discontinuities at distances less than 550 meters and greater than 1,350 meters. This indicates a change in the kind of underground material at these places.

Apart from the above illustrations, the smoothed curves of Fig. 10 show definite maxima and minima from which the depth h is calculated. Using the results of measurements $\sqrt{\epsilon_0} = 2.75$, and using (7), (8), and (9), with $\alpha = 0.75$, the following is obtained:

When

$$f = 1,040 \text{ kc}, d_1 = 830 \text{ meters}, d_2 = 1,185 \text{ meters}, A = 224, \\ B = 204 \times 10^4, \text{ from which } h = 591 \text{ meters.}$$

When

$$f = 940 \text{ kc}, d_1 = 840 \text{ meters}, d_2 = 1,205 \text{ meters}, A = 235, \\ B = 210.1 \times 10^4, \text{ from which } h = 600 \text{ meters}$$

When

$$f = 840 \text{ kc}, d_1 = 850 \text{ meters}, d_2 = 1,225 \text{ meters}, A = 246, \\ B = 216.14 \times 10^4, \text{ from which } h = 582 \text{ meters.}$$

The average value is $h = 591$ meters..

Altitude measurements at Baharya Road gave the barometer reading at Cairo University = 997.8 millibars; barometer reading at receiver site at Baharya Road = 981.7 millibars. Difference = 16.1 millibars, which is equivalent to a difference in level of $16.1 \times 8.38 = 135$ meters. Adding 10 meters from Nile Level, the height of the test point at Baharya Road is 145 meters above Nile Level during the month of July. These results suggest that the water table at this test point is independent of the Nile water. The results, however, agree with those obtained by the variable frequency method mentioned in the previous section.

A NOTE ON THE MODE OF PROPAGATION

The antenna is perhaps the most important part of this system, due to its complicated behavior and lack of rigorous solution for the resulting mode of propagation.

When the antenna is placed on the ground surface, the latter will act as a lossy dielectric because of the presence of conductivity. This conductivity is also inhomogeneous, being relatively greater at the surface layer than at the bottom layers. This is because of the continuous exposure of the surface layer to the ever-changing climatic conditions. The extra conductivity of the surface layer causes relatively strong surface conduction currents to flow in the vicinity of the antenna and will produce the following effects:

1. It will absorb energy, thus reflecting a resistive component into the driving point impedance.

2. It will produce a field which opposes the original field of the antenna, and thus reduces the radiation component and radiation resistance.

3. The reduction in the antenna field in its vicinity will also be accompanied by a change in the reactive component of the driving point impedance. This change, however, may be assumed small in a first order approximation, because most of the energy stored is close to the antenna conductor.

Thus the general effect of the presence of ground surface conductivity is an apparent screening of the power input to the antenna which is thus mainly absorbed instead of being radiated into the appropriate propagation media. However, in this manner, it might appear that the power radiated in air is many times that radiated in the underground medium. Fortunately, the antenna is a more efficient radiator of energy underground than in air by virtue of its relative electrical length in each medium.

In general, the effect of the presence of the extra ground surface conductivity may be reached by assuming an appropriately dimensioned, situated, and resistively loaded image. Owing to the antenna being placed on the boundary, the antenna and its image are almost coincident. Since the image is essentially negative in this case the resulting reduction in the electric field at any point on the ground surface is almost, but not exactly, a complete cancellation. This, perhaps, accounts for the weak field which is observed on the ground surface at all points of reception.

The equipment employed in the field measurements consists of a mobile transmitter and a field strength measuring set with its calibrating signal generator. Both the transmitter and the field strength set are of standard construction but special modifications were made locally in the antenna circuits. The tank circuit of the final power amplifier in the transmitter is coupled to the dipole antenna by means of a carefully balanced transformer in which the degree of balance is controlled and indicated. Similarly, the receiving dipole antenna is coupled to the field strength set by means of a balancing unit and a suitable switching arrangement which enables easy comparison of the antenna-induced emf with the calibrated output of the associated signal generator.

ACKNOWLEDGMENT

Entrusted by the National Research Council of Egypt, the author carried out the work which is the subject matter of this paper at the Electronics Laboratory, Faculty of Engineering, Cairo University, to which he extends his thanks. The field work was made possible with the kind facilities extended by the Quartermaster General, Egyptian Army.

The author wishes also to acknowledge the early work by Dr. H. Löwy under the supervision of Professor H. M. Mahmoud, Professor of electrical engineering, Cairo University, for the determination of the degree of transparency of desert rocks to electromagnetic waves.

A Transmission Line Taper of Improved Design*

R. W. KLOPFENSTEIN†

Summary—The theory of the design of optimal cascaded transformer arrangements can be extended to the design of continuous transmission-line tapers. Convenient relationships have been obtained from which the characteristic impedance contour for an optimal transmission-line taper can be found.

The performance of the Dolph-Tchebycheff transmission-line taper treated here is optimum in the sense that it has minimum reflection coefficient magnitude in the pass band for a specified length of taper, and, likewise, for a specified maximum magnitude reflection coefficient in the pass band, the Dolph-Tchebycheff taper has minimum length.

A sample design has been carried out for the purposes of illustration, and its performance has been compared with that of other tapers. In addition, a table of values of a transcendental function used in the design of these tapers is given.

INTRODUCTION

THE ANALYSIS of nonuniform transmission lines has been a subject of interest for a considerable period of time. One of the uses for such nonuniform lines is in the matching of unequal resistances over a broadband of frequencies. It has recently been shown that the theory of Fourier transforms is applicable to the design of transmission-line tapers.¹ It is the purpose of this paper to present a transmission-line taper design of improved characteristics. The performance of this taper is optimum in the sense that for a given taper length the input reflection coefficient has minimum magnitude throughout the pass band, and for a specified tolerance of the reflection coefficient magnitude the taper has minimum length.

For any transmission line system the applicable equations are

$$\begin{aligned} \frac{dV}{dx} &= -ZI \\ \frac{dI}{dx} &= -YV, \end{aligned} \quad (1)$$

where

- V = the voltage across the transmission line,
- I = the current in the transmission line,
- Z = the series impedance per unit length of line,
- and
- Y = the shunt admittance per unit length of line.

Fig. 1 illustrates the configuration to which the above equations are to be applied.

For nonuniform lines, the quantities Z and Y are known nonconstant functions of position along the line, and the properties of the system are determined through a solution of (1) along with the pertinent boundary

conditions. Through use of the waveguide formalism² (1) is applicable to uniconductor waveguide as well as to transmission line. Strictly speaking, of course, (1) is not precisely applicable to any system since it accounts for the propagation of a single mode only. It furnishes an excellent description, however, as long as all modes but dominant mode are well below cutoff.

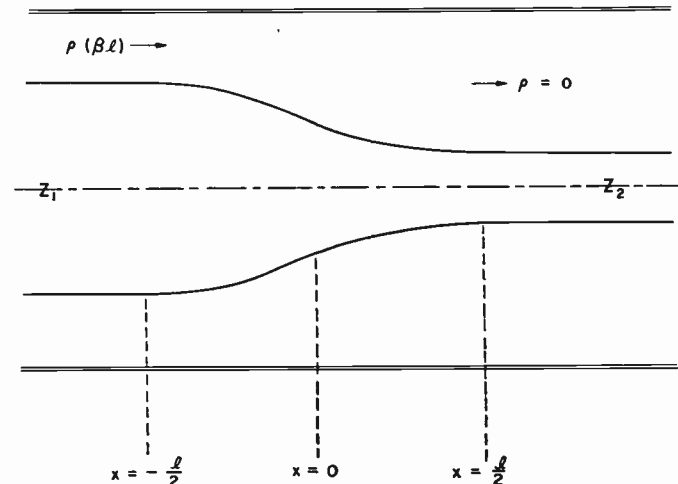


Fig. 1—Tapered transmission-line matching section.

Eq. (1) can be recast in a more directly useful form through the introduction of the quantities

$\gamma = \sqrt{ZY}$ = the propagation constant of the line,

$Z_0 = \sqrt{Z/Y}$ = the characteristic impedance of the line,

and

$$\rho = \frac{V/I - Z_0}{V/I + Z_0} = \text{the reflection coefficient at any point along the line.} \quad (2)$$

These lead to first order nonlinear differential equation³

$$\frac{d\rho}{dx} - 2\gamma\rho + \frac{1}{2}(1 - \rho^2)\frac{d(\ln Z_0)}{dx} = 0. \quad (3)$$

This equation has the advantage that it is in terms of the quantity of direct interest in impedance matching problems. Likewise, a very natural approximation for impedance matching purposes can be made directly in this equation. If it is assumed that $\rho^2 \ll 1$, (3) becomes

$$\frac{d\rho}{dx} - 2\gamma\rho + F(x) = 0,$$

* Original manuscript received by the IRE, June 9, 1955.
† RCA Labs., Princeton, N. J.

¹ F. Bolinder, "Fourier transforms in the theory of inhomogeneous transmission lines," PROC. IRE, vol. 38, p. 1354; November, 1950.

² N. Marcuvitz, "Waveguide Handbook," McGraw-Hill Book Co., Inc., New York, N. Y., ch. 1, p. 7; 1951.

³ L. R. Walker and N. Wax, "Nonuniform transmission lines and reflection coefficients," Jour. Appl. Phys., vol. 17, pp. 1043-1045; December, 1946.

where

$$F(x) = \frac{1}{2} \frac{d(\ln Z_0)}{dx}, \quad (4)$$

which is a first-order linear differential equation in ρ .

SOLUTION OF THE DIFFERENTIAL EQUATION

A solution of the differential equation (4) is sought which satisfies the boundary condition $\rho=0$ at $x=l/2$. An integrating factor for this equation is

$$G(x) = \exp \left[-2 \int_a^x \gamma d\xi \right], \quad (5)$$

where the lower limit of the integral is arbitrary. Applying this to (4) it is found that the solution satisfying the boundary condition is given by⁴

$$\rho(x) = \int_x^{l/2} F(z) \exp \left[-2 \int_z^{l/2} \gamma(\xi) d\xi \right] dz, \quad (6)$$

and, hence, the input reflection coefficient is

$$\rho = \int_{-l/2}^{l/2} F(z) \exp \left[-2 \int_{-l/2}^z \gamma(\xi) d\xi \right] dz. \quad (7)$$

The solution given above is subject only to the restriction that the reflection coefficient is relatively small. It is equally applicable to lossless transmission line, lossy transmission line, and waveguide tapers. The physical interpretation of the solution as given is evident. The incremental reflection at each cross section is given by $F(z)$, and the exponential term expresses the total delay and attenuation of this reflected component at the input of the tapered section relative to incident input wave.

OPTIMAL DESIGN OF TRANSMISSION-LINE TAPERS

An important special case of the general situation considered above is the lossless transmission-line taper as illustrated in Fig. 1. In this case, the characteristic impedance is a real number and is independent of frequency. The wave propagated in the line is essentially TEM in character, and the propagation constant is purely imaginary and proportional to the frequency.

Under these conditions the interior integration of (7) can be carried out, and the input reflection coefficient becomes

$$\rho \exp(j\beta l) = \int_{-l/2}^{l/2} F(z) \exp(-j2\beta z) dz. \quad (8)$$

This relationship can be inverted through the theory of Fourier transforms to obtain

$$F(x) = \frac{1}{\pi} \int_{-\infty}^{\infty} [\rho \exp(j\beta l)] \exp(j2\beta x) d\beta. \quad (9)$$

The analogy between the present problem and the synthesis of radiation patterns from line sources is evident.

⁴ L. R. Ford, "Differential Equations," McGraw-Hill Book Co., Inc., New York, N. Y., ch. 2, pp. 36-39; 1933.

In each case, the quantities of interest are related through the Fourier transform.

In the use of (9) the reflection coefficient is specified so that its value at negative frequencies is equal to the complex conjugate of its value at the corresponding positive frequencies. This is necessary in order that the specified reflection coefficient shall correspond to a physically realizable structure.⁵ This requirement then insures that the transform will be completely real as it must be in order that $F(x)$ have significance in terms of a transmission-line taper.

Collin has recently shown that optimum performance is obtained from a cascaded transformer structure when the power loss ratio is expressed in terms of the Tchebycheff polynomial of degree equal to the number of sections.⁶ This is equivalent to having the input reflection coefficient proportional to the Tchebycheff polynomial of the same degree, when its square is small relative to one [an assumption already made in the derivation of transform pair (8) and (9)].

By allowing the number of sections to increase indefinitely for a fixed over-all length, the results of Collin can be extended to the case of a continuous transmission-line taper. In the case of a cascaded transformer arrangement, a secondary maximum in the reflection coefficient magnitude occurs at the first and at all succeeding frequencies where the individual section lengths become equal to a multiple of a half-wavelength. As the number of sections is allowed to increase without limit for a fixed over-all length, the frequency at which this first secondary maximum occurs also increases without limit so that the pass band consists of all frequencies beyond that for which the reflection coefficient first comes within the specified tolerance.

For maximum bandwidth with a fixed maximum magnitude of reflection coefficient then, input reflection coefficient for a continuous taper takes form

$$\rho \exp(j\beta l) = \rho_0 \frac{\cos[\sqrt{(\beta l)^2 - A^2}]}{\cosh(A)}, \quad (10)$$

which is the limiting form of the Tchebycheff polynomial as its degree increases without limit.⁷ The specification of the parameter A determines the maximum magnitude of reflection coefficient in the pass band which consists of all frequencies such that $\beta l \geq A$. The reflection coefficient magnitude takes on its maximum value $|\rho_0|$ at zero frequency, and it oscillates in the pass band with constant amplitude equal to $\rho_0/\cosh(A)$. A plot of the function given by (10) is shown in Fig. 2 for a number of different values of A .

The inversion of the above specified reflection coefficient through (9) yields⁷

⁵ H. W. Bode, "Network Analysis and Feedback Amplifier Design," D. Van Nostrand Co., Inc., New York, N. Y., ch. 7, p. 106; 1945.

⁶ R. E. Collin, "Theory and design of wide-band multisection quarter-wave transformers," Proc. IRE, vol. 43, pp. 179-185; February, 1955.

⁷ T. T. Taylor, "Dolph arrays of many elements," Tech. Memo. No. 320, Hughes Aircraft Co., Culver City, Calif.; August 18, 1953.

$$\begin{aligned}
 F(x) = & \frac{\rho_0}{\cosh(A)} \left\{ \frac{A^2}{l} \frac{I_1[A\sqrt{1-(2x/l)^2}]}{A\sqrt{1-(2x/l)^2}} \right. \\
 & + \frac{1}{2} \left[\delta\left(x - \frac{l}{2}\right) + \delta\left(x + \frac{l}{2}\right) \right] \left. \right\}, \\
 & |x| \leq l/2, \\
 = & 0, \quad |x| > l/2, \quad (11)
 \end{aligned}$$

where I_1 is the first kind of modified Bessel function of the first order, and δ is the unit impulse function.

The variation of characteristic impedance along the taper can be found by direct integration of $F(x)$, and it is given by

$$\begin{aligned}
 \ln(Z_0) = & \frac{1}{2} \ln(Z_1 Z_2) + \frac{\rho_0}{\cosh(A)} \left\{ A^2 \phi(2x/l, A) \right. \\
 & + U\left(x - \frac{l}{2}\right) + U\left(x + \frac{l}{2}\right) \left. \right\}, \\
 & |x| \leq l/2, \\
 = & \ln(Z_2), \quad x > l/2, \\
 = & \ln(Z_1), \quad x < -l/2. \quad (12)
 \end{aligned}$$

U is the unit step function defined by,

$$\begin{aligned}
 U(z) &= 0, \quad z < 0, \\
 U(z) &= 1, \quad z \geq 0, \quad (13)
 \end{aligned}$$

and ϕ is defined by

$$\phi(z, A) = -\phi(-z, A) = \int_0^z \frac{I_1(A\sqrt{1-y^2})}{A\sqrt{1-y^2}} dy, \quad |z| \leq 1. \quad (14)$$

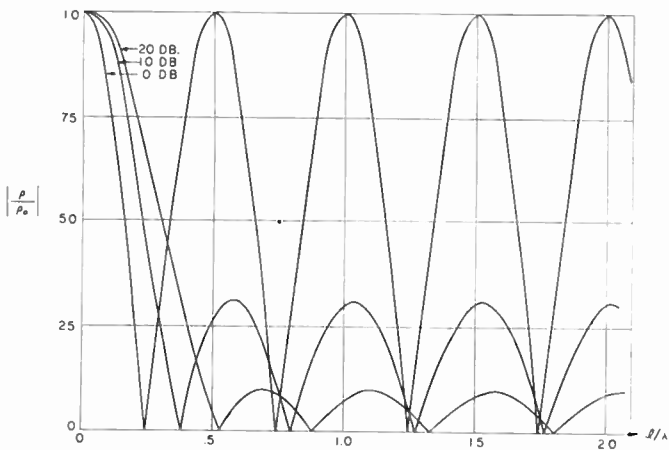


Fig. 2—Response of Dolph-Tchebycheff transmission-line tapers.

Eq. (12) furnishes the information required for the design of a Dolph-Tchebycheff tapered transition. The quantity ρ_0 is determined by the two impedances Z_1 and Z_2 which are to be matched, and A is selected on the basis of the allowed maximum reflection coefficient magnitude in the pass band. One of the interesting aspects of this design is that the taper has a discontinuous change of characteristic impedance at each end as well as a continuous change along the length of the taper. It is interesting to note that when the tolerated reflection

coefficient approaches the initial reflection coefficient ρ_0 , the parameter A approaches zero, and the bandwidth comprises all frequencies from zero to infinity. In this case, the Dolph-Tchebycheff taper design degenerates into the usual quarter-wavelength transformer design with a discontinuous change of characteristic impedance at each end and a constant characteristic impedance at intermediate points.

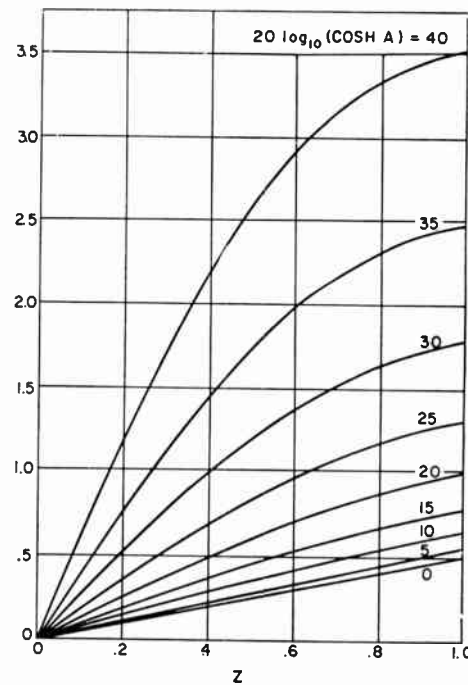


Fig. 3—Plot of the function $\phi(z, A)$.

The function $\phi(z, A)$ is not expressible in closed form except for special values of the parameters. Therefore, this function has been computed through standard integration formulas on an IBM CPC digital computer for a suitable range of values of the parameters. Tabulated values of $\phi(z, A)$ are given to six decimal places in Table I, p. 34, and the function is shown in Fig. 3. The special closed-form relationships

$$\begin{aligned}
 \phi(0, A) &= 0, \\
 \phi(z, 0) &= z/2,
 \end{aligned}$$

and

$$\phi(1, A) = \frac{\cosh(A) - 1}{A^2}, \quad (15)$$

are obtained for the end points of the parameter ranges.

One more comment should be made in regard to the application of the preceding design procedure. If one uses the natural value

$$\rho_0 = \frac{Z_2 - Z_1}{Z_2 + Z_1}, \quad (16)$$

in entering the equation (12), it will be found that the designed taper does not quite fit the final impedances

TABLE I
VALUES OF THE FUNCTION $\phi(z, A)$ FOR $z=0(0.05)1.00$ AND $20 \log_{10}(\cosh A)=0(5)40$

z	$\phi(z, A)$									
	20 $\log_{10}(\cosh A)$									
0	5	10	15	20	25	30	35	40		
0.00	0.000000	0.000000	0.000000	0.000000	0.000000	0.000000	0.000000	0.000000	0.000000	0.000000
0.05	0.025000	0.029593	0.036848	0.048140	0.065590	0.092539	0.134313	0.199460	0.301772	
0.10	0.050000	0.059161	0.073629	0.096137	0.130902	0.184564	0.267698	0.397268	0.600625	
0.15	0.075000	0.088681	0.110276	0.143848	0.195661	0.275567	0.399242	0.591802	0.893707	
0.20	0.100000	0.118128	0.146721	0.191132	0.259597	0.365055	0.528062	0.781511	1.178306	
0.25	0.125000	0.147479	0.182899	0.237850	0.322448	0.452552	0.653321	0.964936	1.451913	
0.30	0.150000	0.176708	0.218746	0.283869	0.383962	0.537610	0.774237	1.140744	1.712272	
0.35	0.175000	0.205794	0.254197	0.329059	0.443899	0.619809	0.890101	1.307751	1.957437	
0.40	0.200000	0.234711	0.289191	0.373296	0.502035	0.698767	1.000282	1.464942	2.185803	
0.45	0.225000	0.263438	0.323667	0.416460	0.558163	0.774142	1.104238	1.611487	2.396134	
0.50	0.250000	0.291950	0.357568	0.458441	0.612094	0.845635	1.201523	1.746753	2.587582	
0.55	0.275000	0.320226	0.390837	0.499134	0.663658	0.912994	1.291792	1.870306	2.759684	
0.60	0.300000	0.348244	0.423420	0.538444	0.712709	0.976019	1.374800	1.981918	2.912359	
0.65	0.325000	0.375982	0.455266	0.576284	0.759120	1.034555	1.450409	2.081555	3.045886	
0.70	0.350000	0.403418	0.486328	0.612574	0.802790	1.088504	1.518582	2.169376	3.160875	
0.75	0.375000	0.430533	0.516559	0.647248	0.843641	1.137814	1.579377	2.245710	3.258228	
0.80	0.400000	0.457305	0.545918	0.680245	0.881619	1.182484	1.632947	2.311049	3.339098	
0.85	0.425000	0.483716	0.574365	0.711518	0.916692	1.222564	1.679531	2.366019	3.404835	
0.90	0.450000	0.509746	0.601865	0.741027	0.948855	1.258145	1.719443	2.411361	3.456938	
0.95	0.475000	0.535377	0.628386	0.768745	0.978123	1.289363	1.753065	2.447905	3.497000	
1.00	0.500000	0.560591	0.653899	0.794653	1.004533	1.316391	1.780835	2.476547	3.526658	

Z_2 and Z_1 at the end points. This fact is an evidence of the approximation $\rho^2 \ll 1$ which was made at the outset in differential equation (4). Discrepancy becomes larger as value of magnitude of ρ_0 increases. This design inconvenience can be eliminated, however, by taking

$$\rho_0 = \frac{1}{2} \ln (Z_2/Z_1), \quad (17)$$

as the initial value of the reflection coefficient instead of the true value of (16). The two expressions are identical to a second order of approximation for small differences between Z_2 and Z_1 , and the use of the second expression will yield a taper design which exactly fits its end-point impedances for all values of Z_2 and Z_1 . The effect of the approximation $\rho^2 \ll 1$ will then be evidenced by a slight deviation from the performance given by (10) in the low-frequency range outside the pass band.

COAXIAL TRANSMISSION-LINE TAPER FROM 50 TO 75 OHMS

As an application of the preceding results, the design of an optimal 50-75 ohm coaxial transmission line taper will be indicated in detail. The taper is to be designed so that the input reflection coefficient magnitude does not exceed about one per cent in the pass band.

The initial value of the reflection coefficient in this case is equal to 0.2. The value of ρ_0 for use in the design of the taper is found from (17) to be

$$\rho_0 = \frac{1}{2} \ln(1.5) = 0.20274. \quad (18)$$

As observed previously, this value does not differ markedly from the zero frequency reflection coefficient.

It will be required that the maximum reflection coefficient magnitude in the pass band shall not exceed one-twentieth of ρ_0 . Thus, from (10)

$$\cosh (.1) = 20,$$

so that

$$.1 = 3.6887. \quad (19)$$

The characteristic impedance contour can now be obtained directly from (12). The resulting Z_0 curve is illustrated in Fig. 4, and the corresponding coaxial line-conductor contour is shown in Fig. 5.

Characteristic impedance has a discontinuous jump from 50 to 50.52 ohms at left-hand end and a corresponding jump from 74.24 to 75 ohms at right-hand end. Characteristic impedance at center of taper is equal to 61.24 ohms, geometric mean between 50 and 75 ohms.

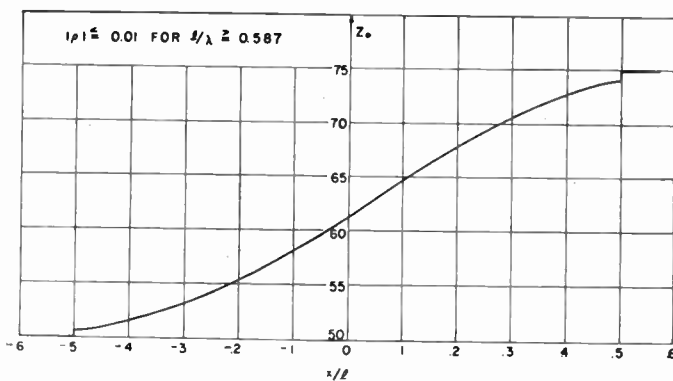


Fig. 4—50-75 ohm Dolph-Tchebycheff tapered transition.

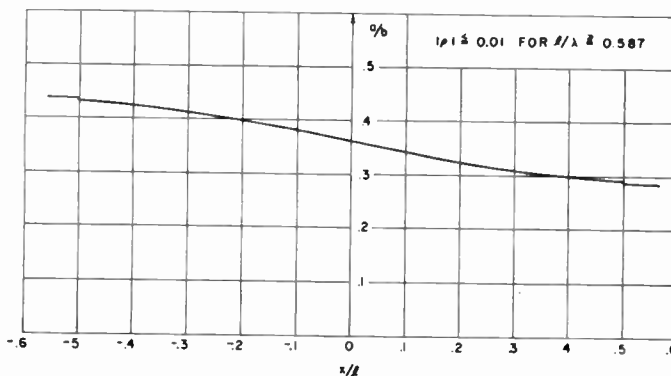


Fig. 5—Inner conductor contour for 50-75 ohm Dolph-Tchebycheff coaxial-line transition.

The performance of this taper is plotted in Fig. 6. The pass band consists of all frequencies greater than that for which $\beta l = 0.587$. For comparison, the performance of an exponential taper⁸ and a hyperbolic taper⁹ has been indicated on the same curve.

⁸ C. R. Burrows, "The exponential transmission line," *Bell Sys. Tech. Jour.*, vol. 17, pp. 555-573; October, 1938.

⁹ H. J. Scott, "The hyperbolic transmission line as a matching section," *Proc. IRE*, vol. 41, pp. 1654-1657; November, 1953.

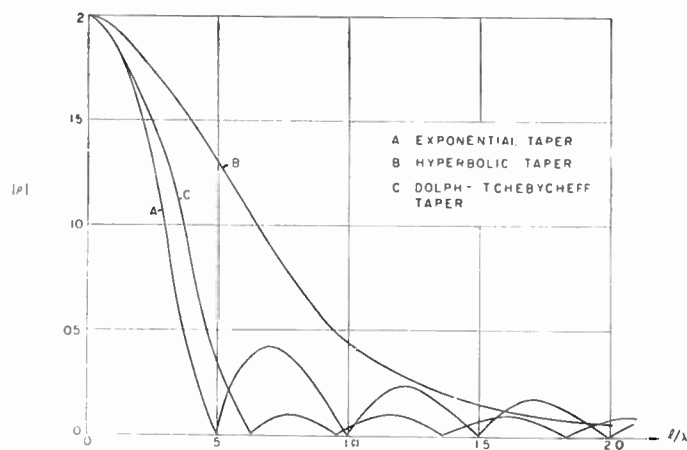


Fig. 6—Performance of 50-75 ohm Dolph-Tchebycheff tapered transition.

CONCLUSION

The theory of the design of optimal cascaded transformer arrangements can be extended to the design of continuous transmission-line tapers. Convenient relationships have been obtained from which the characteristic impedance contour for an optimal transmission-line taper can be found. Alternatively, this impedance contour can be thought of as the envelope of the pointwise specified characteristic impedance of a discrete cascaded transformer arrangement.

The performance of the Dolph-Tchebycheff transmission-line taper treated here is optimum in the sense that it has minimum reflection coefficient magnitude in the pass band for a specified length of taper, and, likewise, for specified maximum magnitude reflection coefficient in the pass band the Dolph-Tchebycheff taper has minimum length.

A sample design has been carried out for the purposes of illustration, and its performance has been compared with that of other tapers. In addition, a table of values of a transcendental function used in the design of these tapers is given in Table I.

A Precision Resonance Method for Measuring Dielectric Properties of Low-Loss Solid Materials in the Microwave Region*

S. SAITO† AND K. KUROKAWA†

Summary—A precision resonance method for measuring the dielectric properties of low loss solid materials has been developed in our laboratory. The dielectric sample to be measured is shaped into a cylindrical disk and inserted into a cylindrical cavity resonator oscillating in the T_{10} mode. ϵ can be measured from the difference

* Original manuscript received by the IRE, April 2, 1955; revised manuscript received, July 6, 1955.

† Institute of Industrial Science, Univ. of Tokyo, Tokyo, Japan.

between the axial lengths of the cavity tuned to the same frequency with and without the sample, and $\tan \delta$ can be found from the difference between the Q 's of the cavity with and without the sample. By making use of a special marker of a resonance point on an oscilloscope, the measurements accuracy can be improved to yield only 1 per cent error in ϵ and 3 per cent error in $\tan \delta$ for various low-loss samples. Such materials as polystyrol, polyethylene, teflon, and glass for high-frequency use were tested at 4,000 mc, 9,000 mc and 24,000 mc.

INTRODUCTION

THE METHODS which have been used to measure the dielectric properties of solid materials in the microwave region fall into two classes: standing wave methods¹⁻³ and resonance methods. The former is suitable for measuring high or medium-loss materials, while the latter is preferable for low-loss materials.

Many researchers³⁻⁶ have already developed several resonance methods for measuring the dielectric properties of low-loss solid and liquid materials. The authors have extended one of these methods by analyzing a way of eliminating completely all residual losses except for the sample loss, which is the most important and difficult problem for the resonance method. Advantages of this new method compared with the earlier papers are as follows:

1. $\tan \delta$ of sample can be obtained without any ambiguity from (7) or (11), by using the measured Q values of cavity with and without sample, and wall losses of empty cavity. Here, it is necessary to locate exciting and pick-up loops or holes at opposite side (No. 1 region of Fig. 1) from movable plunger plate for sample, in order to eliminate coupling losses of external circuits.

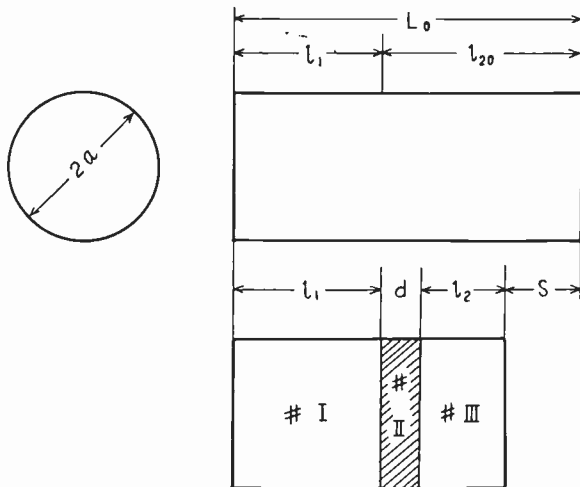


Fig. 1—Dimensions of the cavities with and without the dielectric sample.

2. The accuracy of measurement can be considerably improved by repeating twice measurements at the $\lambda_1/4$ and optimum sample positions as shown in the "typical measuring procedures."

¹ T. W. Dakin and C. N. Works, "Microwave dielectric measurements," *Jour. Appl. Phys.*, vol. 18, pp. 789-796; September, 1947.

² W. H. Surber and G. E. Crough, Jr., "Dielectric measurement methods for solids at microwave frequencies," *Jour. Appl. Phys.*, vol. 19, pp. 1130-1139; December, 1948.

³ C. G. Montgomery, "Technique of Microwave Measurement," McGraw-Hill Book Co., New York, N. Y.; 1947.

⁴ R. L. Sproull and E. G. Linder, "Resonant-cavity measurements," *Proc. IRE*, vol. 34, pp. 305-312; May, 1946.

⁵ F. Horner, T. A. Taylor, R. Dunsmuir, J. Lanib, and W. Jackson, "Resonance methods of dielectric measurement at centimeter wavelengths," *Proc. IEE (London)*, vol. 93, part III, pp. 53-68; January, 1946.

⁶ B. Bleaney, J. H. N. Loubster, and R. P. Penrose, "Cavity resonators for measurements with centimeter electromagnetic waves," *Proc. Phys. Soc. (London)*, vol. 59, pp. 185-199; March, 1947.

3. The accuracy in Q measurements can be improved by making use of a special frequency marker in the measurements of the resonance and half power points. It has been adopted as the standard for measurements of this kind by the Electrical Communication Laboratory of the Japanese Telephone and Telegraph Corporation and is now used widely in Japan.

Since the new precision method of measuring Q employed in this connection is most suitable for measurements involving high values of Q , it is also applicable to measurements of other quantities involving extremely small loss. Measurements of the surface conductivity of metal plates and of the attenuation of waveguide and coaxial line based on the same principle, have been carried out. Their results are briefly described.

PRINCIPLE

Fig. 1 represents a cylindrical cavity resonator which is excited to resonate in the TE_{01} mode. A solid dielectric sample is formed into a cylindrical disk, whose diameter $2a$ is the same as that of the cavity, and is then located perpendicularly to the cylinder axis in a certain position in the cavity. The axial length of the partially filled cavity resonant at a certain frequency is less than that of the cavity resonant at the same frequency without the sample. Let the thickness of the sample be d , and the distances from the surfaces of the sample to the end plates of the cavity be l_1 and l_2 respectively (see Fig. 1). The resonant axial length of the cavity with the sample then is $(l_1 + l_2 + d)$. The resonant axial length of the cavity at the same frequency without the sample is $L_0 = l_1 + l_{20}$, where l_1 and l_{20} are as shown in Fig. 1. Finally, let the difference between the two resonant axial lengths be denoted by shift S . Then the following equation relating these quantities is obtained:

$$\cot \beta_1 l_2 = \cot \beta_1 \{l_{20} - (S + d)\} = \frac{n^2 - n \cot \beta_2 d \cot \beta_1 l_1}{n \cot \beta_2 d + \cot \beta_1 l_1}. \quad (1)$$

Here β_1 , β_2 are the phase constants of the TE_{01} mode in the axial direction in the air and the dielectric sample, respectively, and $n = \beta_2/\beta_1$. The shift S varies with the position of the sample, l_1 , as shown in Fig. 2 and the condition that gives the maximum value of the shift, S_{\max} , is given by

$$\cot \beta_1 l_1 = n \tan \beta_2 d / 2, \quad l_1 = l_2 \pm \nu' / 2\lambda_1 \quad (\text{for } \beta_2 d < \pi). \quad (2)$$

The maximum value S_{\max} satisfies the equation:

$$\cot \beta_1 / 2 (S_{\max} + d) = 1/n \cot \beta_2 d / 2. \quad (3)$$

Defining S_1 and S_2 as the shifts corresponding to $l_1 (= 2\nu' + 1)/4\lambda_1$, and $l_2 = \nu'/2\lambda_1$ respectively, we have

$$\cot \beta_1 (S_1 + d) = 1/n \cot \beta_2 d \quad (4)$$

$$\cot \beta_1 (S_2 + d) = n \cot \beta_2 d. \quad (5)$$

Here ν' is zero or an integer and λ_1 is the guide wavelength in the air-filled guide.

If S is measured corresponding to a certain value of l_1 , β_2 can be calculated from (1), (3), (4) or (5) and the dielectric constant of the sample, ϵ , is given by

$$\epsilon = \frac{\beta_2^2}{(2\pi/\lambda_0)^2} + \left(\frac{\lambda_0}{\lambda_c}\right)^2, \quad (6)$$

where λ_0 is the guide wavelength and λ_c the cut-off wavelength for the TE_{01} mode in the air-filled guide.

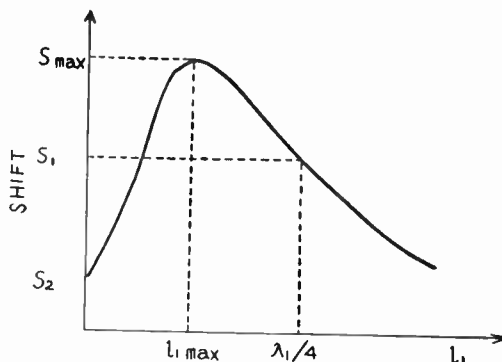


Fig. 2—Relation between the shift and sample position.

$$\Delta = 1.92\sqrt{\lambda_0}A 10^{-5} \frac{2\beta_1^2(R_3^2 - 1) + 2/a(2\pi/\lambda_c)^2 \{(l_1 + l_2R_3^2 + dR_1^2 - L_0) - 1/2\beta_1(1 - 1/n^2)(\sin 2\beta_1l_1 + R_3^2 \sin 2\beta_1l_2)\}}{(2\pi/\lambda_0)^2 \{\epsilon dR_1^2 + \epsilon/2\beta_1(1/n)^2(\sin 2\beta_1l_1 + R_3^2 \sin 2\beta_1l_2)\}}, \quad (13)$$

Next, let us consider the methods for determining $\tan \delta$, the loss tangent of the sample. Associated with cavity measurements there is the frequency variation method and the reactance variation method (or axial length variation method). It is assumed that the cavity in use is of the transmission type and that its exciting and pick-up loops (or holes) are located in the region designated as No. 1 in Fig. 1. When in the frequency variation method $2\delta f$ and $2\delta f_0$, the half-power bandwidths of the resonance curves of the cavity with and without the sample respectively, are measured, $\tan \delta$ can be exactly calculated from

$$\tan \delta = \left[\frac{2\delta f}{f_0} - \frac{\bar{W}_0}{\bar{W}_1 + \bar{W}_2 + \bar{W}_3} \frac{2\delta f_0}{f_0} \right] \left[1 + \frac{\bar{W}_1 + \bar{W}_3}{\bar{W}_2} \right] - \Delta. \quad (7)$$

Here \bar{W}_0 corresponds to the energy stored in the cavity without the sample; \bar{W}_1 , \bar{W}_2 and \bar{W}_3 respectively correspond to the energy stored in regions No. 1, 2 (sample), and 3 of the cavity containing the sample, as shown in Fig. 1. These are obtained as follows:

$$\frac{\bar{W}_0}{\bar{W}_1 + \bar{W}_2 + \bar{W}_3} = \frac{l_1 + \epsilon dR_1^2 + l_2R_3^2 - 1/2\beta_1[1 - \epsilon(1/n)^2](\sin 2\beta_1l_1 + R_3^2 \sin 2\beta_1l_2)}{l_1 + \epsilon dR_1^2 + l_2R_3^2 - 1/2\beta_1[1 - \epsilon(1/n)^2](\sin 2\beta_1l_1 + R_3^2 \sin 2\beta_1l_2)} \quad (8)$$

$$1 + \frac{\bar{W}_1 + \bar{W}_3}{\bar{W}_2} = 1 + \frac{l_1 + l_2R_3^2 - 1/2\beta_1(\sin 2\beta_1l_1 + R_3^2 \sin 2\beta_1l_2)}{\epsilon dR_1^2 + \epsilon/2\beta_1(1/n)^2(\sin 2\beta_1l_1 + R_3^2 \sin 2\beta_1l_2)}, \quad (9)$$

where R_1^2 , R_3^2 are given by

$$\left. \begin{aligned} R_1^2 &= \sin^2 \beta_1 l_1 (1 + 1/n^2 \cot^2 \beta_1 l_1) \\ R_3^2 &= \frac{\sin^2 \beta_1 l_1}{n^2 \sin^2 \beta_1 l_2} \sin^2 \beta_2 d (\cot \beta_1 l_1 + n \cot \beta_2 d)^2 \end{aligned} \right\}. \quad (10)$$

In the reactance variation method, when the differences of the axial lengths $2\delta l_2$ and $2\delta l_{20}$ at the half-power points of the resonance curves of the cavity with and without the sample, respectively, are obtained by varying the axial length l_2 , $\tan \delta$ can be calculated from the equation

$$\tan \delta = \left[\frac{2\delta l_2 - 2\delta l_{20}/R_3^2}{n^2 d R} \right] \left[1 - \frac{1}{\epsilon} \left(\frac{\lambda_0}{\lambda_c} \right)^2 \right] - \Delta, \quad (11)$$

where R is given by

$$R = \sin^2 \beta_1 l_2 \left[1 + \frac{1}{n^2 \tan^2 \beta_1 l_2} + \frac{\cot^2 \beta_1 l_2 \cdot \tan \beta_2 d}{n^2 \beta_2 d} \cdot \left\{ \frac{n^2 \cosec^2 \beta_2 d}{(\cot \beta_1 l_1 \cot \beta_2 d - n)^2} - 1 \right\} \right]. \quad (12)$$

The last term in (7) and (11) is given by

where λ_0 is the wavelength in free space expressed in cm, and A is attenuation coefficient of metal cavity wall relative to pure copper. When cavity is properly designed and manufactured, and value of λ_0/λ_c lies between $0.65 \sim 0.80$, Δ may be as small as $0.1 \sim 0.3 \times 10^{-4}$.

It is interesting to note that the proper loss of the sample can not completely be extracted from the measured Q values of the cavity only, with and without the sample, but another measurement is required to obtain the compensation factor Δ ; i.e., the relative loss factor A . It should be noted that in (7)~(13) cavity wall losses plus coupling losses are taken into account.

For some special cases the above formula may be somewhat simplified. Several cases are listed below.

In the case $S = S_{max}$,

$$\left. \begin{aligned} l_1 &= l_2 \pm \nu'/2\lambda_1, \quad R_1^2 = \sin^2 \beta_1 l_1 \sec^2 \beta_2 d / 2, \quad R_3^2 = 1.00 \\ 1 + \frac{\bar{W}_1 + \bar{W}_3}{\bar{W}_2} &= 1 + \frac{2l_1 - 1/\beta_1 \sin 2\beta_1 l_1}{\epsilon d R_1^2 + \epsilon/2\beta_1(1/n)^2 \sin 2\beta_1 l_1} \\ R &= \sin^2 \beta_1 l_1 \left(1 + \frac{1}{n^2 \tan^2 \beta_1 l_1} + \frac{2}{\beta_2 d} \frac{1}{n \tan \beta_1 l_1} \right) \end{aligned} \right\}. \quad (14)$$

In the case $l_1 = (2\nu' + 1)/4\lambda_1 (\nu' = 0, 1, 2, \dots)$

$$\left. \begin{aligned} R_1^2 &= 1.00, \quad R_3^2 = \cos^2 \beta_2 d + n^2 \sin^2 \beta_2 d, \\ 1 + \frac{\overline{W}_1 + \overline{W}_3}{\overline{W}_2} &= 1 + \frac{l_1 + l_2 R_3^2 \{1 - \sin 2\beta_1 l_2 / 2\beta_1 l_2\}}{\epsilon d \{1 + \sin 2\beta_2 d / 2\beta_2 d\}}, \\ R &= \frac{1 + \sin 2\beta_2 d / 2\beta_2 d}{\cos^2 \beta_2 d + n^2 \sin^2 \beta_2 d} \end{aligned} \right\} \quad (15)$$

In the case $l_2 = \nu'/2\lambda_1 (\nu' = 0, 1, 2, \dots)$

$$\left. \begin{aligned} R_1^2 &= \left(\frac{\sin \beta_1 l_1}{\sin \beta_2 d} \right)^2 \\ &= \left(\frac{\sin \beta_1 (S_2 + d)}{\sin \beta_2 d} \right)^2, \quad R_3^2 = n^2 R_1^2, \\ 1 + \frac{\overline{W}_1 + \overline{W}_3}{\overline{W}_2} &= 1 + \frac{l_1 + 1/2\beta_1 \sin 2\beta_1 (S_2 + d)}{\epsilon d R_1^2 - \epsilon/2\beta_1 (1/n)^2 \sin 2\beta_1 (S_2 + d)}, \end{aligned} \right\} \quad (16)$$

MEASURING EQUIPMENT

General Installation

A block diagram of the measuring equipment is shown in Fig. 3. The klystron is frequency modulated by means of a sawtooth wave derived from the oscilloscope sweep. The signal from the klystron is transmitted through the main waveguide of the directional coupler and variable precision attenuators, and is then fed to the measuring cavity resonator through a pick-up antenna (4,000-mc band) or a small hole (6-mm diameter for 9,000-mc

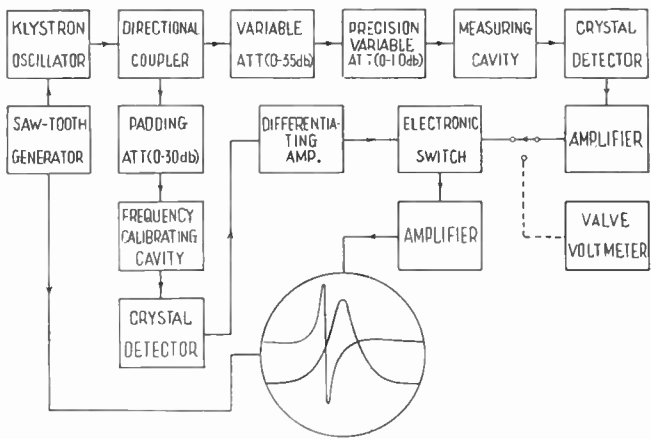


Fig. 3—Block diagram of the measuring equipment.

band, 1×3.5 mm for 24,000-mc band). Part of the signal is attenuated through the directional coupler and the padding attenuator and is fed to the frequency calibrating cavity. The rectified outputs from both cavities are independently amplified, fed to the electronic switch and displayed simultaneously on the oscilloscope. The

klystron oscillator frequency is frequency modulated to sweep through the resonant frequency of the measuring cavity. A typical resonance curve results on the oscilloscope. Since the output of the frequency calibrating cavity is differentiated by an RC circuit and then amplified, the differentiated waveform of the resonance curve appears simultaneously on the screen, as shown in Fig. 3. The (almost) vertical straight line, or more exactly, the point at which this line intersects the abscissa, indicates the resonant frequency of the frequency calibrating cavity. Therefore, when the vertical line, described above, coincides with the resonance curve maximum, the resonant frequency of the measuring cavity can be determined accurately from the tuning plunger reading of the frequency calibrating cavity. Also, the width of the resonance curve at half-power, that is, its damping factor, can be determined precisely from the difference between the two tuning-plunger readings necessary to make the vertical line coincide with the upper and lower half-power points of the resonance curve. The half-power points are determined by means of the calibrated precision attenuator as the points at which the curve is 3.01 db below the top of the resonance curve. Alternately the characteristics of the calibrated crystal detector may be used.

The foregoing method of determining the half-power bandwidth is most suitable for measurements involving high Q (such as the loss measurement of high quality dielectric samples), and is more accurate than any other known method. For low Q -measurement, however, ($Q < 1,000$), its accuracy is decreased by the AM effect of the klystron oscillator, and therefore (for example in the loss measurement of high-loss dielectric samples) the method developed at the Bell Telephone Laboratories⁷ is preferable in such cases. Even in that method the bright spot induced by the differentiated frequency marker is to be preferred over the usual resonance marker because a border point between the bright and dark spots corresponding to the resonant frequency of the calibrating cavity can be observed more clearly on the oscilloscope.

In the reactance variation method of high- Q measurements, the same equipment as shown in Fig. 3 is used. In this case, the frequency marker on the oscilloscope is fixed and the resonance curve is varying in accordance with the variation of the axial length of the measuring cavity. The method to obtain the half power points is just the same as described above.

In the reactance variation method for low- Q measurements, the klystron oscillator is amplitude modulated by means of a square wave. The rectified cavity output is amplified by the tuned audio-amplifier whose output is measured with a vacuum tube voltmeter as shown (in dotted lines) in Fig. 3.

⁷ A. C. Beck and R. W. Dawson, "Conductivity measurements at microwave frequencies," PROC. IRE, vol. 38, pp. 1181-1190; October, 1950.

Fig. 4 shows the complete measuring setup. It involves more than is shown in Fig. 3 so that other measurement methods (described below) are possible in the neighborhood of 9,000 mc.

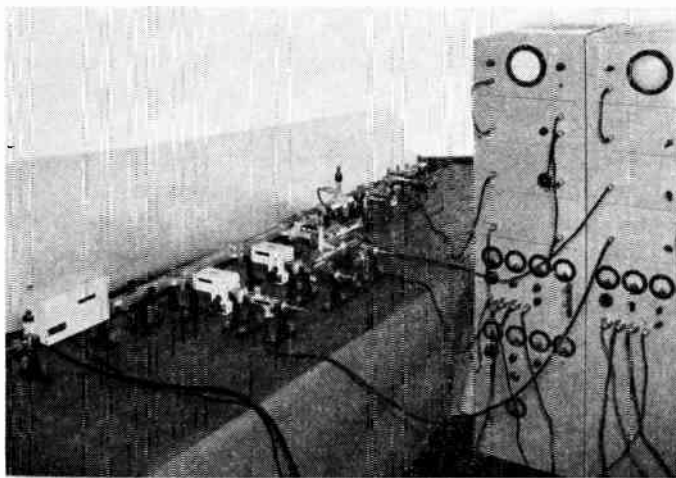


Fig. 4—Complete measuring equipment at 9,000 mc.

Microwave Equipment

The measuring cavities used are cylindrical cavities oscillating in the TE_{01} modes, specifically, the TE_{011} mode in the 4,000-mc band, the TE_{012} mode in the 9,000-mc band, and the TE_{013} and TE_{014} modes in the 24,000-mc band. In order to make the compensation factor, Δ of (13) as small as possible, large diameters, such as 12.5 cm, 5.4 cm and 2.2 cm, are adopted in these frequency bands. Each cavity is provided with a fixed end plate and a movable plunger plate, and the available axial length of the cavity is made long enough to fix sample at the prescribed position and to facilitate tuning over a considerable frequency range. The plunger is advanced with a micrometer screw (one thread per mm), which has a minimum graduation of 1/1,000 mm. All inner dimensions of the cavities are made to within a precision of 3 microns (such an accuracy is not necessarily required for the measuring cavity). The inner surfaces of the cavities are finished by silver plating and their attenuation relative to pure copper is 1.4~2.0 (the relative attenuation is obtained by comparing the Q values of the TE_{01} and the $TE_{01(r-1)}$ modes). The loaded Q 's of the cavities are about 10,000~15,000.

The frequency-calibrating cavities used also oscillate in the TE_{011} , TE_{012} and TE_{014} modes in the respective frequency bands. Their diameters are relatively small (specifically 10.0 cm, 4.4 cm and 1.67 cm) in order to increase the accuracy with which frequency is calibrated. A variation of 1/100 mm in the axial length corresponds to a change in the resonant frequency of about 70 kc, 170 kc and 880 kc at 4,000 mc, 9,100 mc and 24,000 mc, respectively. A variation of 1/1,000 mm in the axial length can be read by means of a double vernier. When a more accurate determination of frequency difference

is required, a small movable rod, attached to the fixed end of the cavity, is inserted into the cavity. For example, a variation of 1/100 mm in rod insertion corresponds to a 2.2-kc change in the resonant frequency at 4,000 mc. The variation in the resonant frequency described above is calibrated to within a precision of 1.5 kc by the heterodyne method.

The variable precision attenuators used are vane-type dissipative attenuators with a range from 0.5 to 1.0 db. They are calibrated by means of a standard cut-off attenuator and their accuracy is about 0.02 db.

Low-Frequency Equipment

The resonance-curve amplifier used consists of three RC coupled stages. The hum which normally results from ac heated filaments is eliminated by the use of dc power obtained from a selenium rectifier. The response of the amplifier is nearly uniform for frequencies ranging from 10 cps to 60 kc.

The output of the klystron and its center frequency should be constant during the measurement. Since it is also necessary to avoid any residual frequency modulation due to hum, battery operation is preferred, but well-stabilized, low hum rectifiers are generally satisfactory sources of klystron cathode and heater voltage. It is necessary to reduce the hum voltage of the klystron repeller source to 0.001 v by adding a decoupling capacitor in the repeller circuit, since, for example, in the 4,000-mc band a residual frequency modulation of 1 kc resulting by a 0.001-v hum voltage causes trouble in these precision measurements.

TYPICAL MEASURING PROCEDURES

Typical procedures for measuring the dielectric properties ϵ and $\tan \delta$ of low-loss dielectric samples are now briefly described.

With the measuring cavity tuned to the measuring frequency f_0 , the axial length of the cavity L_0 and the half-power bandwidth, $2\delta f_0$ (frequency variation method) or $2\delta l_0$ (reactance variation method), are measured.

The sample is then inserted at a distance $l_1 = \lambda_1/4$ from the fixed end of the cavity and the shift of the cavity length, S_1 , as well as the half-power bandwidth, $2\delta f_1$ or $2\delta l_1$, are measured. Using this value of S_1 , p is calculated from the following modification of (4):

$$p \tan p = \frac{1}{1 + S_1/d} q \tan q, \quad (17)$$

where $p = \beta_2 d$, d is the thickness of the sample, $q = \beta_1(S_1 + d)$ and $\beta_1 = v\pi/L_0$. The dielectric constant of the sample, ϵ , is then given by (6).

When greater precision is required, it is preferable to make the measurements with the sample inserted at a distance $l_{1\max}$ from the end; i.e., at the most sensitive position for both ϵ and $\tan \delta$ measurements. To determine $l'_{1\max}$ the shift $S'_{1\max}$ is calculated from the value p obtained from (17), as follows:

$$\tan \beta_1 / 2(S'_{\max} + d) = 2/\beta_1 d [\phi/2 \cdot \tan \phi/2]. \quad (18)$$

Then l'_{\max} is given by

$$l'_{\max} = 1/2 \{ L_0 - (S'_{\max} + d) \}. \quad (19)$$

Next, with a sample insertion of l'_{\max} as obtained above, the shift S_{\max} and the half-power bandwidth $2\delta f_2$ or $2\delta l_2$ are measured. Should the measured value S_{\max} be different from the calculated value S'_{\max} , the insertion must be adjusted so that $l_1 = l_2$. As the shift varies very slightly with a variation in l_1 in the vicinity of l_{\max} , as shown in Fig. 2, l_{\max} may be obtained from the above measured value S_{\max} without any serious error by

$$l_{\max} = 1/2 \{ L_0 - (S_{\max} + d) \}. \quad (20)$$

In this case ϕ is calculated by the following formula:

$$\left. \begin{aligned} \phi/2 \tan \phi/2 &= \frac{1}{1 + S_{\max}/d} q_{\max} \cdot \tan q_{\max}, \\ q_{\max} &= \beta_1/2(S_{\max} + d) \end{aligned} \right\}. \quad (21)$$

Finally, ϵ is obtained from (6). The value of $\tan \delta$ can then be calculated from $2\delta f$ or $2\delta l$ etc., through (7) and (11).

The procedure described above is suitable for the measurement of thin, low-loss samples ($\tan \delta < 20 \times 10^{-4}$, thickness $1.0 \sim 5.0$ mm). In the measurement of high loss or thick samples, on the other hand, it is preferable to insert the sample to such a position that $l_2 = 0$ and to measure the shift S_2 and $2\delta f$. Then, ϕ is given by:

$$\left. \begin{aligned} \tan \phi/\phi &= (1 + S_2/d) \tan q_2/q_2, \\ q_2 &= \beta_1(S_2 + d) \end{aligned} \right\}. \quad (22)$$

In following this method great caution is required, because slight errors in the measured values seriously affect the final values of ϵ and $\tan \delta$. The compensation factor Δ must also be taken into account, because in some cases it may be impossible to neglect.

Next, the method to determine the exact location of the sample within the cavity is briefly described. As it is somewhat difficult to fix the sample precisely at the prescribed position, especially for lower frequency bands, the following method was adopted. First, the movable plunger plate of the cavity is shifted to the prescribed position where the sample is to be located, and the sample is inserted within the cavity until it makes close contact with the plunger plate. The diameter of the sample is made slightly (about $1/10$ mm) smaller than that of the cavity. Then a tiny wedge ($2 \times 2 \times 1$ mm \sim $3 \times 3 \times 2$ mm) made of the same material as the sample is driven between the metal wall of the cavity and the tapered notch of the sample, in order to make the sample stay at the right position and angle within the cavity. The clearance between the cavity wall and the sample can be kept within 1 mm, and therefore the effect on the results of the measurements can be made negligibly small, because there is no electric

field component of the TE_{01} mode near the metal wall.⁸ Finally, the plunger plate is moved away from the sample.

RESULTS

The dielectric properties, ϵ and $\tan \delta$, of polystyrol, polyethylene, teflon, ebonite and glass samples were measured both by the frequency variation method and the reactance variation method, in the 4,000-mc, 9,000-mc and 24,000-mc bands.

The results obtained are described below. Fig. 5 shows the oscilloscope trace of the resonance curves of the cavity and the frequency marker (the lines in the photograph appear broader than in actual practice because of the long exposure necessary to make the fine frequency marking line more visible).

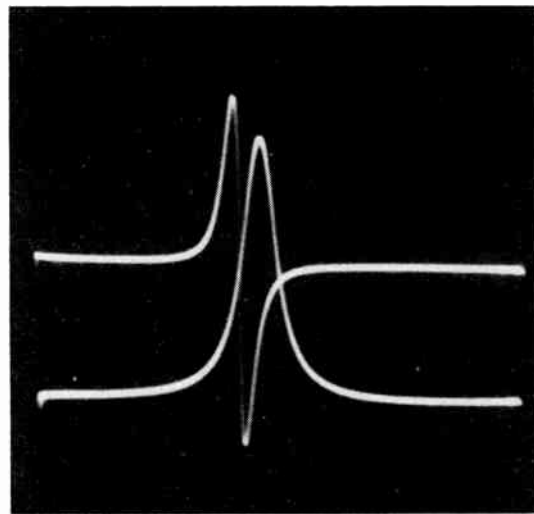


Fig. 5—Resonance curve and frequency marker on the oscilloscope.

First, the results of the measurement of a 3.55-mm thick polystyrol sample, performed at 3,990 mc are described. The results of ϵ measurements for sample positions $l_1 = L_0/2$ and l_{\max} is listed in Table I. From these measured values, ϵ was determined to be 2.570.

TABLE I
MEASURED VALUES OF ϵ FOR POLYSTYROL SAMPLE AT 4,000 mc

f_0	3,990 mc	without sample
L_0 (TE_{011} mode)	5.514 cm	
β_1	0.570	
$2\delta f_0$	0.428 mc	
S_1	0.971 cm	$l_1 = L_0/2$
P	0.423	
ϵ	2.571	
S'_{\max} (Calculated)	1.122 cm	
l'_{\max} (Calculated)	2.017 cm	
S_{\max} (measured)	1.124 cm	$l_1 = l_{\max}$
P	0.422	
S	2.568	
Average value of	2.570 ± 0.1 per cent	

⁸ For example, it has been proved, theoretically, that even the air gap 5 mm in the 4,000-mc band cavity may cause only 0.3 per cent error for the ϵ measurement of the sample $\epsilon = 3$.

The difference between the values of S calculated from β_1 , β_2 , ϵ , etc. obtained above, and the measured values of S were found to be within 5×10^{-2} mm for various sample positions. The values of $\tan \delta$ calculated from the measured half-power bandwidths are listed in Table II, where $\tan \delta'$ and $\tan \delta$ respectively neglect and take into account the compensation factor Δ . The average value of $\tan \delta$ is 5.56×10^{-4} and the maximum deviations in the vicinity of l_{\max} and $l_1 = L_0/2$, i.e., in the vicinity of the optimum sample position, are +1.5 per cent and -2.3 per cent. It should be noted from Table II that the values of $\tan \delta'$ increase with the compensation factor, Δ , which varies from minus to plus value in accordance with the increase of the sample positions l_1 , but the true value of $\tan \delta$ remains nearly constant. Fig. 6 shows the values of S , R_1^2 , R_3^2 , and $l + \bar{W}_1 + \bar{W}_3 / \bar{W}_2$ for various sample positions.

The results of measurements for a polyethylene sample at 3,990 megacycles are listed in Table III. From it, it is noted that the reactance variation method has the same accuracy as the frequency variation method.

Two polyethylene samples whose dielectric properties are expected to be the same were made at 9,000 mc in cavity of TE_{012} mode. Detailed results are in Table

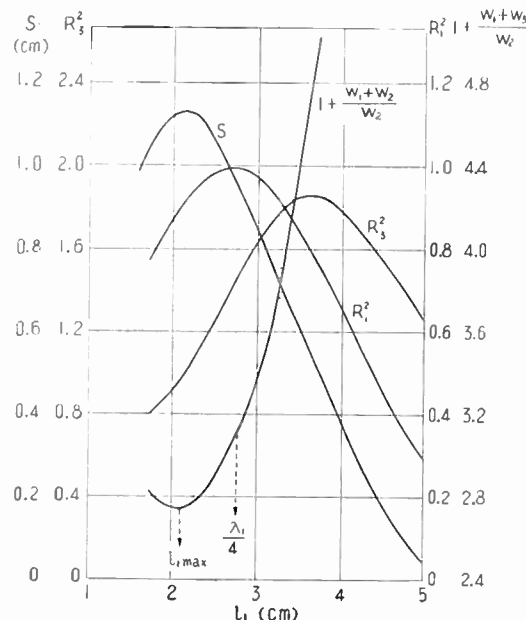


Fig. 6—Relation between the shift S , R_1^2 , R_3^2 , $l + \bar{W}_1 + \bar{W}_3 / \bar{W}_2$ and the sample position l_1 .

IV (next page). By this method, $\epsilon = 2.30$, and $\tan \delta = 2.80 \times 10^{-4}$ was obtained with higher accuracy than possible by any other measurement method.

TABLE II
MEASURED VALUES OF $\tan \delta$ FOR POLYSTYROL SAMPLE AT 4,000 mc

l_1 (cm),	$l + \bar{W}_1 + \bar{W}_3 / \bar{W}_2$,	$2\delta f$ (mc),	$\frac{\bar{W}_0}{\bar{W}_1 + \bar{W}_2 + \bar{W}_3 \cdot 2\delta f_0(\text{mc})}$	$\tan \delta'(10^{-4})$,	$\Delta(10^{-4})$,	$\tan \delta(10^{-4})$
1.645	2.885	1.274	0.637	4.62	-0.548	*5.17
1.895	2.756	1.330	0.578	5.19	-0.338	5.53
2.017 ($l_1 \max$)	2.740	1.335	0.550	5.39	-0.248	5.64
2.395	2.831	1.264	0.481	5.56	+0.0005	5.56
2.757 ($L_0/2$)	3.113	1.188	0.442	5.83	+0.195	5.63
3.145	3.682	1.040	0.417	5.81	+0.382	5.43
3.645	5.053	0.927	0.402	6.61	+0.704	*5.90
4.645	21.38	0.566	0.417	7.98	+1.99	*5.98

Average value and its max deviation; $\tan \delta = 5.61 \times 10^{-4}$ (6.6 per cent, -7.8 per cent)

Average value and its max deviation excluding * values; $\tan \delta = 5.56 \times 10^{-4}$ (1.5 per cent -2.3 per cent)

TABLE III
MEASURED VALUES OF $\tan \delta$ FOR POLYETHYLENE SAMPLE AT 4,000 mc
 $L_0 = 5.518$ cm (TE_{011} mode), $2\delta f_0 = 0.348$ mc, $2\delta l_0 = 1.05 \times 10^{-3}$ cm

Sample position	$l_1 = L_0/2$	$l_1 \max$	Average value
S_1	0.933 cm		
S'_{\max} (calculated)	1.108		
S_{\max} (measured)	1.083 cm		
ϵ	2.292	1.084 cm 2.292	
F.V. $\begin{cases} 2\delta f \\ \bar{W}_0/\bar{W}_1 + \bar{W}_2 + \bar{W}_3 \cdot 2\delta f_0 \\ \tan \delta \end{cases}$	0.815 mc 0.358 mc 3.24×10^{-4}	0.897 mc 0.445 mc 3.02×10^{-4}	$3.13 \times 10^{-4} \pm 3.4$ per cent
R.V. $\begin{cases} 2\delta l \\ 2\delta l_0/R_3^2 \\ \tan \delta \end{cases}$	1.5×10^{-3} cm 0.68×10^{-3} cm 3.10×10^{-4}	2.15×10^{-3} cm 1.05×10^{-3} cm 3.10×10^{-4}	3.10×10^{-4}

{F.V.; frequency variation method}
{R.V.; reactance variation method}

TABLE IV
MEASURED VALUES OF ϵ , $\tan \delta$ FOR TWO POLYETHYLENE
SAMPLES AT 9,000 mc

Sample No.	No. 1 Sample	No. 2 Sample
d	2.30 mm	2.11 mm
S_1	4.966 mm	4.795 mm
p from $l_1 = 3/4 \cdot \lambda_1$	0.571	0.529
S'_{\max}	6.165 mm	
l'_{\max}	3.347 cm	
S_{\max}	6.152 mm	
p from l_{\max}	0.571	
ϵ	2.29	2.31
$l_1 = 3/4 \cdot \lambda_1 / 2\delta f$ ($\tan \delta$)	0.368 mc 0.886 mc 2.75×10^{-4}	0.388 mc 0.881 mc 2.81×10^{-4}
$l_{\max} / 2\delta f$ ($\tan \delta$)	0.873 mc 2.86×10^{-4}	
Average value of \tan	$2.80 \times 10^{-4} \pm 1.8$ per cent	2.81×10^{-4}

$$I_0 = 5.026 (\text{TE}_{012} \text{ mode}), \quad \beta_1 = 1.250$$

In the 24,000-mc band, a 1.55 mm thick teflon sample was measured using the TE_{014} mode. The values found are $\epsilon = 2.09$ and $\tan \delta = 4.32 \times 10^{-4}$. Corresponding results at 4,000 mc were 2.01 and 4.00×10^{-4} .

SOURCES OF ERROR

The sources of error in the measurement of dielectric properties are most conveniently discussed separately for ϵ and for $\tan \delta$.

The sources of error in the dielectric constant measurement can be classified as follows: (1) error due to uncertainty of the position of the sample in the cavity; (2) error due to uncertainty or irregularity of the thickness of the sample measured; (3) error due to the shift S ; (4) error due to the variation of the oscillator frequency; (5) error due to the air gap between the sample and the peripheral metal wall of the cavity. After a detailed investigation of each cause, it was concluded that the error in ϵ can be easily reduced below 1 per cent for sample positions $l_1 = \lambda_1/4$ and l_{\max} , if the sample is well manufactured so that its surface is reasonably flat. For sample position $l_2 = 0$ more cautious measurements are required, because slight errors in the measured values of S and the air gap between the sample and the end plate of the cavity seriously affect the final value of ϵ . This is the case especially for thin samples.

The sources of error in $\tan \delta$ are classified as follows: (1) error due to uncertainty in β_2 and ϵ ; (2) error arising from Q measurements. The latter is the main source of error⁹ in the determination of $\tan \delta$. Since well-calibrated frequency meters, variable attenuators and a low-hum amplifier have been employed in this measurement as discussed above, and since half-power bandwidths can be measured by very fine straight frequency marking lines, total error in Q measurements can be kept within 2 per cent limits for Q ranging from 15,000 to 2,000, as

⁹ G. Birnbaum, S. J. Kryder, and H. Lyons, "Microwave measurements of the dielectric properties of gases," *Jour. Appl. Phys.*, vol. 22, pp. 95-102; January, 1951.

was verified by many experiments. Consequently the error in the values of $\tan \delta$ can be kept below 3 per cent.

OTHER APPLICATIONS OF THE MEASURING EQUIPMENT

As Q measuring equipment is suitable for precision, high Q measurements, it is also applicable to measurements of attenuation (or loss) of waveguide and determination of surface conductivity of metal plates.

Measurement of the Attenuation of Waveguides

The waveguide to be measured (with axial length equal to $n/2 \cdot \lambda_g$) is connected to two adapter waveguides, each of $(2m + 1/4 \cdot \lambda_g)$ axial length. Since the other ends of the adapter waveguides are shorted by end plates and are provided with the exciting and detecting irises, the combination acts as a cavity. After measurement, the waveguide sample is disconnected and the adapter waveguides are connected to each other to constitute a cavity which resonates at the same frequency as the one including the waveguide sample. The attenuation of the sample can then be calculated from the Q values of the two cavities. As an example, the attenuation of drawn WR 112 waveguide samples (axial length equal to 1 foot) was measured by this method in 9,000-mc band. Relative values of measured attenuation, as compared with theoretical attenuation of pure copper waveguide, were found to be: Depending upon their wall roughness, $1.05 \sim 1.25$ for drawn copper waveguide samples, and $1.55 \sim 2.10$ for drawn bronze (90 per cent copper) samples. Accuracy of these measurements is considered to be within 3 per cent.

Measurement of the Surface Loss of Metal Plates

Because the Q of a cylindrical cavity varies with the surface loss of the end plates, the relative surface loss of metal plates can be found from the deviation of the cavity Q (from a standard), when the cavity is fitted at one end with the metal plate in question. The authors measured the relative surface losses of copper plates, silverplated plates, etc., in the 9,000-mc band. A brief report on these measurements was published in a letter in the December, 1954, issue of this journal.

ACKNOWLEDGMENT

This research was carried out at the Institute of Industrial Science, University of Tokyo, over the past several years, under auspices of the Electrical Communication Laboratory, Japanese Telephone and Telegraph Corporation. The authors are indebted to Profs. M. Hoshiai and N. Takagi, University of Tokyo, for their kind advice, and wish to thank S. Seki and other staff members of the Laboratory for helpful discussions. Also, sincere gratitude is extended to K. Niguchi, Shimada Physical and Chemical Industrial Co., (manufacturers of the present equipment), for his kind cooperation and advice, and we are obliged to H. M. Altschuler, Polytechnic Institute of Brooklyn, for his help in correcting our English.

Transistor Amplifiers for Use in a Digital Computer*

Q. W. SIMKINS†, ASSOCIATE MEMBER, IRE, AND J. H. VOGELSONG†, MEMBER, IRE

Summary—Several transistor pulse-regenerative amplifier circuits suitable for use in a 3 megacycle digital computer are described. These circuits all utilize a type of feedback which is essentially external to the transistor. As a consequence, a negative resistance transistor characteristic is not required. Some of these circuits were designed specifically to be relatively tolerant of the slow recovery of reverse impedance found in many germanium diodes.

INTRODUCTION

ONE of the more important units which has been developed for use in a high speed special purpose digital computer is a transistor pulse-regenerative amplifier with external timing. Various circuit configurations for this application, as well as some general design principles, are described in this paper.

Before proceeding further, it would be well to consider the environment of these amplifiers to properly assess their role. The computer for which the amplifiers are intended is synchronous, serial, and binary. The basic pulse rate is 3 megacycles. Storage is provided by delay lines. For delays in the order of word times or less, electrical delay lines are used, while for longer delays requiring larger storage capacities, acoustic delay lines are used. Logical operations such as AND, OR, and INHIBIT are performed by germanium diode circuits. Transformers in the amplifiers provide pulse inversion where necessary for inhibiting.

Pulses are attenuated by the loss in these various passive circuits. In addition, stray capacitance and, in particular, limited bandwidths and nonlinear phase characteristics of delay lines introduce distortion and perturb timing. To offset these effects the regenerative amplifiers are used. At each of these amplifiers, pulses are amplified and reshaped. Under control of a clock signal applied to each amplifier pulses are also retimed.

Different approaches to the design of pulse-regenerative amplifiers are possible. One type of amplifier utilizing base circuit resistance for feedback has been described in detail.¹ The performance of such a circuit is based on its ability to switch between two points of stability on a negative resistance emitter characteristic.² The general type of amplifier to which the scope of this paper will be limited, however, makes use of feedback which is essentially external to the transistor. Fig. 1 shows two logical arrangements for such an amplifier in block form. This principle of external feedback was

applied to vacuum tube circuits by the Bureau of Standards in the SEAC Computer.³

During the course of the investigation to produce a suitable amplifier, various configurations were designed and considered. Initially, a linear amplifier was constructed for use in an arrangement such as indicated in Fig. 1. To improve the efficiency of operation, the operating range was soon extended so that in all succeeding designs the transistor has been driven from below cutoff to some degree of saturation. In the first few models, feedback was used for retiming purposes only.

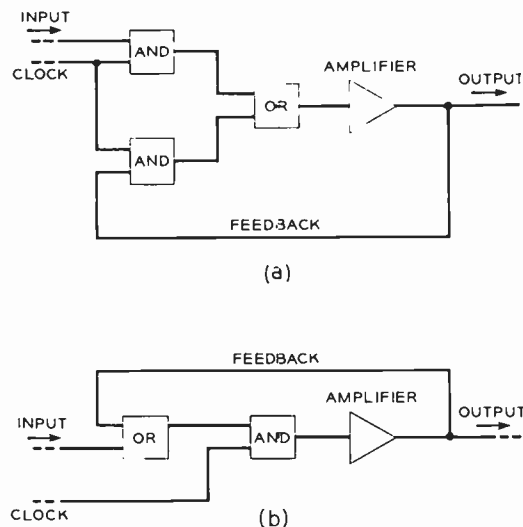


Fig. 1—Logical configurations for a pulse-regenerative amplifier.

Relatively low gain in these models led to the extension of the use of feedback to directly increase the gain. As a beginning in this respect a linear feedback, in which the amount of feedback is directly proportional to the output pulse voltage, was tried. This was found to produce unreliable triggering, since, with the amplifier output load competing with the feedback circuit for current available from the collector, the feedback frequently failed to become fully established. Gated feedback then was produced as a solution to this problem. With this type of feedback, all of the current to be fed back to the emitter becomes available during the first few volts rise at the collector. A back-biased diode can therefore prevent the amplifier load from taking current until the feedback has been established. Limitations in some components presently available, however, cause these circuits to be more complex than would otherwise be necessary. As a consequence of this situa-

* Original manuscript received by the IRE, August 4, 1955.

† Bell Telephone Labs., Inc., Murray Hill, N. J.

¹ J. H. Felker, "Regenerative amplifier for digital computer applications," PROC. IRE, vol. 40, pp. 1584-1597; November, 1952.

² A. E. Anderson, "Transistors in switching circuits," PROC. IRE, vol. 40, pp. 1541-1558; November, 1952. B. G. Farley, "Dynamics of transistor negative resistance," PROC. IRE, vol. 40, pp. 1497-1508; November, 1952.

³ R. D. Elbourn and R. P. Witt, "Dynamic circuit techniques used in SEAC and DYSEAC," PROC. IRE, vol. 41, pp. 1380-1387; October, 1953.

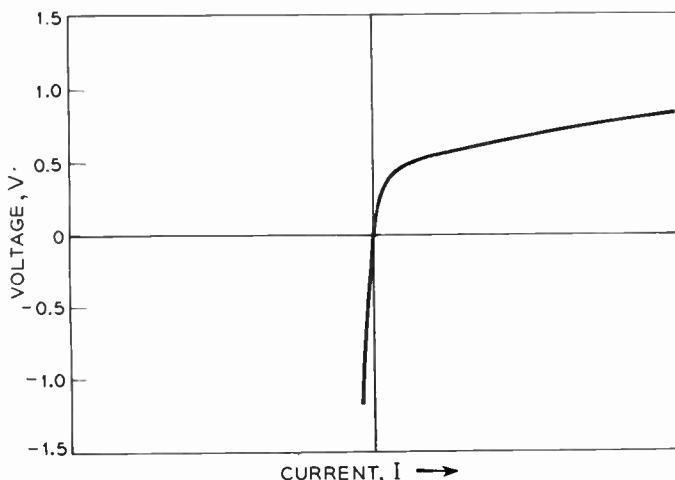


Fig. 2—Typical diode characteristic.

tion, a somewhat simpler amplifier has been designed around a semi-gated feedback. In this circuit, an initial gated feedback current is augmented by additional linear feedback current.

DESIGN OBJECTIVES

The over-all design of the computer and the intended role of the regenerative amplifier, as described in the preceding section, served as a guide in setting the amplifier design objectives. In the succeeding paragraphs, these objectives are discussed.

One of the first considerations in the design of the amplifier is the rise time required in the output pulses. For 3 mc operation with a fifty per cent duty factor the pulse length will be 0.17 microsecond. To provide time margins and to insure proper operation of the logic circuits and delay lines, the flat portion on top of the pulse should be at least 0.08 to 0.10 microsecond in duration. This means that rise and fall times of the order of 0.04 microsecond or less are required. Since the synchronization of the computer is maintained by the clock timing wave, the time relation of the amplifier output pulses with the clock must also be held within about 0.04 microsecond or less.

Another design requirement, gain, should be defined. With amplifiers of the type to be described, a useful definition is the ratio of peak output pulse power to peak input pulse power. (Peak pulse power is the product of pulse voltage and current during the flat-topped portion of the pulse.) Gain will have this meaning in all the material to follow. For a practical computer design, it has been decided that a single amplifier should have at least sufficient gain to drive three other similar amplifiers with one intervening stage of logic. This amounts to from six to ten db gain depending on voltage and current levels employed. Additional gain can be used to make computer design more economical.

Several factors influence the choice of operating voltage and current levels in the amplifier. It is desirable,

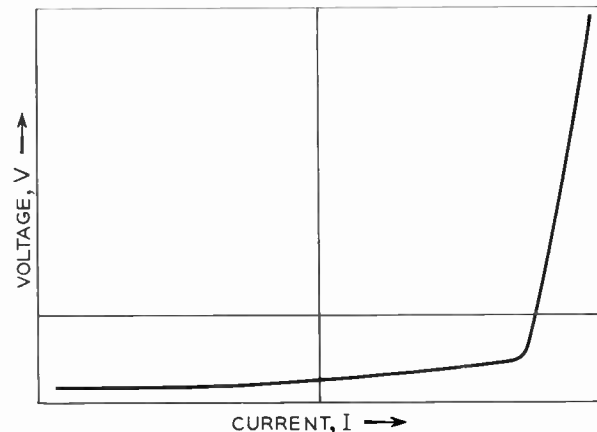
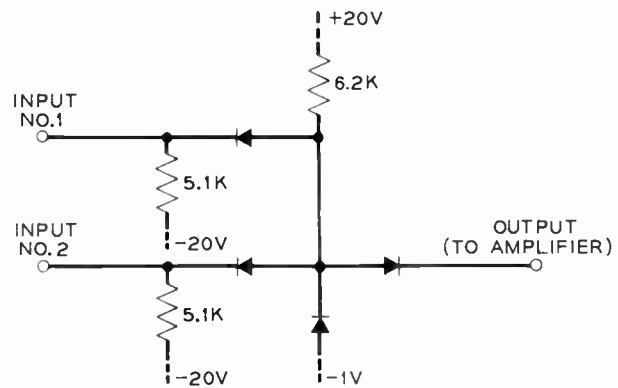


Fig. 3—Diode AND circuit and input V-I characteristic.

of course, to keep power dissipation low, so from this standpoint, both voltage and current levels of signal pulses should be low. On the other hand, minimum pulse voltage depends on the threshold voltage deemed necessary to provide adequate margin at the amplifier input. Also, it is also affected by nonlinear characteristic of germanium diode, as seen in Fig. 2. Stray capacity, and speed of triggering, limit minimum current.

Another important consideration in amplifier design is the nonlinear voltage-current characteristic of diode logic circuits into which amplifier must be capable of operating. As an example, AND circuit and its voltage-current characteristic with one input pulsed appear in Fig. 3. V-I characteristic is seen to have a low incremental impedance region at low voltage and a high incremental impedance region at higher voltages.

COMPONENT LIMITATIONS

Forward and reverse transient effects associated with presently available germanium diodes require special consideration in the design of these regenerative circuits. In practice, the reverse transient has been more troublesome than has the forward transient, solely because in a considerable number of diodes the forward transient effect has been found negligibly small. For this reason, one of the input circuits described in the following section has been designed to have a critical

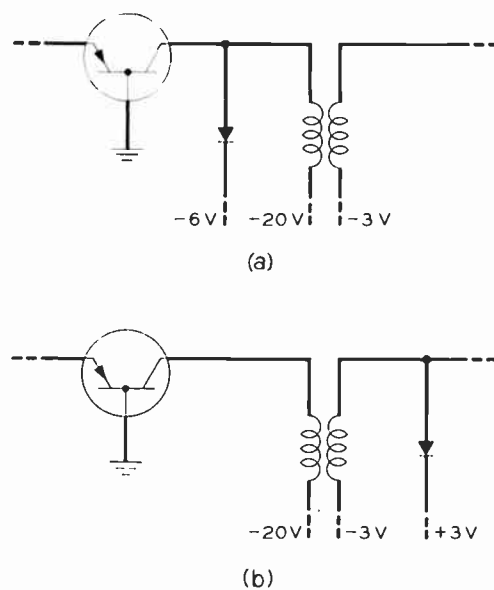


Fig. 4—Transistor output circuits with clipping diodes.

part of the operation depend on changing a diode from the reverse to the forward state, rather than the contrary. In addition, forward current in diodes in sensitive positions is usually limited to less than 5 milliamperes, since transient effects are more pronounced at the higher current levels.

"Minority carrier storage" in transistors presents another limitation. This effect is characterized by a slow return of the collector to a high impedance following an interval in which the collector has been driven to saturation. As a result, pulses are not terminated immediately upon the application of turn-off conditions when the collector is saturated. In the circuits to follow, the combination of a reasonably well controlled emitter current and collector load is used to combat pulse-broadening resulting from hole-storage. Initially, the collector is driven into saturation. As the pulse continues an increasing magnetizing current flows in the mutual inductance of the coupling transformer. This current causes the collector to come out of saturation at approximately the desired time as set by the clock. As a result of differences in transistors and in transformers, not all units reside in the saturated condition for the same interval, so some dispersion in pulse widths is present. The variability appears to be acceptable with no further circuit adjuncts. If further evidence should indicate otherwise, improvement can be obtained through use of a clipping diode as in Fig. 4 to modify the collector load so as to prevent driving the collector to saturation. In this case, the clipped portion of the pulse is no longer available to the external load.

CIRCUIT DESCRIPTIONS

Common Features

In the following sections pulse-regenerative amplifiers of three types are described. They differ mainly in the

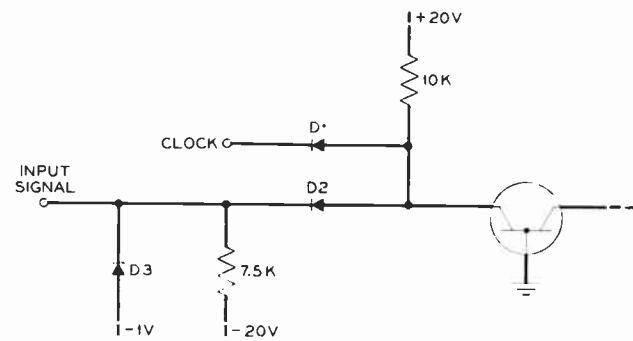


Fig. 5—Pulse-regenerative amplifier input circuit.

manner in which the feedback action takes place. The first type uses a feedback circuit for retiming the pulses, but this feedback is not used to increase the amplifier gain. In the second section several amplifiers with gated feedback are described. Here the feedback enhances the amplifier gain. A gating circuit in the feedback loop permits operation into loads having nonlinear impedance characteristics and insures positive and fast triggering. The third amplifier type described employs semi-gated feedback. In these circuits a combination of gated and linear feedback is used and a somewhat simpler configuration results.

All of the amplifiers to be described have several features in common. They all make use of a grounded base point-contact transistor amplifier which is driven from cutoff to saturation. Since these circuits do not depend on a negative resistance input characteristic, junction transistors should be applicable. Junction transistors with the required bandwidth, power handling capability, and breakdown voltages have not been available in quantity, however. In the circuits to be described, the Western Electric GA-52514 point-contact transistor has proved satisfactory in the grounded base connection. It appears that with point-contact transistors operating under the conditions imposed by the pulse-regenerative amplifier requirements, this is the most satisfactory connection, providing more gain than either the grounded emitter or grounded collector arrangement.

A second feature the circuits have in common is an AND circuit with the incoming signal and the clock as the two inputs. One form of this circuit is shown in Fig. 5. The values of the circuit constants are typical values that can be used to explain the circuit operation. The clock is a 3.0 megacycle sine wave with an amplitude of approximately 5.0 volts rms. In the absence of an input signal and with the clock wave sufficiently positive to cut off the clock diode, D_1 , the potential at the emitter, as set by the voltage divider, is essentially -1.0 volt. Diode D_2 conducts approximately 2.1 milliamperes and the clamp diode, D_3 , conducts about 0.3 millampere.

The voltage-current characteristic of the transistor, as seen from the emitter, varies somewhat from transistor to transistor and also depends on the collector

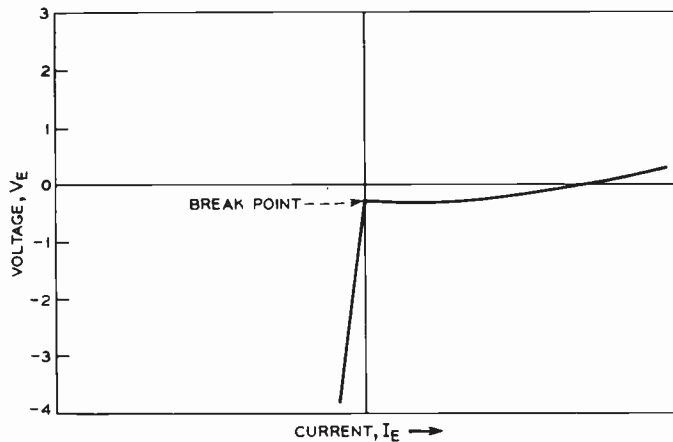


Fig. 6—Typical emitter characteristic for a GA-52514 transistor.

load, but a typical characteristic is shown in Fig. 6. The "break point" is seen to be the point in the characteristic at which the emitter emerges from cutoff, or its high impedance state, to the active region in which the impedance seen at the emitter may be a very small positive resistance or a slightly negative resistance. The break point potential for transistors used in any of the amplifiers to be described is usually within several tenths of a volt of ground potential. The current at the break point is usually positive and less than 50 microamperes.

In the circuit of Fig. 5, it can be seen that in the absence of an input pulse the emitter will be held below the break point and the transistor will be cut off. A coincidence between an input pulse and the positive portion of the clock voltage wave, however, will result in the emitter potential being brought up to the break point and in the circuit of Fig. 5 approximately 2.0 milliamperes of emitter current will result. In this pulse condition, diodes D_3 and D_2 will be held cut off by the input pulse and diode D_1 will be kept back-biased by the positive clock. When the clock swings negative D_1 will conduct and the emitter potential will follow the clock sine wave, cutting off the transistor regardless of the potential on the input signal lead.

The principal disadvantage of the type of input AND circuit shown in Fig. 5 is that it imposes fairly rigid requirements on the transient behavior of diode D_1 . If this diode is slow to recover its high back impedance after forward conduction, the amplifier may be triggered on every time the clock goes positive.

A second type of input AND circuit is shown in Fig. 7. Again, both a positive clock and an input pulse are required to raise the emitter voltage over the break point. With the clock positive and no input pulse present, the emitter voltage can come up to only about -1.0 volt and no emitter current will flow. Diode D_1 clips the clock and therefore limits the flow of current through D_2 to approximately 2.0 milliamperes. This leaves D_3 conducting about 0.4 millampere, thus clamping the emitter potential to -1.0 volt. With an input

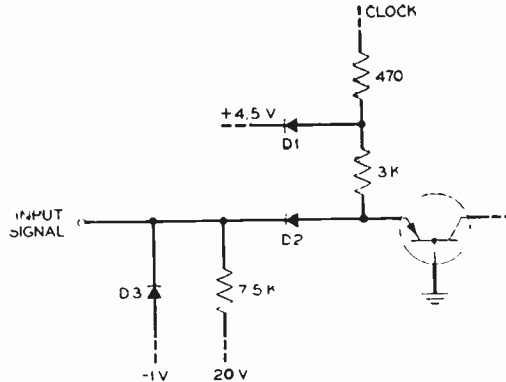


Fig. 7—Pulse-regenerative amplifier input circuit.

pulse present, D_2 and D_3 are cut off and approximately 1.7 milliamperes flows into the emitter. When the clock goes negative, the current source for the emitter is removed, and the transistor turns off. During the negative clock swing, the emitter potential follows the clock.

In this configuration, the reverse transient requirements on the diodes are not so severe. More clock power is required, however, and the pulse rise is slowed down due to the sinusoidal clock waveshape. Considerable improvement could be effected in the performance of this circuit if a square wave clock source were used, but the advantages do not justify the additional complexity of the clock source and the distribution system. The addition of a dc bias of +2 volts to clock has made circuit somewhat more efficient and improves waveshape.

A third feature common to all the amplifier circuits under discussion is the transformer output coupling circuit. The difference in dc voltage levels at the transistor collector and load circuits makes ac coupling necessary. Transformer coupling has several advantages. First, an impedance transformation can be made which results in considerably more usable amplifier gain. Second, with transistor circuits of this type, dc restoration can be more readily obtained with transformer, rather than condenser, coupling. This type of output circuit also provides a more efficient means of supplying the dc power to the transistor collector. Still another advantage is that both positive and negative pulses can be made available at the amplifier output.

Several things should be mentioned in connection with the dc restoring features of transformer coupling. Short rise times are required so very tight coupling is used in these transformers and the leakage inductance is small. The transformer equivalent circuit consists then of the parallel combination of the mutual inductance, shunt capacity, and an equivalent loss resistance which is normally large. To effect complete dc restoration, it is necessary that any energy stored in the mutual inductance and shunt capacity during the pulse interval be dissipated in the interval between pulses. With a 3.0 megacycle pulse repetition frequency, this is 0.17 microsecond. The constants of the transformer and associated circuitry are chosen such that the tuned circuit is slightly less than critically damped and rings at a fre-

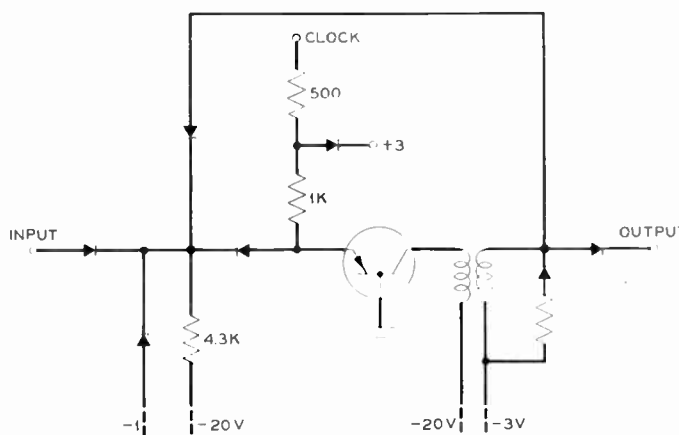


Fig. 8—Pulse-regenerative amplifier with external feedback for timing only.

quency of about 3.0 megacycles. These conditions provide adequate dc restoration with minimum loss. The loss results primarily from the build-up of energy in the transformer mutual inductance in the form of magnetizing current during the pulse interval. This is the energy which has to be dissipated in the interval between pulses. The value of the total equivalent shunt resistance in this interval is quite important to the proper operation of this circuit. If this resistance is too low, the circuit will be overdamped, and the dc restoration will be poor. If the resistance is too high, the overshoot may falsely operate a succeeding amplifier. The transistor collector impedance, which shunts the transformer, is usually of the order of 6 to 15 thousand ohms. To reduce the effect of this large variation and to provide sufficient damping, it is necessary to provide a resistor and a series diode poled, so as to provide a low impedance in the interval between pulses. With this arrangement, little energy is dissipated in the external resistor during the pulse interval, and the circuit efficiency is not significantly impaired.

Most of the amplifiers under discussion require three or four winding transformers. The turns ratio from primary to one of the secondaries called the feedback winding, is normally 3 to 1, while the turns ratio of primary to output windings is usually 2.25 to 1. The mutual inductance of these transformers, as seen from the high or collector side, is nominally 260 microhenries with a maximum variation of ± 20 per cent, while the leakage reactance is only about 1 microhenry. (A reduction in the ± 20 per cent tolerance would be highly desirable.) Stray shunt capacity contributed by transformer itself is approximately 3 micromicrofarads. Additional 2 or 3 micromicrofarads of shunt capacity are due to transistor, its socket, and stray wiring capacity.

Retiming-Feedback Amplifiers

The circuits shown in Figs. 8 and 9 are regenerative amplifiers in which the feedback is used for retiming purposes only. Basically, these two are the same, differing only in the input circuit. In either one, output pulses are returned to the input so that they are terminated

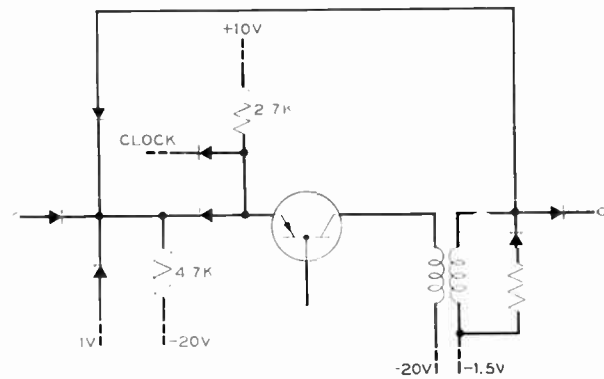


Fig. 9—Pulse-regenerative amplifier with external feedback for timing only.

by the clock rather than the decay of an input pulse. Both circuits are reasonably simple but inherently have rather low pulse gain and require transistors with high pulse current gain to make them useful. Since circuits very similar to these have already been described in some detail,⁴ no further discussion is included here.

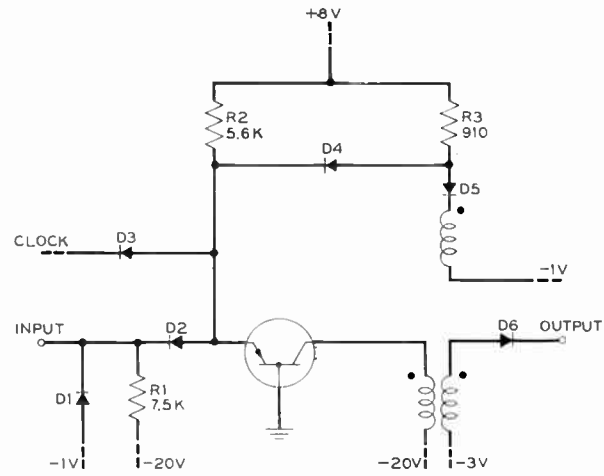


Fig. 10—Gated feedback amplifier.

Gated Feedback Amplifiers

The circuits to be described in this section all make use of a gated feedback path. This term is most readily understood through consideration of the circuit of Fig. 10. The input AND circuit is similar to that shown in Fig. 5 and previously described. As was indicated, emitter current commences at the coincidence of an input pulse and the positive portion of the clock wave. The gated feedback path consists of R_3 , D_3 , D_2 and the feedback winding of the transformer. A current of almost 10 milliamperes normally flows from the +8.0 volt source through R_3 , D_5 , and the feedback winding of the output transformer to the -1.0 volt supply. Diode D_6 is back-biased by several volts so that the initial collector current increment, which flows in response to the emitter current, is in the feedback winding. This winding is poled so that the increment of current opposes the 10

⁴ J. H. Vogelsong, "A transistor pulse amplifier using external regeneration," PROC. IRE, vol. 41, pp. 1444-1450; October, 1953.

milliamperes normally flowing, thereby reducing it and raising the potential at the junction of D_4 and D_5 . When the voltage at this point reaches the emitter voltage, D_4 conducts and part of the current in R_3 flows back to the emitter. This additional emitter current causes still more collector current to flow, diverting more of the current in the feedback winding to the emitter via D_4 . The buildup of feedback continues until D_5 is cut off and all the current in R_3 flows through D_4 into the emitter. Throughout this interval, D_6 is cut off, thus allowing the feedback path to take all the collector current without competition from the output load. When D_5 cuts off, however, the feedback winding sees a very high impedance, and the collector voltage rises, overcoming the back-bias on D_6 , and power is delivered to the load.

The term "gated feedback path" can now be defined as a circuit in which a controlled amount of output current is fed back to the input through a nonlinear impedance. The nonlinear impedance is characterized by a low incremental impedance at currents less than the designed feedback current, and a high incremental impedance to currents greater than this design current. Such a feedback path around a grounded base transistor amplifier, with its emitter biased below cutoff, permits operation as follows:

1. The coincidence of an input pulse and a positive clock raises the transistor emitter potential over the break point and causes a small "trigger" current to flow into the emitter.
2. The resulting collector current is fed back to the emitter through the low impedance of the gated feedback path.
3. The gain in the feedback loop causes the feedback current to increase rapidly until the design amount is reached and the feedback impedance switches to a high value.
4. The output voltage is then permitted to rise and the load is allowed to take the output current. This operation permits a small "trigger" current to control a large output current, thus providing high pulse gain.

While the circuit of Fig. 10 is useful in explaining gated feedback, it has a serious disadvantage. The negative excursion of the clock and the consequent drop in voltage at the junction of D_4 and D_5 results in a pulsating current in the feedback winding and a 3.0 megacycle ripple voltage across it. The likelihood of false amplifier operation is consequently increased. Several means of eliminating this difficulty are proposed and the resulting amplifier circuit configurations are presented in the subsequent paragraphs.

One method of eliminating the ripple voltage across the transformer feedback winding makes use of an additional gate circuit in the feedback path. Fig. 11 is a diagram of a circuit of this type with the conventional AND circuit for the clock input. This circuit differs from the previous circuit, shown in Fig. 10, primarily in the addition of R_4 , D_6 , and D_7 . With this configuration

the gated feedback current normally flows in R_3 , D_5 , and R_4 when the clock is positive. On the negative portion of the clock wave, the current from R_3 is diverted through D_4 and D_5 to the clock. D_6 conducts, however, keeping the potential at the junction of D_5 , D_6 , and D_7 substantially unchanged, and preventing any current from flowing in the feedback winding.

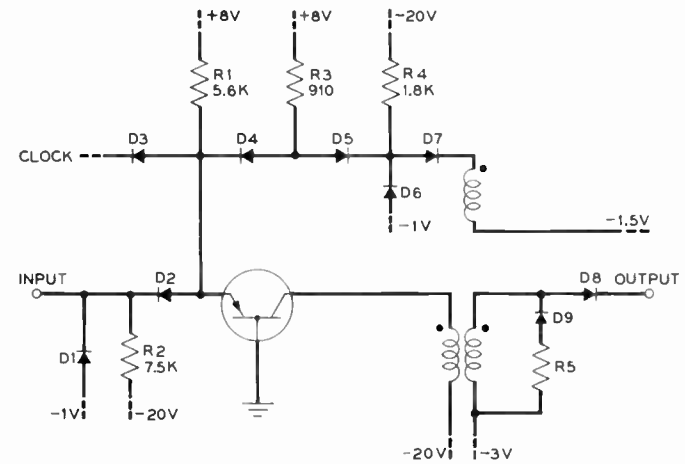


Fig. 11—Gated feedback amplifier.

In the circuit of Fig. 11, just described, both diodes D_3 and D_4 are somewhat critical with regard to reverse transient characteristics. These difficulties are eliminated in the circuit of Fig. 12 which is similar to Fig. 11,

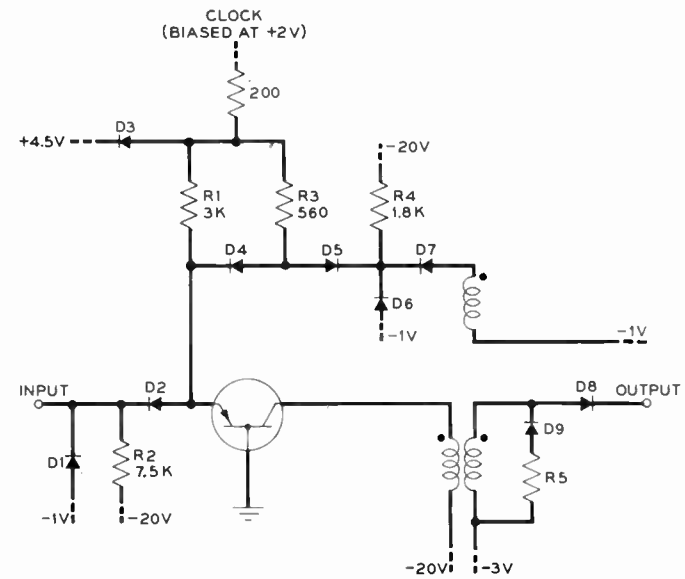


Fig. 12—Gated feedback amplifier.

but makes use of the AND circuit input in which the clock acts as the emitter current source. Both these circuits, however, have rather high dc power dissipation and also contain more components than some of the other circuits to be described.

The circuit of Fig. 13 illustrates another solution to the problem of pulsating current in the feedback winding. Here, the ac clock voltage is supplied to both ends

of the gated feedback current path with a superimposed dc voltage so that the current through R_4 , D_5 and the feedback winding is constant in the absence of an input pulse. The clipping potentials (-2.0 volts and +4.5 volts) are so related to the dc feedback current that diodes D_3 and D_7 commence conduction at about the same time, thus maintaining constant the current in the transformer winding.

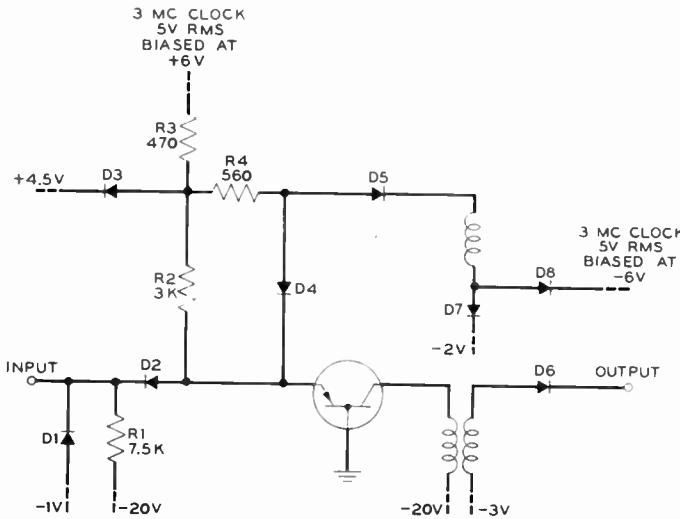


Fig. 13—Gated feedback amplifier.

The following approximate data apply to the amplifier circuit of Fig. 13.

Pulse Power Gain	10 to 12 decibels
Pulse Input Power	7 milliwatts
Clock Power	35 milliwatts
DC Power (Idle Condition)	225 milliwatts

No adverse effects due to poor diode transient response were noted in this circuit operation. Principal objection lies in its complexity, particularly in that two clock voltages biased at different dc levels are required.

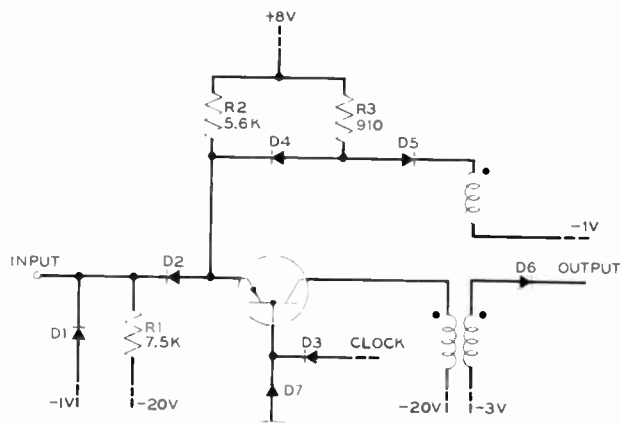


Fig. 14—Gated feedback amplifier with base timing.

Still another circuit employing gated feedback is shown in Fig. 14. This configuration is unique among those presented in that the input AND circuit does not

consist of diodes and resistors alone, but makes use of the transistor as well. It can be seen that the clock is applied to the base through a diode, D_3 . When the clock is positive, D_7 is cut off and D_3 conducts, raising the base voltage and consequently keeping the transistor cut off. On the negative portion of the clock wave D_3 is back-biased and D_7 conducts, holding the base voltage near ground. This permits an input pulse to cause emitter current to flow but keeps the emitter back-biased if no input pulse is present. The feedback circuit is exactly analogous to one previously described and illustrated in Fig. 10. Since the clock is applied on the transistor base rather than at the emitter, there is no difficulty with a pulsating current in the feedback winding of the transformer.

Semi-Gated Feedback Circuits

The final circuits to be described are those which combine some of the characteristics of gated and linear feedback. Fig. 15 is an example of this type with emitter current derived from the clock source. As in the other circuits in which emitter current is provided in this way, this circuit is moderately insensitive to the reverse trans-

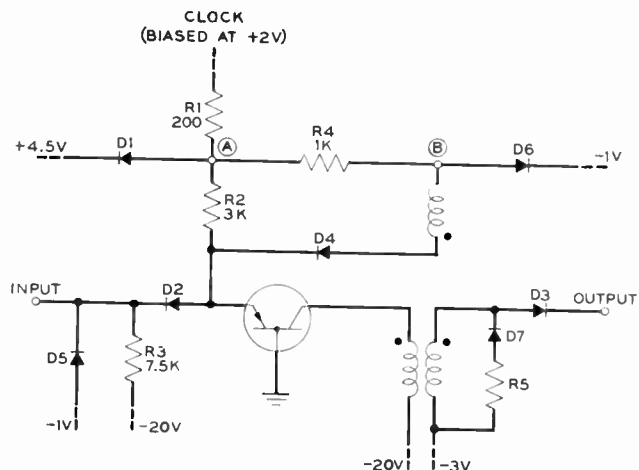


Fig. 15—Semi-gated feedback amplifier.

ient effect in diodes. In comparison with the preceding gated feedback amplifiers, it is relatively simple with low dc dissipation and comparable gain. On the other hand, the clock power required is relatively high, and the pulse turn-off point is less consistent for different transistors. Typical characteristics for this amplifier are:

Pulse Power Gain	10 to 12 decibels
Pulse Input Power	7 milliwatts
Clock Power	40 milliwatts
DC Power (Idle Condition)	100 milliwatts

As in the previous circuits, the feedback is the distinguishing feature of this amplifier, so the description will be centered primarily on it. Again, it will be helpful to consider first how the feedback circuit works when no input signals are applied, and then note the change in its functioning when these signals are present.

During the interval when the applied clock voltage is more negative than -1.0 volt with respect to ground, diodes D_4 and D_6 in Fig. 15 are back-biased. As the clock becomes less negative and reaches approximately -1.0 volt, current commences to flow from the clock source through resistor R_1 . This current divides with essentially one-fourth going into resistor R_2 and three-fourths into resistor R_4 and diode D_6 to -1.0 volt. The current in R_4 and D_6 increases to a maximum of about 5.5 milliamperes where it remains while the positive peak of the clock voltage wave is clipped by diode D_1 . As the clock wave recedes, this current decreases steadily until it becomes zero for applied clock voltages more negative than -1.0 volt. It should be noted that diode D_4 has essentially zero bias during the period when the clock is more positive than -1.0 volt.

When an input signal is applied to the amplifier, the feedback operation is somewhat more involved. With the clock more negative than -1.0 volt, the performance is the same as before. As the clock reaches -1.0 volt, current again commences to flow from the clock source through R_1 , but this time it does not divide immediately. For the short interval until the potential at point A reaches the break point, all of this current flows through R_4 and D_6 to -1.0 volt. By the time it reaches about 1.0 milliampere, however, point A reaches the break point potential, so current begins to flow to the transistor emitter through R_2 . As the clock voltage continues to rise toward the clipping level, the currents through both R_2 and R_4 increase. The R_2 current, which levels off at approximately 1.5 milliamperes, is the trigger current responsible for the initial current in the collector. This collector current, modified by the transformer turns ratio (typically 3:1) is fed back to the emitter via diode D_4 . As long as the current gain around the loop exceeds unity, therefore, emitter and collector currents increase with no increase in the external drive.

Inspection of Fig. 15 shows that the source for the current, through diode D_4 and the transformer feedback winding is the same as that for the current through diode D_6 , namely, the clock supply through resistors R_1 and R_4 . In fact, the current through D_4 represents a diversion of current from D_6 as result of a relatively small voltage induced in the feedback winding. Specifically, this voltage is the difference between the potentials at the emitter and point B , in addition to the forward drop across D_4 , or a total of about 1.5 volts. Until the current through D_4 increases to about 6.0 milliamperes, point B is clamped to -1.0 volt through the low forward impedance of D_6 . While point A is held at about $+5.0$ volts by D_1 , the current through D_4 cannot exceed 6.0 milliamperes until D_6 is cut off. As point B then becomes more negative than -1.0 volt, a second stage of feedback begins.

After D_6 has been cut off, the incremental feedback becomes linear in nature. Each additional volt developed across the feedback winding produces an additional milliampere of feedback current (for $R_4 = 1,000$ ohms).

Since the input impedance at the emitter is low compared to 1,000 ohms, the additional voltage is evidenced primarily by a drop in potential at point B rather than as a rise at the emitter. Typically, point B drops to -5 volts with respect to ground. The buildup of feedback is terminated by the collector being driven to saturation.

To aid the establishment of the full feedback current, diode D_3 is normally back-biased by about 1.5 volts as in the gated feedback circuits. This prevents the load from diverting current from the feedback loop until an appreciable feedback current is provided. The current gain in the loop might otherwise be reduced to the extent that a full output pulse could not be produced. Many of the nonlinear loads to be driven present a very low incremental impedance initially and thereby aggravate this condition. It appears, therefore, that limiting the ratio of linear to gated feedback is desirable, since gated feedback was designed specifically for this condition. Some linear feedback may be used to compensate for the buildup of magnetizing current in the coupling transformer since this quantity is greatest at the end of the pulse interval and is essentially zero at the start. The buildup of magnetizing current should not be allowed to bring the transistor collector out of saturation until the end of the pulse interval, however. When this occurs, the pulse voltage "rolls off." With linear feedback, emitter current is decreased by any shrinkage of the pulse, and the decrease in emitter current acts to reduce the pulse still more.

Decreasing the linear-to-gated feedback ratio in the amplifier of Fig. 15 requires increasing the clock power. On the other hand, a circuit is shown in Fig. 16 in which the ratio is a function of dc, rather than clock, power.

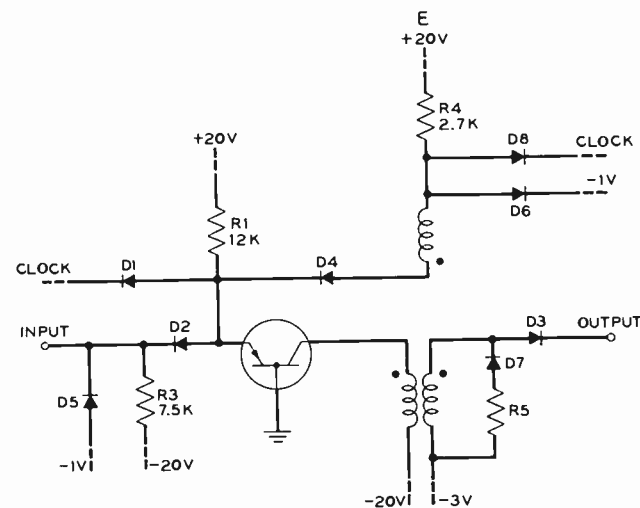


Fig. 16—Semi-gated feedback amplifier.

Specifically, the ratio can be made smaller by an increase in E , the dc supply for the feedback current.

Although the trigger and feedback currents are supplied from dc sources in this amplifier, the basic performance of the feedback circuit is similar to that of the one just described. Slow recovery of reverse impedance in

diode D_1 can degrade performance, however, as in the preceding circuits using the input AND circuit of Fig. 5.

TRANSISTOR CHARACTERISTICS

To provide reasonably uniform circuit performance, several requirements have been established for the transistors. These requirements are listed below and in this form should be interpreted algebraically. The convention of positive currents flowing into the device terminals is used.

1. $I_c (I_e = 8, V_c = -3) \leq -17.0$ milliamperes
2. $I_c (I_e = 0, V_c = -20) \geq -3.0$ milliamperes
3. $f_c (I_e = 1, V_c = -20) \geq 10$ megacycles
4. -0.25 volt \leq Break Point $\leq +0.25$ volt
5. $V_o (I_e = -12, V_c = -10) \geq -0.5$ volt

The quantities in parentheses specify the biasing conditions for the various measurements; all current values are in milliamperes, while voltages are listed in volts.

The first requirement, in conjunction with the second, is to ensure sufficient pulse current gain in the amplifier. In addition, the second requirement also serves to limit the idle condition power dissipation within the transistor. For the third requirement, a lower limit is placed on the alpha cutoff frequency since pulse rise time is related to this quantity, as indicated in the analysis in the Appendix. The range of permissible break points, or emitter cutoff voltages, is limited in the fourth requirement, so that a maximum input trigger voltage can be specified. The final requirement, a minimum limitation on emitter voltage for a specific operating point, is included to ensure return of the transistor to cutoff in response to the clock. Transistors with high base resistance and a consequent $V_o (-12, -10)$ considerably more negative than the limit may "lock-up" in a high conduction state. The following section deals with this condition in more detail.

Lock-up

When this anomalous type of operation occurs, the transistor reaches a high current static condition in which excessive power may be dissipated within the unit. In the material to follow, a heuristic explanation of lock-up, based partially on the static characteristics of the transistor, will be given.

In Fig. 17 the collector characteristics of a typical GA-52514 transistor are shown. Drawn on these characteristics in solid lines is a load line for the normal amplifier load. In normal operation, the transistor starts at point A with zero emitter current. As the emitter current increases, the operating point follows the load line to point B at which the emitter current has reached its peak value. During the "flat top" portion of the pulse, the emitter current is essentially constant. Magnetizing current in the output transformer, however, modifies the solid line load line in the drawing by shifting it to the left. This, of course, is an over-simplified picture of a transient phenomenon, but for our pur-

poses it is adequate. The load line at several times within the pulse interval is shown by the dotted lines. The "droop" on the back edge of the pulse is seen to be the result of the load line moving out of the saturation region. Now, when the clock swings negative and the emitter current starts to decrease, the operating point on the collector characteristics follows the dotted line vertically downward to point C where the characteristic breaks sharply. The operating point then follows the nearly horizontal load line back to point A .

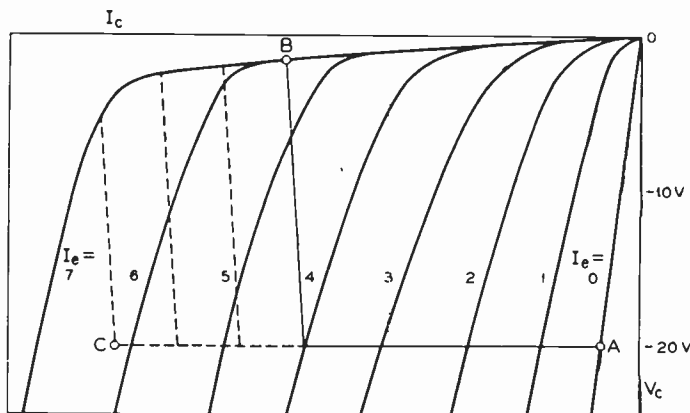


Fig. 17—Typical GA-52514 transistor collector characteristics.

The possibility of lock-up in the high conduction state results from the fact that the emitter current is not supplied from a perfect current source controlled by the clock. Another factor which must be determined, therefore, is the emitter voltage during the turn-off interval. A consideration of the $V_e - I_e$ characteristic shows that the emitter voltage reaches its minimum value at the break in the load line. For the transistor to be turned off, the clock voltage must be sufficiently negative to hold the emitter voltage at or below this critical value for sufficient time. The time required depends on the transient response of the transistor and the degree of saturation of the collector. The delay in turn-off caused by minority carrier storage is minimized in these circuits by virtue of the magnetizing current pulling the transistor out of saturation before the end of the pulse interval.

If the clock does not turn off the transistor at the end of the pulse interval, the load line in Fig. 17 continues to move to the left. At the time of the next negative excursion of the clock, the break in the load line is still further to the left (higher collector current), and the critical emitter turnoff voltage is still lower. As a result, the transistor never turns off. Ultimately, the load line extends so far to the left that the collector voltage drops to the collector supply voltage (-20v.) and the transistor is said to be locked up.

The condition existing at the emitter when a transistor is locked up is of interest. In a number of these particular units the emitter potential drops almost to the potential at the collector, indicating a very low

emitter-to-collector impedance. When this occurs, the power dissipated in the transistor is approximately the product of base current (in the order of 20 milliamperes) and collector voltage (20 volts).

Transistors which might tend to lock up in the amplifier circuit are virtually all eliminated through the imposition of the requirement on V_e (-12, -10). A more desirable requirement would be the emitter voltage corresponding to the break in the load line on the collector characteristic ($V_c = 20$ volts, $I_c \sim 15$ ma). Unfortunately, this corresponds to a rather high power dissipation and could not safely be measured statically. The correlation between V_e (-12, -10) and lock-up in the amplifier circuit has been excellent, however.

It is significant that most transistors of the type employed in this amplifier do not lock up even when the clock voltage is removed. Since during lock-up the collector load is essentially a short circuit, the transistor emitter characteristic (V_e vs I_e) with the collector short circuited is shown in Fig. 18. Superimposed on this characteristic is the emitter load line corresponding to the circuit of Fig. 15. It can be seen that transistors having short circuit emitter characteristics of the type labeled I have no high current point of stability and cannot lock up. Those transistors with characteristics similar to those shown as II and III, however, do have a high current stable point and might potentially lock up. Ideally, all transistors used in the amplifier circuits described in this paper should be of type I.

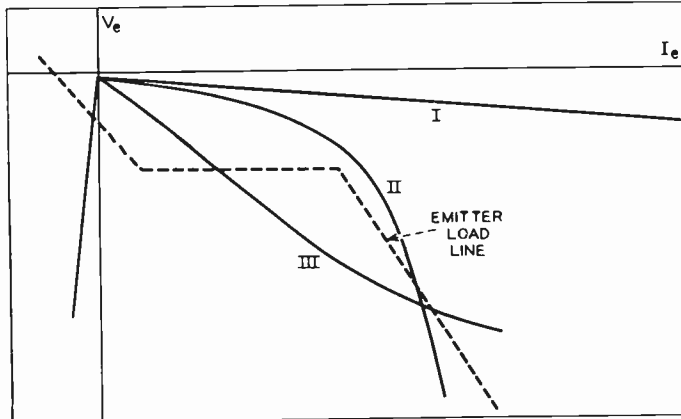


Fig. 18—GA-52514 emitter characteristics.

CONCLUDING REMARKS

Each of the amplifiers described in the preceding sections has been built and tested. Moreover, several hundred semi-gated feedback amplifiers of the type shown in Fig. 15 have been built, and approximately 100 of these have been operating satisfactorily for over 10,000 hours in typical computer circuits. Operating margins of ± 20 per cent or greater, obtained by varying supply voltages independently, have been consistently observed in this equipment.

The performance of the semi-gated feedback amplifier of Fig. 15 appears to be satisfactory and comparable to that of the gated feedback amplifiers such as that shown in Fig. 13, while it is a somewhat simpler circuit. As in several of the amplifier circuits described, the effect of diode reverse transients on amplifier performance is minimized in this configuration.

ACKNOWLEDGMENTS

The authors wish to acknowledge the work of Mrs. J. L. G. Landry in making the many computations for the curves presented.

All of the work on these regenerative amplifiers has been done under contract with the Bureau of Ordnance of the U. S. Navy.

APPENDIX

Amplifier Rise-Time Analysis

As indicated in the discussion of operation, various diodes open and close and the transistor is driven to saturation in these amplifiers during the rise-time interval. Consequently, the performance is quite nonlinear. In the following analysis, the operation is separated into discrete regions in which linear theory is assumed to apply. Many additional simplifying assumptions are made to make the otherwise cumbersome expressions somewhat more manageable as well as interpretable. In spite of these short-cuts (or perhaps because of them), it is believed that the solutions obtained provide a considerable insight into the pulse rise performance of the amplifier. Calculations based on this analysis appear reasonable when compared with experimental results.

The specific circuit for which the analysis is made is the semi-gated feedback amplifier of Fig. 15. With only slight modification, however, the analysis is applicable to the gated feedback amplifiers.

For the semi-gated feedback amplifier, at least five discrete regions can be defined during the pulse rise. The interval of the initial region extends from the instant when trigger current first enters the emitter to the time at which the voltage developed across feedback winding of the transformer is just sufficient to overcome the back-bias on diode D_4 . The duration of this interval is extremely short and is considered negligible in the present analysis. The second interval begins when the first one ends and is terminated when the current through D_4 and the feedback winding rises to the value necessary to cut off diode D_6 (*i.e.*, when this current becomes equal to that flowing through resistor R_4). This is called region I in the work that follows. A third interval which sometimes exists begins at the end of the second and is terminated when the voltage across the output winding has risen sufficiently to just overcome the back-bias on diode D_3 . Again this very short time interval has been ignored.

Two additional regions exist if it is assumed that the amplifier drives a nonlinear load similar to that characterized in Fig. 3. The interval of the first of these load regions commences just as the back-bias of diode D_3 is overcome and lasts until the load current rises to the value corresponding to the break in the load characteristic. This is called region II in the following. The other interval called region III begins as region II ends and is terminated when the transistor collector is driven to saturation.

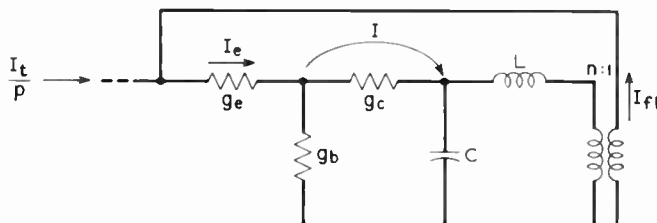


Fig. 19—Equivalent circuit for region I.

Fig. 19 shows the equivalent circuit which is assumed for region I in which feedback current through diode D_4 rises from zero to the approximately 6 milliamperes necessary to cut off diode D_6 —in other words, the gated feedback interval. The transformer equivalent circuit includes a leakage inductance L , a shunt capacitance C , and an ideal transformer with an $n:1$ turns ratio. Additional elements, such as magnetizing inductance or other capacitances are believed less important and are deleted for simplicity. The current I is assumed to be related to the emitter current by the expression,

$$I_e(t) = \frac{1}{a_0} I(t) + \frac{1}{a_0 \omega_c} \frac{dI(t)}{dt}$$

where

$$a_0 = \alpha_0 + (\alpha_0 - 1) \frac{r_b}{r_e} \sim \alpha_0$$

and α_0 is the dc short-circuit current gain of the transistor. The interpretation of ω_c is more apparent if the above relation is expressed in terms of the Laplace complex frequency operator p .

$$I_e(p) = \left(\frac{1}{a_0} + \frac{1}{a_0} \frac{p}{\omega_c} \right) I(p) - \frac{1}{a_0 \omega_c} I(0).$$

If initial conditions are zero; i.e., $I(0) = 0$, then

$$I(p) = \frac{a_0}{1 + \frac{p}{\omega_c}} I_e(p)$$

and ω_c is seen to be the angular frequency at which the factor relating I to I_e is down 3 db from a_0 . Since for all practical purposes a_0 is essentially α_0 , ω_c is essentially the angular α -cutoff frequency of the transistor.

One final assumption should be noted. The trigger current is considered to be a step function. While this is a very close approximation to the actual conditions in the amplifier of Fig. 16, it is somewhat less realistic when used for the amplifier of Fig. 15 in which the trigger current is actually derived from a clipped sine wave voltage operating through a resistor.

Based on these conditions nodal analysis leads to the following characteristic equation for the feedback current:

$$I_{fb} = \frac{I_t}{p} \frac{b_2 p^2 + b_1 p + b_0}{C_3 p^3 + C_2 p^2 + C_1 p + C_0} = \frac{I_t}{p} \frac{Y(p)}{Z(p)}$$

where

$$\begin{aligned} b_2 &= -n^2 C [1 + r_e(g_b + g_c)] \\ b_1 &= g_b + g_c [1 + nr_e g_b - n^2 (1 + r_e g_b)] \\ &\quad + n^2 \omega_c [a_0 - 1 - r_e(g_b + g_c)] \\ b_0 &= \omega_c \{(na_0 + 1)g_b + g_c[1 - n^2(1 + r_e g_b)]\} \\ c_3 &= LC(g_b + g_c) \\ c_2 &= g_b g_c L + (g_b + g_c) \omega_c LC + n^2 C [1 + r_e(g_b + g_c)] \\ c_1 &= g_b + g_c(n - 1)^2 + \omega_c L g_c g_b + n^2 r_e g_c g_b \\ &\quad - n^2 \omega_c C [a_0 - 1 - r_e(g_b + g_c)] \\ c_0 &= \omega_c [g_b(1 - na_0) + g_c(n - 1)^2 + n^2 g_c r_e g_b]. \end{aligned}$$

The time solution for such an equation is:

$$\frac{I_{fb}}{I_t} = \frac{Y(0)}{Z(0)} + \sum_{k=1}^n \frac{\frac{Y(p_k) e^{r_k t}}{p_k \prod_{j=1}^n (p_k - p_j)}}{p_k}, \quad j \neq k$$

where the various p_k 's are the roots of $Z(p)$. Region I ends when I_{fb} equals 6 milliamperes, so with this value substituted in the expression above and I_t set equal to 1.5 milliamperes, the value of t corresponding to the length of the time interval can be determined.

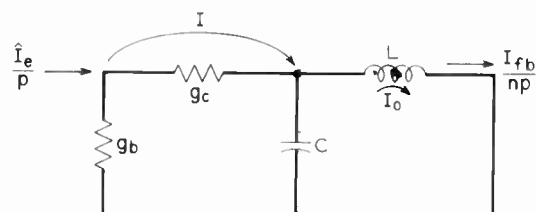


Fig. 20—Equivalent circuit for region II.

The equivalent circuit assumed for the next region (II) is shown in Fig. 20. In this region, the amplifier works into the low incremental impedance portion of the load, and in the equivalent circuit the load is assumed to be a short circuit. The feedback current established during the preceding region is shown here as a step function current generator labeled I_{fb}/np , since this current remains essentially unchanged during this

interval. Similarly, the emitter current is assumed to be a step function current generator labeled \hat{I}_e/p , and on this basis the emitter resistance is deleted.

For this region the characteristic equation defining the load current is:

$$I_0 = \frac{d_2 p^2 + d_1 p + d_0}{p(p + \omega_c)(h_2 p^2 + h_1 p + h_0)}$$

where

$$d_2 = (g_b + g_c)CV_2(0)$$

$$d_1 = \hat{I}_e g_c + I(0)g_b + (g_b + g_c)[\omega_c CV_2(0) - I_L(0)]$$

$$d_0 = \hat{I}_e(a_0 \omega_c g_b + \omega_c g_c) - \omega_c(g_b + g_c)I_L(0)$$

$$h_2 = L C(g_b + g_c)$$

$$h_1 = L g_b g_c$$

$$h_0 = g_b + g_c$$

and

$$\hat{I}_e = I_t + I_{fb}(0)$$

$I_L(0)$ is the current through the leakage inductance at the start of this interval,

$V_2(0)$ is the voltage across the capacitance at the start of this interval, and

$I(0)$ is the initial condition of the current generator in the transistor equivalent network.

$$I(0) \sim L C \frac{d^2 I_{fb}(0)}{dt^2} + \frac{I_{fb}(0)}{n}$$

A time solution can be obtained as before by finding the roots of the denominator of the characteristic equation. By inserting the upper boundary value for I_0 (6 milliamperes), the duration of this region can thus be obtained.

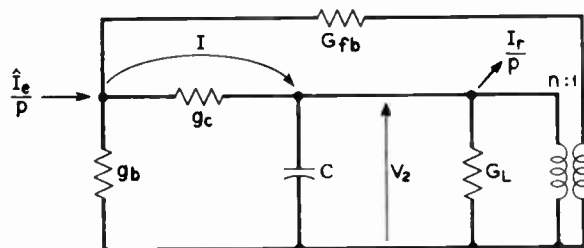


Fig. 21—Equivalent circuit for region III.

For the third and final region of the analysis (III) the equivalent circuit of Fig. 21 is assumed. In this region, the amplifier works into the high incremental impedance portion of the load characteristic. The load is therefore assumed to consist of a conductance, G_L , referred to the primary side of the transformer, in addition to a step function current generator labeled I_r/p . This latter component is necessary to account for the load and feedback currents established in the preceding regions. Another step function current generator labeled \hat{I}_e/p is included as in region II to account for the trigger current plus the

gated feedback current established in region I. In addition, the linear feedback current is introduced to the emitter through G_{fb} .

Leakage inductance is deleted from the equivalent circuit, since the incremental load impedance is high. Also, the initial voltage and current of the condenser are assumed to be zero. I , therefore becomes $I(0)$.

The termination of this region is considered to occur when the pulse voltage rises to 18 volts at the collector, as this is a typical condition existing when the collector reaches saturation. Accordingly, the characteristic equation is written for the pulse voltage developed at the collector and is:

$$V_2(p) = \frac{\hat{I}_e}{p} \frac{k_1 p + k_0}{m_2 p^2 + m_1 p + m_0} + \frac{I(0)}{p} \frac{u_2 p^2 + u_1 p + u_0}{(p + \omega_c)(m_2 p^2 + m_1 p + m_0)}$$

where

$$k_1 = -\left(\frac{G_{fb}}{n} + g_c\right)$$

$$k_0 = \omega_c \left[\frac{G_{fb}}{n} (a_0 - 1) - g_c - a_0 g_b \right]$$

$$m_2 = -C(G_{fb} + g_c + g_b)$$

$$m_1 = \left[(a_0 - 1)\omega_c C G_{fb} - g_c G_{fb} \left(1 - \frac{1}{n} \right)^2 - G_L G_{fb} \right.$$

$$\left. - g_c G_L - \omega_c C g_c - g_b \left(g_c + G_L + \frac{G_{fb}}{n^2} \right) - \omega_c C g_b \right]$$

$$m_0 = \omega_c \left[(a_0 - 1)G_{fb}G_L + \frac{a_0 g_b G_{fb}}{n} - g_c G_{fb} \left(1 - \frac{1}{n} \right)^2 \right.$$

$$\left. - g_c G_L - g_b \left(g_c + G_L + \frac{G_{fb}}{n^2} \right) \right]$$

$$u_2 = g_c + \frac{G_{fb}}{n}$$

$$u_1 = \omega_c \left[G_{fb} \left(1 + \frac{1}{n} - a_0 \right) + 2g_c + g_b \right]$$

$$u_0 = \omega_c^2 [G_{fb}(1 - a_0) + g_b + g_c].$$

While the equations derived are useful, the manner in which rise time is governed by the various parameters is more easily seen from the curves of Figs. 22 and 23, plotted from these equations. In these, the merits of increased transistor cutoff frequency, α , decreased shunt capacitance, and transformer leakage inductance can be noted. For the range of values considered here, leakage inductance appears to have least effect while the other three parameters are somewhat equivalent to one another in influence on the rise time. The total rise times indicated here as ranging from 0.02 to 0.05 microsecond are consistent with measured rise times ranging from 0.03 to 0.05 microsecond.

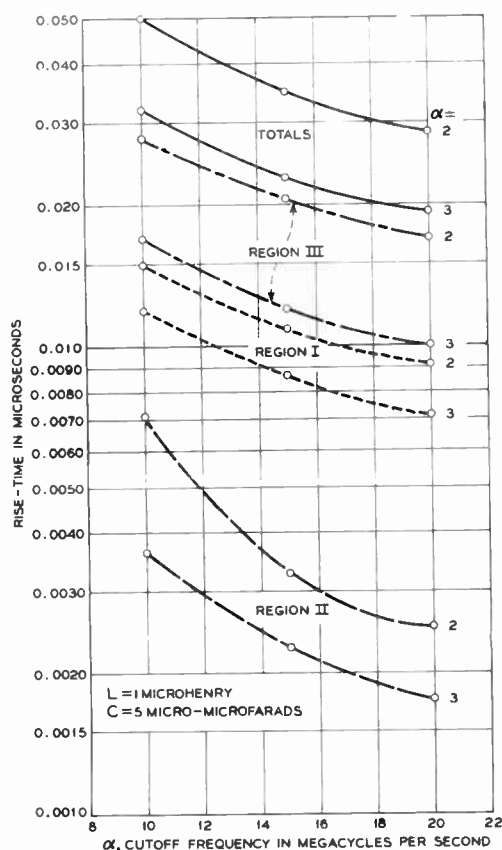


Fig. 22—Computed rise times as a function of the transistor parameters.

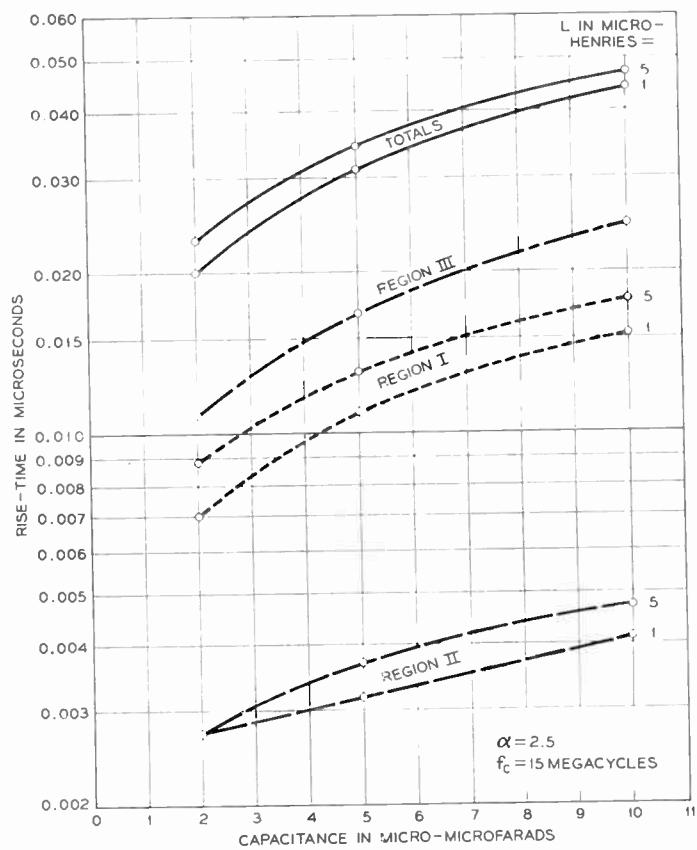


Fig. 23—Computed rise times as a function of the transformer parameters.

A Developmental Wide-Band, 100-Watt, 20 DB, S-Band Traveling-Wave Amplifier Utilizing Periodic Permanent Magnets*

W. W. SIEKIEWICZ† MEMBER, IRE, AND F. STERZER†

Summary—A developmental, 100-watt, S-band traveling-wave amplifier utilizing ceramic "periodic" permanent magnets to focus the electron beam is described. The minimum peak power output of the tube is 100 watts at a gain of at least 20 db at frequencies from 2,000 to 3,800 megacycles per second. At lower power levels, a gain of 36 db has been measured in the center of the frequency band. The operating voltages for the amplifier are below 4,000 volts. The use of "periodic" magnets in place of conventional solenoids or permanent magnets producing uniform magnetic fields effects a considerable reduction in the weight and size of the focusing system. Constructional features of the tube which permit operation with the "periodic" magnet are discussed. The rf characteristics of this amplifier are evaluated, and the complete "package" assembly is described.

* Original manuscript received by the IRE, July 5, 1955; revised manuscript received August 12, 1955. This tube was developed for the U. S. Air Force under Contract No. AF 33(600)-24400, sponsored by the Wright Air Development Center, Dayton, Ohio.

† Tube Division, RCA, Harrison, N. J.

INTRODUCTION

THIS paper describes a developmental, S-band, 100-watt, 20-db traveling-wave amplifier, shown in Fig. 1, which utilizes "periodic" permanent magnets for focusing of the electron beam. The tube operates at a beam duty of 100 per cent and rf power-

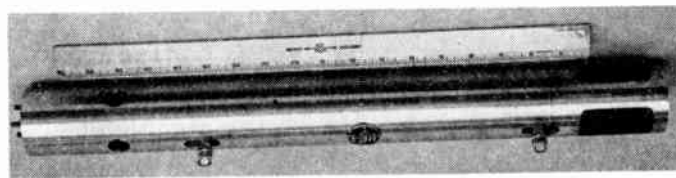


Fig. 1—View of "packaged" traveling-wave power amplifier including "periodic" permanent magnets for beam focusing. The tube is shown in the lower portion of the figure.

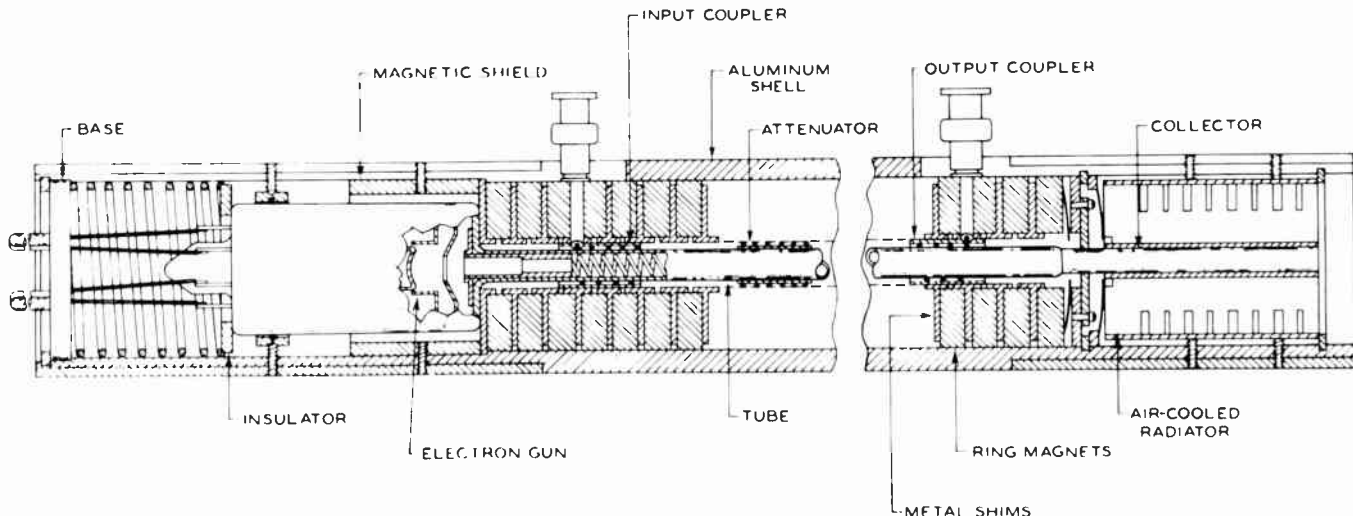


Fig. 2—Schematic diagram of traveling-wave-amplifier assembly.

output duty of 0.1. In the present design, the rf power-output duty cycle is limited to 10 per cent by rf heating of the helix. This basic design is now being modified so that it will also provide continuous rf power operation at a power-output level of at least 100 watts.

The permanent-magnet assembly used in conjunction with this tube weighs 2.8 pounds and replaces a solenoid which, for this application, would weigh about 50 pounds. The use of the permanent magnet also eliminates the power supply required to drive a solenoid. A "packaged assembly" including the tube, the "periodic" permanent magnet, and an air-cooled collector is shown in Fig. 1. A schematic diagram of the assembly is shown in Fig. 2.

DESCRIPTION OF COMPONENTS

Permanent Magnet

The design of a light-weight permanent magnet suitable for use in a "packaged" assembly was a major consideration in the development of this traveling-wave amplifier. The required magnetic-field intensity is reduced by the use of a convergent type of electron gun in which the cathode is shielded from the magnetic field. When purely magnetic means are used for beam focusing, an electron beam launched from a shielded cathode requires a smaller magnetic field for focusing than a beam from a cathode which is partially or totally immersed in a magnetic field.¹ Calculations and preliminary experiments indicated that a uniform magnetic field of 450 gauss would be required over a cylindrical region about $\frac{1}{4}$ inch in diameter and 12 inches long. The weight of a permanent magnet which produced a uniform field of 450 gauss over the required region was considered impractical. However, consideration of the dc parameters and of the electron-beam geometry indicated that permanent magnets producing a "peri-

odic" magnetic field in the region of electron flow could be built with commercially available materials.

The focusing of long electron beams by means of periodic magnetic fields has been described previously.²⁻⁴ The periodic magnet developed for use with the traveling-wave amplifier is shown in Fig. 3. This type of struc-

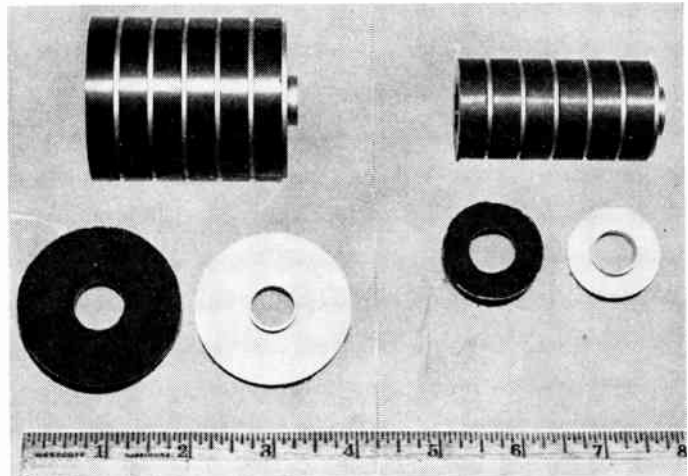


Fig. 3—Sections of "periodic" permanent-magnet assemblies using two different types of magnetic materials. The magnet at the left, made of commercially-available ceramic, weighs 0.510 pound per inch of axial length. The magnet at the right, made of RCA-ceramic ring magnets, weighs 0.200 pound per inch of axial length. Individual ring magnets and shims are shown in the lower portion of Fig. 3.

ture, which consists of a series of ceramic ring magnets separated by metal shims, is considerably lighter in weight than either solenoids, or permanent magnets which produce uniform magnetic fields.

The variation of the axial component of the magnetic field produced by the periodic magnet is very nearly

¹ J. T. Mendel, C. F. Quate, W. H. Yocom, "Electron beam focusing with periodic permanent magnet fields," PROC. IRE, vol. 42, pp. 800-810; May, 1954.

² Kern K. N. Chang, "Beam focusing by periodic and complementary fields," PROC. IRE, vol. 43, pp. 62-71; January, 1955.

³ A. M. Clogston and H. Heffner, "Focusing of an electron beam by periodic fields," J. Appl. Phys., vol. 25, pp. 436-447; April, 1954.

⁴ C. C. Wang, "Electron beams in axially symmetrical and magnetic fields," PROC. IRE, vol. 38, pp. 135-147; February, 1950.

sinusoidal, as shown in Fig. 4. For good focusing, it is necessary that the amplitude and period of the magnetic field in the region of the electron beam satisfy certain conditions.² For operation in the first "pass band" using a magnetically shielded cathode, the following relationship must be satisfied:

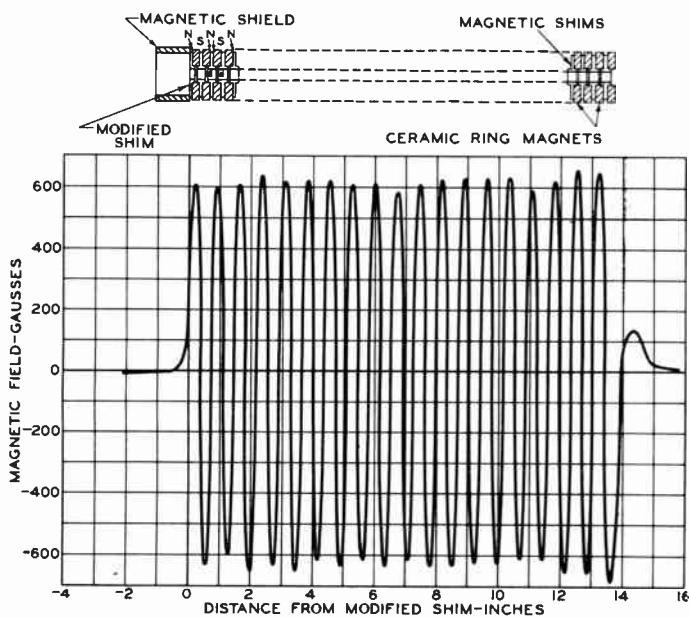


Fig. 4—Magnetic field strength of commercial-ceramic magnet, shown in the upper portion of the figure, along the axis of the traveling-wave amplifier.

$$\frac{eB_0^2L^2}{mV} < 418 \quad (1)$$

where

B_0 = amplitude of the sinusoidal magnetic field in webers per square meter,

L = period in meters,

V = beam (helix) voltage in volts, and

$e/m = 1.759 \times 10^{11}$ coulombs per kilogram.

In addition,

$$B_0 = \sqrt{2}B_b \quad (2)$$

where B_b is the uniform magnetic field required to focus the beam (often called the "Brillouin field"). This field can be expressed as follows:⁵

$$B_b = 8.26 \times 10^{-4} \frac{I^{1/2}}{aV^{1/4}} \quad (3)$$

where I is the beam current in amperes and a is the radius of the electron beam in meters. In practice, the magnetic field required for good focusing of the electron beam is approximately 1.5 to 2 times the theoretical value⁶ calculated from (3).

⁵ J. R. Pierce, "Theory and Design of Electron Beams," D. Van Nostrand Co., Inc., New York, N. Y., p. 143; 1949.

⁶ Mendel, Quate, and Yocom, *op. cit.*

Preliminary experiments showed that the uniform magnetic field required for focusing of the beam in this traveling-wave tube is 450 gauss. When this value is substituted in (2), it is determined that the amplitude of the periodic field should be approximately 635 gauss. When this value is used for B_0 in (1), the value of the period L is calculated to be less than 2 inches. Operation at short periods is desirable because the degree of beam "scalloping" is reduced as the period of the magnetic field becomes smaller.⁷ "Scalloping" is a periodic variation of the beam boundary caused by the periodic nature of the magnetic field. Only a small degree of beam scalloping is permissible in this tube because operation at a high beam-to-helix-diameter ratio is necessary for good rf performance.

A periodic-magnet assembly built of commercially-available ceramic ($\text{BaFe}_{12}\text{O}_{19}$) is shown at the left of Fig. 3. This assembly consists of a series of ring magnets and magnetic shims. The ring magnets, which are axially magnetized, have an outside diameter of 2 inches and are assembled so that their adjoining faces have the same polarity. The cold-rolled steel shims provide a low-permeance path for the flux from the ring magnets to the useful air gap, and also reduce any deviations of the field from axial symmetry.

The inside diameter of the shims should be kept small because the magnetic field strength on the axis increases as the inside diameter of the shims is reduced. With a smaller inside diameter, therefore, the required magnetic field can be obtained with less magnetic material and a lighter structure. Consequently, the radial dimensions of the tube parts and accessories which fit inside the shims are designed to be as small as possible. An inside diameter of the shims of 0.525 inch satisfies both the magnetic and mechanical requirements.

Magnetic materials having a large coercive force make it possible to obtain high field intensities for a design having a small period. Because ceramic magnetic materials have a large coercive force, they are suitable for this application.

Sections of permanent-magnet assemblies built of two different ceramic materials are shown in Fig. 3. The magnet at the left, which is made of commercially available ceramic ($\text{BaFe}_{12}\text{O}_{19}$), has a total weight of 7.1 pounds for its length of $13\frac{7}{8}$ inches. The magnet at the right is made of a new type of magnetic ceramic developed at the RCA Laboratories. This material has a higher energy product at the operating point for this magnetic circuit, and, therefore, permits construction of a smaller and lighter assembly. The total weight of this magnet is 2.8 pounds for a length of $13\frac{7}{8}$ inches. It can be seen that both of the structures shown in Fig. 3 effect a considerable reduction in weight as compared with the solenoid which, for this application, weighs over 50 pounds.

The period of the assemblies shown in Fig. 3 is 40 per cent of the theoretical limit of 2 inches calculated

⁷ *Ibid.*

from (1). The diagram at the top of Fig. 4 shows the constructional features of the commercial-ceramic assembly. The magnetic-field distribution about the axis of the magnet is also shown in Fig. 4. In the region near the electron-gun end of the tube, the desired "launching field" for the electron beam is obtained by the use of a magnetic shield and by the modification of the first shim of the structure. The construction of the magnet using the RCA developmental ceramic is similar to that shown in Fig. 4 except that the outside diameter is $1\frac{1}{4}$ inches. Average peak magnetic-field intensity of the periodic magnet using RCA ceramic is 600 g.

Electron Gun

The electron gun used in the traveling-wave tube is a convergent type in which the cathode is shielded from the magnetic field. The gun has a perveance⁸ of 1.2 micropervs and a mean cathode-current density of 180 milliamperes per square centimeter at a collector current of 250 milliamperes. The initial design of the cathode and the focusing electrodes was based on information given by Pierce⁹ and Helm, Spangenberg, and Field.¹⁰ Electrode shapes were subsequently modified slightly on the basis of actual dynamic measurements to maintain the anode interception as low as possible and to obtain the required perveance. Under normal operating conditions, the current intercepted by the anode is less than 0.2 per cent of the cathode current.

Helix

The helix consists of 0.030 inch molybdenum wire wound at a pitch of 0.100 inch. The helix, which has an inner diameter of 0.218 inch, fits into precision glass tubing.

Helix-to-Coaxial-Line Transducers

"Coupled-helix" transducers are used to feed rf energy into and out of the tube. This method of coupling is based on the transfer of electromagnetic energy obtained between two oppositely-wound helices when the outside helix is designed to have proper pitch and length with respect to the inside helix.^{11,12} Couplers of this type provide a good match over a very wide range of frequencies. The standing-wave ratio of the transducers, measured in the absence of the electron beam, is below 1.7 in the frequency range from 2,000 to 4,000 megacycles per second, as shown in Fig. 5.

⁸ For an electron gun operating under space-charge limited conditions, the cathode current I_c (amps) is related to the anode voltage V_a (volts) as follows: $I_c = K \times 10^{-6} V_a^{3/2}$, where K is the perveance in micropervs.

⁹ Pierce, *op. cit.*

¹⁰ R. Helm, K. Spangenberg and L. M. Field, "Cathode design procedure for electron beam tubes," *Elec. Comm.*, vol. 24, pp. 101-107; March, 1947.

¹¹ O. G. Owens, "Coupled helix attenuators for traveling-wave tubes," Tech. Rept. No. 68, Stanford University, California; August, 1953.

¹² R. Kompfner, "Some theory and experiments on coupled helices"; paper presented at the Conference on Electron Tube Research, Palo Alto, Calif.; June 19, 1953.

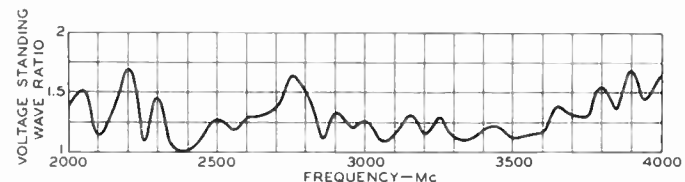


Fig. 5—Voltage standing-wave ratio of "coupled-helix" type of helix-to-coaxial-line transducer as a function of frequency.

The "coupled-helix" transducer is well-suited for use with a periodic magnet because its radial dimensions can be made small. The mechanical construction of the coupler is shown in Fig. 6. The inner conductor of the coaxial line of the transducer is extended to form the outside helix. The coaxial line is brought out through a slot cut in the magnetic shim of the ceramic magnet and through semicircular holes provided in the adjoining ring magnets. Because these modifications to the magnetic circuit are very small, they have a negligible effect on the axial component of the magnetic field.

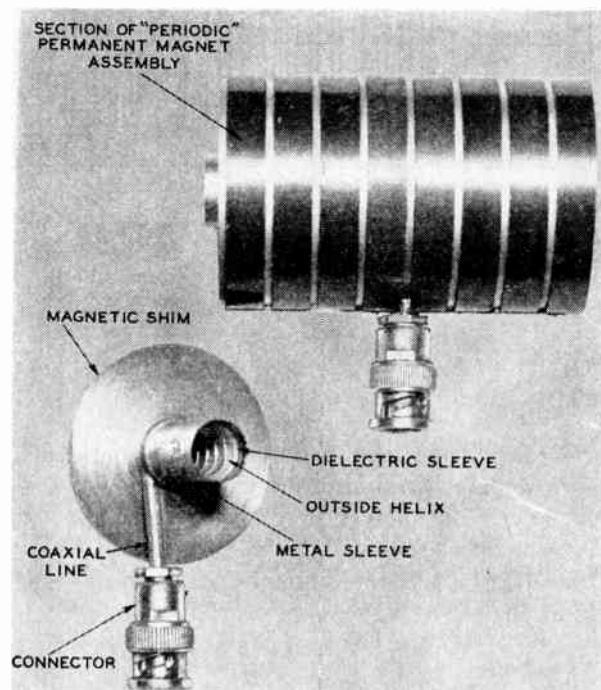


Fig. 6—Coupled-helix type of transducer built into a magnetic shim of "periodic" permanent magnet.

Attenuator

The attenuator used for stabilization of the tube is also of the "coupled-helix"¹³ type, as shown in Fig. 7. The attenuator helix is wound on a thin ceramic sleeve, and carbon is then deposited throughout the volume of the porous ceramic by pyrolysis of methane gas at a temperature of about 1,000 degrees C in a rotating quartz bottle.¹⁴ This attenuator has high power-dissipating capabilities. Attenuation is achieved by the

¹³ *Ibid.*

¹⁴ The application of carbon to the ceramic sleeve was performed at the Pyrofilm Resistor Co., Morristown, N. J., under the direction of Dr. J. M. Hinkle.

transfer of energy from the helix of the tube to the attenuator helix, and the dissipation of the energy in the carbon. A quadrifilar attenuator helix provides more uniform attenuation over the desired range of frequencies. Position of the attenuator along the bulb of the tube is adjusted for best rf performance during preliminary tests; the ceramic sleeve is then sealed to the bulb.

Packaged Design

The packaged design of the developmental traveling-wave amplifier shown in Fig. 1 includes commercial-ceramic ring magnets for focusing of the electron beam and has a total weight of 11 pounds. The use of RCA developmental ceramic permits design of a "package" which is 4.3 pounds lighter. The air-cooled collector is capable of dissipating at least one kilowatt of continuous dc power. The input and output terminals of the amplifier use standard coaxial-line bnc connectors. The total length of the assembly is 21 inches.

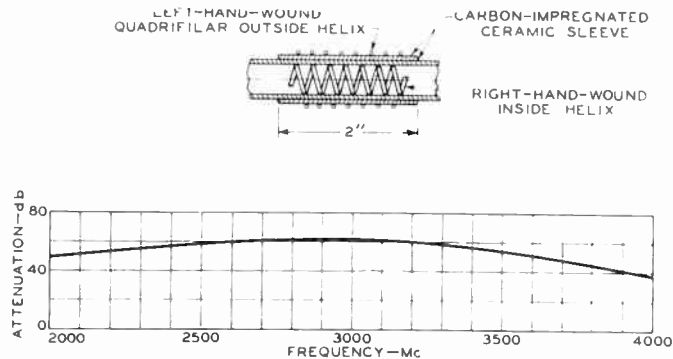


Fig. 7—Coupled-helix type attenuator and its frequency characteristic.

TUBE CHARACTERISTICS

DC Performance

The dc performance of the traveling-wave tube using "periodic" magnets for focusing of the electron beam is as follows: when the tube is operated at the collector current of 250 milliamperes required to provide the desired rf performance, the current intercepted by the helix is less than one per cent of this value.

RF Performance

The design objectives for this tube were a minimum peak power output of 100 watts at a gain of at least 20 db over the widest possible frequency range centered at 3,000 megacycles per second at electrode voltages below 4,000 volts. When a collector current of 250 milliamperes is used and the helix voltage is held constant at 3,750 volts, maximum frequency bandwidth is obtained for large signal levels. Power output and small-signal gain measured under these conditions are shown as functions of frequency in Fig. 8. The rf peak power output obtained at rf peak power inputs of 1 and 0.5 watts is shown by curves *A* and *B*, respectively. A minimum power output of 100 watts at a gain of at

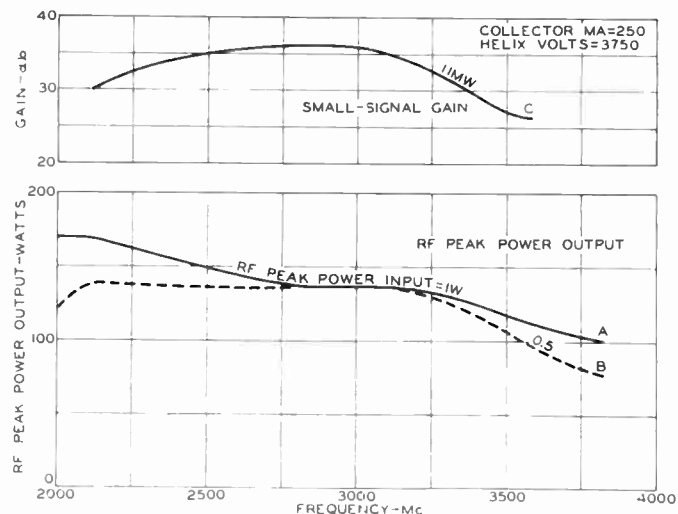


Fig. 8—RF peak power output and small-signal gain as functions of frequency.

least 20 db is obtained at frequencies from 2,000 to 3,800 megacycles per second. When the rf peak power input is 0.5 watt, the tube operates under "saturated" conditions from 2,800 to 3,200 megacycles per second, but below saturation from 2,000 to 2,800 megacycles per second and from 3,200 to 3,800 mcps.

The small-signal gain, measured for an rf peak input power of about 11 milliwatts, is shown by curve *C* of Fig. 8. The small-signal gain is 36 db in the center of the frequency band, but drops to lower values at higher and lower frequencies.

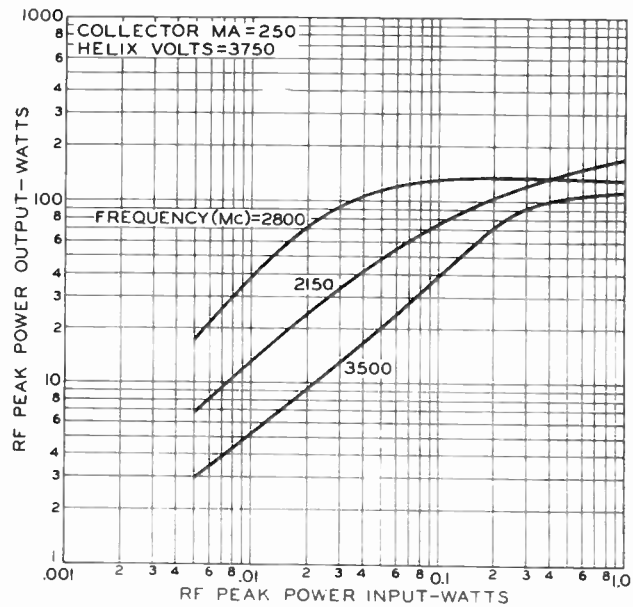


Fig. 9—RF peak power output as a function of rf peak power input.

Peak power output is shown in Fig. 9 as a function of peak power input at three frequencies. Values of helix voltage and collector current are the same as those used in Fig. 8. The tube "saturates" at lower input-power levels in the center of the band than at higher or lower frequencies.

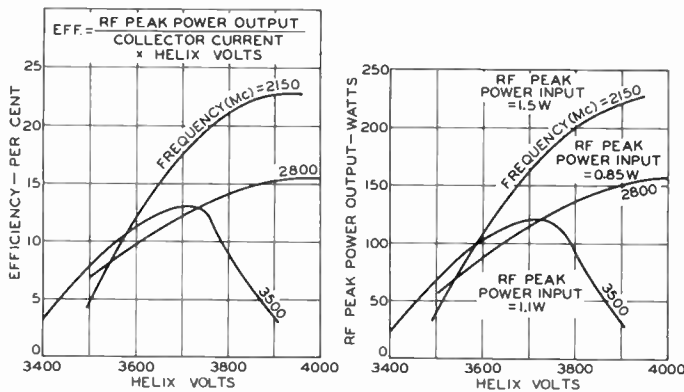


Fig. 10—"Saturated" rf peak power output and efficiency as functions of helix voltage at a collector current of 250 milliamperes.

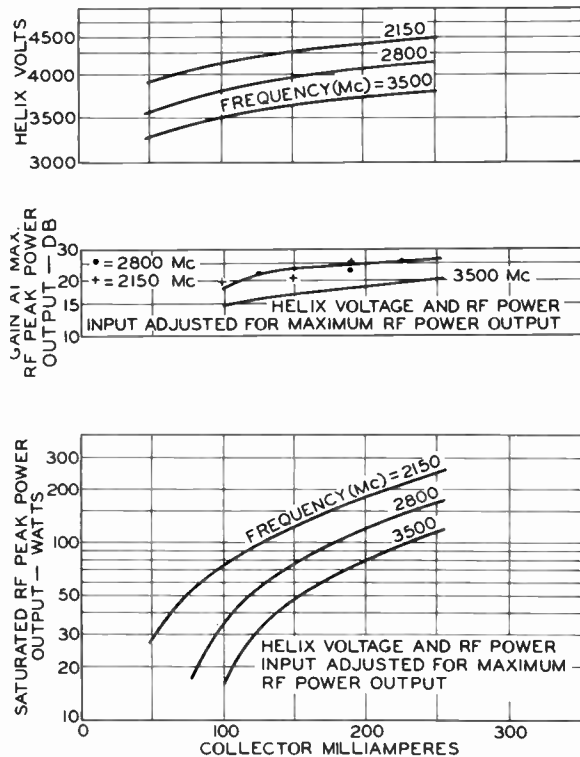


Fig. 11—"Saturated" rf peak power output and corresponding gain and helix voltages as functions of collector current.

If the tube is required to operate over only part of the band, a power output higher than that shown for broadband conditions can be obtained. The "saturated" rf peak power output and efficiency are shown in Fig. 10 as functions of helix voltage at three frequencies. At low frequencies, a peak power output of 230 watts at an efficiency of 22 per cent can be realized by adjustment of the helix voltage to a value favorable for the low-frequency range. This value compares with a power output of 180 watts and an efficiency of 19 per cent when the helix voltage is adjusted for broadband operation.

If the use of a lower power level and gain is desired, the tube can be operated at a reduced collector current. The saturated rf peak power output and corresponding gain and helix voltage are shown in Fig. 11 as functions of collector current.

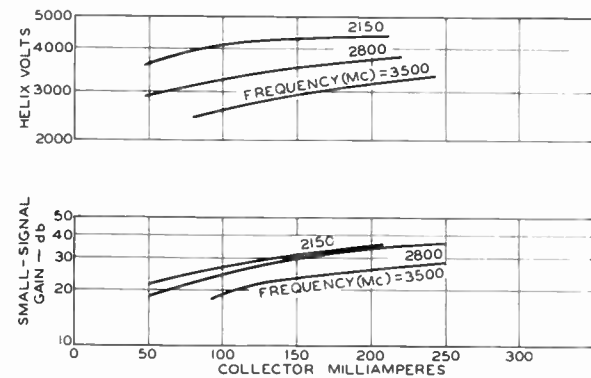


Fig. 12—Maximum small-signal gain and corresponding helix voltage as functions of collector current.

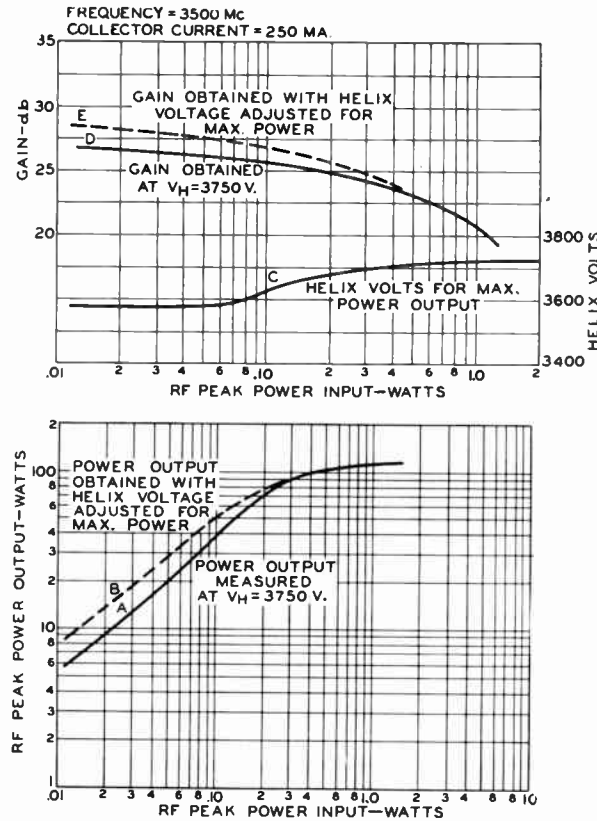


Fig. 13—RF peak power output and gain as functions of rf peak power input at constant and optimized helix voltages at a frequency of 3,500 megacycles per second.

The maximum small-signal gain and the corresponding helix voltage are shown as functions of collector current in Fig. 12. The maximum small-signal gain at any value of collector current is 5 to 10 db higher than the gain at "saturation." In addition, the helix voltage required for maximum small-signal gain is lower than the helix voltage for maximum gain at large signal levels. The rf peak power output and gain are shown in Fig. 13 as functions of rf peak power input at constant and optimized helix voltages at a frequency of 3,500 megacycles per second. The curves of Fig. 13 indicate how the linearity of the tube can be improved by proper adjustment of the helix voltage. Curve D of Fig. 13 shows the gain obtained at a constant helix voltage of

TABLE I

Voltages	below 4,000 volts for wide-band operation.
Collector current	250 milliamperes
Helix current	less than 1 per cent of collector current
DC operation	100 per cent beam duty
RF operation	10 per cent duty ¹⁶
RF power output at constant helix voltage of 3,750 volts	100 to 170 watts at a gain of at least 20 db from 2,000 to 3,800 mc
Small-signal gain	36 db at center frequencies, 28 db at 2,000 mc, 25 db at 3,500 mc
Mechanical features	"Packaged" design including periodic permanent magnet for electron-beam focusing and air-cooled collector
Total length	21 inches
Total weight of "packaged" assembly using commercial-ceramic magnets	11 pounds (weight of permanent magnet alone = 7.1 pounds)
Total weight of "packaged" assembly using RCA-ceramic ring magnets	6.7 pounds (weight of permanent magnet alone = 2.8 pounds)

¹⁶ The present design can be operated at average power-output levels up to 25 watts. The basic design is now being modified so that the tube will also provide continuous rf power operation up to average power outputs of at least 100 watts.

3,750 volts. When the tube is operated under these conditions, the gain is lower than that shown in curve E at small signal levels, but is not affected appreciably at large signals. It is estimated that the helix voltage can be adjusted to give linear operation for power levels up to about 70 per cent of the "saturated" power output.

A summary of the performance data obtained for this developmental traveling-wave tube is shown in Table I.

ACKNOWLEDGMENT

The authors wish to thank Dr. I. Gordon of the RCA Laboratories at Princeton, N. J., for supplying the RCA ceramic used in the magnets, Dr. B. B. Brown and W. J. Dodds for their guidance in the course of this work, E. Bliss for helpful cooperation in the design and evaluation of the tubes, Miss R. Pekarowitz for measurements, R. Pagano for directing construction of the tubes, and other members of the RCA Tube Division for their contributions to the development of the tube described in this paper.

Spurious Modulation of Electron Beams*

C. C. CUTLER†, FELLOW, IRE

Summary—This paper describes spurious modulation effects commonly observed in electron tubes employing high current electron beams. The modulation is caused by positive ions and secondary electrons moving in the beam. It is eliminated by pumping the tube to high vacuum and retarding or deflecting the secondary electrons.

INTRODUCTION

A DIFFICULTY commonly encountered in amplifiers and oscillators employing electron beams is a noise-like modulation of the output at frequencies of around 5 mc and below. Various aspects of this phenomenon have been investigated and explained in part,¹⁻³ but the fact that it keeps being rediscovered⁴⁻⁶ indicates that a clear description of the phenomenon is needed.

* Original manuscript received by the IRE, May 9, 1955; revised manuscript received, July 13, 1955.

† Bell Telephone Labs., Murray Hill, N. J.

¹ J. R. Pierce, "Possible fluctuations in electron streams due to ions," *Jour. Appl. Phys.*, vol. 19, pp. 231-236; March, 1948.

² E. G. Linder and K. G. Hernqvist, "Space charge effects in electron beams and their reduction by positive ion trapping," *Jour. Appl. Phys.*, vol. 21, pp. 1088-1097; November, 1950.

³ K. G. Hernqvist, "Space charge and ion-trapping effects in tetrodes," *PROC. IRE*, vol. 39, pp. 1541-1547; December, 1951.

⁴ T. Moreno, "Some Anomalous Modulation Effects in Reflex Klystrons," paper presented at 10th IRE Conference on Electron Tubes, Ottawa, Can.; June, 1952.

⁵ R. L. Jepsen, "Some Beam Instabilities in Klystrons," paper presented at 10th IRE Conference on Electron Tubes, Ottawa, Can.; June, 1952.

⁶ T. G. Mihran, "Some Experimental Observations of Positive-Ion Oscillations in Long Electron Beams," 13th Annual Conference on Electron Tube Research, Michigan State College; June, 1955.

The effect usually shows up as a modulation of the radio-frequency output of an amplifier or oscillator employing an electron beam which passes through an electric field free region. The modulation appears as noise having a strongest amplitude in the hundreds of kilocycles, but which may have components as low as the audible range and as high as several megacycles. Under some circumstances the modulation is spread out over many octaves, and sometimes will have strong but unstable discrete frequency components. (See Fig. 2.) The amplitude is often as much as 10 per cent modulation of an rf carrier but under severe conditions is as much as 100 per cent modulation, and in some cases has been reduced to as little as 0.01 per cent. The effect is entirely one of modulation, there being no corresponding high-frequency output in the absence of a signal, and no corresponding effect on the noise figure of the tube.

The study to be described indicates that the effects come from three related phenomena. The most prominent is a plasma oscillation of positive ions attracted by the space charge of the electron beam and excited by secondary electrons returning from the collector region. It is strongest in the hundreds of kilocycles, which is near the natural frequency of transverse oscillation of the common positive ions in the normal space-charge field. Another is a relaxation oscillation in the tens of kilocycles, with a period consistent with the time required for electron collisions to produce ions

sufficient for space charge neutralization. The third effect is purely electronic, and appears to be a longitudinal oscillation of secondary electrons in the range of a few megacycles. These effects are strongly influenced by focusing fields, and any and all voltages and currents, even including heater current and cathode temperature.

Both of the ion effects may be eliminated by sufficiently hard pumping (which means vacuums of the order of 10^{-8} mm of Hg in the case of several traveling-wave tube geometries). This leaves a residual modulation noise of around 0.01 per cent due to the random fluctuations⁷ in beam current. The third effect is uncommon, and its elimination simply calls for electric or magnetic field distributions which eliminate secondary electrons from the beam.⁸

No practical use has been found for these effects.

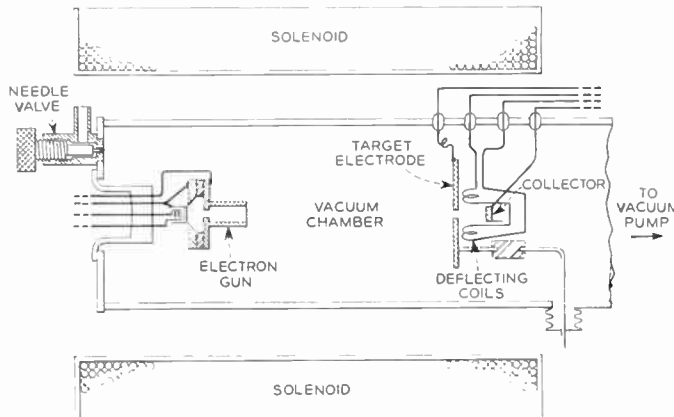


Fig. 1—Apparatus used to study spurious modulation in an electron beam (beam operated at 1,000 volts and 5 milliamperes).

EXPERIMENTAL OBSERVATIONS

In order to avoid confusion with microwave frequency effects, the beam modulation was studied directly, in a demountable continuously pumped chamber shown in Fig. 1 instead of in a traveling-wave tube where it was discovered. The collected beam current was observed in two ways. First the ac component frequencies were measured in a spectrum analyzer, and second, in order to observe the start of the phenomena, the beam was turned on and off with a square wave at a slow rate and observed with an oscilloscope synchronized to observe the starting transient of transmitted

⁷ Shot noise would be an rms current modulation of $\sqrt{2eB/i_0}$ where e is electron charge in coulombs, B is the bandwidth in cycles per second and i_0 is the beam current. Flicker noise would give low frequency components somewhat larger.

⁸ D. Bohm, E. H. S. Burhop, H. S. W. Massey, and R. M. Williams, "A Study of the Arc Plasma," National Nuclear Energy Ser., McGraw-Hill Book Co., Inc., New York, N. Y., Division I, vol. 5, pp. 173-333; 1949.

R. Rompe and H. Steinbeck, "Der plasmatzustand der gase," *Erg. exakten Naturwiss.*, vol. 18, p. 303; 1939.

D. Bohm and E. P. Gross, "Effects of plasma boundaries and plasma oscillations," *Physical Rev.*, vol. 79, pp. 992-1001; September, 1950.

These published works on plasma oscillations lead one to expect an electronic oscillation in the thousands of megacycles. A search was made for such oscillations, but none were found, so we assume they do not exist in the beam geometry and the pressures used.

current.⁹ The total current from the cathode under no circumstances showed any significant modulation during the pulse. Strong modulation was found in the division of current between the target and the collector, however, and this is the current that is described in the following observations.

The apparatus was equipped with a gas inlet, so that the pressure could be varied at will by admitting either hydrogen or nitrogen gas.

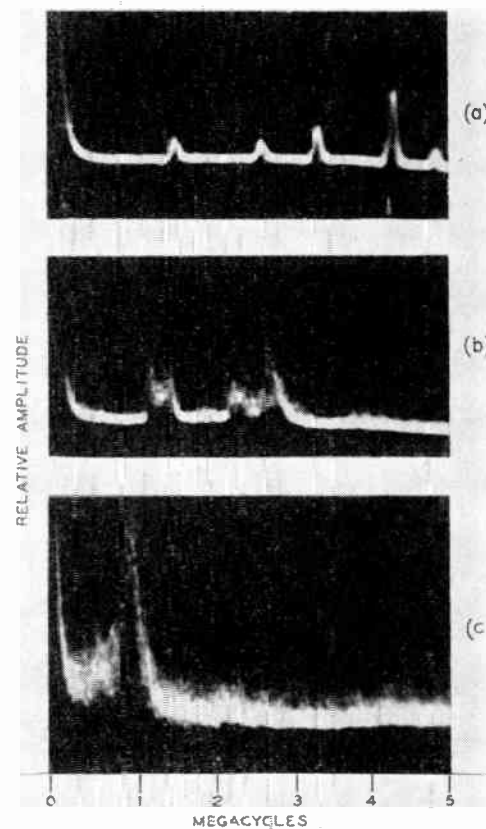


Fig. 2—Spectrum analysis of spurious modulation appearing on the output of a traveling-wave tube. (Courtesy of M. E. Hines.)

The modulation of the collector current was observed with a spectrum analyzer, and gave patterns similar to Fig. 2.¹⁰ The observations were in every particular like those made of the modulation of the microwave energy coming from traveling-wave tubes. This was a good indication that we were studying the same phenomenon as previously observed by Pierce and Hines.^{9,10} The frequencies were generally somewhat lower than in the traveling-wave tube, but this may be explained by the lower-beam currents used.

Fig. 3 shows various oscilloscope patterns of collector current. There were evidently three overlapping phenomena which, to avoid confusion, had best be de-

⁹ Electron beams in traveling-wave tubes were first studied using this pulse technique by J. R. Pierce early in 1947.

¹⁰ These photographs were supplied by M. E. Hines. They were used in his report on spurious modulation effects in traveling-wave tubes at the Fifth Annual Conference on Electron Tubes, at Syracuse University, Syracuse, N. Y., in 1947.

scribed separately, although they usually occurred in concert. The main distinguishing feature between them was the frequency constitution.

ION OSCILLATION

The most predominant effect occurred in a broad spectrum from about 100 kc to 2 mc. The amplitude was critically dependent upon pressure, increasing several orders of magnitude as the pressure was increased from 10^{-7} mm Hg to 10^{-5} mm of Hg. The frequencies in the spectrum increased significantly with increasing electron beam current,¹¹ or if hydrogen was introduced

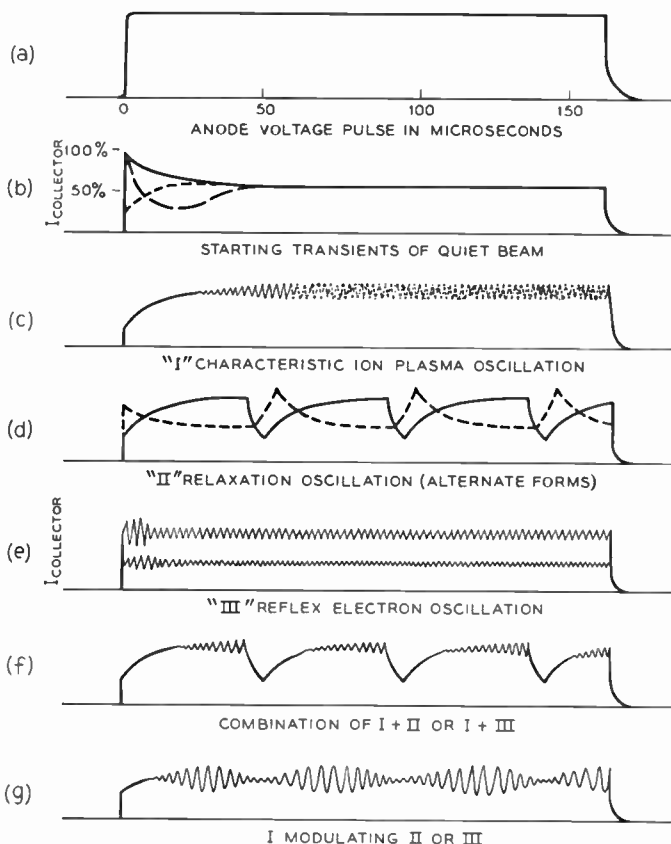


Fig. 3—Oscillograms of collector current from a pulsed electron beam, showing the three types of modulation.

into the system instead of nitrogen. At the lower pressures, the spectrum showed discrete frequencies similar to those in Fig. 2(a), and at higher pressures was more erratic like those in Fig. 2(b) and 2(c). The actual spectrum shape was kaleidoscopically dependent upon anything connected with the tube; *i.e.*, heater power, magnetic field, voltage, etc., but not in a consistent or repeatable fashion.

When the beam was pulsed, the oscillations started slowly, as shown in Fig. 3(c), taking from 10 to 100

¹¹ Linder and Hernqvist, *loc. cit.*, also found, and Pierce, *loc. cit.*, predicted the frequency to be proportional to beam current, but called it "ion density." That it is not the ion density which determines the frequency is evident in the fact that the frequency is not dependent on pressure, and most assuredly at the lower pressures the ion density is affected by the pressure (Bohm and Gross, *loc. cit.*).

microseconds to reach full amplitude, the starting time varying inversely with pressure. They appeared to be sinusoidal at low pressures, and were hashy, not repeating nicely from pulse-to-pulse at higher pressures.

The amplitude was strongly dependent upon the collector-target configuration. When the beam was collected with a symmetrical target configuration, with most of the current either striking the target or the collector, the oscillations tended to be small. When the current was more equally divided the oscillations were stronger, and with either the target displaced or the beam steered off center, the oscillations were very much stronger (under some conditions as much as 20–30 db). When the beam was sharply deflected by a magnetic field near the collector, the oscillations were greatly reduced in amplitude. Maintaining an electric field gradient near the beam also reduced the oscillations by several orders of magnitude. Biasing the collector-target assembly positively usually reduced oscillation amplitude.

With sealed-off tubes it was found that these effects were virtually eliminated at vacuums of the order of 10^{-8} mm of Hg.

All of this evidence points to positive ions oscillating transversely in the space-charge field of the beam. The calculated orbit of a singly-charged ion with an atomic number in the 10's in the space-charge field of the beam has a frequency in the range observed. The period of such an orbit should vary inversely with the charge density (or beam current), as was observed. The time of build-up of oscillation checks roughly with the calculated ionization time based upon the beam current and collision cross section of common atoms. Any large change in the number of positive ions either by electric fields, or by pressure variation gave a corresponding change in the level of oscillation.

The mechanism of the oscillation must involve secondary electrons from the collector, as any reduction in the number of secondaries getting back into the beam reduced the oscillation. It may be that the natural oscillations of ions in the space-charge field are excited by secondary electrons from the collector region. The secondaries add to the space-charge field, which reacts on the positive ions trapped by the space-charge field, which changes the beam focusing, which in turn influences the distribution of secondaries. As symmetry in the collector-beam relationship would accentuate the effect, as was observed. Such oscillations would be critically dependent upon beam-focusing pressure and hence on almost any tube parameter, thus explaining the extreme variability of the oscillation. A more sophisticated explanation of plasma oscillations¹² has been given by Pierce.¹

¹² There is a lot in the literature on plasma ion oscillations (Mihran, *loc. cit.*, and Bohm, Burhop, Massey and Williams, *loc. cit.*) but the usual gas discharge is quite different from our case and does not directly apply. Our pressures are much lower, we have no reason to expect equal numbers of positive and negative charges, or enough free charge to neutralize any applied field, nor are the fast moving electrons in the beam as free to move as electrons in gas discharge.

IONIZATION RELAXATION OSCILLATIONS

Another effect generally mixed with the one mentioned above appeared with a fundamental component between 10 and 100 kc with harmonics at much higher frequencies. It also depended upon pressure, being strong and common with pressures approaching 10^{-5} mm of Hg, and weak and uncommon at pressures around 10^{-7} mm of Hg. Its frequency was critically dependent upon pressure, having a period of the order of the calculated time required for electron collisions to produce sufficient positive ions to neutralize the space charge of the electron beam. When the time function was observed by pulsing the beam, the oscillation usually started at full amplitude and was obviously a relaxation oscillation, as shown in Fig. 3(d), with a period equal to the time required for normal beam transmission to be established. While this was a long time at very low pressures (the oscillations were sometimes audible), the amplitude became vanishingly small as the pressure was decreased. Sometimes the period described only appeared as a modulation of a higher-frequency component, as in Fig. 3(g), and it often appeared in combination with a higher frequency oscillation, as in Fig. 3(f). When the surrounding cylinder was biased negatively, the oscillations were greatly enhanced, and when the cylinder was positive, the oscillations were sharply reduced.

These effects may be explained by the trapping of ions in the space charge of the beam. The ion density presumably builds up until a critical value is reached, probably the point where ions begin to spill over, influencing the electron focusing near the gun, and thus displacing or sharply defocusing the beam. This quickly releases the trapped ions sufficiently so that at least some of them escape and have to be replaced by new ionization. The process then repeats, giving the relaxation type of oscillation observed.

SECONDARY ELECTRON OSCILLATION

The third effect was almost certainly not an ion effect. It was observed from 1 mc to 15 mc, was strongest with the lowest pressures, and sometimes would start within one or two microseconds of turning on the electron beam, as indicated in Fig. 3(e). It depended strongly upon secondary electrons, and could be increased in frequency and amplitude by elevating the potential of the cylinder surrounding the electron beam, or eliminated by reducing the potential below that of the collector.

This oscillation is presumed to be caused by secondary electrons oscillating longitudinally between the cathode and collector. Electrons released at the collector, returning with a few volts of energy, can influence the focusing at the gun, and thus influence the primary electron beam, thereby changing the secondary electron distribution. Slow secondaries have the proper velocity to explain the period of the observed oscillations. The variation of the velocity of secondaries with cylinder potential would explain the electronic tuning, and elimination of secondaries, of course, would stop the oscillation.

A cousin to the above is a rather uncommon, single-frequency, low-amplitude oscillation at 2 or 3 mc, which disappeared with the slightest applied electrical gradient. It is thought to be an oscillation of slow electrons between scallops in the electron beam.

CONCLUSION

The various beam modulation effects described usually occur simultaneously with overlapping spectra, and they intermodulate, the higher-frequency components often showing sidebands due to the lower-frequency oscillations. All three are easily locked in with an ac voltage near the natural frequency of oscillation applied to any electrode. It is not surprising that the spectrum is erratic, since there are many modes of possible oscillation and there are no really stable elements to control the frequencies; the pressure, electron emission, gas constitution, and applied fields all being critically involved.

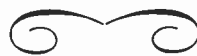
The happy conclusion is that the unwanted effects are eliminated by simply adequately outgassing the parts and pumping the tube to a good vacuum, and in some cases deflecting the secondary electrons produced at the collector.

Unfortunately, proposed systems which would use ions to help beam focusing^{2,3,13,14} are impractical unless one can either show that the oscillations are not harmful in the particular application, or one can invent some way to make the pesky things stand still.

This work was done with the assistance of C. F. Chapman, and was stimulated by J. R. Pierce, M. E. Hines and many other colleagues at the Bell Telephone Laboratories.

¹³ M. E. Hines, G. W. Hoffman, and J. A. Saloom, "Positive ion drainage in magnetically focused electron beams," *Jour. Appl. Phys.*, vol. 26, pp. 1157-1162; September, 1955.

¹⁴ E. L. Ginzton and B. H. Wadia, "Positive-ion trapping in electron beams," *PROC. IRE*, vol. 42, pp. 1548-1553; December, 1954.



Negative Resistance Regions in the Collector Characteristics of the Point-Contact Transistor*

L. E. MILLER†

Summary—The negative resistance regions in the active portion of the point-contact collector characteristics are characterized in terms of three unique types of anomalies in the current multiplication properties of the device. While the interaction of the α anomalies and the associated circuitry result in a measuring circuit instability, the negative resistances are true device properties which are attributable to variations in the collection efficiency of the reverse biased collector junction.

INTRODUCTION

CERTAIN ANOMALIES in the output characteristics of various types of germanium point-contact transistors have been noted from time to time during the testing of experimental and production units. These phenomena appear as negative resistance regions in the active portion of the characteristic. Their incidence varies widely from type to type and is essentially zero in a few types presently being manufactured.

It is convenient to examine these phenomena by displaying the collector V - I characteristics on an oscilloscope using emitter current as the other independent parameter. This may be accomplished by applying a sinusoidal voltage to the collector and using the collector voltage and current as the ordinate and abscissa respectively. A convenient circuit for this purpose is shown in Fig. 1. In Fig. 2 is shown the typical appearance of a number of the more commonly-found types of negative resistance regions when displayed by the circuit of Fig. 1. The general nature of these anomalies has been found to be highly stable. That is, the size and shape of the anomalies do not change appreciably with shelf life or with length of operation at maximum-rated power dissipation. For any given transistor, they appear only in a specified region and the device exhibits normal characteristics at any point outside this region. The anomalies usually appear well within the maximum-rated power dissipation limits of the device. Although individual types of anomalies occur most frequently in separate transistor types, a number of types may occur in the same transistor type.

The seriousness of this situation is obvious if one considers the effect of such a negative resistance region in the operating range of some oscillator and amplifier applications.

Although the discussions to follow are confined to n type transistors, similar anomalies are observed in p type point-contact transistors. It appears that if appropriate changes in sign are made the same considerations will apply.

* Original manuscript received by the IRE, March 7, 1955; revised manuscript received July 7, 1955.

† Bell Tel. Labs., Inc., Allentown, Pa.

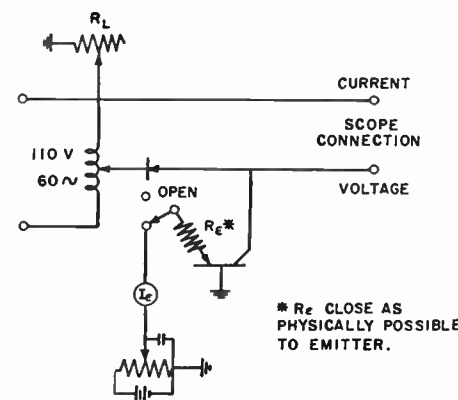


Fig. 1.—Transistor output characteristic sweeper.

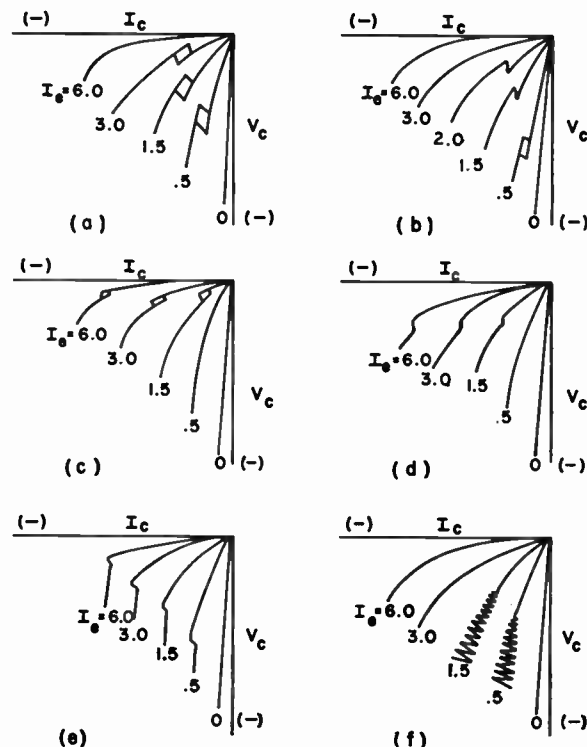


Fig. 2.—Some typical transistor negative resistance regions.

CHARACTERIZATION

The multiplicity of the various forms which these negative resistance regions exhibit makes it necessary to characterize them with some care. It has been convenient to divide them into three major categories because it has been found that there are at least three separate and distinct causes (which, however, may be

interdependent) for their occurrence in the output characteristics of the point-contact transistor.

The other characteristics of the transistor provide a means of partial characterization of the negative resistance regions. All of the transistors with anomalies in the output characteristics exhibit corresponding anomalies in the feedback and transfer characteristics. However, not all of them show a corresponding anomaly in the input characteristics.

It will also be useful to examine the small signal α versus emitter current characteristic as a part of the characterization, since each type of collector characteristic anomaly has associated with it a unique α anomaly. This relation will be discussed in the subsequent sections. The first category of anomaly may be identified as the kind which does not have its counterpart in the input characteristic of the transistor. This category is illustrated by Figs. 2(a) and 2(b) and will be termed a Type 1 negative resistance region.

This type of negative resistance region, which appears as a sudden increase in collector current with a slight increase in collector voltage, is related to a region of operating instability resulting from an abnormally high value of current multiplication in this region. Fig. 3(a) illustrates the appearance of this type of negative resistance region as an oscillographic presentation and Fig. 3(b) depicts the corresponding family of current multiplication vs emitter current curves with collector voltage as the parameter. The peak in the α curve appears at high emitter current for low collector voltage and moves through a maximum to low values of emitter current for increasing collector voltage. Those units which have this type of anomaly exhibit peak values of α , sometimes as high as 100, for collector voltages which correspond to the $I_c - V_c$ region where the anomaly occurs. The α characteristic has normal peak values of α for all other values of collector voltage.

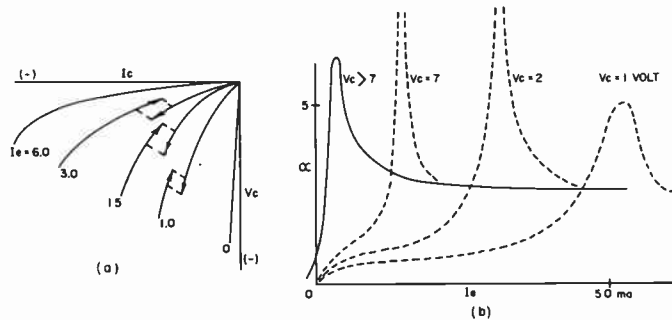


Fig. 3—Correlation between $I_c - V_c$ negative resistance regions and α vs emitter current anomalies.

Fig. 4 shows the low frequency tee network equivalent circuit of the transistor and the equation which is the criterion for stability¹ in this circuit. This equation,

$$\frac{r_m}{R'_c} < 1 + \frac{R'e}{R'b} + \frac{R'e}{R'c} \quad (1)$$

¹ R. M. Ryder and R. J. Kircher, "Some circuit aspects of the transistor," *Bell Sys. Tech. Jour.*, vol. 28, pp. 367-400; July, 1949.

where the primed R 's include both internal and external resistive elements, predicts that the transistor will exhibit a negative resistance region similar to the solid curve in Fig. 4 whenever the inequality does not hold. A normal curve denoted by the dotted line results for the other alternative.

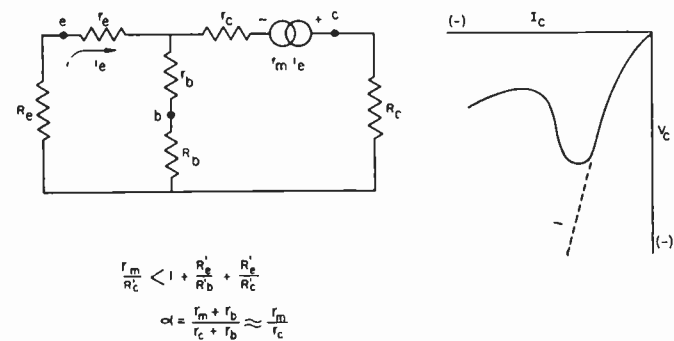


Fig. 4—Negative resistance output characteristic.

Since the quantity on the left of (1) is related to α by

$$\alpha = \frac{r_m + r_b}{r_e + r_b} \approx \frac{r_m}{r_e} \text{ (for small } r_b) \quad (2)$$

$$\approx \frac{r_m}{R'c} \text{ (for small external collector resistance)} \quad (2)$$

and the quantities on the right of (1) remain relatively constant for any given circuit, the transistor will exhibit a negative resistance region whenever α exceeds a certain value which will be determined by the relative magnitude of the collector resistance and the collector load. Therefore, a high, narrow, α peak, which is extremely variable with collector voltage (such as shown on Fig. 3(b)) results in a localized instability as the collector is swept through the range of voltages at which it occurs. The occurrence and size of the anomaly and whether circuit changes will affect it may be predicted from the height of the peak, the area under it, and the values of collector voltage for which it occurs.

The α emitter current characteristic provides a convenient method for additional characterization of the negative resistance regions. The step-back in collector current with an incremental increase in collector voltage such as illustrated in Figs. 2(c) and 2(d) is related to a different type of anomaly in the α emitter current curves and will be termed a Type 2 anomaly. In these cases a secondary peak appears in the α curve at relatively low collector voltages and moves to higher values of emitter current with increasing collector voltage. This type of negative resistance region is shown on Fig. 5(a). On Fig. 5(b) is the associated α emitter current characteristic. The size of this secondary α peak with respect to the primary peak and its voltage sensitivity completely determines the characteristics of this type of negative resistance region in the following manner:

The collector current at any particular collector voltage can be represented as

$$I_c = I_{e0}(V_e) - \alpha I_e \quad (3)$$

where I_{e0} represents the saturation current at zero emitter bias and $\bar{\alpha}$, the average α up to the emitter current I_e . For low values of collector voltage and large values of emitter current

$$I_c = -\bar{\alpha} I_e \quad (4)$$

where the average α is defined as

$$\bar{\alpha} = 1/I_e \int_0^{I_e} \alpha(I_e) dI_e. \quad (5)$$

Therefore, for these conditions and for any given emitter current, the collector current is directly proportional to the area under the α emitter current characteristic. Referring to Fig. 5(b), the secondary peak moves to higher values of emitter current quite rapidly as the collector voltage is increased, while the primary peak remains relatively constant. In terms of output characteristic it is seen, at constant emitter current, the average α (and hence collector current) undergoes a sudden decrease as collector voltage is increased through range of voltages at which secondary α peak occurs.

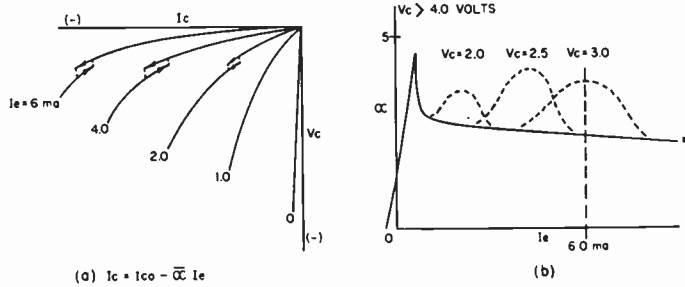


Fig. 5—Correlation between I_c-V_c negative resistance regions and α vs emitter current anomalies.

Transistors with both the first and second category of negative resistance region just described exhibit normal characteristics everywhere except in the immediate regions of the anomaly. The third separate and distinct category of negative resistance region is distinguished from the others because the device does not regain its original characteristics at operating points beyond the region of operation defined by the presence of the anomaly. Typical examples of this type are shown in Figs. 2(e) and 2(f). The anomaly in this type can take on many forms such as the oscillations shown in Fig. 2(f), the ohmic form illustrated by Fig. 2(e), or other variations depending on the impedances in the measuring equipment. This is the type of negative resistance region discussed by D. E. Thomas.² The transistors which will oscillate in almost any circuit usually contain anomalies which fall into this category as do most vhf point-contact transistors. Although the negative resistance regions which fall into this category take on many different forms and can be changed in appearance by changing the impedance levels in the measuring equipment, they are all characterized by one common feature.

² D. E. Thomas, "Stability considerations in the parameter measurements of vhf point-contact transistors," Proc. IRE, vol. 42, pp. 1636-1644; November, 1954.

At zero or small values of collector voltage, the normal characteristic curve is obtained with typical values of ohmic base resistance (feedback resistance). As the voltage is increased to the point at which the anomaly appears, the base resistance takes on very large values and remains large for all values of voltage beyond this point. The negative resistance of the region coupled with the large positive feedback afforded by the increased base resistance is the cause for many of the oscillators such as illustrated in Fig. 2(f). In many cases, units of this type exhibit an enhanced emitter current which shows an ohmic dependence on collector voltage for all voltages greater than the value at which the anomaly initially occurs. The voltage at which it occurs may be decreased by applying additional forming pulses.

EXPERIMENT AND DISCUSSION

Concepts of Point-Contact Transistor Alpha

In the discussion to follow, considerable use will be made of terms which are intimately connected with the physics of the device. For this reason a short summary of the concepts of current multiplication in point-contact transistors as first elucidated by Bardeen and Brattain³ will be presented.

The point-contact transistor consists of a pair of spring contacts on a germanium wafer which is soldered or bonded to a broad area "base" contact. In this configuration it is desired to maintain the base as an ohmic contact (one which will pass current of either polarity with equal facility). A point contact on germanium displays rectifying properties which are related in a rather complex fashion to the difference in work function between the metal and the semiconductor. When the point is biased in the reverse direction it will act as a high impedance to flow of current. In the forward direction the contact will display a low impedance through the mechanism of injection of minority carriers. In the point-contact transistor the emitter is normally biased in the forward condition resulting in a high minority carrier concentration in the region of the emitter. In *n* type germanium in which the minority carriers are holes, this results in a positively charged region under the emitter point. Since the holes are minority carriers, the statistical probability of recombination with electrons is high. The collector is usually biased in the reverse direction and the reverse current is determined by the physical properties of the collector region. The collector reverse current passing through the ohmic spreading resistance of the bulk material results in a collector field. This field, in turn, is in such a direction as to cause the minority carriers injected by the emitter to drift to the collector. Holes drifting across the reverse biased *p-n* junction at the collector result in a space charge. Charge neutrality requires the neutralization of this space charge. This is accomplished by the emission of electrons from the collector. Since there is a basic difference

³ J. Bardeen and W. H. Brattain, "Physical principles involved in transistor action," Phys. Rev., vol. 73, pp. 1208-1225; April, 1949.

in the drift mobility of holes and electrons, a current multiplication which is determined by the ratio of mobilities results.

Current multiplication values in excess of those predicted from this picture have been observed and a variety of theories have been proposed to account for these. However, a consideration of these models is not essential to the discussion to follow.

Electrical forming consists of discharging a charged condenser through the collector in the reverse direction. This is used primarily to increase the collector current, hence the collector drift field. Such a field results in a focusing action for the efficient collection of minority carriers. The variety of anomalies discussed in this paper apparently results from a complicated set of interactions between the collector and emitter fields.

Mechanism for the Type 3 Negative Resistance Region

The cause of the Type 3 anomaly illustrated in Figs. 2(e) and 2(f) yields most easily to experimentation. The high base resistance implies an excessive interaction of the collector region with the emitter point, as does the ohmic dependence of enhanced emitter current on collector voltage. This can be shown to be the case by moving the emitter point with respect to the formed collector, as in a micromanipulator transistor. Decreasing the point spacing on a unit of any kind will cause a negative resistance region of this type to appear, while increasing the separation will cause it to disappear. A large increase in base resistance appears to be coincident with the onset of this negative resistance region.

Since all of the units which are normally known as oscillators exhibit this high base resistance, it is important to know whether the high base resistance results in oscillations or the oscillations result in a measurement of abnormally high base resistance. If one observes the wave form of the signal obtained during the measurement of base resistance, one can confirm that there is an increase in the amplitude of the signal which is normally used to measure base resistance before the unit breaks into oscillation. That is, the high base resistance causes many units to oscillate in ordinary circuits rather than the converse.

The high base resistance associated with a Type 3 anomaly indicates that the collector space charge has penetrated to the emitter, so that variations in collector current result in more than the usual amount of variation in emitter voltage. One may make use of a third electrode to measure floating potentials in the space between emitter and collector to check this possibility. This experimental arrangement is shown in Fig. 6(a). Using a close spacing between emitter and collector results in a Type 3 anomaly for normal forming, as shown by Fig. 6(b). The slightly increased point-spacing obtained by using a second emitter results in the disappearance of the anomaly so that a normal family of characteristics is displayed, Fig. 6(c). The third electrode, now called the probe, is present at a point such

that if it were used as an emitter a Type 3 negative resistance curve would be obtained. This is illustrated in Fig. 6(b).

Measurements taken on this probe, as the characteristics of the unit shown in Fig. 6(c) are displayed, indicate that only a fraction of the full collector voltage appears at the probe. Strictly speaking, the Type 3 anomaly is not the result of the sudden punch-through of collector voltage to the emitter but rather results when the potential under the point increases gradually through a range which is small compared with the total collector voltage variation. The low r_b before the negative resistance region indicates the presence of an emitter field which prevents interaction between emitter and collector. The high r_b beyond the break in the curve suggests that, at this potential, the collector field has succeeded in overwhelming the emitter field.

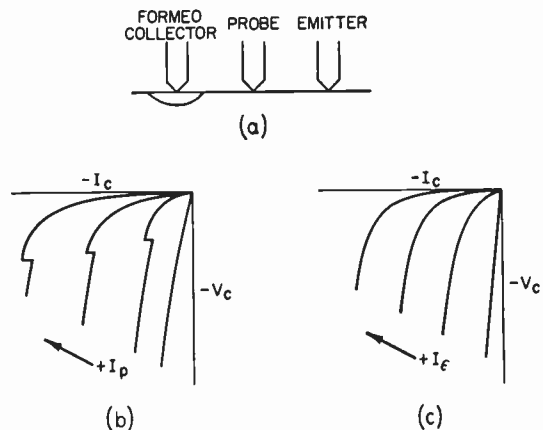


Fig. 6—Collector characteristics for the three electrode experiment.

The experimental procedure just discussed may be used to verify the presence of such regions of interacting electric fields. The α vs emitter current characteristics at several collector voltages for the unit illustrated in Fig. 6(c) are shown in Fig. 7(a). The α curve increases quite rapidly with collector voltage, from zero for zero collector voltage to its final limiting value at about $V_c = 1$ v. For no applied collector voltage, there is, of course, no current gain. The probe potential increases positively as a monotonic function of emitter current (see Fig. 7(b)). This implies that the emitter field extends some considerable distance into the germanium from the emitter, that the germanium is at a positive potential under the probe due to a concentration of minority carriers (holes) which are injected by the emitter, and, further, that the magnitude of this potential increases with the number of injected carriers.

With the application of a collector voltage some current multiplication occurs with a resultant increase in electron flow. This increase in electron flow results in a change in the probe potential to a negative value which is dependent on the magnitude of currents flowing.

One may infer from these measurements that the volume encompassed by the emitter field, which is of

opposite sign to the collector field, is sharply dependent on the currents flowing through the region. This means that the distance over which no collector drift field exists is extremely variable and dependent on the operating point of the device.

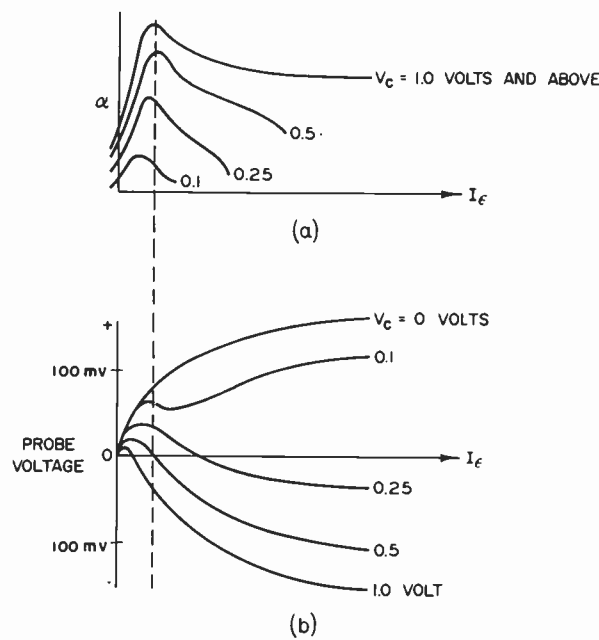


Fig. 7—Probe potential as a function of α characteristics.

Since, in the absence of a drift field, the holes injected by the emitter do tend to move by diffusion alone, recombination processes may become significant. Any significant recombination results in a change in transport efficiency which in turn affects α . The Type 3 anomaly almost always has associated with it a region of enhanced α . It is suggested, therefore, that the collector field under the emitter is sufficient, at the voltage at which the Type 3 anomaly occurs, to decrease the size or eliminate completely the positively-charged region under the emitter point where the carriers move by diffusion. There are a number of other convincing facts to support this conclusion:

1. The frequency cutoff of α in all regions before the negative resistance region is relatively low and agrees with predictions based on the conductivity modulation model.⁴ At all points beyond the negative resistance region the frequency cutoff takes on larger values which coincide closely with calculations based on the drift model.⁵
2. All hf units, whether they are formed as transmission or switching types, exhibit Type 3 anomalies in some portion of their characteristics.
3. All those hf units which will oscillate in any given circuit, unless special precautions are taken, fall into

the category of the Type 3 anomaly. The oscillations are the result of the negative resistance and the accompanying hf response which tends to sustain oscillation.

It appears that the dependence of the frequency response of any given point-contact unit on electrical forming is based on the necessity of increasing the collector field under the emitter to such an extent that the region where the carriers move by diffusion is effectively reduced. The Type 3 anomaly occurs at the biases at which a positively-charged region under the emitter no longer inhibits the drift of holes from emitter to collector. Since at this point the interaction between emitter and collector is increased, causing the base resistance to increase to large values, the device loses part of its usefulness as a small signal amplifier.

The conclusion which one is forced to draw is that there will be an upper frequency limit for any given point-contact structure which will be imposed by the maximum tolerable base resistance, or the negative resistance region, which is a manifestation of this high base resistance.

MECHANISM FOR THE TYPE 2 NEGATIVE RESISTANCE REGION

The explanation for the Type 2 anomaly follows from the discussion of the Type 3. A transistor can have both a Type 2 and a Type 3 anomaly as shown on Fig. 8(a), or it can have a Type 2 which changes into a Type 3 as the biases are changed as illustrated in Fig. 8(b). Often a Type 2 will change to a Type 3 as one observes the characteristics on a curve tracer. This occurs because the sweep measurements are being carried out at biases corresponding to the transition point shown on Fig. 8(b).

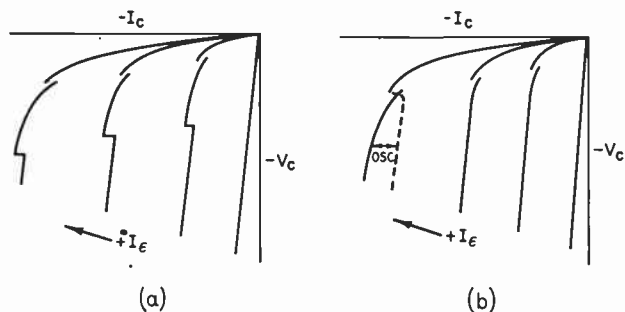


Fig. 8—Collector characteristics containing Types 2 and 3 anomalies.

Both types exhibit high base resistances and both have peculiar peaks in the α vs emitter current characteristic. The difference between the two appears to be one of degree rather than kind, the Type 2 representing a Type 3 which recovers its original characteristics of α and low base resistance. If one measures the base resistance of a unit containing a Type 2 anomaly while sweeping collector voltage through the range at which the anomaly occurs, a high value is obtained. It resumes the normal low value at biases beyond this point. This increase in base resistance may be associated with a

⁴ J. E. Thomas, unpublished work.

⁵ W. Shockley, "Electrons and Holes in Semiconductors," D. Van Nostrand Co., New York, N. Y., pp. 106-108; 1950.

decrease in the size of the positively-charged region under the emitter. This, in turn, results in a more efficient transport factor with the consequent enhanced α .

This hypothesis may be checked by repeating the three-probe experiment described in the previous section. One may form a transistor such that it contains both Type 2 and Type 3 negative resistance regions. Making use of the wider point-spacing afforded by the third electrode results in the disappearance of the Type 3 but not the Type 2 anomaly. These results are illustrated in Fig. 9(a), (b), and (c). Fig. 10(a) shows the α emitter current characteristic which is associated with the output characteristics shown in Fig. 9(c). The secondary α peak appears at relatively low collector voltage and moves in a characteristic fashion to higher emitter currents for increasing collector voltage. The probe potentials for collector voltages which correspond to those for the α curves shown are plotted in Fig. 10(b).

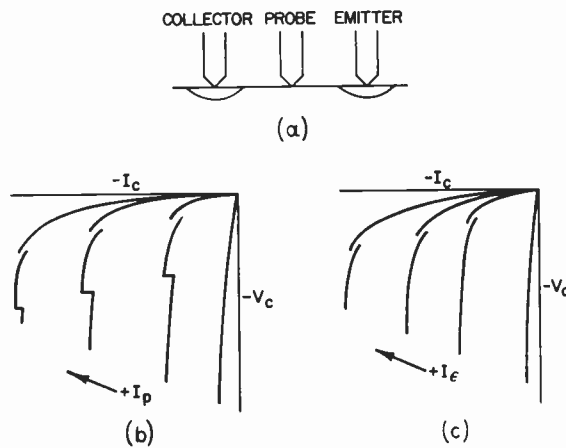


Fig. 9—Collector characteristics for the three-electrode experiment.

These curves show that the potential between the emitter and collector goes to a more negative value as the unit is swept through the region where the α peak occurs and then returns to a more or less "typical" value. This change in probe potential appears to reflect the changing size of the region of positive charge under the emitter point. In the region where the secondary α peak occurs this volume contracts to such an extent that the transport efficiency increases with a resultant increase of α . As the emitter current increases still further the increased hole density in the region under the point builds up the size of the region of positive charge resulting in the drop in α .

Whether a Type 2 or 3 anomaly will occur depends on the magnitude and rate of change of collector field with respect to changing bias. If the collector field is expanding quite rapidly as the collector voltage is increasing, one might expect a large amount of interaction between the negative collector field and the positive emitter field under the emitter point. This in turn would result in a Type 2 anomaly. This accounts for the fact that the Type 2 anomaly occurs at relatively low voltages while

α is still changing quite rapidly with collector voltage. The Type 3 anomaly, however, almost always occurs at higher voltages than the Type 2. At this voltage, the α has reached its final limiting values.

Finally, one can confirm that this change in drift space potential results in the enhanced α rather than the converse. A unit which is formed so that it does not exhibit a secondary α peak can be made to exhibit one by the application of a positive potential to the probe electrode. It is presumed that the resultant increased hole concentration in the drift space effectively changes the size of the positively-charged region under the emitter resulting in changes in transport efficiency.

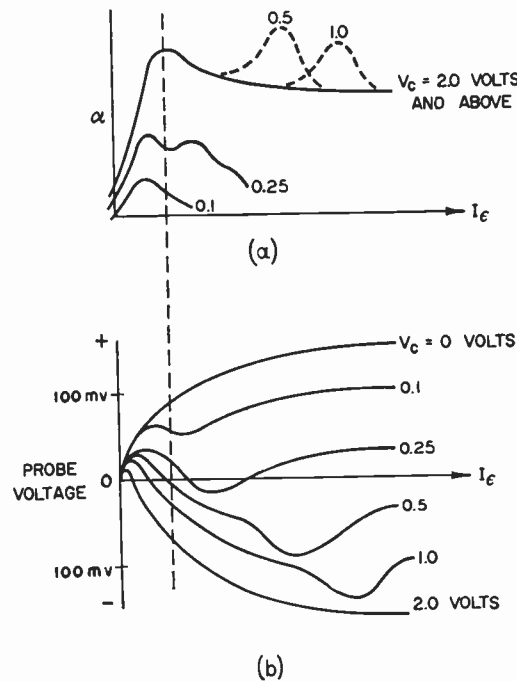


Fig. 10—Probe potential as a function of α characteristics.

INVESTIGATION OF THE TYPE 1 NEGATIVE RESISTANCE REGION

In the characterization of the negative resistance regions it was pointed out that the Type 1 anomaly does not have its counterpart in the input characteristic of the transistor. This suggests that the emitter is not basically involved in the formation of this type of anomaly. This can be verified experimentally by forming a transistor containing a Type 1 anomaly and then removing the emitter point. Minority carriers may be supplied by illuminating the germanium surface. If one sweeps out the collector characteristics using light intensity as the parameter, the same negative resistance region in the characteristics is displayed as though a metallic emitter point were used. One may also move the collector point about within the limitations of the formed region or replace the original point used to form the transistor with another without significantly affecting the appearance of the negative resistance region. These facts appear to indicate that the cause of

the negative resistance region is attributable to some anomalous behavior in or near the formed region. This is also suggested by the fact that the anomalies can appear or disappear during a particular forming schedule. All units containing Type 1 negative resistance regions, however, are characterized by reverse currents which are lower than those for the same type of unit containing no anomaly. There is no direct physical explanation for this anomaly but statistical evidence will be presented to suggest that its presence is related to the donor concentration in the formed region of the collector.

Pfann⁶ has observed that the reverse current for formed point-contact collectors is dependent on the donor concentration in the collector wire. The data summarized in Fig. 11 represent the results of a carefully designed experiment in which experimental transistors were made utilizing a series of phosphor bronze wires with increasing phosphorous concentration. These

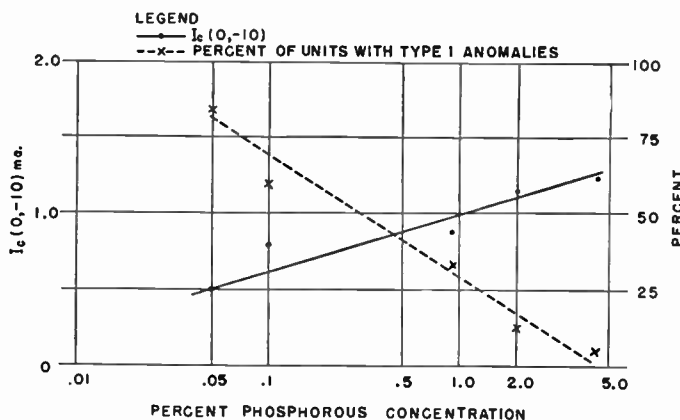


Fig. 11—Variation in transistor parameters with point wire composition.

units were formed to the same large signal forming objective of average α . The figure shows that the frequency of occurrence of the Type 1 anomaly, other design variables held constant, is dependent on the donor concentration in the collector wire. More accurately, since matter is transferred from collector to germanium during forming,⁷ the occurrence of a Type 1 anomaly is dependent on the amount of donor in the formed region as a result of the forming sequence. The graph also shows that a low I_{c0} distribution is probably incompatible with an anomaly free product.

Since the Type 1 anomaly can appear or disappear during any particular forming sequence, and since the absolute amount of donor in the formed regions cannot decrease significantly, one must presume that the relative amount of donor may increase or decrease during the forming sequence. This implies that the transfer and distribution of both acceptor and donor impurities in the germanium during forming is of importance in

⁶ W. G. Pfann, "Significance of composition of contact-point in rectifying junctions on germanium," *Phys. Rev.*, vol. 81, p. 882; March, 1951.

⁷ L. B. Valdes, "Transistor forming effects in N-type germanium," *Proc. IRE*, vol. 40, pp. 445-448; April, 1952.

the determination of the properties of the formed collector junction. Copper has been suggested as one of the possible acceptors involved in the forming phenomenon.⁸ Thermally-induced acceptors have also been suggested.⁹ Both may be involved since Valdes¹⁰ reports as high as 10^{20} atoms of Cu/cc have been measured by radioactive techniques in a heavily formed region and has observed damage to the germanium surface in the vicinity of a formed region. In either case, the diffusion coefficients of donor and acceptor¹¹ are sufficiently different so that we might expect forming efficiency to be time dependent. Table I shows that I_{c0} (the reverse cur-

TABLE I

Parameter	0.10 Per cent Phosphorous Phosphor Bronze		0.9 Per cent Phosphorous Phosphor Bronze	
Time Constant $I_c(0, -10)$ (Average)	250 μ sec 0.72 ma	5 μ sec 1.00 ma	250 μ sec 0.82 ma	5 μ sec 1.10 ma
Percent of Units Containing Type 1 Anomalies	42 per cent	8 per cent	33 per cent	0 per cent

rent of the collector junction) and the α characteristics of the formed collector may be controlled by varying the time constant of the condenser discharge forming pulse. These data were obtained by empirically adjusting the amplitudes of the long and short pulses so that each unit could be formed to the same large signal objectives with one forming pulse. Each sub-group represents approximately 25 units. The table shows that one may reduce the incidence of α anomalies by increasing the point wire donor concentration, as was indicated in Fig. 11, but an even more effective way of achieving the same result is to reduce the time constant of the forming pulse. In any event, however, a higher I_{c0} is associated with an anomaly free product.

The potential measuring techniques described in the two previous sections were applied also to the study of the Type 1 anomaly. Very pronounced changes in drift potential are observed in the bias regions corresponding to the presence of the high α peaks, and application of potentials to the probe on units containing such anomalies enables one to change the properties of the α peak significantly.

One may summarize the implications of these experiments as follows:

1. The Type 1 anomaly is a phenomenon which is most closely associated with the properties of the collector junction, appearing most often when reverse currents are low, in turn a property of lightly formed units.
2. The forming process involves the transfer of acceptor and donor atoms into the bulk of the germanium and it

⁸ Valdes, *ibid.*

⁹ R. C. Longini, "Electric forming of n-germanium transistors using donor alloy contacts," *Phys. Rev.*, vol. 84, p. 1254, December, 1951.

¹⁰ Valdes, *op. cit.*

¹¹ C. S. Fuller, "Diffusion of donor and acceptor elements into germanium," *Phys. Rev.*, vol. 86, pp. 136-137; April, 1952.

is the distribution of these impurities at or near the collector junction which determines its properties; a relatively high donor concentration results in a high reverse current and normal α characteristics, while a relatively low donor concentration results in low reverse currents and anomalous α characteristics.

3. Significant changes in drift potential observed when the transistor is operated at biases in the region of the Type 1 anomaly suggest that this anomaly is a result of variations in collection efficiency of the formed collector point at different operating biases.

CONCLUSIONS

The negative resistance regions in point-contact collector characteristics which appear as a measuring circuit instability are the combined result of device properties and the associated circuitry. While the appearance of each type of negative resistance region may vary with the termination impedances of the measuring equipment, the anomalies are the result of true negative resistance regions. Negative resistance regions are possible whenever the current gain of a device is greater than one. Each of the three general types of point-contact negative resistance regions has associated with it a unique anomaly in the current gain-emitter current

characteristics which features pronounced variations in current multiplication over relatively short ranges of operating bias. The observed negative resistances are directly attributable to such changes in current gain.

The cause of each of the α anomalies in turn is traceable to variations in the collector drift potential which exists in the bulk of the germanium between emitter and collector. The additivity of the fields from the reverse biased collector junction and the forward biased emitter junction provides a continuously varying field (with respect to changing dc bias) through which the minority carriers injected at the emitter are transported to the collector. The efficiency of multiplication (α), therefore, is a function of the relative amount of diffusion (near the emitter) and drift, (near the collector) which the injected minority carrier must undergo in its motion from emitter to collector.

Other device properties such as base resistance and the frequency cutoff of α are also related to such variations in drift potential.

ACKNOWLEDGMENT

The author is indebted to N. J. Herbert for many helpful suggestions and constant encouragement, and has profited greatly from many discussions with J. H. Forster.

The Dependence of Transistor Parameters on the Distribution of Base Layer Resistivity*

J. L. MOLL†, ASSOCIATE MEMBER, IRE, AND I. M. ROSS†

Summary—This paper presents a method of analyzing transistor behavior for any base-layer impurity distribution. In particular, expressions are derived for emitter efficiency γ , transverse sheet resistance R , transit time τ , and frequency cut-off f_a . The parameters γ and R are functions only of the total number of impurities in the base layer. The analysis is used to derive γ , R , τ and f_a for four different distributions—uniform, linear, exponential, and complementary error function. For each of these distributions a transistor base-layer design equivalent in R and f_a is obtained. Comparison shows that for equivalent parameters the nonuniform distributions permit the use of wider base layers, but require greater maximum impurity concentrations and must be operated at high current densities.

INTRODUCTION

THE DEPENDENCE of transistor parameters on geometry and conducting characteristics of emitter, base, and collector has been discussed for the case of minority carrier transport across the base layer

* Original manuscript received by the IRE, July 22, 1955; revised manuscript received September 20, 1955.

† Bell Telephone Labs. Inc., Murray Hill, N. J.

by pure diffusion.^{1,2} This case is realized physically by having a base layer of uniform resistivity throughout. The dependence of frequency response on base layer thickness for transistors with uniform base layer resistivity is well known. High frequencies require thin base layers, making the fabrication of high frequency transistors difficult.

If the resistivity varies across the base layer from emitter to collector the change in equilibrium majority carrier concentration results in "built in" fields which may aid or retard the flow of minority carriers across the base layer. In particular, if the donor concentration (for $p-n-p$) decreases from the emitter to collector the resultant fields will aid the flow of minority carriers across the base layer with a resultant decrease in transit

¹ W. Shockley, M. Sparks, and G. K. Teal, "P-n junction transistors," *Phys. Rev.*, vol. 83, pp. 151-162; July, 1951.

² J. M. Early, "PNIP and NPIN junction transistor triodes," *Bell Sys. Tech. Jour.*, vol. 33, pp. 517-533; May, 1954.

time and increase in the frequency cut-off of the transport factor as compared to the case of pure diffusion.

The enhancement of frequency cut-off by an appropriate resistivity gradient eases the fabrication problem somewhat, and a quantitative calculation of the effects of the resistivity gradient on frequency and transit time as well as the effects on other transistor parameters was desired.

In addition to effects on the frequency behavior of the transport factor, the distribution of base layer impurities can effect the behavior with frequency of the emitter efficiency, γ . The total number of impurities as well as geometry determine the low frequency emitter efficiency and the base resistance r_b . Some of the effects of an exponential distribution of impurities have been discussed.^{3,4} This paper presents a method of analyzing transistor behavior for any base layer impurity distribution. The analysis is used to give a simple comparison of the properties resulting from four different distributions.

THEORY FOR A GENERAL DISTRIBUTION

Assumptions

- A one-dimensional geometry will be analyzed.
- The base layer thickness is large compared to a mean free path for charge carriers. Hence the motion of carriers can be represented by a diffusion plus drift equation.
- The mobility of carriers is constant. This is not true for impurity densities greater than about $10^{16}/\text{cc}$, but the assumption of constancy does not radically alter the final results.
- The density of "minority" carriers is small compared to the density of "majority" carriers; i.e., no conductivity modulation effects. Also the density of "majority" carriers is small enough that Maxwell-Boltzman statistics apply; i.e., nondegenerate semiconductors.

e) Recombination in the base layer is negligible. This assumption implies that the dc transport factor β is unity. Hence the component of current carried by minority carriers is constant (in the dc case) across the base layer. Actually, this is not an unduly restrictive assumption since the effect of a finite minority carrier lifetime in the base layer can be calculated from the relation

$$1 - \beta = \frac{\tau}{\tau_p} \quad (1)$$

where

τ = average minority carrier transit time

τ_p = minority carrier lifetime in the base layer

β = fraction of emitted holes (for $p-n-p$) that reach the collector.

³ H. Krömer, "Der driftransistor," *Naturwiss.*, vol. 40, pp. 578-579; November, 1953.

⁴ H. Krömer, "Zur theorie des diffusions- und des drifttransistors," *Arch. elekt. Übertragung*, vol. 8, pp. 223-228, 363-369, 499-504; 1954.

Basic Equations

Fig. 1 illustrates the general configuration that will be considered. The theory will be obtained for an n type base region.

The zero of the spatial coordinate x will be taken at the emitter-base junction and it will be assumed that the holes are collected at $x=w$. There may be space-charge widening effects on the base layer in some of the configurations that will be considered. In such cases w will vary with collector voltage but these effects will be neglected in this analysis.

Let $N(x)$ = excess donor density in the base layer (see Fig. 1).

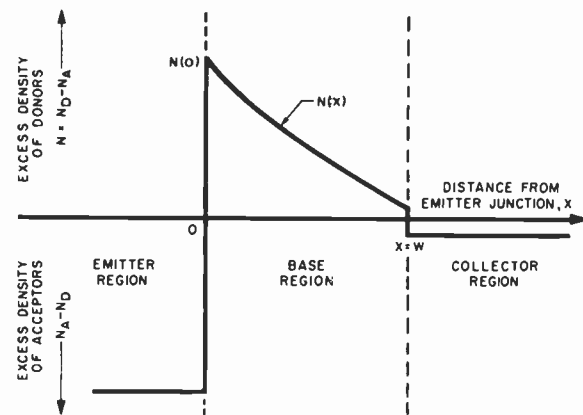


Fig. 1—General distribution of donors and acceptors in structures to be analyzed.

Then if $N \gg n_i$ it is approximately true^{5,6} that

$$n \approx N \cong n_i e^{\psi - \phi} / kT \quad (2)$$

where n = electron density, n_i the intrinsic value of electron density. ϕ is the Fermi potential and ψ is the electrostatic potential.

From (2) we obtain

$$E = - \frac{d\psi}{dx} = - \frac{kT}{q} \frac{1}{N} \frac{dN}{dx} \quad (3)$$

= "built in field."

Also the hole current density I_p is given by⁷

$$I_p = q\mu_p p E - qD_p \frac{dp}{dx}. \quad (4)$$

Where I_p is the hole current, μ_p and D_p are mobility and diffusion constants for holes in n type material, and p is hole density. Substituting (3) into (4) we obtain

$$I_p = - qD_p \left[\frac{p}{N} \frac{dN}{dx} + \frac{dp}{dx} \right]. \quad (5)$$

The steady state solution to (5) with the boundary condition that $p=0$ at $x=w$ is

⁵ The condition $N \gg n_i$ limits the accuracy of calculation to $n > 5 \times 10^{13}$ for Ge at room temperature.

⁶ W. Shockley, "Electrons and Holes in Semiconductors," New York, D. Van Nostrand, 1950, p. 304.

⁷ *Ibid.*, p. 299.

$$p = \frac{I_p}{qD_p} \frac{1}{N(x)} \int_z^w N dx. \quad (6)$$

The hole concentration, p_0 , in the base layer adjacent to the emitter junction can be obtained from (6), and is of interest since this quantity is related to the emitter voltage by the boundary condition⁸

$$p_0 = p_{n0} e^{qV_E/kT} \quad (7)$$

where p_{n0} = thermal equilibrium value for hole concentration in the base layer at the emitter junction and V_E = emitter voltage. The hole concentration p_0 is

$$p_0 = \frac{I_p}{qD_p N_0} \int_0^w N dx. \quad (8)$$

where N_0 is defined as the excess donor concentration in the base layer adjacent to the emitter junction.

Derivation of Fundamental Transistor Parameters

The transverse sheet resistance R of the base layer is given as the reciprocal of the integrated transverse conductance⁹ and is very nearly

$$\frac{1}{R} = q\mu_n \int_0^w N dx \quad (9)$$

where R = resistance/square and μ_n = electron mobility. For any fixed geometry, the ohmic base resistance is directly proportional to R . Thus, for circular geometry the ohmic base resistance for the active region between emitter and collector¹⁰ is

$$r_b' = \frac{R}{8\pi} = \frac{1}{8\pi q\mu_n N w} \quad (10)$$

for uniform base layer.

The dc emitter efficiency is defined as

$$\gamma = \frac{I_p}{I_p + I_n} \quad (11)$$

where I_n and I_p are the electron and hole currents respectively crossing the emitter junction.

The electron current I_n is¹¹ (for uniform resistivity in the emitter)

$$I_n = \frac{qD_n}{L_n} \frac{n_i^2}{P_0} (e^{qV_E/kT} - 1) \quad (12)$$

where P_0 is the acceptor concentration in the emitter region, L_n is the diffusion length for electrons in the emitter¹² and D_n is the diffusion constant for electrons in the emitter region.

From (7), (8) and (9) we obtain

⁸ *Ibid.*, p. 312.

⁹ *Ibid.*, p. 16.

¹⁰ Early, *op. cit.*

¹¹ Shockley, *op. cit.* p. 314.

¹² For emitter regions less than a diffusion distance thick, L_n must be replaced by a distance dependent on the emitter geometry and recombination velocity at the emitter surfaces.

$$I_p = q^2 D_p \mu_n R n_i^2 e^{qV_E/kT}. \quad (13)$$

For $V_E \gg kT/q$ (12) and (13) give

$$\gamma = \frac{R}{R + \frac{1}{q\mu_n L_n P_0}}. \quad (14)$$

This expression neglects possible differences in mobility between emitter and base regions but does give the general form of the dependence of γ on the geometrical parameters. Note that the second term in the denominator of (14), which arises from electron current into the emitter, could be written as the transverse sheet resistance of a slice of the emitter which is one electron diffusion length thick. Eq. (14) shows that the dc emitter efficiency is a function only of the sheet resistance of the base layer and the conducting properties of the emitter region. Also, for a given emitter region, γ approaches 1 as R is increased. This places a lower limit on R consistent with high dc γ . This requirement conflicts with the general objective of low ohmic base resistance.

The average transit time for holes, τ , is given by

$$\tau = \int_0^w \frac{dx}{v} \quad (15)$$

where v is the average velocity at position x . The velocity is related to the current I_p by the relation

$$I_p = pqv. \quad (16)$$

A substitution for p from (6) gives

$$\frac{1}{v} = \frac{1}{D_p N(x)} \int_x^w N(x) dx, \quad (17)$$

hence,

$$\tau = \int_0^w \left[\frac{1}{D_p N(x)} \int_x^w N(x) dx \right] dx. \quad (18)$$

The alpha of a transistor, defined as the ratio of change in collector current to corresponding change in emitter current can be written as the product of γ , β , and α^* where γ is the emitter efficiency, β is the transport factor and α^* is the ratio of total collector current to minority carrier current at the collector junction. For the purposes of this paper, we assume that α^* is unity. Both γ and β decrease in magnitude as frequency is increased so that the frequency cut-off of alpha is determined by a combination of the frequency behavior of γ and β . We will consider the frequency cut-off of γ and β separately.

In the transistor of Fig. 1, a drift-field exists in the base layer which forces the holes in the base layer to drift towards the collector junction. In this case, as distinguished from that of the uniform base layer, the frequency cut-off of the transport factor is not proportional

to the reciprocal of transit time. In fact we will have a phase shift in β without the corresponding fall off in amplitude.

A general relation between transit time τ and frequency cut-off can be obtained from the following consideration: The frequency cut-off of β (defined as the frequency where the magnitude of β has fallen to $1/\sqrt{2}$ of its low frequency value) is proportional to the frequency with which infinitely narrow spikes of holes can be emitted at the emitter and still be distinguishable when they have reached the collector. The spike of current will start as a very narrow bunch of holes which simultaneously drifts and diffuses towards the collector.¹³ To a first order, the effects of drift and diffusion can be considered separately so that we can say that in time τ (transit time) the bunch has spread in space to a width of

$$d \sim \sqrt{D_p \tau}. \quad (19)$$

If we take d as the closest spacing of the bunches that are still distinguishable, the spacing in time of the spikes must then be

$$t = \tau \frac{d}{w} \quad (20)$$

or

$$f_\beta \sim \frac{1}{t} = \frac{w}{\sqrt{D_p \tau^{3/2}}} \quad (21)$$

f_β = frequency cut-off of β .

The values of transit time and frequency cut-off for the uniform case have been calculated.¹⁴ From these results (25), (26) the relationship of (21) can be reduced to,

$$f_\beta = \frac{1}{\pi \sqrt{D_p}} \frac{w}{(2\tau)^{3/2}}. \quad (22)$$

The nature of the assumptions used in obtaining (22) limits its accuracy to within about 20 or 30 per cent. However, the direction of error should be the same for all distributions.

SPECIFIC DISTRIBUTIONS

The quantities R , τ , and f_β will be discussed for four specific donor distributions in the base layer. The excess donor distributions will be taken as *a*) Uniform, *b*) Linear, *c*) Exponential, and *d*) Complementary error function. In cases *b*), *c*) and *d*) it will be assumed that the concentration decreases from emitter to collector. As before, the collector junction will be taken at $x=w$. The uniform case has been extensively discussed and will

¹³ W. Shockley, "Transistor electronics: imperfections, unipolar and analog transistors," Proc. IRE, vol. 40, pp. 1289-1313; November, 1952 gives a more comprehensive discussion of simultaneous drift and diffusion of a bunch of carriers.

¹⁴ Shockley, *et al.*, *op. cit.*

be taken as the basis of comparison for all of the other distributions. The subscripts 0, lin, exp, erfc will be used to designate cases *a*, *b*, *c*, and *d* respectively to facilitate the comparison.

Uniform

$$N(x) = \text{constant} = N_0. \quad (23)$$

From (9)

$$\frac{1}{R_0} = q\mu_n w N_0. \quad (24)$$

From (10)

$$\tau_0 = \frac{w^2}{2D_p}. \quad (25)$$

Also, the frequency cut-off for the uniform case is

$$f_0 = \frac{D_p}{\pi w^2}. \quad (26)$$

Linear

$$N(x) = N_0 \left(1 - \frac{x}{w}\right) \quad (27)$$

$$\frac{1}{R_{\text{lin}}} = \frac{1}{2} q\mu_n N_0 w = \frac{1}{2R_0} \quad (28)$$

$$\tau_{\text{lin}} = \frac{w^2}{4D_p} = \frac{1}{2} \tau_0 \quad (29)$$

and from (22) and (26)

$$f_{\text{lin}} = \frac{2\sqrt{2}}{\pi} \frac{D_p}{w^2} = 2\sqrt{2} f_0. \quad (30)$$

Exponential

$$N(x) = N_0 e^{-x/L} - N_1. \quad (31)$$

Collector junction is at $x=w$ where $N(x)=0$; hence

$$\frac{w}{L} = \ln \frac{N_0}{N_1}. \quad (32)$$

(Actually, in the examples considered here, collection occurs at a place in the base region where the concentration of donors is at least as high, or higher, than the concentration of acceptors in the collector region. However, for purposes of comparison, the same conditions are assumed for all distributions.)

$$\frac{1}{R_{\text{exp}}} = \frac{1}{R_0} \left[\frac{1}{\ln \frac{N_0}{N_1}} - \frac{N_1}{N_0} \left(\frac{1}{\ln \frac{N_0}{N_1}} + 1 \right) \right]. \quad (33)$$

Fig. 2 shows a plot of R_{exp}/R_0 as a function of N_0/N_1

$$\tau_{\text{exp}} = \frac{w^2}{2D} \left[\frac{2}{\ln \frac{N_0}{N_1}} - \frac{2}{\left(\ln \frac{N_0}{N_1} \right)^2} \int_1^{N_1/N_0} \frac{\ln u \, du}{1-u} \right]. \quad (34)$$

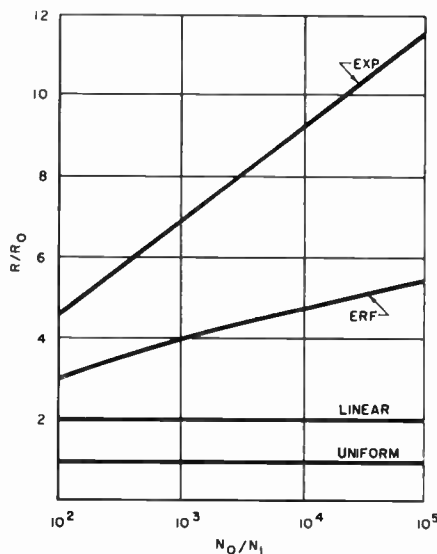


Fig. 2—Effect of various impurity distributions, on base layer resistance.

In (34), the dimensionless parameter u is introduced to demonstrate the dependence of transit time only on N_0/N_1 . We can rewrite (34) as

$$\tau_{\text{exp}} = \tau_0 f \left(\frac{N_0}{N_1} \right) \quad (35)$$

where $f(N_0/N_1)$ is the multiplier of $w^2/2D_p$ in (34). Fig. 3 shows a plot of τ_{exp}/τ_0 as function of N_0/N_1 ,

$$f_{\text{exp}} = f_0 \left(f \left(\frac{N_0}{N_1} \right) \right)^{-3/2}. \quad (36)$$

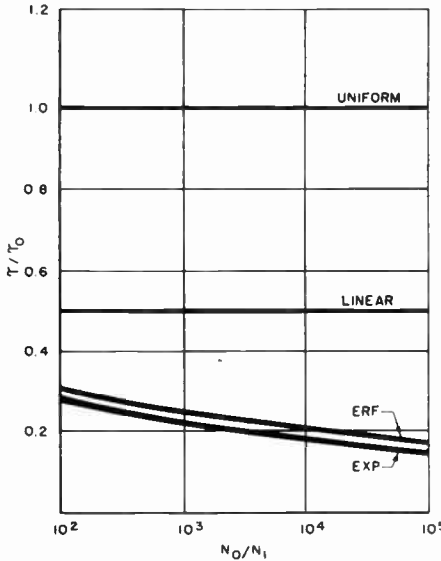


Fig. 3—Effect of various impurity distributions on transit time.

Fig. 4 has a plot of f_{exp}/f_0 as a function of N_0/N_1 .

Complementary Error Function

$$N(x) = N_0 \operatorname{erfc} \frac{x}{L} - N_1 \quad (37)$$

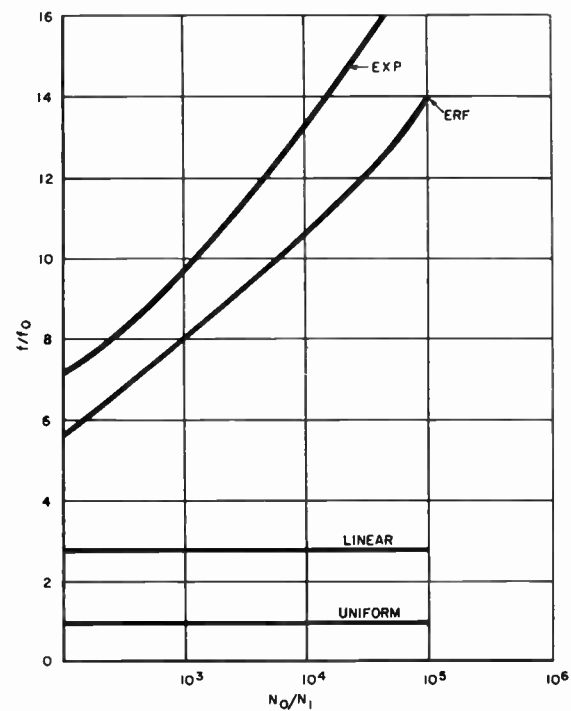


Fig. 4—Effect of various impurity distributions on frequency cut-off of β .

and it will be assumed that $N(x) = 0$ at $x = w$ or

$$N_0 \operatorname{erfc} \frac{w}{L} = N_1 \quad (38)$$

$$\frac{1}{R_{\text{erfc}}} = q \mu_n N_0 w \left(\frac{L}{w \sqrt{\pi}} (1 - e^{-w^2/L^2}) \right) \quad (39)$$

$$\therefore \frac{1}{R_{\text{erfc}}} = \frac{1}{R_0} \left(\frac{L}{w \sqrt{\pi}} (1 - e^{-w^2/L^2}) \right). \quad (40)$$

Fig. 2 also shows a plot of R_{erfc}/R_0 as a function of N_0/N_1 . Also,

$$\tau_{\text{erfc}} = \frac{w^2}{D_p} \int_0^1 \frac{\int_\xi^1 \left(\operatorname{erfc} \frac{\eta w}{L} - \frac{N_1}{N_0} \right) d\eta}{\operatorname{erfc} \frac{\xi w}{L} - \frac{N_1}{N_0}} d\xi. \quad (41)$$

In (41), the dimensionless parameters have been introduced so that integral is a function only of N_1/N_0 and w/L which is a function of N_1/N_0 . We may write

$$\tau_{\text{erfc}} = \tau_0 g \left(\frac{N_1}{N_0} \right) \quad (42)$$

where

$$g \left(\frac{N_1}{N_0} \right) = 2 \int_0^1 \frac{\int_\xi^1 \left(\operatorname{erfc} \frac{\eta w}{L} - \frac{N_1}{N_0} \right) d\eta}{\operatorname{erfc} \frac{\xi w}{L} - \frac{N_1}{N_0}} d\xi. \quad (43)$$

Fig. 3 shows a plot of $\tau_{\text{erfc}}/\tau_0$ as a function of N_0/N_1 .

Also,

$$f_{\text{erfo}} = f_0 \left(g \left(\frac{N_0}{N_1} \right) \right)^{-3/2}. \quad (44)$$

Fig. 4 has a plot of f_{erfo}/f_0 as a function of N_0/N_1 .

DISCUSSION

We have obtained formulas relating some of the fundamental transistor parameters to the distribution of impurities in the base layer. A direct comparison between the attainable transistor parameters is desirable however. The essential transistor parameters which affect the behavior of transistors include base resistance, frequency cut-off of β , low frequency γ , frequency cut-off of γ , collector capacitance, low frequency collector-emitter voltage feedback, space charge layer widening effects on α .

In order to reduce collector capacitance and mitigate "punch through limitations" it has been proposed that a high resistivity layer be included between the base and collector.¹⁵ This has the effect of forcing the space charge region to extend towards the collector rather than in the direction of the base layer. In this case, the number of base layer donor atoms which are included within the space charge region is essentially independent of the distribution of donors in the base layer, and is a function only of collector voltage. Thus, the effect of collector voltage on transverse base layer sheet resistivity does not depend on the distribution of donors in the base layer. The effects of collector voltage on collector-emitter feedback and low frequency γ are also independent of the distribution of carriers in the base layer, but are a function of the total number of impurity centers. The requirements of high dc γ and low r_b' make it necessary to compromise the value of R (base layer sheet resistivity) and this compromise is independent of donor distribution.

The parameters that are a function of donor distribution in the transistor structure that we have hypothesized are f_α , the frequency cut-off, and N_0 , the density of donors in the base at the emitter junction. The density N_0 is a large factor in determining the behavior of the emitter junction at high frequencies. For thin base layers and low resistivity emitter regions, the high frequency behavior of the emitter junction may be approximated by the parallel combination of an emitter resistance r_E and emitter transition region capacitance C_{TE} . On a unit area basis, and for a junction approximating a step¹⁶

$$C_{TE} \sim \sqrt{N_0} \quad (45)$$

$$r_E \sim \frac{1}{I_E}. \quad (46)$$

¹⁵ Early, *op. cit.*

¹⁶ W. Shockley, "The theory of $p-n$ junctions in semiconductors and $p-n$ junction transistors," *Bell Syst. Tech. Jour.*, vol. 28, pp. 435-489; July, 1949.

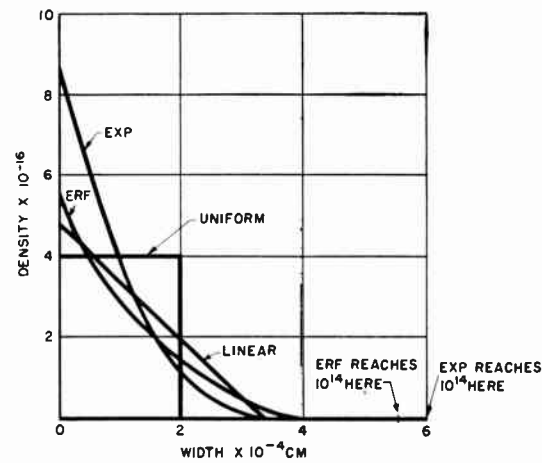


Fig. 5—Equivalent base layer designs.

The current which flows into C_{TE} does not contribute to hole flow so that the emitter has a frequency cut-off (frequency cut-off of γ) proportional to the reciprocal of the time constant.

$$t_E = r_E C_{TE}, \quad (47)$$

but

$$r_E C_{TE} \sim \sqrt{N_0 / I_E}. \quad (48)$$

Hence, if the ratio $\sqrt{N_0 / I_E}$ remains constant, the emitter cut-off frequency remains constant. (Actually, C_{TE} is a function of the forward voltage, but this variation is slow compared to the variation of I_E with voltage.)

In practice, the relation in (48) means that in order to attain higher frequencies it will be necessary to operate transistors at higher current densities. Also, to attain a given cut-off frequency in the emitter, the operating current density is a function of the base layer donor distribution.

In particular, distributions with high N_0 require higher emitter current densities than those with low N_0 to attain the same γ frequency cut-off. However, it will now be shown that, for equal base resistances and the required higher current density consistent with high γ frequency cut-off, the distributions with high N_0 actually operate at lower hole concentration. Eq. (8) shows that, if the total number of impurities in the base layer is fixed, the maximum hole density p_0 is given by

$$p_0 \propto \frac{I_p}{N_0}. \quad (49)$$

Furthermore, if $I_p/\sqrt{N_0}$ is constant, then

$$p_0 \propto \frac{1}{\sqrt{N_0}}. \quad (50)$$

To present a concrete comparison of the base layer designs, four Ge base layers equivalent in R and f_α were obtained by a cut and try process from Figs. 2, 3, and 4. These base layer designs are shown in Fig. 5. It is

assumed for this comparison that the density of acceptors in the collector is 10^{14} and for the uniform case the density of donors is $4 \times 10^{16}/\text{cm}^3$ and $W = 2 \times 10^{-4} \text{ cm}$.¹⁷ It is seen from Fig. 5 that the nonuniform distributions require greater maximum donor concentrations than does the uniform case. Thus for equal γ cut-off frequency the nonuniform distributions must operate at higher current (and power) density than does the uniform distribution, but at a lower hole density. Also, the uniform case requires a narrower base region than do the nonuniform cases.

We have not attempted to account for variation of mobility across the base layer in the analysis. In the

¹⁷ This example is essentially the 200 mcps f_α transistor given by J. M. Early in reference 2.

¹⁸ M. B. Prince, "Drift mobilities in semiconductors, I. Germanium," *Phys. Rev.*, vol. 92, pp. 681-687; November 1, 1953.

examples of Fig. 5, this would certainly have an effect since at $N = 4 \times 10^{16}$ the hole drift mobility¹⁸ in Ge is only 1,100 while at 10^{16} (roughly the last third of the transit for the exponential case) the mobility is approximately 1,800. The increased mobility at the end of the transit would be at least partially compensated by the lower mobility at the beginning of the transit so that exact estimation of this effect is difficult.

ACKNOWLEDGMENT

The authors are indebted to R. W. Hamming who was of great assistance in the computing of transit times, and to the reviewer who pointed out an error in the treatment of the exponential case.

Surface Resistance and Reactance of Metals at Infrared Frequencies*

J. R. BEATTIE† AND G. K. T. CONN†

INTRODUCTION

IN A METAL the electrical current density and the field strength decay exponentially at high frequencies as the distance z from the surface increases. Thus

$$J = J_0 \exp(-z/\delta), \quad (1)$$

where J is the current density and δ is the skin depth. By Maxwell's theory δ is related to σ , the direct current conductivity, so that

$$\delta = c/\sqrt{(2\pi\omega\sigma)}; \quad (2)$$

ω is the angular frequency. At 10^9 cycles per second, δ is of the order of microns in metals of high conductivity. The ratio R of the electric field gradient to the current per unit square at the surface is a convenient definition of resistance at high frequencies, and

$$R = 1/(\sigma\delta) = \sqrt{(2\pi\omega/\sigma c^2)}. \quad (3)$$

At high radio-frequencies R may be obtained by measuring the Q of resonators made of the material under

study.¹⁻⁴ Measured values usually exceed those calculated from (3) but good electro-polished surfaces give close agreement. The discrepancies are almost certainly caused by surface roughness; the presence of strain or impurity in the surface layers appears to be of less practical importance.

At infrared frequencies, greater than 10^{12} cycles per second, (3) is inadequate. Writing $CZ/4\pi$ as the ratio of the electric to the magnetic field strengths at the surface of the metal,^{5,6} we define the real and imaginary components of the surface impedance, Z respectively as the surface resistance R and the surface reactance X . R may be determined from measurements of the intensity of reflected radiation. If R_0^2 is the ratio of reflected to incident intensity, then to a close approximation

$$1 - R_0^2 = CR/\pi. \quad (4)$$

¹ F. A. Benson, "Wave-guide attenuation and its correlation with surface roughness," *Proc. IEE*, vol. 100, pp. 85, 213; 1953.

² F. A. Benson, "Attenuation in nickel and mild-steel waveguides at 9375 Mc/s," *Proc. IEE*, vol. 101, pp. 38; 1954.

³ A. C. Beck and R. W. Dawson, Correction to "Speed of electronic switching circuits," *PROC. IRE*, vol. 38, p. 1181; October, 1950.

⁴ R. C. Chambers and A. B. Pippard, "Properties of Metallic Surfaces," Institute of Metals, p. 28; 1952.

⁵ J. A. Stratton, "Electromagnetic Theory," McGraw-Hill Book Co., Inc., New York, N. Y.; 1941.

⁶ G. E. H. Reuter and E. H. Sondheimer, "Theory of the anomalous skin effect in metals," *Proc. Roy. Soc. A*, vol. 195, p. 336; 1948.

* Original manuscript received by the IRE, May 31, 1955; revised manuscript received August 11, 1955.

† Dept. of Physics, University of Sheffield, Sheffield, England.

Rubens and Hagen⁷ measured R_0^2 for many metals and this early work was taken to vindicate (3) at infrared frequencies. Recently, considerable doubt has been cast on this view which is in conflict with modern theories.^{8,9} Though R and X are related,¹⁰ both must be measured if investigation is limited to a particular frequency range. This work shows that X is much larger than R so that measurements of R_0^2 alone are of limited value.

The experimental methods used in the infrared are essentially optical and it is natural to describe the behavior of materials studied in terms of a complex refractive index $n - jk$. Save under special theoretical conditions (Reuter and Sondheimer) this refractive index is equivalent to reciprocal of surface impedance and

$$Z = R + jX = 4\pi/c(n - jk). \quad (5)$$

R and X have a more direct practical significance for the present purpose and will be used to describe the experimental results. The simple theory of electron relaxation gives^{6,11,12}

$$R = \sqrt{\left(\frac{2\pi\omega}{c^2\sigma}\right)} \cdot \sqrt{-\omega\tau + \sqrt{(1 + \omega^2\tau^2)}}, \quad (6)$$

$$X = \sqrt{\left(\frac{2\pi\omega}{c^2\sigma}\right)} \cdot \sqrt{\omega\tau + \sqrt{(1 + \omega^2\tau^2)}}. \quad (7)$$

τ is the relaxation time, that is the interval between electron collisions. In each expression the factor which forms (3) is multiplied by a function of τ .

The behavior of a number of specimens of silver, aluminum, copper, and nickel is discussed below; these have been studied in the range 2.5 to 15×10^{13} cycles per second. Suitable values of τ and σ have been chosen to fit these results. The consequent values of σ do not in general agree with accepted figures of the direct current conductivity and the origin of this is discussed. In some cases the temperature coefficient of σ has been measured. Nickel specimens show undoubted departure from (6) and (7); probable explanation that this is caused by internal photoelectric transitions between d - and s -bands.

EXPERIMENTAL METHOD

The only measurements of the optical constants of metals in the infrared region, ν less than 10^{14} cycles per second, from which both R and X may be deduced, are

⁷ H. Rubens and E. Hagen, "On some relations between the optical and electrical qualities of metals," *Phil. Mag.*, vol. 7, p. 162; 1904.

⁸ N. F. Mott and C. Zener, "Optical properties of metals," *Proc. Camb. Phil. Soc.*, vol. 30, p. 249; 1934. The dispersion of free or metallic electrons in terms of optical constants n and k is discussed in this paper.

⁹ R. B. Dingle, "The anomalous skin effect and the reflectivity of metals," *Physica*, vol. 19, p. 348; 1953.

¹⁰ T. S. Robinson, "Optical constants by reflection," *Proc. Phys. Soc. B*, vol. 65, p. 910; 1952.

¹¹ N. F. Mott and H. Jones, "Properties of Metals and Alloys," 1936.

¹² O. O. Wolfe, *Proc. Phys. Soc. B*, vol. 65, p. 910; 1952.

those of Försterling and Fréedericksz.¹³ Opaque films of silver, copper, gold, iridium, and platinum were examined over the limited range of 5.9×10^{13} to 5×10^{14} cycles per second. In studies of relaxation it is important to extend measurements to frequencies at least as low as 3×10^{13} cycles per second. The experimental methods which have been developed^{14,15} are applicable over the whole range of infrared frequencies but attention has so far been limited to frequencies larger than 2.5×10^{13} cycles per second since ample radiant flux is available, relaxation effects can be measured and there is no reason to suppose that, with metals, information is lost by this limitation.

Plane polarized radiation falls at an oblique angle on a specimen and the elliptically polarized light which is reflected is analyzed by a second plane polar. At a given angle of incidence ϕ , two parameters ρ and Δ are measured; ρ is the amplitude ratio of the two reflection coefficients and Δ is the relative phase of these two components polarized parallel and perpendicular to the plane of incidence. Then, to a close approximation,¹⁶

$$R + jX = \frac{4\pi}{c \tan \phi \sin \phi} \frac{1 - \rho \exp(i\Delta)}{1 + \rho \exp(j\Delta)}. \quad (8)$$

R and X are usually determined with an accuracy of 1 or 2 per cent.

SPECIMENS

The depth to which radiation of wavelength λ penetrates an absorbing medium is $\lambda/4\pi k$ or $c/2\omega k$;¹⁷ in most metals it is of the order of 10^{-6} cm. Roughness or contamination of the surface may therefore seriously influence Z though the defects are small compared with a wavelength of visible light and therefore not obvious to microscopic examination. Since such defects cannot be eliminated entirely it is important to examine, in the case of each metal, a number of surfaces prepared in different ways. Specimens of bulk material have been prepared by buffing, by mechanical polishing, by chemical etching, and by electropolishing of annealed material. Opaque metal films have been made by condensing the metal vapor on glass at room temperatures; these were deposited at pressures lower than 10^{-6} mm Hg. It is well-known that the electrical conductivity of thin films is significantly lower than that of bulk material; using the technique of multiple-beam interferometry to determine the thickness, the direct current conductivity was measured.¹⁷

¹³ V. Försterling and Fréedericksz, "Optical constants of certain metals in the infrared," *Ann. Phys.*, vol. 40, p. 201; 1913.

¹⁴ J. R. Beattie and G. K. T. Conn, "Optical constants of metals in the infrared principles of measurement," *Phil. Mag.*, vol. 46, p. 222; 1955.

¹⁵ J. R. Beattie, "Optical constants of metals in the infrared-experimental methods," *Phil. Mag.*, vol. 46, p. 235; 1955.

¹⁶ If $\omega \ll 1/\tau$ so that there is no reactive term, this reduces to (1).

¹⁷ S. Tolansky, "Multiple-Beam Interferometry," Clarendon Press, Oxford, England; 1948.

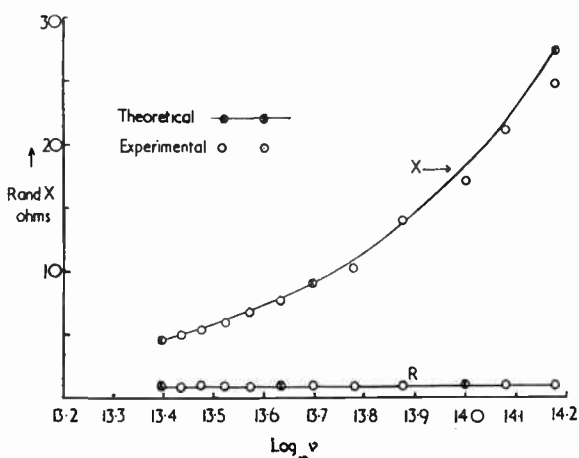


Fig. 1—Surface resistance R and reactance X of evaporated silver as a function of frequency.

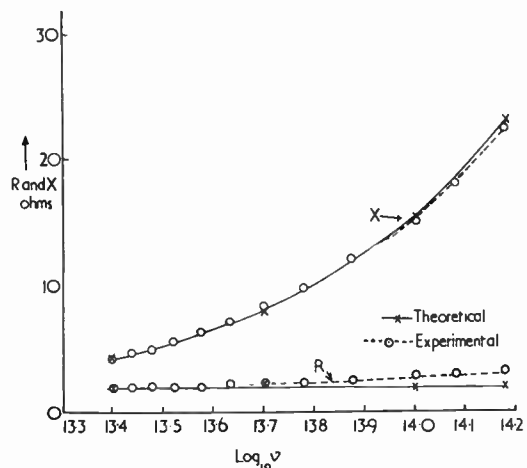


Fig. 2—Surface resistance R and reactance X of evaporated aluminum as a function of frequency.

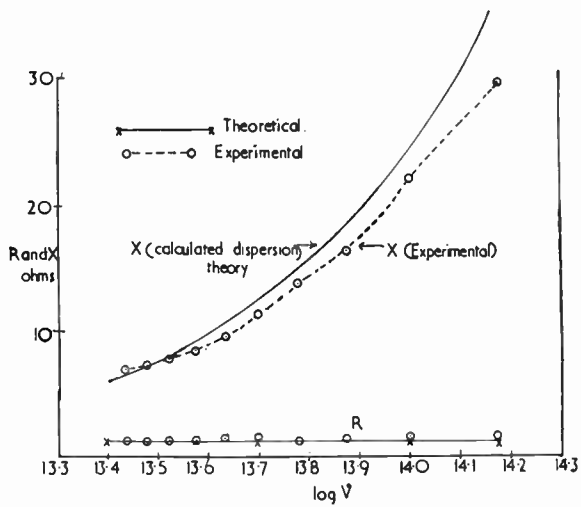


Fig. 3—Surface resistance R and reactance X of a copper surface, mechanically polished, plotted against frequency.

EXPERIMENTAL RESULTS

Results which are typical of silver, aluminum, and copper are shown in Figs. 1, 2 and 3 in which R and X

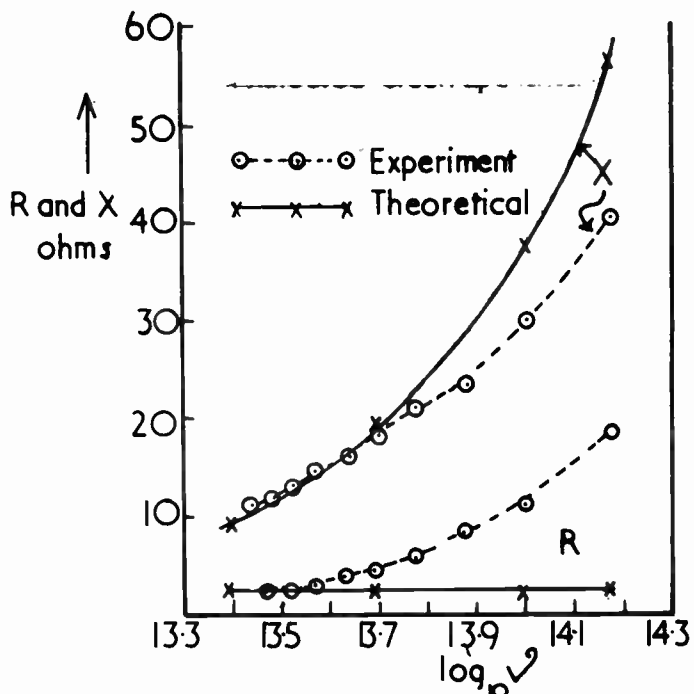


Fig. 4—Surface resistance R and reactance X of annealed electro-polished nickel plotted against frequency. At higher frequencies the experimental points depart significantly from the calculated dispersion curve.

are plotted as functions of frequency. The curves drawn are calculated from (6) and (7). The values of σ and τ used for this purpose were chosen to fit the experimental results at low frequencies since there is evidence that the dispersion of metallic electrons, described by (6) and (7), is the only significant influence at such frequencies.¹⁸ σ and τ are given by the equations

$$\sigma = 2\pi\omega/(RXc^2) \quad \text{and} \quad \tau = -(R^2 - X^2)/(2RX\omega). \quad (9)$$

These follow immediately from (6) and (7). The simple theory of electron relaxation is vindicated by the close correspondence between the experimental points and the theoretical curves. The importance of the reactive component X is obvious. It may be noted that in all cases investigated the value of σ which is deduced is considerably less than that measured with direct currents.

Fig. 4 is representative of specimens of nickel. Clearly (6) and (7) are not adequate; the significant influence of absorption other than by conduction electrons is briefly discussed elsewhere.¹⁹ At low frequencies this absorption is trivial and (9) has been used in this region to calculate τ and σ ; the latter is again much less than that measured with direct currents.

A summary of many experimental measurements is given in Table I. τ and σ are listed with γ the effective number of "free" electrons per unit volume which is calculated from the simple expression¹¹

¹⁸ J. R. Beattie and G. K. T. Conn, "Optical constants of metals in the infrared-silver, copper, and nickel," *Phil. Mag.*, in press.

¹⁹ J. R. Beattie and G. K. T. Conn, "Resonance absorption of nickel in the infrared region," *Phil. Mag.*, in press.

TABLE I
SUMMARY OF EXPERIMENTAL RESULTS*

Metal	Preparation	$\sigma_{E.S.U.}$	τ secs.	γ/atom	$\sigma_{D.C.}/\sigma$	$\alpha_{D.C.}/\alpha$
Silver	Evaporated	23.4×10^{16}	1.75×10^{-14}	0.90	1.4	—
	Mechanically polished	19.5×10^{16}	1.61×10^{-14}	0.81	2.9	4
	Metal-polish	12×10^{16}	2.05×10^{-14}	0.39	4.8	—
	Etched	6.9×10^{16}	3.3×10^{-14}	0.14	8.4	—
Aluminum	Evaporated	11.6×10^{16}	6.1×10^{-14}	1.28	1.3	—
Copper	Evaporated	12.4×10^{16}	1.41×10^{-14}	0.41	2.0	—
	Mechanically polished	13.5×10^{16}	1.80×10^{-14}	0.35	3.9	—
	Electrolytically polished	9.1×10^{16}	1.41×10^{-14}	0.30	5.7	—
	Scratched	4.9×10^{16}	1.06×10^{-14}	0.21	10.6	—
Nickel	Evaporated	3.16×10^{16}	1.02×10^{-14}	0.14	1.5	5.5
	Mechanically polished	2.68×10^{16}	0.81×10^{-14}	0.14	4.3	20
	Electrolytically polished	3.93×10^{16}	1.24×10^{-14}	0.14	2.9	4.6
	Etched	1.47×10^{16}	1.32×10^{-14}	0.05	7.8	—

* With evaporated films $\sigma_{D.C.}$ is that of the film not the bulk value. $\alpha_{D.C.}$ is the temperature coefficient of the direct current conductivity of bulk material and α the temperature coefficient of σ measured at infrared frequencies.

$$\sigma = \gamma e^2 \tau / m. \\ (m \text{ denotes the mass of an electron}).$$

Figures for the conductivity of each metal vary considerably with treatment of the surface. The general, and obvious, conclusion may be drawn that rougher surfaces show lower value of σ but even the most brilliant mirror finish, however obtained, yields figures which fall short of those measured with direct currents. Such discrepancies may be caused by surface irregularities of the order of 10^{-6} cm, an interpretation which finds some support in the behavior of liquid metals. Color is also lent to this view by the temperature coefficients listed. These were obtained by measuring the R and X of specimens at 250° C and were very much smaller than the figures commonly accepted. Elimination of the influence of surface roughness may eventually permit a more

satisfactory explanation in terms of "anomalous skin effect";^{6,9} a discussion on such lines is premature at this stage. For normal metals at room temperature Reuter and Sondheimer showed that, assuming specular reflection of electrons at the surface of the metal, the anomalous skin effect is not important. Dingle discusses in detail the influence of diffuse electron reflection and it appears not impossible that a theoretical treatment on these lines may account for the low values of σ_0 reported. Dingle's theory, however, predicts a departure from the form of classical dispersion contrary to these results for silver, copper, and aluminum.

ACKNOWLEDGMENT

We must acknowledge grants for apparatus from the Research Fund of the University of Sheffield and from the Royal Society.



Transverse-Field Traveling-Wave Tubes with Periodic Electrostatic Focusing*

R. ADLER†, FELLOW, IRE, O. M. KROMHOUT†, AND P. A. CLAVIER†, MEMBER, IRE

Summary—Traveling-wave tubes are described in which the wave-propagating structure constitutes a smooth, balanced transmission line for radio frequency signals while at the same time providing a space-periodic focusing field at zero frequency. Experimental structures for the 500–900 mc band have wave velocities of 1 to 2 per cent of light and characteristic impedances of about 500 ohms.

A simplified theoretical analysis is given, based on the readily visualized concept of transverse electron waves in a focusing field. In order to get gain, the electron stream must travel faster than the circuit wave by a substantial margin which is determined by the strength of the focusing field. The gain is proportional to the square root of the beam current.

Experimental data are presented concerning the relation between focusing field and effective beam velocity, and between beam current and gain. They are in good agreement with the theory.

Noise figures as low as 6 db have been measured.

THIS PAPER deals with traveling-wave tubes in which the high-frequency signal fields and the periodic electron motions which correspond to these fields are perpendicular to the direction of wave propagation and of electron flow. The electron stream in these tubes is shaped like a thin, flat ribbon; it originates at a long, narrow, cathode, passes through focusing and collimating slits and enters the interaction space, where it is kept thin by a chain of electrostatic lenses.

The experimental tubes described in the following were designed for the uhf band, 500 to 900 mc. The principles of their operation, however, are not restricted to any particular band and same type of structure or a similar one may be used on other frequency ranges.

THE TUBE STRUCTURE

The Slow-Wave Circuit

The wave-propagating structure, shown schematically in Fig. 1, is symmetrical about a center plane which is also the mid-plane of the thin electron stream. On each side of the center plane there is a helical winding which has the cross-sectional shape of a thin rectangle. High frequency signals are applied to this balanced structure from a push-pull source and the amplified signals are delivered to a push-pull load. In the center plane the electric field is purely transverse for reasons of symmetry; longitudinal components exist outside the center plane but for the dimensions employed these components are small enough to remain negligible throughout the region of electron flow.

The helices used in the experimental tubes were wound on rail-shaped ceramic bars having a cross section of 0.550 inch \times 0.63 inch. Each helix was bifilar, being made up of two interlaced windings, each of 44 turns per inch. The spacing between the two helices

* Original manuscript received by the IRE, August 10, 1955; revised manuscript received, September 19, 1955.

† Research Dept., Zenith Radio Corp., Chicago 39, Ill.

was varied from 0.064 inch to as little as 0.010 inch.

Propagation velocities of the transverse field wave on such structures were measured over the range of frequencies from a few mc up to 1,000 mc by observing the length of standing waves along the helices. For this purpose the two interlaced windings of each helix were

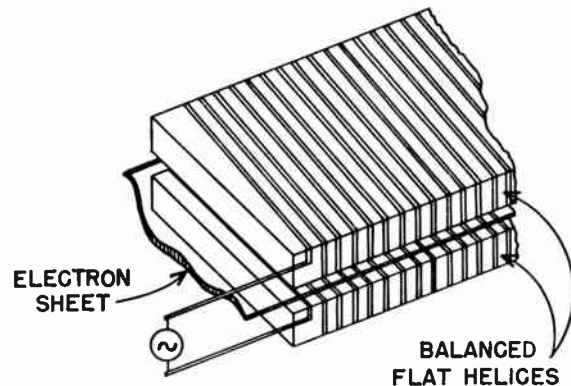


Fig. 1—Balanced wave propagating structure, with electron stream along center plane.

connected together at both ends. At the lower frequencies the standing waves were measured by shorting the helices together at one end and observing the frequencies for which the impedance is zero at the other end; above 400 mc, where end effects were no longer negligible, the field pattern along the helices was explored with the aid of a small movable inductive probe.

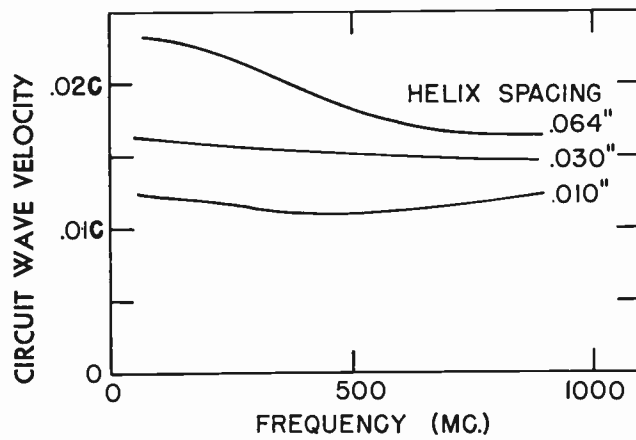


Fig. 2—Phase velocity of balanced flat helices (in terms of light velocity c) vs frequency for three values of spacing between helices. Spacing of 0.030 inch is used in present tubes.

Fig. 2 shows some of the results of these measurements. For the widest spacing, the propagation velocity is more than 2 per cent of light at low frequencies but falls off rapidly toward higher frequencies. For the narrowest spacing, low frequency propagation is slower than 1 per cent of light and after an initial drop, a

slight increase of velocity occurs toward the higher frequencies. At 0.030 inch spacing, the velocity in the range from 500 to 900 mc is practically constant at 1.5 per cent of light. Thus, the circuit wavelength λ is 0.365 inch at 500 mc and 0.197 inch at 900 mc. The corresponding propagation constants ($\gamma = 2\pi/\lambda$) are 17.2 per inch at 500 mc and 31.7 per inch at 900 mc. With a spacing $D = 0.030$ inch between the helix surfaces, the product $\gamma \cdot D$ becomes 0.52 at 500 mc and 0.95 at 900 mc. These figures are of interest with respect to the theoretical analysis which follows later.

In addition to the transverse field wave, the structure shown in Fig. 1 can also propagate a longitudinal wave. It is of interest to know the velocity of this wave because if it accidentally coincided with the velocity of electron flow, traveling-wave amplification of the conventional kind would occur. Measurements show that the longitudinal mode on this structure is 90 per cent faster than the transverse mode at 500 mc and 40 per cent faster at 900 mc.

Returning now to the transverse field, the characteristic impedance of such a structure can be defined like that of a two-wire transmission line, as the square of the voltage between corresponding points on the two helices divided by the power flow. The transverse field in the center plane is generated by that same voltage. A known perturbation of the transverse field, produced for instance by inserting a sheet of mica between the two helices, causes a drop in phase velocity from which the characteristic impedance can be computed. For 0.030-inch spacing, the structure described above measures several thousand ohms at very low frequency, about 600 ohms at 500 mc and 400 ohms at 900 mc.

The 0.030 inch spacing was used in all experimental tubes. A phase velocity of 1.5 per cent of light corresponds to the speed of electron flow at 57 volts; this illustrates the magnitude of the voltages employed in such tubes.

Beam Forming and Focusing

Fig. 3 illustrates the electron gun which was used. The first slot following the cathode is held at negative potential; it serves to control the total current and to confine the active portion of the cathode to a narrow strip of high density. The following accelerator slot is held at about 400 volts to produce the required field at the cathode. After passing the accelerator the beam enters a retarding field and diverges; a small slice, about 10 to 15 per cent of the total cathode current in the present tubes, is selected by the third slot which is only 0.005 inch wide. This slot, together with the metallic mounting brackets for the ceramic bars and with the helices themselves, forms an entrance lens which projects the collimated beam into the interaction space.

The two centering wires shown in Fig. 3—one electrically connected to the third slot, the other brought out separately—make it possible to start beam along the center plane in spite of accidental asymmetries in the gun, and study effects of incorrect beam centering.

Space charge forces, if left to themselves, would make the thin beam grow rapidly thicker; periodic electrostatic focusing is used to prevent this. In a recent paper¹ it was pointed out that the spatial period of such a focusing system must be of a certain minimum size if orderly beam flow is important; unless the thickness of the beam is small compared to the spatial period, transverse motions impressed upon the beam at one point along its travel soon turn into turbulence. The pitch of the windings used in these tubes (0.023 inch) is not nearly large enough to serve as spatial period; thus it

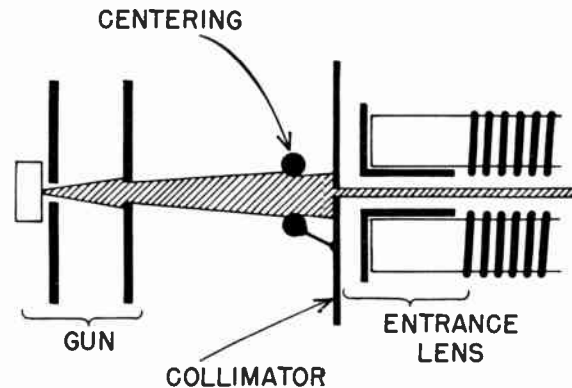
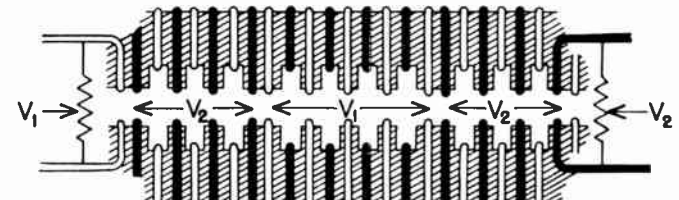


Fig. 3—Profile of electron gun, showing small slice of beam selected by narrow third slot.

is not possible to obtain suitable focusing by applying two different dc potentials to two interlaced uniform windings in the manner described by Tien² without changing some important parameter by a large factor. This did not appear practical.

What is required here is a structure which combines the uniformly distributed high frequency properties of a smooth transmission line with the space-periodic dc field needed for focusing. Several alternatives which combine these properties were studied. The structure finally chosen is shown in Fig. 4. This is still a bifilar



PERIODIC FOCUSING

Fig. 4—Edgewise view of bifilar winding arrangement for electrostatic focusing. Shaded areas represent the notched ceramic forms; the two separate windings on each form, shown in white and black, are held at separate dc potentials V_1 and V_2 .

helix pair, with the two windings on each bar operated at two different dc potentials V_1 and V_2 . But the turns are no longer of uniform cross section; instead, one winding is exposed to the electron stream while the

¹ R. Adler, O. M. Kromhout, and P. A. Clavier, "Resonant behavior of electron beams in periodically focused tubes for transverse signal fields," PROC. IRE, vol. 43, pp. 339-341; March, 1955.

² P. K. Tien, "Bifilar helix for backward-wave oscillators," PROC. IRE, vol. 42, pp. 1137-1143; July, 1954.

other is recessed into grooves cut into the ceramic form, thus shielded from the electron stream by the first winding. At regular intervals, the recessed and the exposed windings interchange their roles. This is accomplished by arranging the grooves in such a pattern that a winding of constant pitch alternately drops into one group of grooves and rides between the grooves of the next group. A bifilar winding of constant pitch is thus made to form a periodic focusing structure with a spatial period which may be made as long as desired. In the experimental tubes, this period equals 0.20 inch or nine times the pitch.

The depth of the recesses is only 0.015 inch, a little less than one-quarter of the minor cross-sectional dimension of the winding. This is not enough to cause any substantial change in the propagation properties of the structure; each bar still acts essentially like a uniform bifilar helix.

The over-all length of the bars is 2.25 inches, and the wound length a little less than two inches. This is rather short for a traveling-wave tube, but not too short to provide useful gain, and it simplifies the task of putting windings on the fragile ceramic bars.

Terminations

In the frequency range between 500 and 900 mc, the characteristic impedance of the helix pair is not very much higher than the 300 ohms commonly used in balanced transmission lines for this range. To obtain a reasonably good match to such lines, quarter-wave sections of intermediate impedance are provided at both ends of the structure. This is done by increasing the distributed capacity of the last three bifilar turns.

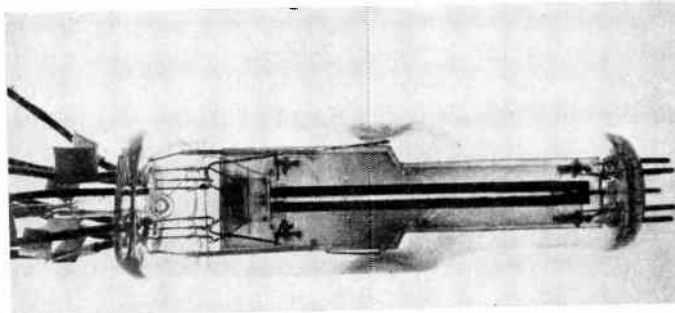


Fig. 5—Transverse-field traveling-wave tube. Flat helix surfaces are perpendicular to plane of photograph. Electron gun at left; two of the wires at left and two of the base pins at right form the 300-ohm balanced input and output lines.

At each end of each helix, the two bifilar windings are connected together through small barium titanate discs which constitute short circuits for signal frequencies. This makes it possible to save four external connections: only the two low-voltage windings are brought out through one end of the tube, and only the two high-voltage windings through the other.

Fig. 5 shows a complete tube, photographed to give the effect of a cross-sectional view. Fig. 6 shows the tube parts including an assembled helix pair (spaced somewhat farther apart than in the experimental tubes) and a single, partly wound ceramic bar.

ELEMENTARY ANALYSIS OF THE TRANSVERSE FIELD TUBE

Transverse Electron Waves

A general theory of the transverse field traveling wave tube has long been available in the literature.³ It treats the interaction between slow-wave circuits and electron streams throughout the range of relative velocities and focusing fields.

Elementary considerations regarding the mechanism of interaction in transverse fields teach us that substantial effects will occur only if a certain numerical relation exists between velocities, focusing field and signal frequency. Since practical tubes must obey this relation, we might reasonably ask whether a simplified analysis might not be made for this special case. It turns out that the resulting simplification is considerable, and that the analysis correctly predicts the performance of practical tubes.

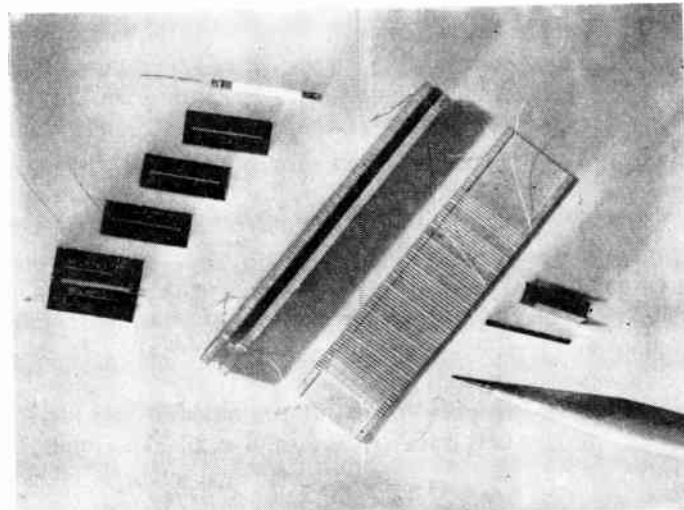


Fig. 6—Components of tube, from left to right: bracket for supporting helices, slots for electron gun, and cathode; pair of helices in position as mounted in tube; partially wound helix showing bifilar winding; collector and capacity-loading element for matching.

Consider a slow-wave circuit on which waves, excited by a generator of angular frequency ω , travel in the $+z$ direction at a velocity u . An observer at a fixed point anywhere along the circuit notes an electric field which alternates at the frequency ω . A moving observer finds a different frequency, because of the Doppler effect; if his speed of motion u_B coincided with u , he would observe zero frequency. Generally, the frequency ω_A which he observes is

$$\omega_A = \omega \left(1 - \frac{u_B}{u} \right). \quad (1)$$

If the observer travels faster than the wave ($u_B > u$), ω_A becomes negative; as in the familiar case of a beat note passing through zero, the minus sign merely signifies a reversal of phase rotation.

³ J. R. Pierce, "Traveling-Wave Tubes," D. Van Nostrand Co., Inc., New York, N. Y., ch. XIII; 1950.

In some instances the sense of phase rotation is not important. For these we can write

$$\frac{u_E}{u} = 1 \pm \frac{|\omega_A|}{\omega}. \quad (2)$$

A case in point is the excitation of a resonator by a driving force of appropriate frequency. If the observer carries such a resonator, tuned to some fixed frequency ω_E which he wishes to be excited by the field, he can accomplish this even though $\omega_E \neq \omega$, by traveling at one of the two suitable speeds u_E given by (2).

An electron in a focusing field represents this kind of an observer. In a homogeneous magnetic field, electrons may easily be thrown into large transverse motion if the driving force acts at the cyclotron frequency; a periodic electrostatic focusing field, on the other hand, exerts upon each electron an elastic restoring force and thus again renders it resonant at a well-defined frequency.¹

An electron stream of velocity u_E in a focusing field, which establishes a transverse resonant frequency ω_E , will therefore react strongly to a circuit wave whose velocity u and signal frequency ω are properly related. We may use (2) to obtain the two suitable wave velocities:

$$u_{12} = \frac{u_E}{1 \pm \frac{\omega_E}{\omega}} \quad (3)$$

and the propagation constants $\gamma_1 = \omega/u_1$, $\gamma_2 = \omega/u_2$:

$$\gamma_{12} = \frac{\omega \pm \omega_E}{u_E} = \frac{\omega}{u_E} \pm \gamma_E \quad (4)$$

where $\gamma_E = \omega_E/u_E$.

Once an electron stream has been exposed, even for a short portion of its travel, to one of the two signal fields described by (3), its electrons will keep on oscillating at their resonant frequency ω_E while they move forward. Thus (3) and (4) describe the velocities and propagation constants not only of two kinds of slow-wave circuits capable of influencing the stream, but also of two free transverse electron waves which may exist on the stream. These waves—one faster and one slower than the stream—are evidently similar to the familiar longitudinal space-charge waves first described by Hahn and Ramo;⁴ the analogy between transverse field traveling-wave tubes operated with a focusing field and velocity-modulating traveling-wave tubes working under high space charge conditions was pointed out by Pierce.⁵ It is important, however, to remember the differences. The two transverse electron waves are separated not because of space charge but only because of the focusing field; their separation remains the same regardless of current density as long as the focusing

field is not changed, and generally they are quite far apart in velocity: a separation of less than ± 10 per cent is rare, and ± 25 per cent is common in practical tubes.

If the two electron waves exist at the same time, they beat with each other and form a standing wave. Since the difference between the two propagation constants [from (4)] is $2\gamma_E$, the length of a standing wave is

$$\Delta z = \frac{2\pi}{2\gamma_E} = \frac{\pi}{\gamma_E} = \pi \frac{u_E}{\omega_E}. \quad (5)$$

A simple physical interpretation of this standing-wave picture is given in Fig. 7. Here, an electron stream guided by a focusing field passes between a pair of short deflectors. Electrons which receive a transverse impulse while passing the deflectors oscillate transversely at the frequency ω_E and thus cross the center plane at time intervals separated by half cycles, or π/ω_E ; during each of these intervals they cover a distance $\Delta z = u_E(\pi/\omega_E)$, the length of one standing wave. It might be noted that the experiment illustrated in Fig. 7 is easily performed; there is no restriction on the signal frequency to be applied to the deflectors, and any convenient signal down to zero frequency may be used. Since the forward velocity u_E is generally known rather accurately, direct observation of the trajectories, for instance by means of off-center targets, is a convenient means for measuring the transverse resonant frequency ω_E in periodically focused structures.

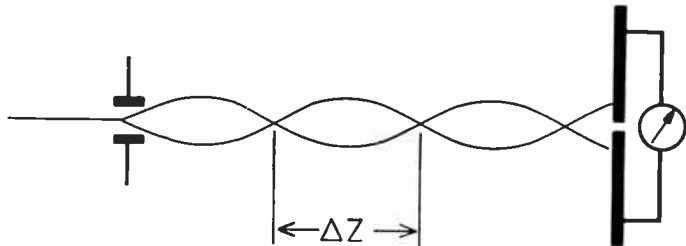


Fig. 7—Electron trajectories in focusing field. Electrons pass a short deflection field before entering. The results of two opposite deflections are shown for a pictorial representation of the standing-wave analogy. Electrons strike one or the other collector depending on number of center-plane crossings. This number can be determined by varying the focusing field.

The Interaction Process

Having now established the relations between velocities and frequencies associated with transverse electron waves on a stream which flows in a focusing field, we proceed to examine the interaction process between such a stream and a slow-wave circuit capable of carrying a transverse electric field. We will assume that the undisturbed propagation velocity of the slow-wave circuit has been made equal to the velocity of one of the two unmodified electron waves; the other electron wave must then have an entirely different velocity and its propagation constant will remain relatively unaffected by the presence of the slow-wave circuit. We shall limit study to interaction between the circuit wave and that electron wave which travels at the same velocity.

⁴ Simon Ramo, "The electronic-wave theory of velocity-modulated tubes," PROC. IRE, vol. 27, pp. 757-763; December, 1939.

⁵ Pierce, *op. cit.*, p. 169.

Each of these two waves, originally, has the same propagation constant γ . As a result of their interaction, we expect γ to be perturbed, so that the field will be

$$E = E_0 \exp [j(\omega t - \gamma z) + \alpha z] \quad (6)$$

To an electron moving at the speed u_E this appears as if it were a field

$$E_E = E_0 \exp [j\omega_A + \epsilon]t \quad (7)$$

where

$$\epsilon = \alpha \cdot u_E. \quad (8)$$

The sign of ω_A (7) may be positive or negative, depending on whether we have chosen the faster or the slower electron wave.

Under the influence of E_E , the electron moves transversely with an excursion

$$y = y_0 \exp [j\omega_A + \epsilon]t \quad (9)$$

a velocity

$$\dot{y} = [j\omega_A + \epsilon]y \quad (10)$$

and an acceleration

$$\ddot{y} = [j\omega_A + \epsilon]^2 y = -[\omega_A^2 - \epsilon^2]y + 2j\omega_A\epsilon y. \quad (11)$$

The first term on the right side of (11) represents an acceleration \ddot{y} proportional to the excursion y but of opposite sign; this is characteristic of periodic motion, and it is taken care of by the elastic force which the focusing field exerts. Let us now assume that $\epsilon \ll |\omega_A|$; if we then adjust the focusing field so that $\omega_E^2 = \omega_A^2 - \epsilon^2$, we find that to a good approximation

$$\omega_E \approx |\omega_A|. \quad (12)$$

The condition $\epsilon \ll |\omega_A|$, stated in physical terms, means that each electron performs primarily a harmonic motion at the frequency ω_A ; growth, decay or phase change are insufficient to overshadow the harmonic character of this motion. As will be shown later, the condition $\epsilon \ll |\omega_A|$ is more easily met than infringed in practice.

The second term on the right side of (11) calls for an external driving force. A transverse field E produces an acceleration $\ddot{y} = (e/m)E$; thus

$$2j\omega_A\epsilon y = \frac{e}{m} E \quad (13)$$

and

$$y = \frac{e}{m} \frac{E}{2j\omega_A\epsilon}. \quad (14)$$

Eq. (14) relates the transverse excursion y of an electron at any point in the tube to the transverse signal E at the same point. It thus describes the electron wave as a function of the circuit wave. Let us now turn to the current which the electron wave induces in the circuit.

This circuit contains two metallic surfaces, spaced by a distance D , between which the electron stream flows.

We may simplify the analysis by assuming that D is smaller than the circuit wavelength divided by 2π , or $\gamma D < 1$. Under this restriction the field changes only gradually with z and y and it becomes permissible to consider each increment dz of the slow-wave circuit a small lumped condenser in which the transverse field is homogeneous.

The current induced in such an incremental condenser at a point z is determined by the transverse motion of the stream $\partial y / \partial t$ at that point, not by the transverse velocity \dot{y} of the individual electrons. All electrons, however, which start at the same time travel through the same signal field and all are subject to the same elastic force. Thus all electrons arriving at a point z at a given instant have acquired the same excursion y from the signal. Hence the excursion of the entire stream at point z , at any instant, is determined by (14).

The field E when measured at a fixed point has the frequency ω ; therefore the transverse excursion of the electron stream at a point z is given by

$$y(z) = \frac{e}{m} \frac{E(z)}{2j\omega_A\epsilon} \exp j\omega t. \quad (15)$$

The transversely moving stream, with a charge density ρ per unit length, induces in the adjacent slow-wave circuit a current per unit length

$$i = \rho \frac{\partial y}{\partial t} \frac{1}{D}. \quad (16)$$

From (15) and (16),

$$i = \frac{e}{m} \frac{\rho}{D} \frac{E}{2\epsilon} \frac{\omega}{\omega_A}. \quad (17)$$

Substituting the voltage on the circuit v and the spacing D for the field E , and dividing by the voltage,

$$\frac{i}{v} = \frac{e}{m} \frac{\rho}{D^2} \frac{1}{2\epsilon} \frac{\omega}{\omega_A}. \quad (18)$$

Now when an external current $-i$ (amperes per unit length) is injected, current flowing outward would be counted positive, into a transmission line of characteristic impedance Z , it splits up into the two parallel halves of the line and produces a voltage increment $\partial v / \partial z = -\frac{1}{2}iZ$. Since the voltage along the line varies as $v = v_0 \exp \alpha z$, $\partial v / \partial z = \alpha v$; hence $-\frac{1}{2}iZ = \alpha v$ and

$$\frac{i}{v} = -\frac{2\alpha}{Z}. \quad (19)$$

Combining now (18) and (19), and replacing ϵ by $\alpha \cdot u_E$ according to (8), we find

$$-\frac{2\alpha}{Z} = \frac{e}{m} \frac{\rho}{D^2} \frac{1}{2\alpha u_E} \frac{\omega}{\omega_A}. \quad (20)$$

or

$$\alpha^2 = -\frac{1}{4} \frac{e}{m} \frac{\rho}{D^2} \frac{Z}{u_E} \frac{\omega}{\omega_A}. \quad (20)$$

We may now use some well-known relations: $u_E \cdot \rho = I$ (the dc beam current) and $m \cdot u_E^2 = 2e \cdot V$ (where V is the dc beam voltage). With their help, (20) becomes:

$$\alpha^2 = -\frac{ZI\omega}{8VD^2\omega_A}. \quad (21)$$

α corresponds to the perturbation in the propagation constant in (6). If ω_A is negative (stream faster than wave), $\pm\alpha$ represents the gain or loss per unit length of two waves, both having the original velocity u ; with a voltage v_1 applied to the input end, the voltage along the slow-wave circuit becomes

$$v = v_1 \cosh \alpha z. \quad (22)$$

If, on the other hand, ω_A is positive (stream slower than wave), an input signal splits up into two waves of unchanging amplitude but modified velocity (propagation constants $\gamma \pm \alpha$) and the combined voltage on the slow-wave circuit is

$$v = v_1 \cos \alpha z. \quad (23)$$

Eqs. (22) and (23) describe what happens when the input signal is applied to the slow-wave circuit. For this simple and important case, the two resulting waves have equal starting fields which add up to match the input field, and equal but opposite electron motions which cancel each other initially. Eq. (10) shows that this cannot be quite correct: if the initial excursions y_1 and y_2 of the two waves are equal and opposite, the two transverse velocities \dot{y}_1 and \dot{y}_2 are equal but not exactly opposite, because of the factor $[j\omega_A + \epsilon]$ in one and $[j\omega_A - \epsilon]$ in the other. But at least for $\epsilon \ll |\omega_A|$, the approximation is good and no third wave is needed to satisfy the boundary conditions at the input.

It was stated previously that the condition $\epsilon \ll |\omega_A|$ is more easily met than infringed. Inspection of (21) might lead one to believe that reducing ω_A would increase α and thus quickly lead to an infringement. But if one wants to reduce ω_A he must also reduce ω_E , which means weakening the focusing field. This leads to a very rapid drop in the maximum possible dc current which the tube can carry.⁶ In practice it appears to be quite difficult to build a tube which violates the rule.

EXPERIMENTAL RESULTS

Velocity and Gain

Eq. (3) predicts that if the signal frequency ω is kept constant and ω_E is varied, beam velocity u_E must be varied in a certain way to maintain maximum gain. This was tested in an experimental tube at three signal frequencies; the potential difference between high and low dc voltages was varied in steps, and each time average beam velocity was adjusted for maximum gain.

The transverse electron resonant frequency ω_E as a function of the two dc voltages was determined by the method illustrated in Fig. 7, using zero frequency deflection. For this purpose a separate tube was built in

which the helix windings were replaced by a series of flat plates; the spatial period of the focusing field formed by these plates corresponded to that in the traveling-wave tube. Upon leaving the focusing field the beam was collected by a pair of target anodes, so that its final direction could be determined. The effective electron velocity u_E was computed by totaling the transit times for the high and low voltage sections. The circuit wave velocity u was measured by the method described in connection with Fig. 2; it corresponded to 55 volts at the highest frequency and to 60 volts at the lowest. Fig. 8 shows the experimental points; the dashed line represents the theoretical relation.

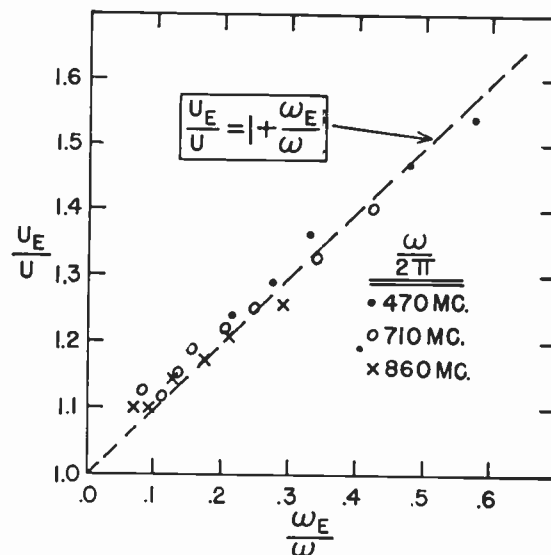


Fig. 8—Ratio of electron velocity to phase velocity in function of the ratio of transverse resonant frequency to signal frequency, for maximum gain.

Experimental tubes are normally operated at a ratio ω_E/ω of 0.1 to 0.25; thus the effective beam voltage is normally 20 to 60 per cent above the voltage which would correspond to the circuit wave velocity. It might be noted that these beam voltages are too low for any accidental interaction with the longitudinal mode.

If the tube is operated at an effective electron velocity lower than the circuit wave velocity, the ratio ω_A/ω becomes positive. The dc voltages can then be adjusted so that $\omega_E = \omega_A$, and the combined signal voltage on the helix becomes a cosine function of distance according to (23). Under these conditions, for a helix of length L , there exists a value of beam current I for which $\alpha \cdot L = \pi/2$. From (23) one would expect a null in the output signal at this particular adjustment, similar to the Kompsner dip in more conventional traveling-wave tubes.⁷ This has been observed experimentally for several values of ω_E ; the information so obtained is useful in calculating tube parameters. For example, with an effective electron velocity corresponding to 45 volts, and an $\omega_E/2\pi$ of 123 mc, a null was observed for

⁷ R. Kompsner, "On the operation of the traveling-wave tube at low level," *Jour. Brit. IRE*, vol. 10, pp. 283-289; August-September, 1950.

⁶ Adler, Kromhout, and Clavier, *op. cit.*; eq. (25).

$I = 81$ microamperes. The signal frequency was 710 mc and $L = 1.93$ inches. With $\alpha = \pi/2L$, the characteristic impedance Z can be calculated from (21); it is found to be 460 ohms. This is in reasonable agreement with the value found by inserting a dielectric between the helices and measuring the change in phase velocity.

Fig. 9 is a plot of gain-over-cold against beam current, for three different signal frequencies: 470 mc, 710 mc, and 860 mc. Two curves are shown for 710 mc, for two different values of ω_E . As one would expect from (21), the gain for a given beam current is higher for the smaller ω_E ; however, with the stronger focusing field one can get more beam current through the tube, and the maximum gain is higher than for the weaker focusing field. The dashed line on Fig. 9 represents the theoretical gain-over-cold for 710 mc with an $\omega_E/2\pi$ of 123 mc; it includes a small correction for the 2.6 db distributed cold loss at this frequency.

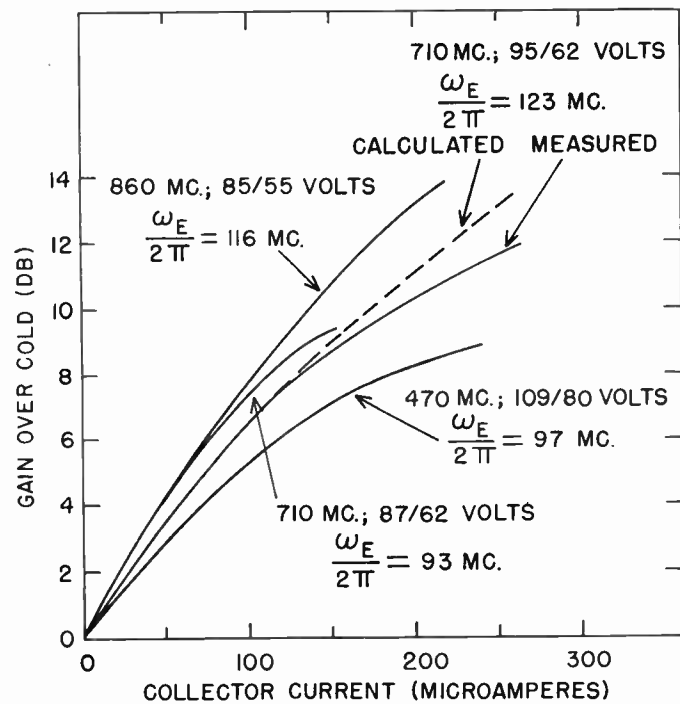


Fig. 9—Gain vs collector current for various signal and resonant frequencies. The potentials from which the resonant frequencies were calculated are listed next to the signal frequency.

No attenuator was used in the tube on which these measurements were made. With helices only about two inches long, the gain was not high enough to render an attenuator necessary; leaving it off made it much easier to compare theory and experiment.

The value of Z used in the calculation was the one obtained by the null method described earlier. The experimental curve follows the theoretical curve closely for the lower beam currents but begins to fall short of the theoretical gain for the higher currents. This is probably due to the fact that at these currents a considerable part of the beam is lost to the helices. For example, at dc voltages of 95 and 62 volts, the helices intercept 8

μ for 100 on the collector, 32 μ for 200 on the collector, and 83 μ for 260 on the collector.

As mentioned previously, there is little dispersion in these helices over the frequency range of interest. As a result, if ω_E is left approximately constant, the effective electron velocity must be adjusted as the signal frequency is varied in order to maintain maximum gain according to (3). This was done in taking the data for Fig. 9; the average beam voltage decreases as ω increases. If the beam voltage is not readjusted but left at the optimum setting for 710 mc, and the current is adjusted to give a gain-over-cold of 10.5 db at that frequency, the gain is down to 9.5 db at 570 mc and to 9.0 db at 860 mc. It should be pointed out that no voltage adjustment with frequency would be necessary if the helices were designed to have the proper positive dispersion. This was verified on the present tube by observing that the voltage did not need to be readjusted as the signal frequency was varied between 850 and 1,300 mc; in this region the helices have a slight amount of positive dispersion.

Overload effects are observed at unusually low signal levels. Electrons move transversely in response to the signal and because of the small spacing D , they cannot go very far without striking a winding. An increase of helix current at the expense of collector current is readily observed at output voltages of the order of 100 millivolts; this is in good agreement with the relation between field and electron excursion given in (15).

Noise Figure

The noise figure of the tube ranged from 6 to 8 db over the frequency range 470 to 860 mc. This was found by measuring the improvement in noise figure of a television receiver, obtained when the traveling-wave tube was placed in front of it. Table I shows the improvement at three signal frequencies.

TABLE I

Signal frequency	Noise figure, receiver alone	Noise figure, receiver with TWT	Insertion gain of TWT
470 mc	16.1 db	11.1 db	6.2 db
710 mc	15.0 db	10.2 db	7.5 db
860 mc	16.4 db	10.1 db	8.4 db

The best noise figures which can currently be obtained with special triodes range from 4 to 7 db at 500 mc and from 6 to 9 db at 1,000 mc. The receiver used in measuring the traveling-wave tube was, of course, not equipped with such triodes.

The noise figure of the transverse-field traveling-wave tube depends critically on the accuracy with which the beam is positioned in the center plane. This can be demonstrated by using the small centering electrode in the gun to deflect the beam in the y direction at the start of the interaction space. As the beam is swept through the centered position, the noise output of the tube goes through a distinct minimum, while the gain goes through a maximum.

It has been pointed out⁸ that the noise figure of a transverse-field traveling-wave tube has no theoretical minimum and depends primarily upon the width of the limiting apertures in the gun: the smaller the aperture width, the better the noise figure. The current through the aperture, however, decreases when the aperture is narrowed. Therefore, a compromise must be made. The experimental tubes described in this paper probably do not represent an optimum choice from the standpoint of noise figure.

It is interesting to note that as far as noise is concerned, electrostatic focusing has a definite advantage over magnetic focusing. The tube is not affected by transverse fluctuations in the beam parallel to the

⁸ G. Wade, K. Amo, and D. A. Watkins, "Noise in transverse-field traveling-wave tubes," *Jour. Appl. Phys.*, vol. 25, pp. 1514-1520; December, 1954.

center plane of the flat helices. In the case of magnetic focusing, such fluctuations are rotated by the magnetic field and converted into transverse fluctuations perpendicular to the center plane which the tube can amplify. With electrostatic focusing, on the other hand, no such rotation occurs.

CONCLUSION

The results of measurements on experimental tubes show good agreement with the theory. Gains of useful magnitude are readily obtained. Noise figures as low as 6 db have been measured and the chances for further improvement look promising. It appears that the transverse-field traveling-wave tube with periodic electrostatic focusing is well suited for low noise high frequency amplification.

A Simplified Method of Solving Linear and Nonlinear Systems*

R. BOXER†, MEMBER, IRE, AND S. THALER†

Summary—A simplified method for obtaining the response of linear and nonlinear systems, without knowledge of the roots of the system characteristic equation, is described. The solutions are given as time series representing the values of the response at equally spaced instants of time. Initial conditions are introduced easily through the use of the Laplace transform. It is shown that the Laplace transform of a linear system may be approximated by a z-transform, allowing the time series to be obtained by synthetic division. Two examples for linear constant coefficient systems are worked out including the solution of a third-order system and a first-order differential equation. The results are compared with the exact solutions obtained by analytic means.

The same methods are then extended to the solution of time-varying, nonlinear, and time-lag systems. An example of each type is worked out in detail to illustrate the wide applicability of the technique. A discussion of error considerations is included.

INTRODUCTION

THE RESPONSE of a network to an applied signal is usually initially defined implicitly by an integro-differential equation. The methods for obtaining an explicit solution fall into two broad classes—analytic methods which yield a solution in functional form, and numerical methods which yield a solution as a sequence of numerical values. In the more simple problems, the analytic methods have the advantage of permitting one to obtain a functional solution which contains the original network parameters in explicit

form. As the order of the differential equation increases, this advantage is lost and numerical methods may provide a solution with less labor. Recently, methods have been published which endeavor to systematize the numerical approach into easily used disciplines of wide applicability.¹⁻⁸ These methods are based upon a number series expansion, the coefficients of which are the values of the desired time function at times that correspond to the particular term of the number series expansion. Madwed extends Tustin's method of deriving number series utilizing the time domain only.¹ Unfortunately Madwed's method utilizes cumbersome notation and manipulation.

Cruickshank utilizes jump functions in approximating the solution of continuous linear systems.⁴ The method

¹ A. Madwed, "Number Series Method of Solving Linear and Nonlinear Differential Equations," Rep. No. 6445-T-26, Instrumentation Lab., MIT; April, 1950.

² J. R. Ragazzini, and A. R. Bergen, "A mathematical technique for the analysis of linear systems," *PROC. IRE*, vol. 42, pp. 1645-1651; November, 1954.

³ A. Tustin, "A method of analysing the behavior of linear systems in terms of time series," "A method of analysing the effects of certain kinds of nonlinearity in closed-cycle control systems," *Jour. IEE, Proceedings at the Convention on Automatic Regulators and Servomechanisms*, vol. 94, Part II-A, pp. 130ff; May, 1947.

⁴ A. J. O. Cruickshank, "A note on time series and the use of jump functions in approximate analysis," *Proc. IEE*, vol. 102, Part C, pp. 81-87; March, 1955.

⁵ J. Oswald, "Filtres en echelle elementaires," *Cables and Trans.*, vol. 7, pp. 325-358; October, 1953.

⁶ J. G. Truxal, "Numerical analysis for network design," *TRANS. IRE*, vol. CT-1, pp. 49-60; September, 1954.

* Original manuscript received by the IRE, June 9, 1955; revised manuscript received, August 18, 1955.

† Rome Air Development Center, Griffiths AF Base, Rome, N. Y.

requires knowledge of the zeros of the characteristic equation for each of the individual transfer functions in the system.

Ragazzini and Bergen have applied z -transform theory, which was developed for the analysis of sampled data systems, to the solution of continuous linear systems with successful results. In a typical system, the method requires that the Laplace transform of the individual network blocks be known in factored form; i.e., the roots of the characteristic equations of the individual blocks must be known. In addition, a fictitious network block known as a "triangle generator" must be inserted in the network loop. This entails considerable complication to the equations, especially when the loop itself is of any complexity.

In this paper, a method will be described which utilizes the z -transform directly to obtain the responses of linear and nonlinear continuous systems. A knowledge of the roots of the characteristic equation will not be required nor will a "triangle generator" be necessary. The simplicity of obtaining the result by the process of long division when dealing with linear systems by the other methods will be retained and extended to the solution of time varying and nonlinear differential equations.

Before describing the theory, it is advantageous to summarize the procedure to be used. This should emphasize the simplicity of the method. Assume that one has the Laplace transform of an output response. This could have been obtained by taking the Laplace transform of a differential equation including initial conditions, or by manipulation of Laplace transfer functions. The Laplace transform of the response will usually be available in the following form:

$$F(S) = \frac{a_0 + a_1S + a_2S^2 + \dots + a_kS^k + \dots + a_nS^n}{b_0 + b_1S + b_2S^2 + \dots + b_kS^k + \dots + b_mS^m}. \quad (1)$$

The steps to obtain the time response are:

1. Express the function $F(S)$ as a rational fraction in powers of S^{-1} by dividing the numerator and denominator by S^n .
2. Substitute for S^{-k} a rational fraction in powers of z^{-1} obtained from Table I and rearrange $F(S)$ as a rational fraction in powers of z^{-1} .
3. Divide the resulting expression by T , where T is the time interval between points at which the solution is desired.
4. Expand the fraction by synthetic division into a series of the form

$$D_0 + D_1z^{-1} + D_2z^{-2} + \dots + D_nz^{-n} + \dots, \quad (2)$$

where D_n , the coefficient of z^{-n} , is the approximate value of the time response at $t = nT$.

LINEAR SYSTEMS

Assume an arbitrary function of time $f(t)$ as shown in Fig. 1(a). The Laplace transform of $f(t)$ is defined by

$$F(S) = \int_0^\infty f(t)e^{-St}dt, \quad (3)$$

while the inverse Laplace transform is given by

$$f(t) = \frac{1}{2\pi J} \int_{C-J\infty}^{C+J\infty} F(S)e^{St}dS. \quad (4)$$

Fig. 1(b) indicates symbolically the result of sampling the function $f(t)$ utilizing shifted unit impulses. The result is a series of impulses at times $t = nT$. The areas of the impulses are equal to the amplitudes of the function $f(t)$ at corresponding times $t = nT$.⁷ The Laplace transform of the sampled function is given by⁸

$$F^*(e^{ST}) = \sum_{n=0}^{\infty} f(nT)e^{-SnT}. \quad (5)$$

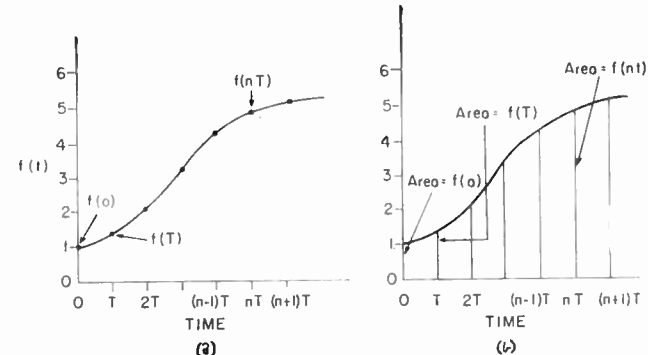


Fig. 1—(a) Arbitrary function of time; (b) Sampled function of time (symbolic).

If the substitution

$$z = e^{ST} \quad (6)$$

is made in (5), the result is the shorthand notation known as the z -transform;

$$F^*(z) = \sum_{n=0}^{\infty} f(nT)z^{-n}. \quad (7)$$

The inverse z -transform is given by

$$f(nT) = \oint F^*(z)z^{n-1}dz, \quad (8)$$

where the contour is taken around a circle centered at the origin in the z -plane and including all the singularities of $F^*(z)$.⁹ The relationship (6) conformally maps the $J\omega$ axis of the s -plane into a unit circle about the origin in the z -plane.

Although the z -transform defined by (7) is given in series form, it can usually be expressed in closed form for the functions of time arising in engineering practice.⁷ A simplified method for accomplishing this has been reported.¹⁰ The result will appear as

⁷ J. R. Ragazzini and L. A. Zadeh, "The analysis of sampled data systems," *Trans. AIEE*, vol. 71, Part II, pp. 225-232; November, 1952.

⁸ E. I. Jury, "Analysis and synthesis of sampled data control systems," *AIEE Commun. and Elec.*, vol. 73, pp. 332-346; September, 1954.

⁹ C. Holtsmith, D. F. Lawden, and A. E. Bailey, "Characteristics of sampling servo systems," *Automatic and Manual Control*; Butterworth's Scientific Publications; London, pp. 377-407; 1952.

¹⁰ R. Boxer, "Frequency analysis of computer systems," *PROC. IRE*, vol. 43, pp. 228-229; February, 1955.

$$F^*(z) = \frac{a_0 + a_1 z^{-1} + a_2 z^{-2} + \cdots + a_n z^{-n}}{b_0 + b_1 z^{-1} + b_2 z^{-2} + \cdots + b_m z^{-m}}. \quad (9)$$

An advantage of the z -transform is evident in that division of the numerator by the denominator will yield the coefficients $f(nT)$ as defined by (7) directly, without resorting to the inversion integral of (8).²

It would be desirable to utilize this characteristic of z -transform theory in the analysis of nonsampled systems. To do this, one uses the inverse Laplace Integral of (4),

$$f(t) = \frac{1}{2\pi J} \int_{C-J\infty}^{C+J\infty} F(S)e^{St} dS, \quad (10)$$

which can be expressed for a contour on the $J\omega$ axis of the s -plane as

$$\begin{aligned} f(t) &= \frac{1}{2\pi J} \int_{-J\pi/T}^{J\pi/T} F(S)e^{St} dS \\ &+ \frac{1}{2\pi J} \int_{J\pi/T}^{J\infty} [F(S)e^{St} + F(-S)e^{-St}] dS. \end{aligned} \quad (11)$$

Fig. 2 illustrates the manner in which the contour on the $J\omega$ axis is divided into two sections in (11). The part of the contour shown between $-(\pi/T) \leq \omega \leq (\pi/T)$ is given by the first integral of (11). The second integral is for the remaining portion of the contour $\omega > (\pi/T)$, $\omega < -(\pi/T)$.

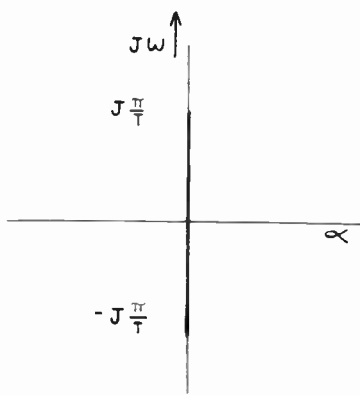


Fig. 2—Contour taken in complex frequency plane S for approximate solution.

If $F(S)$ has poles on the real frequency axis between $-(\pi/T)$ and π/T , the path of integration is modified to pass to the right of such poles. If $1/T$ is chosen sufficiently large, the first integral of (11) will yield a good approximation of $f(t)$ and the second integral may be discarded. The error is then given by

$$e(t) = \frac{1}{2\pi J} \int_{J\pi/T}^{J\infty} [F(S)e^{St} + F(-S)e^{-St}] dS. \quad (12)$$

Further considerations regarding the error will be discussed in the error consideration section.

The approximation to $f(t)$ is given by $f_A(t)$ as

$$f_A(t) = \frac{1}{2\pi J} \int_{-J\pi/T}^{J\pi/T} F(S)e^{St} dS. \quad (13)$$

Letting $t = nT$,

$$f_A(nT) = \frac{1}{2\pi J} \int_{-J\pi/T}^{J\pi/T} F(S)e^{SnT} dS. \quad (14)$$

Eq. (6) can be solved for S :

$$S = \frac{1}{T} \ln z, \quad (15)$$

which is substituted into (14)

$$f_A(nT) = \frac{1}{2\pi J} \int_{-J\pi/T}^{J\pi/T} F\left(\frac{1}{T} \ln z\right) e^{nT(1/T) \ln z} d\left(\frac{1}{T} \ln z\right) \quad (16)$$

$$f_A(nT) = \frac{1}{2\pi J} \oint \frac{1}{T} F\left(\frac{1}{T} \ln z\right) z^{n-1} dz, \quad (17)$$

where the contour is a unit circle in the z -plane.

Two aspects of (17) should be pointed out. The substitution $S = (1/T) \ln z$ given by (15) is exact for principal values of the logarithm as can be seen by¹¹

$$S = \frac{1}{T} \ln e^{ST} \quad (18)$$

$$S = \left(\frac{1}{T}\right)(ST). \quad (19)$$

Thus, the term $F[(1/T) \ln z]$ is exactly equal to $F(S)$ for $-(\pi/T) \leq \omega \leq (\pi/T)$. Furthermore, if equation (17) is compared with equation (8), it is seen that it has the form of an inverse z -transform except for the constant multiplier $1/T$. However, since $F[(1/T) \ln z]$ is a transcendental function instead of a ratio of polynomials in z^{-1} , it is not directly expandable, by synthetic division, into a series of powers of z^{-1} . This relatively simple procedure, synthetic division, is applicable only if a suitable approximation can be found. It is well known that if $F(S)$ is expanded in a series of descending powers of S

$$F(S) = a_1 S^{-1} + a_2 S^{-2} + \cdots, \quad (20)$$

a functional solution of the form

$$f(t) = a_1 + a_2 t + a_3 \frac{t^2}{2!} + \cdots \quad (20a)$$

can be obtained. However, an attempt to expand $F(S)$ in ascending powers of S is usually not valid. We are, therefore, led to rearrange $F[(1/T)/\ln z]$ as a rational fraction of two polynomials in powers of $S^{-1} = T/\ln z$.

Polynomial approximations for the function of $T/\ln z$ can be obtained from a number of definitions of $\ln z$. The definition selected was

$$\ln z = 2[u + \frac{1}{3}u^3 + \frac{1}{5}u^5 + \cdots], \quad (21)$$

where:

$$u = \frac{1 - z^{-1}}{1 + z^{-1}}.$$

¹¹ F. H. Raymond, "Analyse du fonctionnement des systèmes physiques discontinus," *Ann. Tele. Commun.*, vol. 4, pp. 8-9; July, 1949; pp. 250-256; September, 1949; p. 307; pp. 347-357; October, 1949.

This definition was selected because the series converges relatively rapidly and further, when this series is used to approximate $1/S = T/\ln z$ the result has the same phase as $1/S$ for $S = J\omega$. Using this definition, we obtain

$$\frac{1}{S} = \frac{T}{\ln z} = \frac{T/2}{u + \frac{1}{3}u^3 + \frac{1}{5}u^5 + \dots}. \quad (22)$$

Then by synthetic division we obtain a Laurent series,

$$\begin{aligned} \frac{1}{S} &= \frac{T}{\ln z} \\ &= \frac{T}{2} \left[\frac{1}{u} - \frac{1}{3}u - \frac{4}{45}u^3 - \frac{44}{945}u^5 + \dots \right]. \end{aligned} \quad (23)$$

Series expansions for S^{-K} can be obtained by raising both sides of (23) to the K th power. Table I was constructed by retaining the principal part and the constant term of the Laurent series. This yields a result of the form

$$S^{-K} \approx \frac{N_K(z^{-1})}{(1 - z^{-1})^K} = F_K(z^{-1}), \quad (24)$$

where N_K is a polynomial in powers of z^{-1} . The right-hand side of (24) is called the "z-form" for S^{-K} .

Since $z = e^{j\omega T}$, both sides of (24) have a pole of order K at $S = 0$. The right-hand side has additional poles and zeros but these occur sufficiently far out on the real frequency axis so as not to introduce appreciable errors where T is chosen so that π/T is greater than the highest frequency of interest.

It might appear that the inclusion of additional terms from the series definition of S^{-K} would improve accuracy. However, an attempt to do this introduces additional poles in the z-form leading to increased rather than smaller errors.

The z-forms obtained by this procedure are given in Table I for $K = 1, 2, 3, 4, 5$.

Column 4 of Table I gives the frequency spectrum of the z-form obtained by substituting the expression $z = e^{-j\omega T}$ into the forms of column three. As noted earlier, there is no phase shift between the actual spectrum of column two and the derived z-forms.

$$\theta_{0A}^*(z) = \frac{6T^2(z^{-1} + z^{-2})}{(12 + 6T + T^2) - (36 + 6T - 9T^2)z^{-1} + (36 - 6T - 9T^2)z^{-2} - (12 - 6T + T^2)z^{-3}}. \quad (27)$$

To note the effect of using only a finite number of terms of the inverse log expansions, the frequency spectrum of the z-forms may be expanded into the series shown in column 5 of Table I. The first term of each series is identical to the exact frequency spectrum of column 2. The magnitude of the coefficients indicates that the z-form approximation improves as K becomes larger. In all cases, the series reduces to the exact spectrum in the limit as T becomes zero.

$$\frac{.316z^{-1} + .864z^{-2} + 1.15z^{-3} + 1.16z^{-4} + 1.06z^{-5} + .987z^{-6} + \dots}{19 - 33z^{-1} + 21z^{-2} - 7z^{-3}} \frac{6z^{-1} + 6z^{-2}}{6z^{-1} + 6z^{-2}}. \quad (29)$$

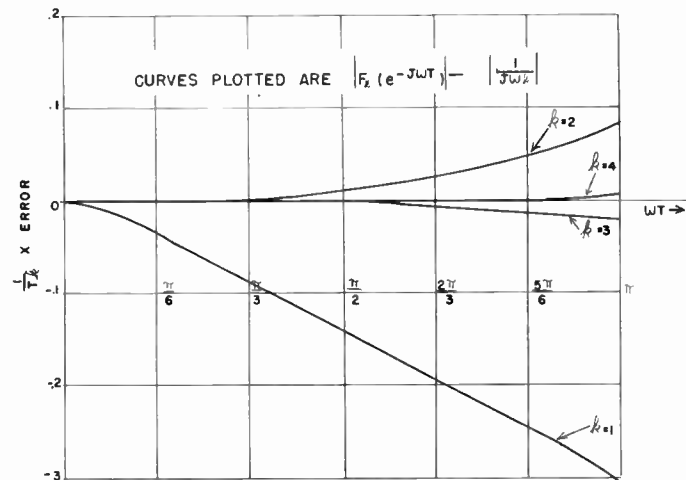


Fig. 3—Spectrum amplitude error between z-forms and exact Laplace forms.

Fig. 3 plots the error between the z-form spectrum and the actual spectrum for the various values of K .

Example 1—Third Order System

The first example will be based upon the third-order system shown in Fig. 4. With a step input as shown, the Laplace transform of the output is given by

$$\theta_0(S) = \frac{1}{S^3 + S^2 + S}. \quad (25)$$

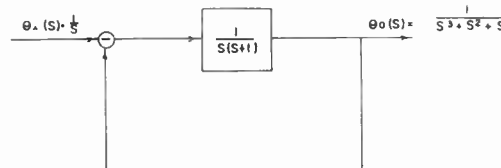


Fig. 4—Typical feedback system used in example.

Following the step-by-step procedure outlined in the introduction, the transform is expressed in powers of S^{-1} :

$$\theta_0(S) = \frac{S^{-3}}{1 + S^{-1} + S^{-2}}. \quad (26)$$

Substituting the corresponding forms from Table I and dividing the result by T ,

The solution is obtained by choosing T and dividing the denominator of (27) into the numerator. A discussion of the choice of T will be given in the section on error analysis. At this point, assume $T = 1.0$, causing the output to be expressed as

$$\theta_{0A}^*(z) = \frac{6z^{-1} + 6z^{-2}}{19 - 33z^{-1} + 21z^{-2} - 7z^{-3}}. \quad (28)$$

Carrying out the long division process,

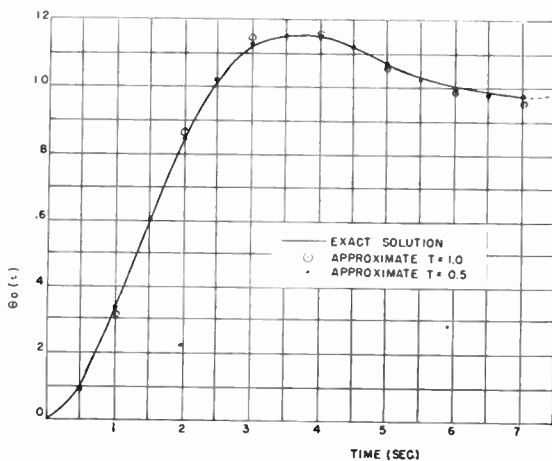


Fig. 5—Exact and approximate solution to third-order system.

These points are plotted in Fig. 5, together with the exact solution.

The accuracy improves if smaller values of T are taken. This will be indicated by letting $T=0.5$ in the example just considered. Substituting $T=0.5$ into (27).

$$Y_{0A}^*(z) = \frac{1.5z^{-1} + 1.5z^{-2}}{15.25 - 36.75z^{-1} + 30.75z^{-2} - 9.25z^{-3}}. \quad (30)$$

Carrying out the long division process,

$$\frac{15.25 - 36.75z^{-1} + 30.75z^{-2} - 9.25z^{-3}}{1.5z^{-1} + 1.5z^{-2}} \cdot \frac{.0984z^{-1} + .335z^{-2} + .610z^{-3} + .853z^{-4} + \dots}{.0984z^{-1} + .335z^{-2} + .610z^{-3} + .853z^{-4} + \dots}. \quad (31)$$

The points obtained in this case are plotted on Fig. 5.

Example 2—Solution of Differential Equation

The method described in this paper is applicable to the solution of integro-differential equations. To do this,

$$\frac{.00714 + .085z^{-1} + .163z^{-2} + .233z^{-3} + .296z^{-4} + .354z^{-5} + \dots}{12.6 - 24z^{-1} + 11.4z^{-2}} \cdot \frac{.09 + .9z^{-1} + .09z^{-2}}{.09 + .9z^{-1} + .09z^{-2}}. \quad (37)$$

one takes the Laplace transform of the equation including any initial conditions in the usual way, and then proceeds exactly as above. If the numerator of $F(S)$ is only one degree less than the denominator, the solution as a function of time will exhibit an instantaneous rise to an initial value at time $t=0$. It is usually worthwhile in such cases to eliminate from $F(S)$ the high frequencies implied by the instantaneous rise. This is very readily done by using synthetic division to reduce the degree of the numerator. This is best illustrated by a simple example; namely

$$\frac{dY}{dt} + Y = 1. \quad (32)$$

Assuming an initial condition $Y(0)=u$, the Laplace transform $Y(S)$ is

$$Y(S) = \frac{1 + Su}{S(S + 1)} = \frac{Su + 1}{S^2 + S}. \quad (33)$$

The methods described previously may be used to obtain the solution to (33). Alternatively, the high-frequency component can first be removed by dividing the denominator of (33) into the numerator once. This yields a quotient u/S and remainder $(1-u)$. Thus

$$Y(S) = \frac{u}{S} + \frac{1-u}{S^2 + S}. \quad (34)$$

In this procedure, the step function of amplitude u is added to the result obtained after operating upon $(1-u)/S^2+S$.

In general, the following rules can be stated:

1. If the degree of the denominator of the Laplace transform is higher than the degree of the numerator by two or more, proceed directly.
2. If the degree of the numerator is one less, equal to, or greater than the degree of the denominator, divide until the remainder meets the criterion of Rule 1.

In the example under consideration, let $u=.1$. Expressing the second term of (34) in powers of S^{-1} ,

$$Y_1(S) = \frac{0.9S^{-2}}{1 + S^{-1}}. \quad (35)$$

$$\frac{.0984z^{-1} + .335z^{-2} + .610z^{-3} + .853z^{-4} + \dots}{.0984z^{-1} + .335z^{-2} + .610z^{-3} + .853z^{-4} + \dots}.$$

Substituting the z -forms of Table I and dividing by T ,

$$Y_{1A}^*(z) = \frac{0.9T(1 + 10z^{-1} + z^{-2})}{(12 + 6T) - 24z^{-1} + (12 - 6T)z^{-2}}. \quad (36)$$

Letting $T=0.1$ and carrying out the long division,

$$\frac{.00714 + .085z^{-1} + .163z^{-2} + .233z^{-3} + .296z^{-4} + .354z^{-5} + \dots}{12.6 - 24z^{-1} + 11.4z^{-2}} \cdot \frac{.09 + .9z^{-1} + .09z^{-2}}{.09 + .9z^{-1} + .09z^{-2}}.$$

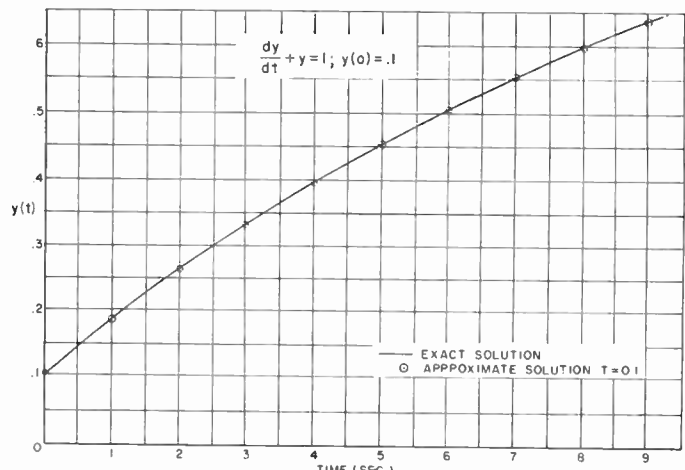


Fig. 6—Exact and approximate solution of first-order differential equation having initial condition.

This result is plotted in Fig. 6 after adding the step function of amplitude 0.1.

TABLE I
Z-FORMS

S^{-K}	$(J\omega)^{-K}$	$z\text{-Form} = F_K(z^{-1})$	$F^K(e^{-J\omega T})$	$F^K(e^{-J\omega T})$
S^{-1}	$-\frac{J}{\omega}$	$\frac{T}{2} \frac{1+z^{-1}}{1-z^{-1}}$	$-J \frac{T}{2} \cot \frac{\omega T}{2}$	$-\frac{J}{\omega} + \frac{J\omega T^2}{12} + \frac{J\omega^3 T^4}{720} + \dots$
S^{-2}	$-\frac{I}{\omega^2}$	$\frac{T^2}{12} \frac{1+10z^{-1}+z^{-2}}{(1-z^{-1})^2}$	$T^2 \left(\frac{1}{12} - \frac{1}{4} \csc^2 \frac{\omega T}{2} \right)$	$-\frac{1}{\omega^2} \frac{\omega^2 T^4}{240} - \frac{\omega^4 T^6}{6048} - \dots$
S^{-3}	$\frac{J}{\omega^3}$	$\frac{T^3}{2} \frac{z^{-1}+z^{-2}}{(1-z^{-1})^3}$	$J \frac{T^3}{8} \frac{\cos \frac{\omega T}{2}}{\sin^3 \frac{\omega T}{2}}$	$\frac{J}{\omega^3} - \frac{J\omega T^4}{240} - \frac{J\omega^3 T^6}{3024} - \dots$
S^{-4}	$\frac{1}{\omega^4}$	$\frac{T^4}{6} \frac{z^{-1}-4z^{-2}+z^{-3}}{(1-z^{-1})^4} - \frac{T^4}{720}$	$\frac{T^4}{48} \left(\frac{2+\cos \omega T}{\sin^4 \omega T} - \frac{1}{15} \right)$	$\frac{1}{\omega^4} + \frac{\omega^2 T^6}{3024} + \frac{\omega^4 T^8}{34560} - \dots$
S^{-5}	$-\frac{J}{\omega^5}$	$\frac{T^5}{24} \frac{z^{-1}+11z^{-2}+11z^{-3}+z^{-4}}{(1-z^{-1})^5}$	$-J \frac{T^5}{24} \left[\frac{\cos \frac{3\omega T}{2} + 11 \cos \frac{\omega T}{2}}{\sin^5 \frac{\omega T}{2}} \right]$	$-\frac{J}{\omega^5} + \frac{J\omega T^6}{6048} + \frac{J\omega^3 T^8}{34560} + \dots$

TIME-VARYING SYSTEMS

The general form of a linear differential equation with time-varying coefficients may be expressed as

$$\frac{d^n}{dt^n} [f_n(t)Y] + \frac{d^{n-1}}{dt^{n-1}} [(f_{n-1}(t)Y)] + \dots + f_0(t)Y = f(t), \quad (38)$$

where $f_n(t)$, $f_{n-1}(t)$, ..., $f_0(t)$ are functions of the independent variable t . This type of differential equation can be solved using the z -forms of Table I by the following procedure:

1. Obtain the Laplace transform of (38) in the usual manner including initial conditions.
2. Proceed as in the constant coefficient case discussed above. In performing the long division process, however, change the values of C_n, \dots, C_0 at each step in the division process to the values at the corresponding times of the functions

$$\begin{aligned} C_n &= f_n(t) \\ C_0 &= f_0(t). \end{aligned} \quad (39)$$

In general

$$C_i = f_i(t). \quad (40)$$

The justification for the above procedure is outlined in the Appendix.

To illustrate the procedure, a simple time-varying equation, the exact solution of which is easily available, will be used. Let

$$\frac{dY}{dt} + tY = t. \quad (41)$$

The exact solution, assuming $y(0) = 0$, is

$$Y = 1 - e^{-t^2/2}. \quad (42)$$

Following the procedure outlined, (41) is rewritten

$$\frac{dY}{dt} + CY = t. \quad (43)$$

Taking the Laplace transform, considering C constant, and $Y(0) = 0$,

$$Y(S) = \frac{1}{S^3 + CS^2}. \quad (44)$$

Expressing as powers of S^{-1} ,

$$Y(S) = \frac{S^{-3}}{1 + CS^{-1}}. \quad (45)$$

Substituting the z -forms of Table I and dividing by T ,

$$Y_A^*(z) = \frac{T^2(z^{-1} - z^{-2})}{(2 + CT) - (6 + CT)z^{-1} + (6 - CT)z^{-2} - (2 - CT)z^{-3}}. \quad (46)$$

Letting $T = 0.4$,

$$Y_A^*(z) = \frac{.16z^{-1} + .16z^{-2}}{(2 + .4C) - (6 + .4C)z^{-1} + (6 - .4C)z^{-2} - (2 - .4C)z^{-3}}. \quad (47)$$

The long division process is carried out letting $C=0.4$ during the first step of the division, 0.8 during the second step, and 1.2 during the third step, and so forth, yielding

$$(2 + .4C) - (6 + .4C)z^{-1} + (6 - .4C)z^{-2} - (2 - .4C)z^{-3}) \cdot 16z^{-1} + .16z^{-2}$$

The solution obtained is plotted on Fig. 7 together with the exact solution.

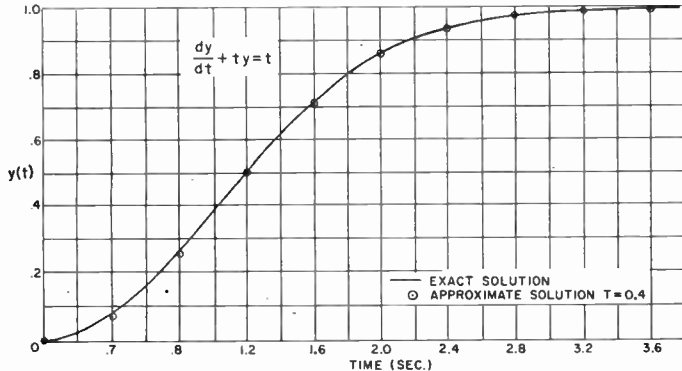


Fig. 7—Exact and approximate solution of differential equation with time-varying coefficient.

The limitations upon the form of the time varying coefficients have not been fully examined. Difficulties are encountered if these coefficients become infinite at a value t in the range of interest. It is believed however, that the method is applicable to the type of equations that arise from physical systems. It appears that a minimum limitation upon the form of the coefficients is that they be Laplace transformable.

In addition to the derivation shown in the Appendix, the time-varying situation can be related to the Laplace transform by making use of an approximation to the Laplace integral definition. This will be illustrated for the case in which the coefficients $f_n(t)$, $f_{n-1}(t)$... $f_0(t)$ are polynomials in t . A well-known relation from Laplace transform theory is

$$L[tf(t)] = -\frac{d}{ds}F(S). \quad (49)$$

For the methods of this paper, the Laplace transform definition

$$F(S) = \int_0^\infty f(t)e^{-St}dt \quad (50)$$

can be approximated by

$$F(S) = \sum_{n=0}^{\infty} f(nT)e^{-SnT}T. \quad (51)$$

Differentiating with respect to S ,

$$\frac{dF(S)}{dS} \approx -\sum_{n=0}^{\infty} nTf(nT)e^{-SnT}T. \quad (52)$$

Since n cannot be taken outside the summation sign, the equivalent z -form for $-dF(S)/dS$ can be expressed as

$$\sum_{n=0}^{\infty} nTf(nT)z^{-n}T. \quad (53)$$

$$\frac{.0741z^{-1} + .266z^{-2} + .503z^{-3} + .714z^{-4} + \dots}{(.16z^{-1} + .16z^{-2})} \quad (48)$$

The factor nT is identically equivalent to the factor C of (43).

NONLINEAR SYSTEMS

Nonlinear differential equations may be solved in a manner similar to that for the time varying linear equation. The regression equation is arrived at through the long division process as in the time varying case. The factors such as C_n , C_{n-1} , ... C_0 , however, must now represent functions of the dependent variable.

In general, a nonlinear differential equation can be expressed in the following form:

$$\begin{aligned} \frac{d^n}{dt^n} \left[f_n \left(Y, \frac{dY}{dt}, \dots \right) Y \right] + \frac{d^{n-1}}{dt^{n-1}} \left[f_{n-1} \left(Y, \frac{dY}{dt}, \dots \right) Y \right] \\ + \dots + f_0 \left(Y, \frac{dY}{dt}, \dots \right) Y = f(t), \end{aligned} \quad (54)$$

for which the rules of procedure are

1. Obtain the Laplace transform of (54) in the usual manner including initial conditions.

2. Proceed as in the constant coefficient case. In performing the long division process, however, change the values of C_n ... C_0 at each step in the division process to the most recent values available for

$$\begin{aligned} C_n &= f_n \left(Y, \frac{dY}{dt}, \dots \right) \\ C_{n-1} &= f_{n-1} \left(Y, \frac{dY}{dt}, \dots \right) \\ &\dots \\ C_0 &= f_0 \left(Y, \frac{dY}{dt}, \dots \right). \end{aligned} \quad (55)$$

In general

$$C_i = f_i \left(Y, \frac{dY}{dt}, \dots \right). \quad (56)$$

In other words, in the first step, values of C_n , C_{n-1} , ... C_0 are obtained from the initial conditions for Y , dY/dt The result of the first division is a new value of Y to be used in calculating C_n , C_{n-1} ... C_0 for the second step in the division. New values to be used for the derivatives of Y with respect to t are calculated from the new values of the dependent variables. The process is awkward to describe in words, but is simple in concept.

As an illustration, let

$$\frac{dy}{dt} + y^2 = 1. \quad (57)$$

The exact solution of (57) obtained by standard means, assuming $y(0)=0$, is

$$Y = \tanh t. \quad (58)$$

In carrying out the procedure outlined above, (57) is written

$$\frac{dy}{dt} + CY = 1. \quad (59)$$

The Laplace transform, assuming C to be constant expressed in powers of S^{-1} is

$$Y(S) = \frac{S^{-2}}{1 + CS^{-1}}. \quad (60)$$

Substituting the z -forms of Table I and dividing by T yields

$$Y_A^*(z) = \frac{T(1 + 10z^{-1} + z^{-2})}{(12 + 6CT) - 24z^{-1} + (12 - 6CT)z^{-2}}. \quad (61)$$

Letting $T=0.1$,

$$Y_A^*(z) = \frac{0.1(1 + 10z^{-1} + z^{-2})}{(12 + 0.6C) - 24z^{-1} + (12 - 0.6C)z^{-2}}. \quad (62)$$

Carrying out the long division procedure yields

$$\frac{.00833 + 0.100z^{-1} + .199z^{-2} + .295z^{-3} + .390z^{-4} + \dots}{(12 + 0.6C) - 24z^{-1} + (12 - 0.6C)z^{-2}} \cdot \frac{0.1 + 1.0z^{-1} + 0.1z^{-2}}{z^{-1}}. \quad (63)$$

The solution obtained is plotted on Fig. 8 together with the exact solution.

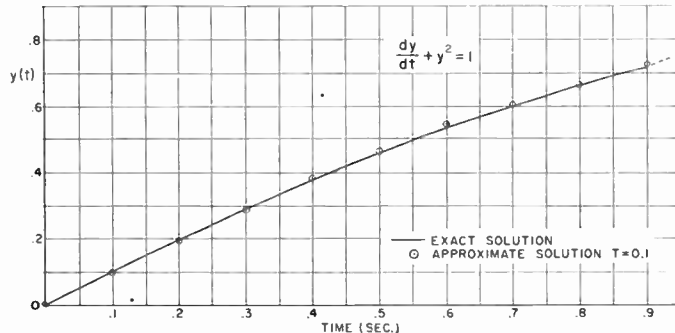


Fig. 8—Exact and approximate solution of nonlinear differential equation.

In the above example, the value of the dependent variable at $t=nT$ was utilized in calculating the value of the dependent variable at $t=(n+1)T$. The derivation in the Appendix indicates that the proper value to be

used in calculating Y at $t=(n+1)T$ is based upon the value of Y one is seeking. This is unavailable, obviously, necessitating the use of the previous value of Y as described above. An improvement in accuracy would result, if each step of the division were iterated. For the same degree of accuracy as obtained in the above example, iteration would permit a larger value of T to be used. Whether the amount of labor saved in the reduction in the number of basic division steps is appreciable compared with the labor involved in the iteration process has not been fully explored. The authors believe that it is advantageous to improve the accuracy by choosing a smaller value of T .

SYSTEMS CONTAINING TIME LAGS

Systems that contain time lags are readily manipulated through the use of the z -forms. One requirement must be met; namely, the choosing of the sampling interval T must be such that T is an integral submultiple of the time-delay. The trivial system of Fig. 9, con-

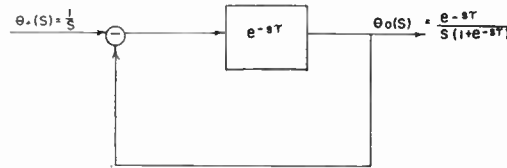


Fig. 9—Feedback system containing time lag.

sisting of a delay line with a unity feedback path, will serve as an illustration of the procedure. For a step

input the Laplace transform of the output is

$$\theta_0(S) = \frac{e^{-S\tau}}{S(1 + e^{-S\tau})}, \quad (64)$$

where τ is the time lag. Expressing (64) in powers of S^{-1} ,

$$\theta_0(S) = \frac{e^{-S\tau} S^{-1}}{1 + e^{-S\tau}}. \quad (65)$$

Substituting the z -form and dividing by T ,

$$\theta_{0A}^*(z) = \frac{e^{-S\tau}(1 + z^{-1})}{2(1 - z^{-1}) + 2e^{-S\tau}(1 - z^{-1})}. \quad (66)$$

Assuming a sampling period T such that $\tau=3T$ causes

$$e^{-S\tau} = e^{-3ST} = z^{-3}. \quad (67)$$

Substituting (67) into (66)

$$\theta_{0A}^*(z) = \frac{z^{-3} + z^{-4}}{2 - 2z^{-1} + 2z^{-3} - 2z^{-4}}. \quad (68)$$

Carrying out the long division process,

$$\frac{0 + 0 + 0 + 0.5z^{-3} + z^{-4} + z^{-5} + 0.5z^{-6} + 0 + 0 + 0.5z^{-9} + \dots}{2 - 2z^{-1} + 2z^{-3} - 2z^{-4})0 + 0 + 0 + z^{-3} + z^{-4}}. \quad (69)$$

The result is shown in Fig. 10 together with the exact solution.

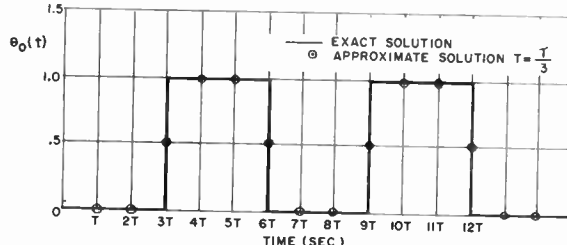


Fig. 10—Exact and approximate solution to system containing time lag.

ERROR CONSIDERATIONS

Contributions to the total error that result through the use of the method are based upon two factors. The error is due in part to the use of truncated series for the inverse logarithms, and to the fact that the contour of (13) is the finite path along the imaginary axis in the s -plane from $-J\pi/T$ to $+J\pi/T$. As $T \rightarrow 0$, the error goes to zero because the contour then becomes infinite and the z -forms become exact, as can be seen from column 5 of Table I, where all the terms of the series except the first go to zero. Thus, the smaller the value of T chosen, the more accurate the result.

The z -forms were derived using the maximum number of terms compatible with realizing a denominator of the form $(1 - z^{-1})^K$. Since a more accurate approximation to the logarithm results when more terms of the series are included, an explanation of the limitation on the number of terms is in order. To deal with a specific case, the inverse logarithm series for $K=1$ will be used. Repeating the series for convenience,

$$\begin{aligned} \frac{1}{S} &= \frac{T}{2} \left[\frac{1 + z^{-1}}{1 - z^{-1}} - \frac{1}{3} \left(\frac{1 - z^{-1}}{1 + z^{-1}} \right) - \frac{4}{45} \left(\frac{1 - z^{-1}}{1 + z^{-1}} \right)^3 \right. \\ &\quad \left. - \frac{44}{945} \left(\frac{1 - z^{-1}}{1 + z^{-1}} \right)^5 + \dots \right]. \end{aligned} \quad (70)$$

Following the rules outlined, only the first term is taken, yielding

$$\frac{1}{S} \approx \frac{T}{2} \frac{1 + z^{-1}}{1 - z^{-1}}. \quad (71)$$

The expression indicates that there is a single order pole at $z^{-1}=1$ in the z -plane. This is equivalent to a single order pole in the s -plane at $S=0$. This is shown in Figs. 11a and 11b. The location of the pole indicates

that the time response should be a constant. Carrying out the long division in terms of z^{-1} for (71) after dividing by T yields

$$\frac{\frac{1}{2} + z^{-1} + z^{-2} + z^{-3} + z^{-4} + \dots}{2 - 2z^{-1})1 + z^{-1}}. \quad (72)$$

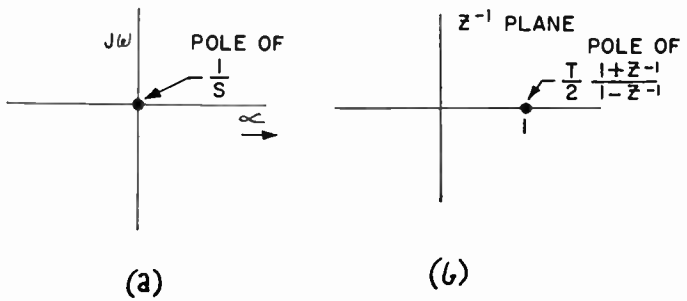


Fig. 11 (a) Pole of Laplace forms; (b) Pole of z -form.

The result (with the exception of the point at $t=0$) is a sampled unit step. Fig. 12 plots this response.

If the second term of the series given by (70) is included, the result would be

$$\frac{1}{S} \approx \frac{T}{3} \frac{1 + 4z^{-1} + z^{-2}}{1 - z^{-2}}, \quad (73)$$

$$\frac{1}{S} \approx \frac{T}{3} \frac{1 + 4z^{-1} + z}{(1 - z^{-1})(1 + z^{-1})}. \quad (74)$$

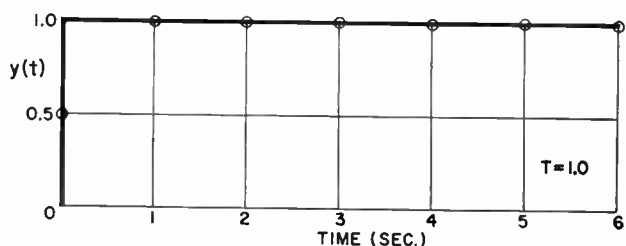


Fig. 12—Time domain solution of first-order z -form using one term of inverse log series.

This indicates that there are single order poles at $z^{-1}=1$ and $z^{-1}=-1$. The response due to the pole at $z^{-1}=1$ yields the constant, while the pole at $z^{-1}=-1$ causes an oscillation at half the sampling frequency. Carrying out the division indicated by (73) after dividing by T leads to

$$\frac{\frac{1}{3} + \frac{4}{3}z^{-1} + \frac{2}{3}z^{-2} + \frac{4}{3}z^{-3} + \frac{2}{3}z^{-4} + \dots}{3 + 0 - 3z^{-2})1 + 4z^{-1} + z^{-2}}. \quad (75)$$

The result is plotted in Fig. 13. The desired value of unity is obtained between the sampling points. Excluding the first point, the average of any two succeeding values of (75) is the correct result between the times at which the two values are taken. With this understanding, the method of this paper can be applied to the solution of a Laplace transform that does not contain other than S^{-1} terms. Thus, if

$$F(S) = \frac{1}{S+1} = \frac{S^{-1}}{1+S^{-1}}, \quad (76)$$

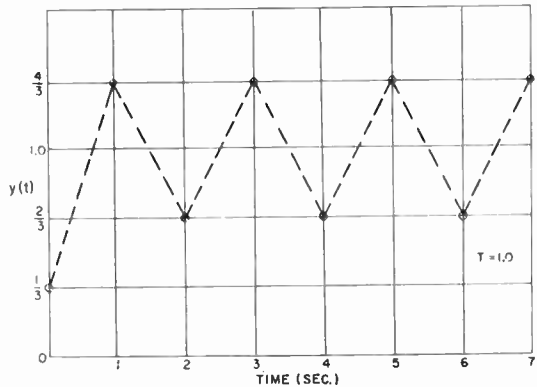


Fig. 13—Time domain solution of first-order z -form using two terms of inverse log series.

one may substitute (73) into (76) obtaining after division by T :

$$F_A^*(z) = \frac{1 + 4z^{-1} + z^{-2}}{(3 + T) + 4Tz^{-1} + (T - 3)z^{-2}}. \quad (77)$$

Choose a value for T in (77) and carry out the long division procedure. Then average succeeding values which will yield the result midway between the sampling points to greater accuracy than that obtained using the z -form of Table I for a given choice of T .

If the third term of the series of (70) is included, there results

$$\frac{1}{S} \approx \frac{T}{45} \frac{13 + 111z^{-1} + 230z^{-2} + 236z^{-3} + 111z^{-4} + 13z^{-5}}{(1 - z^{-1})(1 + z^{-1})^4}. \quad (78)$$

This form contains the pole at $z^{-1}=1$, but has a multiple order pole at $z^{-1}=-1$, causing an unstable response. Rules for obtaining the correct response could be worked in a manner similar to the discussion associated with Fig. 13, but they would be fairly complicated. Possibly the rules for removing the undesirable oscillations could be obtained using the suggestions made by Huggins in relation to a similar problem.¹² This may merit further investigation.

In general, therefore, taking more terms of the inverse logarithm series introduces unwanted poles, complicating the methods for obtaining the desired result. The difficulties are enhanced when the Laplace transform forms one is working with contain various powers of S^{-1} as is usually the case. Since the forms given in

Table I do not introduce undesirable responses and can be made as accurate as desired by choosing smaller values of T , it is recommended that those forms be used.

In theory, the error due to the use of the finite contour in the s -plane can be obtained by evaluating (12). In practice, the evaluation is difficult to perform, and is not recommended as standard procedure. Until simplified procedures for calculating the error are evolved, the successful use of the method is based upon the judicious choice of the value T . The choice of T can be made in a number of ways. In solving a typical feedback problem, one can always choose a highest frequency of interest and then base the choice of T upon the highest frequency of interest being down a specified number of db at some subharmonic of the sampling frequency.

In any event, one can always choose a value of T , obtain a solution, and then compare results with that obtained for a smaller value of T until the change in the least significant figure of interest is negligible.

DISCUSSION

The paper has presented a systematic procedure for the approximate solution of linear, time-varying and nonlinear systems, including those containing time lags. An advantage of the method other than the technical advantages described in the introduction is that the z -forms of Table I are substituted into standard Laplace transforms. The Laplace transform method is well known, allowing one to couple the methods of this paper with other knowledge readily available; *i.e.*, initial and final theorems, Nyquist criteria, frequency response and the convenient method the Laplace transform affords for the introduction of initial conditions.

Further research should extend the applicability of the method. Among the fields that should be investi-

gated are better methods of choosing T , a simple way of obtaining a quantitative value for the error and utilization of the technique for synthesis.

In conclusion, it should be pointed out that a definite relationship exists, to an extent not yet determined, to the methods of numerical analysis. This is indicated by the fact that (71) is the z -transform for the trapezoidal rule of integration, while (73) is the z -transform of Simpson's $\frac{1}{3}$ rule. Summation of the first two terms of the series given in (21) is the z -transform of Simpson's $\frac{3}{8}$ rule. The z -transforms of these integration formulas have been derived by Salzer, using the numerical analysis relations directly, in connection with integration programming for digital computers.¹³

¹² W. H. Huggins, "A low pass transformation for z -transforms," TRANS. IRE, vol. CT-1, pp. 69-70; September, 1954.

¹³ J. M. Salzer, "Frequency analysis of digital computers operating in real time," PROC. IRE, pp. 457-466; February, 1954.

APPENDIX: JUSTIFICATION OF PROCEDURES

A differential equation with functional coefficients may, in general, be written in either of two forms. The first is

$$\frac{d^n}{dt^n} (f_n Y) + \frac{d^{n-1}}{dt^{n-1}} (f_{n-1} Y) + \cdots + f_0 Y = f(t), \quad (79)$$

where the f_i are functions of the independent variable t , the dependent variable y and its derivatives. The second form is:

$$g_n \frac{d^n Y}{dt^n} + g_{n-1} \frac{d^{n-1}}{dt^{n-1}} Y + \cdots + g_0 Y = g(t), \quad (80)$$

where the g_i are similarly functions of t , y and the derivatives of y .

A differential equation having the form of (80) may be expressed in the form of (79) through the use of the following relation:

$$\frac{d^n}{dt^n} g_n Y = \sum_{k=0}^n C_k^n \left(\frac{d^k}{dt^k} g_n \right) \left(\frac{d^{n-k}}{dt^{n-k}} Y \right), \quad (81)$$

where the C_k^n are the binomial coefficients.

One can justify the application of the procedures given in the body of the paper to equations of the form of (79). The procedures are applicable to the form (80) if the functions of g_i are slowly varying, otherwise the conversion to form (79) must be accomplished. To illustrate this point, consider

$$\frac{d^2 Y}{dt^2} + g_1(t) \frac{d Y}{dt} + g_0(t) Y = f(t). \quad (82)$$

After conversion to the form (79),

$$\frac{d^2}{dt^2} Y + \frac{d}{dt} [g_1(t) Y] + \left[g_0(t) - \frac{d}{dt} g_1(t) \right] Y = f(t). \quad (83)$$

If $g_1(t)$ is slowly varying so that

$$g_0(t) \gg \frac{d}{dt} g_1(t); \quad \frac{d}{dt} g_1(t)$$

may be neglected and it is not necessary to perform the conversion.

In (79), let $h_i = f_i Y$, obtaining

$$\frac{d^n}{dt^n} h_n + \frac{d^{n-1}}{dt^{n-1}} h_{n-1} + \cdots + h_0 = j(t). \quad (84)$$

To simplify the discussion, without loss of generality, let (84) be of the second order,

$$\frac{d^2}{dt^2} h_2 + \frac{d}{dt} h_1 + h_0 = f(t). \quad (85)$$

The Laplace transform is given by

$$S^2 H_2(S) - S h_2(0) - h_2'(0) + S H_1(S) - h_1(0) \\ + H_0(S) = F(S), \quad (86)$$

where

$$H_i(S) = \int_0^\infty h_i(t) e^{-St} dt$$

$$F(S) = \int_0^\infty f(t) e^{-St} dt$$

Rearranging (86),

$$S^2 H_2(S) + S H_1(S) + H_0(S) \\ = F(S) + S h_2(0) + h_2'(0) + h_1(0). \quad (87)$$

If $F(S)$ is available as a rational function of S , the procedure is somewhat different than instances in which $F(S)$ is not so available. The procedure for $F(S)$ not rational will be discussed subsequently.

Needless complication in this discussion is avoided, without loss in generality, by choosing a particular function $F(S)$. Let $F(S) = 1/S$, in which case (87) becomes

$$H_2(S) + \frac{1}{S} H_1(S) + \frac{1}{S^2} H_0(S) \\ = \frac{1}{S^3} + \frac{1}{S} h_2(0) + \frac{1}{S^2} [h_2'(0) + h_1(0)]. \quad (88)$$

Utilizing the z -forms of Table I, one obtains

$$H_2(s) + \frac{T}{2} \frac{1+z^{-1}}{1-z^{-1}} H_1(S) + \frac{T^2}{12} \frac{1+10z^{-1}+z^{-2}}{(1-z^{-1})^2} H_0(S) \\ = \frac{T^3}{2} \frac{z^{-1}+z^{-2}}{(1-z^{-1})^3} + \frac{T}{2} \frac{1+z^{-1}}{1-z^{-1}} h_2(0) \\ + \frac{T^2}{12} \frac{1+10z^{-1}+z^{-2}}{(1-z^{-1})^2} [h_2'(0) + h_1(0)]. \quad (89)$$

It should be noted that (89) reduces to (88) in the limit as $T \rightarrow 0$. The difference equation that will be obtained from (89) represents an approximation to the original differential equation.

Clearing fractions in (89)

$$12(1-z^{-1})^3 H_2(S) + 6T(1-z^{-1}-z^{-2}+z^{-3}) H_1(S) \\ + T^2(1+9z^{-1}-9z^{-2}-z^{-3}) H_0(S) \\ = 6T^3(z^{-1}+z^{-2}) + 6T(1-z^{-1}-z^{-2}+z^{-3}) h_2(0) \\ + T^2(1+9z^{-1}-9z^{-2}-z^{-3}) [h_2'(0) + h_1(0)]. \quad (90)$$

Dividing both sides of (90) by T yields the z -transform of proper difference equation. Difference equation is obtained by taking inverse z -transform, which leads to

$$12h_2(t) - 36h_2(t-T) + 36h_2(t-2T) - 12h_2(t-3T) \\ + 6Th_1(t) - 6Th_1(t-T) - 6Th_1(t-2T) \\ + 6T^2h_1(t-3T) + T^2h_0(t) + 9T^2h_0(t-T) \\ - 9T^2h_0(t-2T) - T^2h_0(t-3T) \\ = 6T^2u_1 + 6T^2u_2 + (6u_0 - 6u_1 - 6u_2 + 6u_3)h_2(0) \\ + T(u_0 + 9u_1 - 9u_2 - u_3)[h_2'(0) + h_1(0)], \quad (91)$$

where t takes on the values nT ; $n = 0, 1, 2, \dots$, and

$$u_n = 1 \text{ for } t = nT$$

$$u_n = 0 \text{ for } t \neq nT.$$

If the numeric values of $h_1(0)$, $h_2(0)$ and $h'_2(0)$ are inserted in the right-hand side of (91), and if the usual

The methods given in the body of the paper would yield for (92) the following z-transform expression:

$$Y_A^*(z) = \frac{T^2(z^{-1} + z^{-2})}{(2 + TC) - (6 + TC)z^{-1} + (6 - TC)z^{-2} - (2 - TC)z^{-3}}. \quad (98)$$

Performing the synthetic division indicated by (98),

assumption is made that $h_0(t)$, $h_1(t)$, and $h_2(t)$ are zero for negative arguments, then the solution of the above difference equation is found to give exactly the same results as are obtained by the synthetic division process described in the body of the paper. A simple example will serve to clarify this. Given the differential equation

$$\frac{d^2Y}{dt^2} + \frac{d}{dt}(tY) = 1, \quad (92)$$

the Laplace transform assuming zero initial conditions is

$$S^2Y(S) + SL[tY] = \frac{1}{S} \quad (93)$$

$$Y(S) + \frac{1}{S} L[Y] = \frac{1}{S^3}. \quad (94)$$

Substituting the z -forms of Table I to obtain the approximate Laplace transform

$$Y_A(S) + \frac{T}{2} \frac{1+z^{-1}}{1-z^{-1}} L_A[C_n Y] = \frac{T^2}{2} \frac{z^{-1}+z^{-2}}{(1-z^{-1})^3}, \quad (95)$$

where $Cn = t = nT$; for $n = 0, 1, 2, \dots$. Dividing by T to obtain a z -transform and then taking the inverse transform yields

$$(2 + TC_n)Y_n - (6 + TC_{n-1})Y_{n-1} + (6 - TC_{n-2})Y_{n-2} \\ - (2 + TC_{n-3})Y_{n-3} = T^2u_2 + T^2u_2. \quad (96)$$

Solving this difference equation, assuming

$$C_n = 0; \quad t < 0$$

The first three values are

$$\begin{aligned} y(0) &= 0 \\ y(1) &= \frac{T^2}{2+T} \\ y(2) &= \frac{T^2}{2+2T} + \frac{T^2(6+T)}{(2+2T)(2+T)}. \end{aligned} \quad (97)$$

It is seen that the sequence of values obtained by the synthetic division propagates in the same way as the results given by (97).

Considering the case in which $F(S)$ is not available as a rational function of S in (87) one may express the equation as

$$H_2(S) + \frac{1}{S} H_1(S) + \frac{1}{S^2} H_0(S) \\ = \frac{1}{S^2} F(S) + \frac{1}{S} h_2(0) + \frac{1}{S^2} [h_2'(0) + h_1(0)]. \quad (100)$$

Using the z -forms of Table I, dividing by T to obtain the z -transform, and then taking the inverse z -transform yields the following difference equation:

$$\begin{aligned}
& 12h_2(t) + 24h_2(t-T) + 12h_2(t-2T) + 6Th_1(t) - 6Th_1(t-T) \\
& \quad + T^2h_0(t) + 10T^2h_0(t-T) + T^2h_0(t-2T) \\
& = T^2f(t) + 10T^2f(t-T) + T^2f(t-2T) + 6h_2(0)(u_0 - u_2) \\
& \quad + T[h_2'(0) + h_1(0)][u_0 + 10u_1 + u_2]. \tag{101}
\end{aligned}$$

The synthetic division process equivalent to this difference equation is derived in the following manner. The original differential equation is

$$\frac{d^2}{dt^2}(f_2 Y) + \frac{d}{dt} f_1(Y) + f_0(Y) = f(t). \quad (102)$$

Obtain the Laplace transform in accordance with the rules outlined for variable coefficients (time-varying or nonlinear);

$$S^2 C_2 Y(S) - S f_2(0) y(0) - f_2'(0) Y(0) - f_2(0) Y'(0) \\ + S C_1 Y(S) - f_1(0) Y(0) + C_0 Y(S) = F(S). \quad (103)$$

Rearranging and solving for $Y(S)$,

$$Y(S) = \frac{\frac{1}{S^2}F(S) + \frac{1}{S}f_2(0)Y(0) + \frac{1}{S^2}q(0)}{C_2 + \frac{1}{S}C_1 + \frac{1}{S^2}C_0} \quad (104)$$

Where

$$q(0) = f_2'(0)Y(0) + f_2(0)Y'(0) + f_1(0)Y(0).$$

Utilizing the z -forms of Table I, and dividing by T , the following z -transform is obtained:

$$Y_A^*(z) = \frac{\frac{T^2}{12} \frac{1+10z^{-1}+z^{-2}}{(1-z^{-1})^2} F^*(z) + \frac{T}{12} \frac{1+10z^{-1}+z^{-2}}{(1-z^{-1})^2} q(0) + \frac{1}{2} \frac{1+z^{-1}}{1-z^{-1}} [f_2(0)Y(0)]}{C_2 + \frac{T}{2} \frac{1+z^{-1}}{1-z^{-1}} C_1 + \frac{T^2}{12} \frac{1+10z^{-1}+z^{-2}}{(1-z^{-1})^2} C_0}. \quad (105)$$

But

$$F(z) = \sum_{n=0}^{\infty} f(nT)z^{-n}$$

which can be inserted in (105). After clearing fractions one then can proceed with the synthetic division leading to the same results that are obtained from the solution of (101).

Two further comments are appropriate in this Appendix. First, it can be shown that the procedures of this paper yield values of $y(nT)$ such that

$$\begin{aligned} \lim_{T \rightarrow 0} Y(nT) &= \frac{1}{2}Y(0) \quad \text{for } n = 0 \\ \lim_{T \rightarrow 0} Y(nT) &= Y(0) \quad \text{for } n \neq 0 \end{aligned} \quad (106)$$

where $Y(0)$ is the exact solution at $t = 0$.

Second, if initial conditions are neglected in taking the Laplace transform, the method yields a difference equation approximating the system with considerably less algebraic manipulation. This difference equation can be used for computation after the first values of the solution are calculated by any means whatever.

ACKNOWLEDGMENT

The authors wish to express their appreciation to D. L. Ashcroft for his helpful suggestions made during the development of the technique covered by this paper.

Multi-Beam Velocity-Type Frequency Multiplier*

YUKITOKO MATSUO†

Summary—One of the limitations imposed upon a conventional frequency multiplier using a double-cavity klystron is the restriction of rf output caused by the mutual repulsion of electrons. To overcome this difficulty a multibeam velocity-type frequency multiplier was proposed by the author, and theoretical and experimental investigations were made.

Another type of multibeam frequency multiplier has been proposed by R. Kompfner, but as far as the author is aware, this tube has not yet been fully examined experimentally nor theoretically because of the complexity of the physical structure.

Experiments made on a tentative model of the proposed frequency multiplier with two electron beams disclosed that much higher output power compared with conventional klystron multipliers could be derived. It is believed that the new tube is promising in providing a novel means of generating microwave signals of multiplied frequencies.

INTRODUCTION

AT THE PRESENT time, crystal detectors are used as frequency multipliers in the generation of millimeter waves, but the multiplied power obtainable therefrom is very small. This is the primary drawback of such frequency multipliers. On the other hand, beam current in double-cavity klystrons contain

large quantities of higher-order harmonics and are used as frequency multipliers in the centimeter regions. Drawbacks experienced with double-cavity klystrons, however, are in the debunching force in the electron beam, which increase with large beam current. If the debunching force is reduced to some extent by some sort of way, the multiplied power will be greater. Herein lies the possibility of an effective method of generating millimeter waves by extracting powerful harmonic power from the beam.

Hereupon, in 1951, the author proposed a new type of multibeam velocity-type frequency multiplier consisting of several individual beams, thus providing an increased total beam current without serious debunching effect inherent to all high beam density.¹ This multiplier tube is provided with a single input and an output cavity common to all the beams. These electron beams, with different dc velocities, are velocity-modulated in common by the input cavity, while the energy of the harmonics generated in each beam are picked up by the output cavity. This type of frequency multiplier will be termed the velocity-type, hereafter.

* Original manuscript received by the IRE, May 21, 1955; revised manuscript received, June 16, 1955.

† Dept. of Physics, Osaka University, Osaka, Japan.

¹ Y. Matsuo "On the new type of frequency multiplier," The Record of the General Meeting of the Kansai Branches of I.E.E. and I.E.C.E. of Japan, October, 1951.

R. Kompsner proposed another type of multibeam frequency multiplier, employing the same number of input cavities with the number of electron beams, in which the driving high-frequency voltages are impressed on each input cavity at different phases.² This method is pretty troublesome, if not impossible, in maintaining definite phase difference between the driving voltages, and it also involves added difficult procedure in the mechanical arrangement. For convenience, this type will be termed the phase-type frequency multiplier.

The authors have carried out theoretical studies on the multibeam velocity-type multiplier as well as the phase-type multibeam frequency multiplier. For simplicity, two-beam velocity-type frequency multipliers have been constructed and tested in the centimeter region; *i.e.*, 8 cm~3 cm, whose results will be dealt with in the present paper.

OPERATION OF THE TUBE

The operation of the multi-beam velocity-type multiplier is outlined as follows.

The current components at the *m*th harmonic of the klystron, i_m , are given by

$$i_m = 2I_0 J_m(mX) \cos(m\omega t - \theta_0), \quad (1)$$

here,

$X = (V/2V_0)(\omega l/u_0)$ = bunching parameter,

V_0 = accelerating voltage,

l = drifting length,

$\theta_0 = \omega l/u_0$ = dc transit angle,

V = driving rf voltage,

I_0 = beam current,

u_0 = dc velocity.

Transverse debunching results in the reduction of the beam current that passes through the output gap caused by the loss of current collected at the circumference of the cavity gap. Hence, the reduction of rf current caused by transverse debunching is affected approximately by a factor,³

$$1 - \frac{X}{6} (hl)^2, \quad (2)$$

here,

$$(ha)^2 = \frac{60I_0}{\beta V_0},$$

$$\beta = \frac{u_0}{c}, \quad a = \text{beam radius}, \quad c = \text{light velocity}.$$

By the effect of transverse debunching, neglecting the effect of longitudinal debunching which is equivalent to

² R. Kompsner, "Velocity modulation results of further consideration," *Wireless Engr.*, vol. 17, pp. 478-488; November, 1940.

³ D. R. Hamilton, J. K. Knipp, and J. B. H. Kuper, "Klystrons and Microwave Triodes," McGraw-Hill Book Company, New York, N. Y., pp. 209-217, 285-293; 1948.

assuming a constant Bessel function independent of the beam current, the rf power is proportional to

$$I_0^2 \left\{ 1 - \frac{X}{6} (hl)^2 \right\}^2 = I_0'^2.$$

This is to say that the rf power is not proportional to the square of the beam current as indicated in the simple klystron theory. Since this transverse debunching effect is based upon the assumption of $X < 1$, it is not rigorously true for $X > 1$, however, it may serve to explain the general behavior of this type of tube. From (2), it follows that the effect of transverse debunching is proportional to I_0 , and inverse proportional to V_0^3 .

On the other hand, longitudinal debunching causes a reduction in the value of bunching parameter at the output gap. In this case the bunching parameter is expressed as follows.³

$$X' = X \frac{\sin hl}{hl}. \quad (3)$$

Increase of beam current affects X' in such a way as to reduce the maximum value of $J_m(mX')$. However, the longitudinal debunching effect caused by the increase of beam current may be compensated by adjusting the accelerating voltage. The optimum voltage in the actual adjustment is achieved by maximizing the amplitude of i_m as expressed by (1), wherein I_0' , as well as $J_m(mX')$ is also a function of V_0 . In a beam of finite cross section with a conducting wall, however, there is no longitudinal debunching at the outer edge of the beam, and it should be noted that there is a variation in the bunching parameter with different radial position within the beam. Hereupon, there is an effective bunching parameter which must be taken equal to the mean bunching parameter. This effect decreases the rf current of the *m*th harmonic, since the mean bunching parameter necessarily reduces the value of the Bessel function $J_m(mX')$ from its maximum value determined by the optimum X' . Though it was found experimentally that the wall effect did not extend so far into the beam,³ it must be remembered that the wall effect might play an important role as the harmonic order, *m*, is taken large.

At any rate, it may be concluded that the rf power is not proportional to the square of the beam current caused by such debunching effects. There certainly is a maximum value to the rf power at some value of beam current, say, I_0 . Therefore, instead of increasing the beam current I_0 to increase the rf power which cannot exceed the maximum power, a number of beams, whose beam currents are I_0 , are adopted, and their bunches may be made to pass through the output gap successively with the definite time intervals by changing their dc velocities (see Fig. 1). If $m\theta_0 = 2\pi n$ (*n* = integer) is set for each beam by adjusting each velocity, (1) is written for *N* beams as follows:

$$i_{m,N} = 2 \{ I_0' J_m(mX_1') + I_0'' J_m(mX_2') + \dots + I_0^{(N)} J_m(mX_N') \} \cos m\omega t. \quad (4)$$

Primes show the bunching effects. As the velocities of each beam are different, each bunching parameter has a different value.

In the phase-type, $X_1' = X_2' = \dots = X_N'$, and $I_0' = I_0'' = \dots = I_0^{(N)}$, so the rf power of the m th harmonic is proportional to $\{NI_0' J_m(mX_1')\}^2$, which is N^2 times the rf power of one beam. But in the velocity-type, if $J_m(mX_1')$ is adjusted to its maximum value, the values of other Bessel functions become smaller than $J_m(mX_1')$. Also, the beam currents $I_0', I_0'', I_0''', \dots$, and $I_0^{(N)}$ are not equal, because their beam velocities are different. Consequently, the rf power of the m th harmonic is smaller than that of the phase-type. However, if the "B-type arrangement" which will be stated later is adopted, the rf power of the m th harmonic will approach that of the phase-type fairly closely.

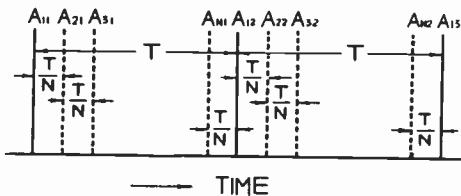


Fig. 1—A-type arrangement of the bunching centers (N =Number of beams).

THE ARRANGEMENT OF THE BUNCHING CENTERS OF THE BEAMS

Fig. 1 shows the general order of the bunching centers of N beams that arrive successively at the output gap. In Fig. 1, N is the beam number, T is the period of the driving voltage, $A_{11}, A_{12}, \dots, A_{21}, A_{22}, \dots$, and A_{N1}, A_{N2}, \dots are the bunching centers of the first, second, and the N th beam, respectively. In this notation, the first subscript represents the beam number and the second represents the successive bunching centers of the beam specified by N . This arrangement of the order of beam bunches will be termed the "A-type," and it contains the nN th harmonics (n =integer). However, it does not necessarily require that the time intervals between each bunching center are T/N . Another arrangement, wherein, for instance, $N=2$, is shown in Fig. 2(a). In this case, the 4th harmonic is predominant among the rest of the harmonics. This arrangement will be called the "B-type." Large difference of velocity between each beam leads to large difference of the bunching parameters, X' , of each beam. Therefore, when one beam is adjusted to its optimum bunching, it follows that the others will depart from their optimum bunching. Hence, the B-type arrangement, Fig. 2(a), is richer in the 4th harmonic than the A-type arrange-

ment, Fig. 2 (b). In general, we assume that there are N beams. One of the beams, say the first beam, will be adjusted to its optimum bunching. The beam the bunching center of which arrives at the output gap next to the bunching center of the first beam will be called the second beam, and so forth. In order to get the m th harmonic (in general, $m \geq N$), one should take the time difference between the bunching centers of the first and

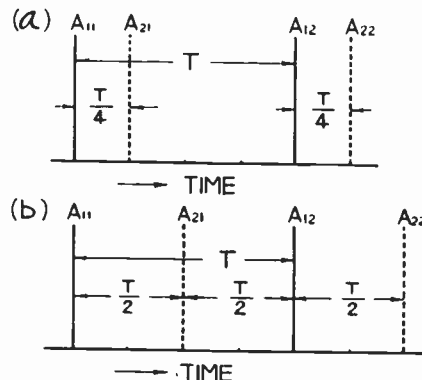


Fig. 2—(a) An example of the B-type arrangement of the bunching centers (Number of beams: 2, $m=4$). (b) A-type arrangement (Number of beams: 2).

the $(b+1)$ th beam as bT/m ($b=1, 2, 3, \dots, N-1$). For large m , the values of the bunching parameters of each beam approach each other closely, whereby the multiplied rf power of the velocity-type approaches fairly close to that of the phase-type. However, when the successive bunching centers are made too close to each other, overlapping of bunches occurs which gives rise to undesirable debunching. Cut-and-try means of adjustment seem to be the only way of overcoming this effect.

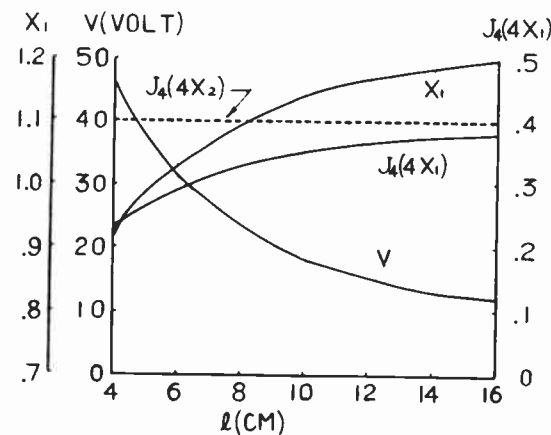


Fig. 3—Relation between $J_4(4X_1)$ and drifting space length l , when $N=2$, $\lambda=20$ cm and $V_{02}=500$ volts (A-type arrangement).

For example, when $N=2$, $\lambda=20$ cm and the accelerating voltage of one beam, V_{02} , is kept constant at 500 volts (V_{02} meaning V_0 in Fig. 7), the Bessel function $J_4(4X_1)$ of the other beam is calculated for the drifting space length l and is shown in Fig. 3, maintaining the

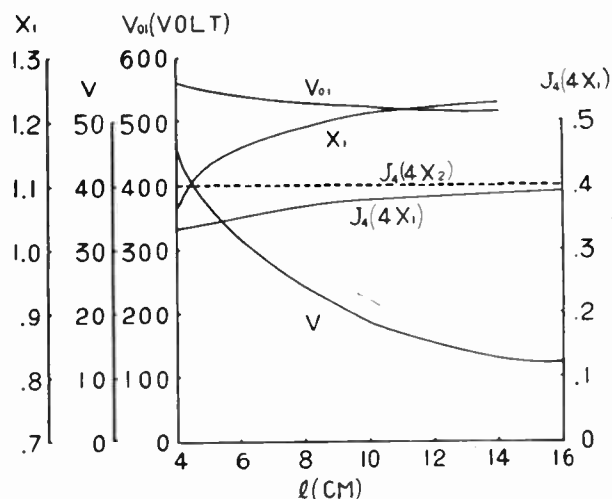


Fig. 4—The relation between $J_4(4X_1)$ and the drifting space length l , when $N=2$, $\lambda=20$ cm and $V_{02}=500$ volts. (The time difference of the flight of both beams to output gap is $T/4$).

Bessel function $J_4(4X_2)$ to its maximum value by adjusting the high frequency driving voltage for each drifting space length. As these Bessel functions are in proportion to the magnitudes of the 4th harmonic contents of each beam, the multiplied power is proportional to $\{J_4(4X_1)+J_4(4X_2)\}^2$, neglecting the debunching

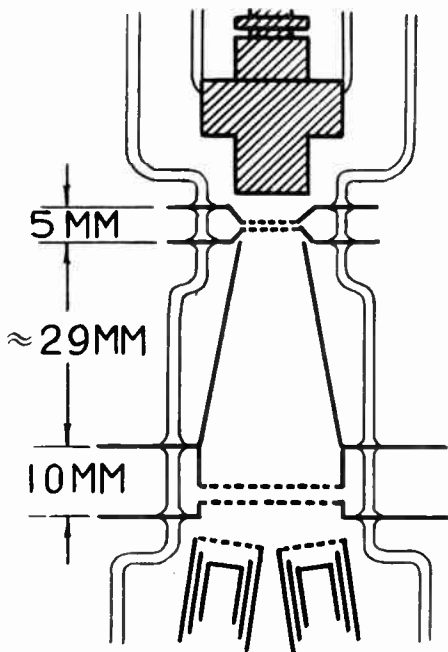


Fig. 5—Cross section of the two-beam velocity-type frequency multiplier.

effects of electrons. In Fig. 3, the arrangement of bunching centers belongs to the A-type.

Fig. 4 shows the case in which the bunching centers of both beams are arranged as in Fig. 2(a). From Fig. 3 and Fig. 4, the rate of increase of the value of Bessel function, $J_4(4X_1)$, for the B-type arrangement is found.

In these figures, V represents the high-frequency driving voltage, and V_{01} represents the accelerating voltages of the other beam (V_{01} meaning $V_0 + V_d$ in Fig. 7).

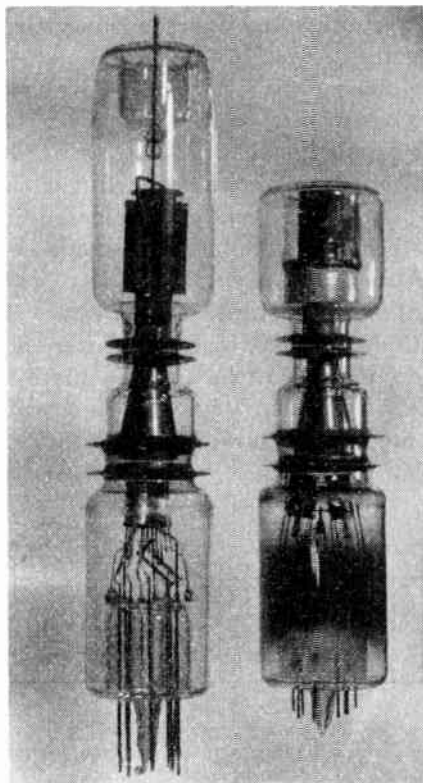


Fig. 6—Appearance of the two-beam velocity-type multiplier.

CONSTRUCTION OF TUBE AND EXPERIMENTAL SETUP

The internal construction and external appearance of the velocity-type frequency multiplier are illustrated in Figs. 5 and 6, respectively. Each of the two electron guns is given an inclination to the center axis to facilitate the passage of the electron beams through the aperture of the output cavity. The connection diagram of this tube is shown in Fig. 7. The velocity of the first beam, "1," which is faster than that of the second beam "2," is varied by the voltage V_d . Unbalance of both beams due to different grid potentials relative to each cathode is very small if beam 2 is operated in the vicinity of the temperature limited condition. This condition may be the cause of instability by fluctuation in cathode temperature, and therefore this condition is not the best one. Methods of overcoming this point are being considered, but the objections did not prevent obtaining the desired results. Electron paths of both beams are affected little by adjusting the difference voltage V_d . Therefore the ratio of the collector current to the total current is almost invariable for the difference of voltage applied between the two beams. The wavelength of the driving high frequency voltage was about 22.5 cm. As the output was detected by a crystal detector having a square

law character, the detected crystal current may be considered proportional to the output power, which is designated by P_0 with an arbitrary unit. Experiments were carried out up to the harmonic order of $m=7$.

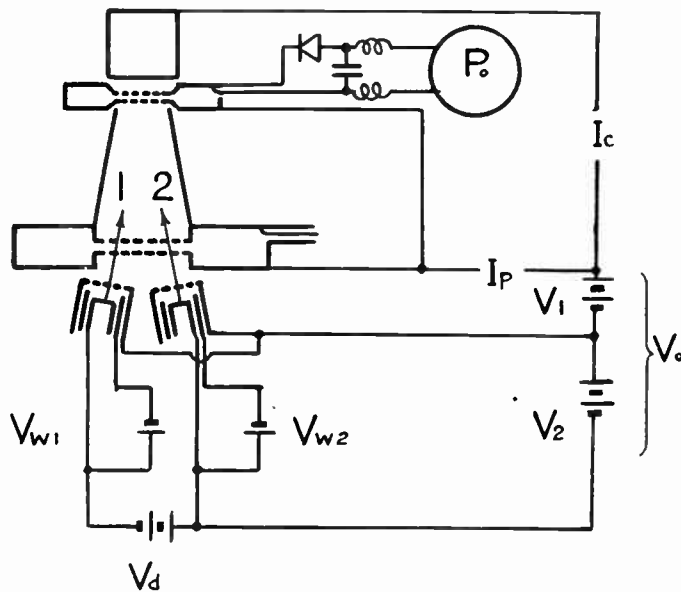


Fig. 7—Connection diagram.

EXPERIMENTAL RESULTS

Effect Due to Velocity Difference

The 4th harmonic power P_0 and the collector current I_c vs the difference voltage V_d are shown in Fig. 8. At $V_d=0$, the accelerating voltage is adjusted for maximum harmonic power P_0 , while maintaining constant the driving voltage and the filament voltage. The difference in the time of arrival of the bunching centers of both beams at the output gap for extremum points of P_0 is calculated from the experimental results of Fig. 8 and is shown in Fig. 9. Here, A_{21} and A_{22} are the bunching centers of beam 2 in Fig. 7. At $P_0=0$ and $V_d \approx 50$ volts in Fig. 8, the bunching centers of beam 2 lag about $T/8$ from those of beam 1, wherein 4th harmonic powers induced by the bunching centers of both beams are out of phase as shown in Fig. 9. In Fig. 9, the sinusoidal wave represents the 4th harmonic induced by the bunching center A_{21} in the output cavity. Points of maximum power are explained in the same way. From this figure, the power at $V_d \approx 390$ volts is seen to be smaller than that at $V_d \approx 150$ volts. This is due to the reduction of the harmonic content of beam 1 for large difference voltages. In Figs. 8 and 9, it is clear that condition at $V_d \approx 150$ volts corresponds to *B*-type arrangement of Fig. 2(a), and that condition at $V_d \approx 390$ volts corresponds to *A*-type arrangement of Fig. 2(b).

Effect Due to Current Density

If the parameters are adjusted in favor of the m th harmonic, which is proportional to the Bessel function

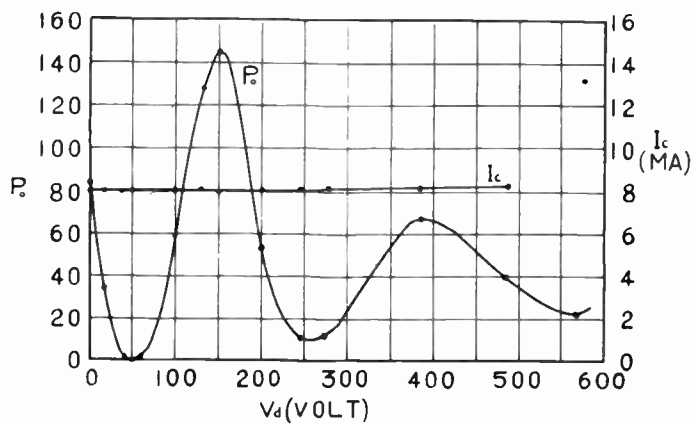


Fig. 8—The 4th harmonic power vs the difference voltage ($\lambda_4 = 5.64$ cm).

$J_m(mX_2)$ of beam 2, the velocity of which is less than that of beam 1, the condition that maximizes the slow beam power output does not simultaneously satisfy the optimum condition of $J_m(mX_1)$ of beam 1. Nevertheless, the reduction of $J_m(mX_1)$ is compensated to some extent by the decreased transverse debunching effect of beam 1 caused by the larger accelerating voltage.

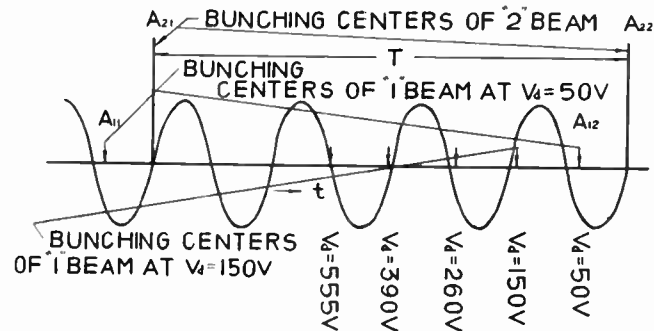


Fig. 9—Time relation between the bunching centers of beam 1 and beam 2 at the output gap (calculated from the result of Fig. 8).

Fig. 10 shows a typical relation between the collector current and the third harmonic power. Here, the output is adjusted so as to be at its maximum for each collector current, maintaining constant the driving voltage. Curve C shows the case where there is no velocity difference between both beams; curve D shows the case when the time difference of the flight of both beams to the output gap is $T/3$. In Fig. 10, the maximum power of curve D is about twice as large as that of curve C. If both beams have equal current densities, and if the debunching effects are not considered for simplicity, the maximum power ratio of both cases, $\{ [J_3(3X_1) + J_3(3X_2)] / J_3(3X_1) \}^2$, is calculated only from the values of Bessel functions. Therefore, the maximum power for curve D is about 2.9 times that of curve C, which is slightly different according to the operating voltage. The reason why the experimental result is smaller than 2.9 is due to the electron path of both beams. This will be explained later.

In the region of small collector currents, the power for curve *C* is little affected by the debunching forces and follows the square law character, as expected theoretically. Hence the power for curve *C* is larger than that for curve *D*.

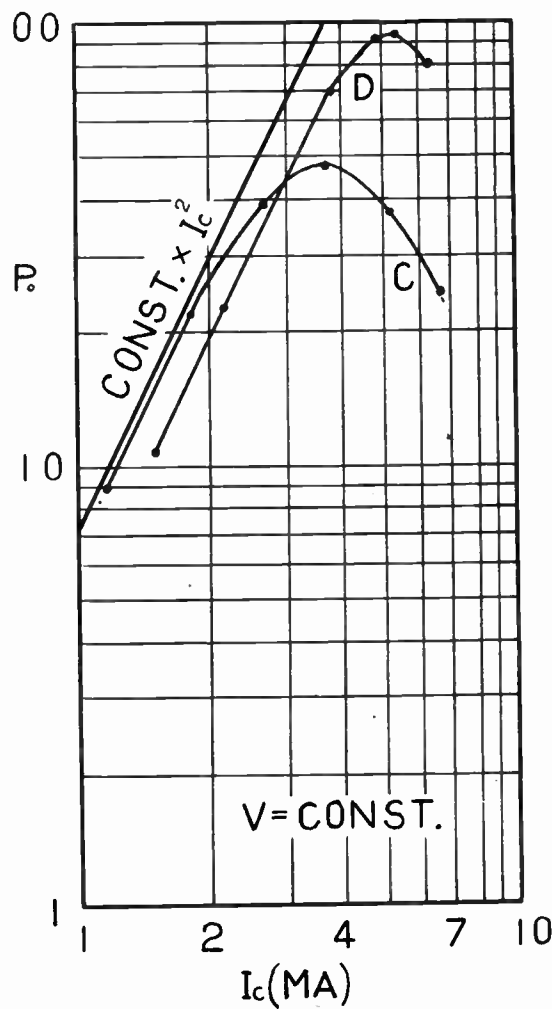


Fig. 10—The 3rd harmonic power vs the collector current. Curve *C*: without velocity difference between both beams. Curve *D*: with velocity difference between both beams.

Fig. 11 shows the 3rd harmonic power for the various values of collector current. In this figure, curves *A* and *B* are results obtained for beam 1 and beam 2, separately. Curve *C* is the superposed result of both beams without velocity difference, and curve *D* is that with velocity difference. If electron paths of both beams coincide with each other, although it is impossible to realize such an electron gun, curves *A*, *B* and *C* will fall on the same curve. In this ideal case, the maximum power ratio of curve *D* to curve *C* and therefore the maximum power ratio of curve *D* to curves *A* or *B* is about 2.9, in accord with the above statement. If the paths of both beams

miss the center of the output gap, the ratio of the former becomes smaller, but the ratio of the latter stays almost invariable. In Fig. 11, the maximum power of curve *D* is more than 2.9 times the maximum power of curve *A* or *B*. That the ratio is greater than 2.9 may be due to the fact that the transverse debunching effect is smaller in beam 1, since the velocity of beam 1 is faster than that of beam 2.

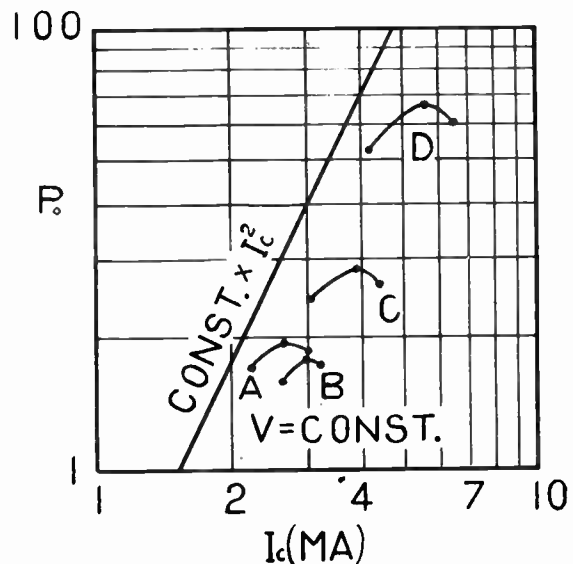


Fig. 11—The third harmonic power versus the collector current. Curve *A* and Curve *B*: Curves for beam 1 and beam 2.

In these above experiments, wave interaction between two beams of different velocity is not considered in the present case, owing to the fact that two beams are far apart from each other along their entire path except at output gap. Results of Fig. 8 and Fig. 9 are in good accord with the discussions, neglecting effects of wave interaction. Therefore, it is justified to assume that wave interaction, in construction of the tube as employed here, is of the second-order phenomena.

ACKNOWLEDGMENT

The author wishes to thank heartily Professor K. Okabe of Osaka University, Dr. T. Hayashi, and Prof. S. Mito of the Osaka City University who kindly directed the author, and Dr. S. Nakajima, Mr. Y. Yasuoka, Mr. K. Shiozawa, and Mr. C. Shibata of J. R. C. and Mr. K. Takashima and Mr. T. Misugi of Kobe Kogyo Electric Co., Ltd. who helped fabricate the testing tubes. The author is also much indebted to Dr. T. Hatano, Tokyo Shibaura Electric Co. Ltd., for his useful discussion and to Mr. Y. Yamane for his valuable assistance in carrying out the experiment.

IRE Standards on Terminology for Feedback Control Systems, 1955*

COMMITTEE PERSONNEL

Subcommittee on Terminology for Feedback Control Systems

M. R. AARON, *Chairman* 1954-55

J. C. LOZIER, *Chairman* 1952-54

M. R. Aaron
G. R. Arthur
V. Azgapetian

C. F. Rehberg

M. Cooperstein
J. O. Edson
T. Flynn

F. Zweig

L. Goldman
J. C. Lozier
L. H. O'Neill

Committee on Feedback Control Systems 1954-55

J. E. WARD, *Chairman*

M. R. Aaron
G. S. Axelby
G. A. Biernson
V. B. Haas, Jr.
R. J. Kochenburger

D. P. Lindorff
W. K. Linvill
D. L. Lippitt
J. C. Lozier
T. Kemp Maples
W. M. Pease

E. A. Sabin
P. Travers
R. B. Wilcox
S. B. Williams
F. R. Zatlin

Standards Committee 1955-56

E. WEBER, *Chairman*

M. W. BALDWIN, JR., *Vice-Chairman*

R. F. SHEA, *Vice-Chairman*

L. G. CUMMING, *Vice-Chairman*

J. Avins
W. R. Bennett
J. G. Brainerd
P. S. Carter
P. S. Christaldi
A. G. Clavier
J. E. Eiselein
A. W. Friend
V. M. Graham
R. A. Hackbusch
H. C. Hardy

P. J. Herbst
Hans Jaffe
Henry Jasik
A. G. Jensen
J. L. Jones
J. G. Kreer, Jr.
E. A. Laport
A. A. Macdonald
Wayne Mason
D. E. Maxwell
K. R. McConnell

H. R. Mimno
M. G. Morgan
G. A. Morton
H. L. Owens
P. A. Redhead
C. H. Page
R. Serrell
R. M. Showers
H. R. Terhune
J. E. Ward
W. T. Wintringham

Definitions Coordinator

M. W. BALDWIN, JR.

1. INTRODUCTION

1.1. Prior to the preparation of this standard, no complete and self-consistent set of terminology appeared to fulfill the requirements of the IRE. Because of a wide variation in the terminology used by different industries

and professional societies it was difficult to choose a terminology acceptable to all fields. Therefore, a compromise has been made among existing terminologies used in the electrical field.

* Reprints of this standard, 55 IRE 26.S2 may be purchased while available from the Institute of Radio Engineers, 1 East 79 Street, New York, N. Y., at \$0.50 per copy. A 20 per cent discount will be allowed for 100 or more copies mailed to one address.

2. DEFINITIONS

2.1 Signals

2.1.1. Loop Input Signal. An external signal applied to a feedback control loop.

2.1.2. Loop Output Signal. The controlled signal extracted from a feedback control loop.

2.1.3. Loop Feedback Signal. The signal derived as a function of the loop output signal and fed back to the mixing point for control purposes.

2.1.4. Loop Actuating Signal. The signal derived by mixing the loop input signal and the loop feedback signal.

2.1.5. Loop Error Signal. The loop actuating signal in those cases in which it is the loop error (See 2.4.10).

2.1.6. Loop Return Signal. The signal returned via a feedback control loop to a summing point, in response to a loop input signal applied to that summing point, and subtracting from the loop input signal.

Note: The loop return signal is a specific type of loop input signal.

2.1.7. Loop Difference Signal. The output signal from a summing point of a feedback control loop produced by a particular loop input signal applied to that summing point.

Note: The loop difference signal is a specific type of loop actuating signal.

2.2. Points and Paths

2.2.1. Mixing Point. In a block diagram of a feedback control loop, a symbol indicating the relationship of one output to two or more inputs, such that the value of the output at any instant is a function of the values of the inputs at that instant.

Note: If a mixing device in practice contains dynamic elements, these shall be considered as transfer elements in one or more of the signal paths entering or leaving the mixing point.

2.2.2. Summing Point. A mixing point whose output is obtained by addition, with prescribed signs, of its inputs.

2.2.3. Multiplication Point. A mixing point whose output is obtained by multiplication of its inputs.

2.2.4. Forward Path. In a feedback control loop, the transmission path from the loop actuating signal to the loop output signal.

2.2.5. Feedback Path. In a feedback control loop, the transmission path from the loop output signal to the loop feedback signal.

2.2.6. Through Path. In a feedback control loop, the transmission path from the loop input signal to the loop output signal.

2.3. Transfer Functions

2.3.1. Transfer Function. A relationship between one system variable and another that enables the second variable to be determined from the first.

2.3.2. Transfer Ratio. The transfer function from one system variable to another in a linear system, expressed as the ratio of the Laplace transform of the second variable to the Laplace transform of the first variable, assuming zero initial conditions.

2.3.3. Loop Transfer Function. The transfer function of the transmission path formed by opening and properly terminating a feedback loop.

Note: One example of proper termination is a zero impedance generator driving the opened loop, and an output termination for the opened loop equal to the impedance facing the generator.

2.3.4. Loop Transfer Ratio. The transfer ratio of a loop return signal to the corresponding loop difference signal.

2.3.5. Forward Transfer Function. In a feedback control loop, the transfer function of the forward path.

2.3.6. Feedback Transfer Function. In a feedback control loop, the transfer function of the feedback path.

2.3.7. Return Transfer Function. In a feedback control loop, the transfer function which relates a loop return signal to the corresponding loop input signal.

2.3.8. Difference Transfer Function. In a feedback control loop, the transfer function which relates a loop difference signal to the corresponding loop input signal.

2.3.9. Through Transfer Function. In a feedback control loop, the transfer function of the through path.

2.3.10. Actuating Transfer Function. In a feedback control loop, the transfer function which relates a loop actuating signal to the corresponding loop input signal.

2.4. General

2.4.1. Feedback Control Loop. A closed transmission path, which includes an active transducer and which consists of a forward path, a feedback path, and one or more mixing points arranged to maintain a prescribed relationship between the loop input signal and the loop output signal.

2.4.2. Feedback Control System. A control system, comprising one or more feedback control loops, which combines functions of the controlled signals with functions of the commands to tend to maintain prescribed relationships between the commands and the controlled signals.

2.4.3. Feedback Control System, Linear. A feedback control system in which the relationships between the pertinent measures of the system signals are linear.

2.4.4. Feedback Control System, Nonlinear. A feedback control system in which the relationships between the pertinent measures of the system input and output signals cannot be adequately described by linear means.

Note: A system can be either *quasi-linear* or *nonlinear*, depending upon operating conditions and performance requirements.

2.4.5. Feedback Control System, Quasi-Linear. A feedback control system in which the relationships between the pertinent measures of the system input and output signals are substantially linear despite the existence of nonlinear elements.

Note: A system can be either *quasi-linear* or *nonlinear*, depending upon operating conditions and performance requirements.

2.4.6. Feedback Regulator. A feedback control system which tends to maintain a prescribed relationship between certain system signals and other pre-determined quantities.

Note 1: This definition is intended to point out the fact that some of the system signals in a regulator are adjustable reference signals.

Note 2: It should be noted that *servomechanism* and *regulator* are not mutually exclusive terms; their application to a particular system will depend on the method of operation of that system.

2.4.7. Servomechanism. A feedback control system in which one or more of the system signals represent mechanical motion.

Note: It should be noted that *servomechanism* and *regulator* are not mutually exclusive terms; their application to a particular system will depend on the method of operation of that system.

2.4.8. Command. An independent signal from which the dependent signals are controlled according to the prescribed system relationships.

2.4.9. Disturbance. An undesired command.

2.4.10. Loop Error. The desired value minus the actual value of the loop output signal.

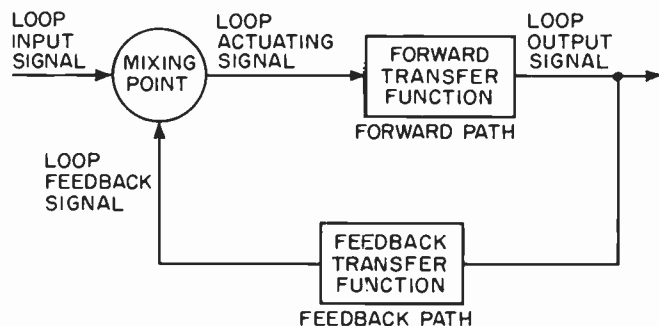
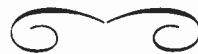


Fig. 1

3. EXAMPLE

3.1. Application of the standard terminology to a typical block diagram is shown in Fig. 1.



CORRECTION

E. A. Gerber, author of the correspondence "Temperature Coefficient of AT Cut Quartz Crystals," which appeared on page 1529 of the October, 1955, issue of the PROCEEDINGS OF THE IRE, has brought the following

correction to the attention of the editors.

In the first column, twelfth line from the bottom of the page, the term *feet* should be replaced by the term *minutes*.

Correspondence

Scattering Matrix Measurements on Nonreciprocal Microwave Devices*

I read with considerable interest the letter by A. C. MacPherson¹ describing a method of measuring the scattering matrix elements of nonreciprocal microwave four-pole. We have worked out a strikingly similar technique early this year and have been using it in our laboratory.² Since our method gives a somewhat more rapid measurement of the scattering matrix parameters, we believe it warrants description.

A two-port microwave device (Fig. 1) is described by

$$\Gamma_1 = S_{11}d_1 + S_{12}d_2$$

$$\Gamma_2 = S_{21}d_1 + S_{22}d_2,$$

where d_1 and d_2 represent the waves incident on the device, and Γ_1 and Γ_2 represent the outgoing waves.

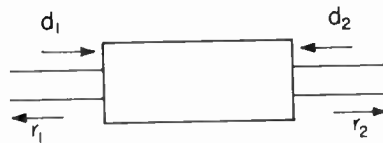


Fig. 1—Two-port microwave device.

Then

$$\Gamma_1 = r_1/d_1 = S_{11} + S_{12}d_2/d_1$$

$$\Gamma_2 = r_2/d_2 = S_{22} + S_{21}d_1/d_2,$$

where we have denoted r_1/d_1 and r_2/d_2 by Γ_1 and Γ_2 ; these complex reflection coefficients are measurable by slotted lines. In particular, if $|d_2| = |d_1|$, so that $d_2/d_1 = e^{j\theta}$, then

$$\Gamma_1 = S_{11} + S_{12}e^{j\theta}$$

$$\Gamma_2 = S_{22} + S_{21}e^{-j\theta}.$$

If the angle θ is adjusted to be first zero (with respect to some reference plane) and then π , we have

$$\Gamma_1^{(a)} = S_{11} + S_{12} \quad (\theta = 0) \quad (1)$$

$$\Gamma_1^{(b)} = S_{11} - S_{12} \quad (\theta = \pi).$$

Therefore,

$$S_{11} = \frac{\Gamma_1^{(a)} + \Gamma_1^{(b)}}{2} \quad (2)$$

$$S_{12} = \frac{\Gamma_1^{(a)} - \Gamma_1^{(b)}}{2}.$$

* Received by the IRE, August 26, 1955. Work carried out under AF Contract No. 19(604)-1084, while the writer was a General Communications Company Fellow in Applied Physics.

¹ Measurement of microwave nonreciprocal four-poles, PROC. IRE, vol. 43, p. 1017; August, 1955.

² Crutt Lab., Harvard University, Prog. Rep. No. 34, Contract NS ORI-76, p. 8; Jan., 1955. *Ibid.*, No. 35, p. 7; April, 1955. A complete description with a discussion of errors is given in Gordon McKay Laboratory, Harvard University, Prog. Rep. No. 1, Contract AF 19(604)-1084; July, 1955.

A similar set of equations holds for S_{21} and S_{22} . Thus, if two measurements of Γ_1 ($\Gamma_1^{(a)}$) and $\Gamma_1^{(b)}$) are made, S_{11} and S_{12} are determined by (2); similarly, S_{21} and S_{22} are determined from two measurements of Γ_2 .

The measurement setup is illustrated in Fig. 2. The device under test is to be inserted at plane $a-b$. The procedure is as follows:

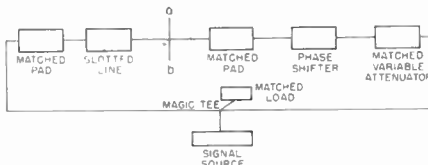


Fig. 2—Test set-up.

1. With a straight section of waveguide inserted at plane $a-b$, adjust the variable (uncalibrated) attenuator until an infinite vswr is observed in the slotted line. Then $|d_2| = |d_1|$. Set the phase shifter so that a minimum in the standing wave occurs at the desired reference plane; the setting on the phase shifter corresponds to $\theta = \pi$. If the phase shifter is uncalibrated, it may be calibrated at this point by adjusting it until a maximum in the standing wave appears at the previously selected reference plane, at which time the phase shifter is set for $\theta = 0$. This completes the calibration adjustments and takes the place of the measurement of Bg_1/Bg_2 suggested by MacPherson.

2. Insert the unknown at plane $a-b$ and measure $\Gamma_1^{(a)}$ and $\Gamma_1^{(b)}$ for the two positions of the phase shifter. S_{11} and S_{12} are then determined.

3. Turn the device end-for-end and repeat step 2, measuring $\Gamma_2^{(a)}$ and $\Gamma_2^{(b)}$, thus determining S_{21} and S_{22} .

If a second slotted line is used at the right of the plane $a-b$, as suggested in MacPherson's Fig. 2, the whole measurement described above is carried out without removing the device, once the calibration adjustments of step 1 are made.

This procedure is somewhat more convenient than that described by MacPherson, although it is obvious that his procedure will give a more accurate measurement of S_{11} and S_{12} .

Finally, a consideration of errors shows that for reasonable accuracy the pads (or Unilines) must be well-matched, as emphasized by MacPherson. The commercial Unilines with which we are familiar are not sufficiently well-matched to use without additional matching devices. On the other hand commercial pads have proven adequate of themselves for our purposes.

Professors C. L. Hogan, J. E. Storer, and Dr. E. G. Fubini gave valuable suggestions in connection with this problem.

J. E. PIPPIN
Gordon McKay Lab.
Harvard University
Cambridge, Mass.

A New Treatment for Parabolic Reflector Problems*

Parabolic reflectors are often used at microwave frequencies to obtain a high directivity and large antenna gain. The ordinary procedure is to calculate the reflected field strength at a point by the ordinary ray treatment—considering the reflection at the parabolic reflector. A slight modification of this procedure is to consider it on the image basis.

Suppose O is a line source at the focus of the parabolic cylinder reflector PQV shown in Fig. 1. Considering only the transverse section in the plane of the paper, the field strength due to the reflected wave at any point on the right of the reflector can be calculated on the assumption that the radiation is coming from a line source LL' (the directrix of the parabolic reflector) which emits a parallel beam of radiation. Thus the problem of calculating the reflected field strength at any point is simplified. The actual field strength is the superposition of the direct field strength due to the source proper over this reflected field strength.

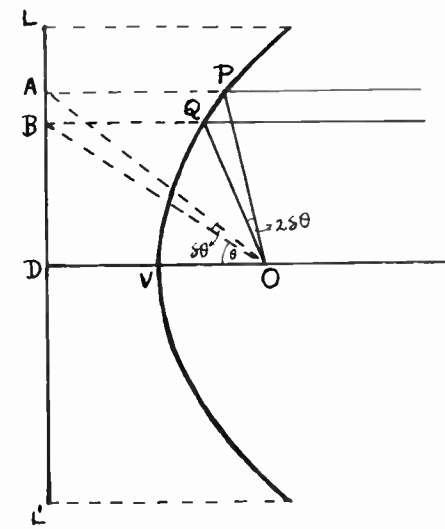


Fig. 1

In order to calculate the field strength we should also know the intensity distribution along the image. If the ray OQ makes an angle 2θ with the axis OV , then (from the properties of the parabolic cylinder) the image of O in the reflector element near Q will be the point B on the directrix, and $\angle QOB = \angle QBO$. Also, as QB is parallel to OD , $\angle QBO = \angle BOD$. Therefore, $\angle BOD$ is half $\angle QOD$ or $\angle BOD = \theta$. Similarly, if a portion PQ of the parabola makes an angle 2θ at O , then its image AB will make an angle θ at the same point. Now,

* Received by the IRE March 18, 1955. Revision received, August 15, 1955.

$$AB = (OB) \cdot \delta\theta \cdot \sec \theta = (OD) \cdot \delta\theta \sec^2 \theta.$$

The power radiated by the source O is proportional to $2\delta\theta$, and, since OD is constant, the intensity I at the point B of the image (directrix) is proportional to $\cos^2 \theta$ where $\theta = \angle DOB$.

The above treatment can be easily extended to the three-dimensional case in which the image will be a plane sheet perpendicular to the axis.

B. CHATTERJEE

Indian Institute of Technology
Kharagpur, India

A Method of Launching Surface Waves*

In order to launch surface waves efficiently the field pattern of the launching device should be matched as closely as possible to the pattern of the wave. A very good match can be obtained with the systems shown in Fig. 1. The principle of the method is to maintain the phase velocity of the wave constant throughout the system.

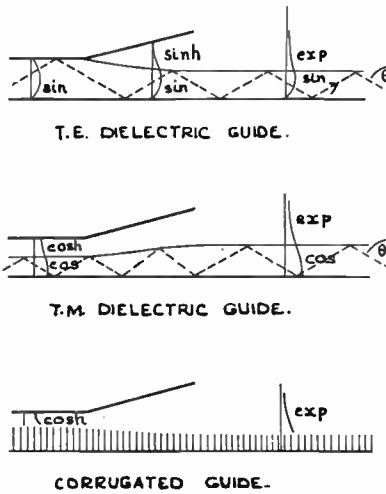


Fig. 1

In the diagrams the vertical amplitude variation of the component of field perpendicular to the paper, and the wave normal of the elementary criss-crossing plane waves in the dielectric are shown. The phase velocity in the dielectric guides is given by $c/n \sin \theta$, where c is the velocity of light, n is the refractive index of the dielectric, and θ is the angle between the wave normal of the elementary plane waves in the dielectric and the vertical. In the corrugated guide the angle of the elementary wave is complex, and the phase velocity is given by $c/\sin \phi$, where $\sin \phi = \sec 2\pi d/\lambda$, d being the depth of the slots outside the horn.

Experiments with the first system showed that if the horn was tapered gradually the radiation loss was very small indeed.

* Received by the IRE, September 26, 1955.

This letter is based on work done at the Telecommunications Research Establishment, Malvern, England, in 1946.

J. D. LAWSON
Atomic Energy Res. Establishment,
Harwell, England.

Noise Reduction in CW Magnetrons*

In two-way microwave systems operating in both directions simultaneously, the noise voltage in the receiver due to the local transmitter may well be as large as the received signal. The reduction of noise in transmitting tubes is thus highly desirable.

The rf output of self-excited oscillators in general, and of magnetrons in particular, is a function of the parameters of the power supply. Experiments have shown that this is usually true for the noise output too, specifically, that the fluctuations in anode current are usually correlated with the rf noise, which appears as modulation of a sinusoidal carrier wave.¹ Thus one expects that increasing the impedance of the power supply will reduce the noise output by reducing the anode current fluctuation.

The AM and fm noise modulations of the magnetron have been measured using a crystal video receiver; for fm detection, an off-tune resonant cavity acting as a microwave discriminator is included.² Several types of S- and X-band magnetrons have been tested; the figures illustrate the measurements on a typical RK5609, a 100-watt cw S-band tube, in which the carrier to noise ratio in the AM measurements is about 70 db.

Fig. 1 shows the power in the anode current fluctuations in the frequency band from 2 kc to a variable upper frequency limit

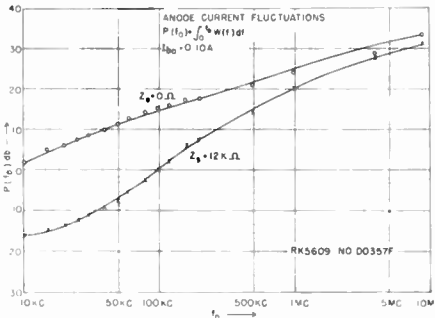


Fig. 1—Anode current fluctuations.

which appears as abscissa with either zero or twelve thousand ohms in the anode line. The unregulated noise output rises at 3 db per octave which is characteristic of white noise. The increased impedance reduces the amount of noise present by 15 to 18 db at low frequencies. Above 1 mc the regulation

¹ Received by the IRE, September 26, 1955.
² D. Middleton, W. M. Gottschalk, and J. B. Wiesner, "Noise in cw magnetrons," *Jour. Appl. Phys.*, vol. 24, pp. 1065-1066; August, 1953.

³ W. M. Gottschalk, "Direct detection measurements of noise in cw magnetrons," *TRANS. IRE, PGED*, vol. 1, no. 4, pp. 91-98; December, 1954.

becomes less effective and the noise again increases at 3 db per octave.

Fig. 2 shows the corresponding measurements on the AM noise. The noise reduction here follows that in the anode current as regards both amplitude and frequency. The narrow bandwidth of the microwave components eliminates the noise above a few megacycles per second.

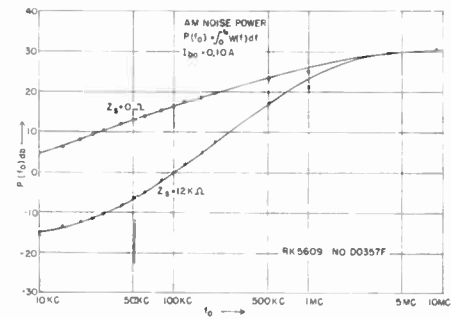


Fig. 2—AM noise power.

The fm measurements are shown in Fig. 3. The cavity which acts as discriminator is tuned above the frequency of the magnetron, which gives a noise output about 6 db greater than when the cavity is tuned below the magnetron. The frequency dependence of the regulated output is the same as for the anode current, but the maximum noise reduction is about 6 db less, for the high peak shown in the figure and about 12 db less for the low peak (not shown). In one tube type, no reduction of fm noise was possible, although the AM noise was reduced as usual.

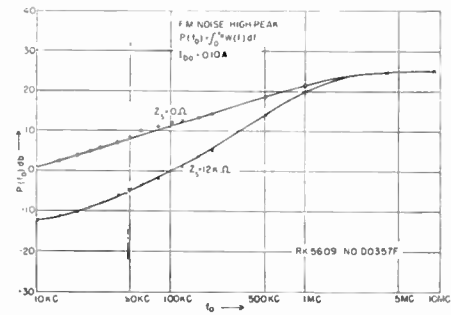


Fig. 3—FM noise high peak.

Correlation measurements showed that for these tubes the fm noise voltage was uncorrelated with the anode current fluctuations.

On approximately a dozen cw magnetrons, we have found that the AM noise output can be reduced by as much as 25 db and the fm noise output by 15 db by adding impedance in the anode line in order to reduce the anode current fluctuations.³

R. L. KRUEE
RCA Aviation Systems Lab.
Waltham, Mass.
J. A. MULLEN
Res. Div. Raytheon Mfg. Co.
Waltham, Mass.

This work was done entirely under the auspices of Research Division, Raytheon Manufacturing Co., Waltham, Mass.

Russian Vacuum-Tube Terminology*

The list of Russian terms given below is a continuation of several such lists of radio terms and circuit notations already published in these columns primarily for the benefit of engineers engaged in foreign-equipment evaluation.

As noted in a previous article the ordinary Russian word for tube is лампа (lampa) with трубка (trubka) reserved for special-

purpose tubes. In the present list of tube terms, it may be seen that two methods of noun modification are used in Russian: (1) an adjective, (2) a prepositional phrase introduced by the preposition *co* or *so* (with). For example, "glass tube" is expressed by (1) стеклянная лампа or (2) лампа со стеклянным баллоном (tube with glass envelope). Other examples of (2) are cold-cathode tube and hot-cathode tube which in Russian are literally "lamp with cold cathode" and "lamp with preheated cath-

ode," respectively. Russian has no word for oscillator, using simply "generator"; thus, oscillator tube is literally "generator tube." X-ray is rendered in Russian by "Rentgen," a transliteration from the German "Roentgen."

G. F. SCHULTZ
Indiana University
Bloomington, Ind.

* Received by the IRE, October 3, 1955.

all-metal tube	цельнометаллическая лампа
amplifier tube	усилительная лампа
cathode-ray tube	катодолучевая трубка
cold-cathode tube	лампа с холодным катодом
detector tube	детекторная лампа
dissector tube	диссекторная трубка
gas tube	газовая лампа (трубка)
gas-filled tube	газонаполненная лампа
general-purpose tube	универсальная лампа
glass tube	стеклянная лампа
high-vacuum tube	высоковакуумная лампа
hot-cathode tube	лампа с подогревным катодом
klystron	клистрон
magnetron	магнетрон
mercury-vapor tube	рутная лампа
metal-glass tube	металлическо-стеклянная лампа

mixer tube	смесительная лампа
multielectrode tube	многоэлектродная лампа
multiple-unit tube	многоизменная лампа
oscillator tube	генераторная лампа
oscillating tube	генерирующая лампа
phototube	фототрубка
power tube	мощная лампа
receiving tube	приемная лампа
rectifier tube	выпрямительная лампа
thermionic tube	термионная лампа
transmitting tube	передающая лампа
thyatron	тиратрон
twin-diode tube	сдвоенная диодная лампа
variable-mu tube	лампа "вари-му"
water-cooled tube	лампа с водяным охлаждением
X-ray tube	рентгеновская трубка

Contributors

For a biography and photograph of R. Adler, see p. 345 of the March, 1955 issue of PROCEEDINGS OF THE IRE.



J. R. Beattie was born in British Honduras in 1922. He was educated in Montrose, Scotland, and studied at St. Andrews University.



J. R. BEATTIE

He received a commission in the radar branch of the R.A.F. in 1942, and served in the United Kingdom and later with a mobile radar unit on the Continent.

At present, Mr. Beattie is a lecturer in the physics department of the University of Sheffield. His research studies are concerned mainly with the infra-red and the solid state.

Mr. Beattie is a member of the Physical Society of London.



R. Boxer was born on August 6, 1927, in New York, N. Y. He received the B.E.E. degree in 1949 from the Cooper Union and

the M.E.E. degree from Syracuse University in February, 1955.

From 1949 to 1950, Mr. Boxer was employed as a project engineer at the Wright Air Development Center, Dayton, Ohio.

Since 1950, he has been with the Rome Air Development Center, Rome, N. Y., engaged in the development of control systems involving aircraft and guided missiles. He is the author of several publications concerned with the analysis of air traffic control, fuel and aerodynamic characteristics, sampled data systems, and digital computers.

Mr. Boxer is an associate member of Sigma Xi.



For a biography and photograph of P. A. Clavier, see p. 345 of the March, 1955 issue of PROCEEDINGS OF THE IRE.



G. K. T. Conn was educated in Canada and at the Universities of Aberdeen and Cambridge in Great Britain.

He is presently a reader in the department of physics in the University of Sheffield.



G. K. T. CONN

In his research work, Dr. Conn has been investigating the application of optical techniques to the study of the solid state. He is also studying the mechanism of conduction in thin films and vacuum physics.

He is a fellow of the Physical Society of London, and the Cambridge Philosophical Society, and a member of the Faraday Society.



For a photograph and biography of C. C. Cut'er, see page 231 of the February, 1955 issue of the PROCEEDINGS OF THE IRE.



R. S. Duncan was born in New York City, N. Y. on October 19, 1911. He received the E.E. degree from Cornell University in

1933 and the S.M. in E.E. from Massachusetts Institute of Technology in 1935.

Since 1936 he has been a member of the technical staff of Bell Telephone Laboratories. He worked with a special group on the design of filters and networks until 1950. Since then he has been concerned with the design and development of inductors.

Mr. Duncan is a member of Tau Beta Pi, Eta Kappa Nu, and Phi Kappa Phi.

M. A. H. EL-SAID

This project was sponsored by the Marconi Wireless Telegraph Co. in England, and the General Radio Co. in the United States.

Since 1949, he has occupied the post of assistant professor of radio engineering at Cairo University, and was recently assigned by the National Research Council to investigate the geophysical prospection of underground water by radio methods.

R. W. George (A'31-SM'44) was born in Jamestown, N. D., on July 19, 1905. He received the B.S. degree in electrical engineering from Kansas State College in 1928. Since that time he has been with RCA.

At Riverhead, N. Y. he worked in the fields of high frequency propagation, measuring equipment, radio relays, and other phases of communications. He transferred to the David Sarnoff Research Center at Princeton, N. J. in 1951 where he has been concerned mostly with the development of electromechanical filters. He is a member of Sigma Xi.

T. Honma was born in 1923 in Yamagata-ken, Japan. He received his degree from Yamagata University in 1942 and



R. S. DUNCAN



M. A. H. EL-SAID

This project was sponsored by the Marconi Wireless Telegraph Co. in England, and the General Radio Co. in the United States.

Since 1949, he has occupied the post of assistant professor of radio engineering at Cairo University, and was recently assigned by the National Research Council to investigate the geophysical prospection of underground water by radio methods.



R. W. GEORGE

search Center at Princeton, N. J. in 1951 where he has been concerned mostly with the development of electromechanical filters.

He is a member of Sigma Xi.



T. HONMA

served in the armed forces during World War II.

After the war, Mr. Honma was a member of the research staff of the Matsuda Research Laboratory of Tokyo Shibaura Electric Co. His major field of work has been the study of microwave measurement and microwave relay systems.

Mr. Honma is a member of the Institute of Electrical Communication Engineers of Japan.



R. W. KLOPFENSTEIN

This project was sponsored by the Marconi Wireless Telegraph Co. in England, and the General Radio Co. in the United States.

Since 1949, he has occupied the post of assistant professor of radio engineering at Cairo University, and was recently assigned by the National Research Council to investigate the geophysical prospection of underground water by radio methods.

Dr. Klopfenstein is a member of Sigma Xi, Phi Kappa Phi, and the Mathematical Association of America.

For a biography and photograph of O. M. Kromhout, see p. 346 of the March, 1955 issue of *PROCEEDINGS OF THE IRE*.

K. Kurokawa was born on August 14, 1928, in Tokyo, Japan. He received the B.S. degree in electrical engineering from the University of Tokyo in 1951.

Since then, as a graduate student at the university, he has been engaged in research on microwave measurements. He was a participant in the Foreign Student Summer Project at the Massachusetts Institute of Technology in 1954.



K. KUROKAWA

Mr. Kurokawa is a member of the Institute of Electrical Engineers of Japan, and a member of the Institute of Electrical Communications Engineers of Japan.

Y. Matsuo was born on July 12, 1919, in Osaka, Japan. He was graduated from the electrical engineering department of Yonezawa Technical College in 1940, and joined Tokyo Shibaura Electric Co., Ltd.

From 1943 to 1945 he was engaged in the development of uhf tubes and radar techniques at the Naval Technical Institute. In 1945, Mr. Matsuo joined the physics department

of Osaka University where he is presently concerned with research in the development of uhf tubes.

Mr. Matsuo is a member of the Institute of Electrical Engineering and Electrical Communication of Japan.



Y. MATSUO

L. E. Miller was born on September 30, 1923. He received his B.S. degree in engineering physics from Lafayette College in 1949. He was a member of the technical staff of the Central Research Laboratory of General Aniline and Film Corp. from 1949 to 1952. During this period, his work was concerned primarily with the theory of the photographic process. His major efforts were physical-electronic instrumentation and measurements, and a consideration of solid-state physics in relation to formation of photographic latent image.

Mr. Miller became a member of the technical staff of Bell Telephone Laboratories in July, 1952, and has been concerned with the final development of semiconductor devices. He is a member of the American Physical Society.

For a biography and photograph of J. L. Moll, see p. 1978 of the December, 1955 issue of *PROCEEDINGS OF THE IRE*.

I. M. Ross was born in Southport, England, on August 15, 1927. He received the B.A. and M.A. degrees in engineering from

the University of Cambridge in 1948 and 1952. He received the Ph.D. degree from Cambridge in 1952 for an investigation of low-frequency noise in vacuum tubes and semiconductors.



IAN M. ROSS

Dr. Ross became a member of the technical research staff of Bell Telephone Laboratories in February, 1952, and since that time has worked in transistor physics and development.



S. SAITO

S. Saito was born on September 17, 1919, in Tokyo, Japan. He graduated from the electrical engineering department of the University of Tokyo in 1941. During World War II he was engaged in research on microwave radar for the Naval Technical Research Institute in Tokyo.

He returned to the University of Tokyo after the war, and was appointed as an assistant professor in 1947. In

1951, he received the Ph.D. degree from the University of Tokyo.

For his research on microwave measurements at the Institute of Industrial Science of the University, he was awarded the Akiyama and Shida Memorial Prize by the Institute of Electrical Communication Engineers of Japan, and the Hattori Hoko Prize from the Hattori Hoko Kai Foundation in 1953.

During the present academic year, he is studying at the Research Laboratory of Electronics of M.I.T. as a Fulbright research scholar. He is a member of the Institute of Electrical Engineers of Japan, and of the Institute of Electrical Communication Engineers of Japan.

N. Sawazaki was born in Wakayama-ken, Japan, on April 16, 1913. He graduated from Waseda University in 1938, and received the Ph.D. in engineering in 1952.

During the war he designed and developed radio altimeter and radar equipment in the Tokyo Shibaura Electric Co. Since the war, Dr. Sawazaki has engaged in studies connected with microwave measurement and microwave relay systems at the Matsuda Research Laboratory of Tokyo Shibaura Electric Co., in Kawasaki, where he is chief of research in communication.



N. SAWAZAKI

Dr. Sawazaki is secretary of the Institute of Electrical Communication Engineers of Japan, and a member of the Institute of Electrical Engineers of Japan.

❖

W. W. Siekanowicz (A'49-M'55) was born on January 3, 1928, in Poland. He received the B.S. degree in electrical engineering from the Imperial College of Science and Technology, London University, England, in 1948, and the M.S. degree in electrical engineering from Columbia University in 1950.



W. SIEKANOWICZ

He has been employed in the Tube Division of RCA at Harrison, New Jersey since July of 1950 and has specialized in the development of traveling-wave tubes.

Mr. Siekanowicz holds membership in Sigma Xi.

❖

Q. W. Simkins (S'49-A'50) was born on May 4, 1926, in Camden, N. J. He received the B.S.E.E. degree from Cornell University in 1949.



Q. W. SIMKINS

Since his graduation, Mr. Simkins has been a member of the technical staff of Bell Telephone Laboratories, where he has been engaged in the design of transistor and magnetic core digital computer circuits. He has also done research studies concerned with telephone switching systems and circuits.

Mr. Simkins is a member of Eta Kappa Nu, and Tau Beta Pi.

❖

F. Sterzer was born in Vienna, Austria, on November 18, 1929. He received the B.S. degree in physics from the City College of New York in 1951,



F. STERZER

and the M.S. and Ph.D. degrees in physics from New York University in 1952 and 1955, respectively.

He worked for the Allied Control Co. in New York City from 1952 to 1953. During the school year of 1953 to 1954 he was an instructor in physics at the Newark College of Engineering in Newark, N. J., and a research assistant

at New York University working on microwave spectroscopy. He joined the Tube Division of RCA in Harrison, N. J., in October, 1954. His work with the microwave tube advanced development activity is concerned primarily with traveling-wave tubes and backward-wave oscillators.

Dr. Sterzer is a member of Phi Beta Kappa, Sigma Xi, and the American Physical Society.

❖

H. A. Stone, Jr. (A'54) was born in New York City, N. Y. on July 7, 1909. He received the B.S. degree in physics from Yale in 1933.



H. A. STONE, JR.

Mr. Stone joined the Bell Telephone Laboratories in 1936. Until 1953, he was engaged in the design of inductors. From 1953 to the present he has been components development engineer for Bell Telephone Laboratories in charge of an organization devoted to the development of inductors, capacitors, and resistors. He is a member of AIEE.

❖

S. Thaler was born on June 17, 1917, in New York, N. Y. He received the B.E.E. from the College of the City of New York in 1940. From 1940 to 1948, he was with the Signal Corps.



S. THALER

Since 1948, Mr. Thaler has been at the Rome Air Development Center in Rome, N. Y. where he has engaged in the development of digital tracking devices.

He is an associate member of the American Institute of Electrical Engineers, as well as IRE.

❖

J. H. Vogelsong (M'54) was born on October 30, 1925, in York, Pa. In 1949, he received the B.S. degree in electrical engineering from Lehigh University.



J. H. VOGELSONG

Since his graduation, he has been a member of the technical staff of Bell Telephone Laboratories. He has been engaged in the design of digital computer circuits, and is currently working on a military communications study.

Mr. Vogelsong is a member of Phi Beta Kappa, Tau Beta Pi, and Eta Kappa Nu.

IRE News and Radio Notes

ANNUAL AWARDS FOR 1956 ARE ANNOUNCED BY THE IRE

F. J. Bingley, color television research engineer of the Philco Corp., has been named to receive the Vladimir K. Zworykin Television Prize Award for 1956 for his contributions to colorimetric science as applied to television. The award is made annually for outstanding contributions to electronic television.

The Browder J. Thompson Memorial Prize for 1956 was awarded to J. E. Bridges, research engineer of the Zenith Radio Corp., for his paper entitled "Detection of Television Signals in Thermal Noise," which appeared on page 1396 of the September, 1954 issue of the PROCEEDINGS OF THE IRE. The award is made annually to an author under thirty years of age at date of submission of manuscript for a paper recently published by the IRE which constitutes the best combination of technical contribution and presentation of the subject.

The awards will be presented during the IRE National Convention in New York City, March 19-22.

IRE NATIONAL CONVENTION SET FOR MARCH 19-22

On Monday, March 19, New York City will be the focal point of the engineering world when the 1956 IRE National Convention gets underway. Over 40,000 engineers and scientists are expected to be on hand as a full four-day program of sessions, exhibits, and social events unfolds at the Waldorf-Astoria Hotel and Kingsbridge Armory.

The convention will start at 10:30 Monday morning with the Annual Meeting in the Waldorf's Grand Ballroom. This meeting is held especially for members to meet their officers and hear them discuss current plans and activities of the IRE. The program will feature a well-known speaker who will discuss a subject of interest to all engineers.

A comprehensive program of fifty-five technical sessions and professional group symposia is being prepared by the Technical Program Committee with the assistance of all twenty-four professional groups. The sessions will be held at the Waldorf-Astoria, nearby Belmont-Plaza, and at the Kingsbridge Armory. The highlight of the program will be a special Tuesday evening session devoted to Space Satellites. Full details of the program will be announced in the March issue of the PROCEEDINGS.

Plans are being made to publish again the *IRE Convention Record*. It will contain all available papers presented at the convention.

The Radio Engineering Show this year will comprise over 700 exhibits, covering almost every conceivable new development in radio and electronic equipment, materials, and techniques. To accommodate this display, approximately 100 exhibits will be located in the Kingsbridge Palace, just a block

and a half from the Kingsbridge Armory. Free and continuous bus service will be provided between the Armory and Waldorf-Astoria for the convenience of convention registrants.

The social activities will get underway Monday evening with a "get-together" cocktail party in the Grand Ballroom of the Waldorf. Climax of the convention will be the Annual Banquet, which this year will feature a speaker of national importance. Also on the program will be presentation of the IRE Awards for 1956 by A. V. Loughren, President.

An attractive and entertaining program is being planned for the wives of members. Visits to a famous art gallery, a leading department store, and West Point are included, as well as a luncheon-fashion show, matinees at Broadway plays, and a sightseeing tour of New York. The center for women's activities will be located in the Regency Suite on the fourth floor of the Waldorf-Astoria.

NEW IRE MILITARY ELECTRONICS PROFESSIONAL GROUP FORMS

The Professional Group on Military Electronics recently formed an active new group.

IRE members interested in joining it should contact J. Q. Brantley, Jr., Membership Committee Chairman, Cornell Aeronautical Laboratory, Buffalo Airport, New York. Any persons interested in starting chapters in their area should contact E. A. Speakman, Guided Missiles Division, Fairchild Engine and Aircraft Corporation, Wyandanch, L. I., New York.

OFFICERS ELECTED FOR 1956

At its meeting on November 2, 1955, the Board of Directors announced the election of the following IRE officers and directors:

President, 1956: Arthur V. Loughren, Hazeltine Corporation, Little Neck, Long Island.

Vice-President, 1956: Herre Rinia, Philips Research Laboratories, Eindhoven, Holland.

Directors-Elected-at-Large, 1956-1958: E. W. Herold, Radio Corporation of America, Princeton, New Jersey; J. R. Whinnery, University of California, Berkeley, California.

Regional Directors, 1956-1957: Region One, C. R. Burrows, Cornell University, Ithaca, New York; Region Three, J. G. Brainerd, University of Pennsylvania, Philadelphia, Pennsylvania; Region Five, J. J. Gershon, DeVry Technical Institute, Chicago, Illinois; Region Seven, C. F. Wolcott, Gilfillan Brothers, Inc., Los Angeles, California.

Calendar of Coming Events

IRE-ASQC Second National Symposium on Reliability and Quality Control, Hotel Statler, Washington, D. C., Jan. 9-10

IRE National Simulation Symposium, Dallas, Tex., Jan. 19-21

AIEE Winter General Meeting, Hotel Statler, New York City, Jan. 30-Feb. 3

IRE Symposium on Microwave Theory and Techniques, U. of Pennsylvania, Philadelphia, Pa., Feb. 2-3

Western Computer Conference, Fairmont Hotel, San Francisco, Calif., Feb. 8-10

IRE Annual Southwestern Conference, Oklahoma City, Okla., Feb. 9-11

Annual Banquet of Washington Section, Hotel Statler, Washington, D. C., Feb. 11

IRE-AIEE-U. of P. Conference on Transistor Circuits, U. of Pennsylvania, Philadelphia, Pa., Feb. 16-17

IRE-AIEE Scintillation Counter Symposium, Shoreham Hotel, Washington, D. C., Feb. 28-29

IRE National Convention and Radio Engineering Show, Waldorf-Astoria Hotel and Kingsbridge Armory, New York City, Mar. 19-22

PGIE-AIEE-ISA Conference on Magnetic Amplifiers, Syracuse, N. Y., Apr. 5-6

Seventh Regional Technical Conference and Trade Show, Hotel Utah, Salt Lake City, Utah, Apr. 11-13

Tenth Annual Spring Television Conference of the Cincinnati Section, Engineering Society of Cincinnati Building, Cincinnati, Ohio, Apr. 13-14

New England Radio Engineering Meeting, Sheraton Plaza Hotel, Boston, Mass., Apr. 23-24

PGCT-PIB Symposium on Non-linear Network Theory, Engineering Society Building, New York City, Apr. 25-27

URSI Spring Meeting, National Bureau of Standards, Washington, D. C., Apr. 30-May 3

IRE-RETMA-AIEE-WCEMA Electronic Components Symposium, U. S. Department of Interior, Washington, D. C., May 1-3

National Aeronautical and Navigational Conference, Hotel Biltmore, Dayton, Ohio, May 14-16

JOHN V. N. GRANGER WINS 1955 REGIONAL AWARD

John V. N. Granger, a Senior Member of IRE, was presented recently with the 1955 Regional Electronics Achievement Award at WESCON in San Francisco. Joseph M. Pettit, Director of IRE Region 7, presented this annual regional award for recognition of contributions to electronics to Dr. Granger.

Dr. Granger is assistant chairman of the Engineering Department and head of the Aircraft Radiation Systems Laboratory at Stanford Research Institute, Palo Alto, California. He is also a civilian member of the Panel on Antennas and Propagation, Committee on Electronics, Research and Development Board, and since 1951 he has been Chairman of the Subpanel on Airborne Antennas.



J. M. Pettit (right), Director of IRE Region Seven, congratulates J. V. N. Granger, award recipient.

Prior to 1949 and his coming to SRI, Dr. Granger was a Research Fellow in electronics and group leader of the Antenna Group at the Electronics Research Laboratory, Harvard University. He obtained the A.B. degree in mathematics from Cornell College, the M.S. degree in communications engineering, and the Ph.D. degree in applied physics from Harvard University.

Dr. Granger is retiring Chairman of the Palo Alto Subsection and Editor of the *IRE Transactions on Aeronautical and Navigational Electronics*. In 1951 he was Chairman of the Technical Program Committee at the IRE West Coast Convention. He is a member of Sigma Xi, the American Physical Society, and Commission VI of the U. S. National Committee of the International Scientific Radio Union.

TENTH SPRING TELEVISION CONFERENCE WILL BE IN APRIL

The Tenth Annual Spring Television Conference, sponsored by the Cincinnati Section of the IRE, will be held on Friday and Saturday, April 13 and 14, at the Engineering Society of Cincinnati Building, 1349 East McMillan St., Cincinnati, Ohio.

Requests for advertising and exhibition privileges should be referred to Arthur B. Ashman, Cincinnati and Suburban Bell

Telephone Company, 225 East Fourth Street, Cincinnati 2, Ohio. Information concerning advance registration or hotel reservations may be obtained from Reuben Nathan, Crosley Division, Avco Mfg. Corporation, Glendale-Milford Road, Everdale, Ohio. Information on other matters may be obtained from Stanley M. Stuhlbarg, Chairman of Publicity Committee, Crosley Division, Avco Mfg. Corporation, 4890 Spring Grove Avenue, Cincinnati 32, Ohio.

SOUTHWESTERN CONFERENCE AND SHOW MEETS AT OKLAHOMA CITY

Oklahoma City, with its central location and proximity to the Air Force's largest procurement, supply, and maintenance depot, the Civil Aeronautic Authority's world-wide training center, the educational plants of the University of Oklahoma and Oklahoma City University, and the petroleum industry, is the site of this year's Southwestern Regional Conference and Electronics Show which will be held February 9-11.

At Oklahoma City's Municipal Auditorium the Zebra Room has been engaged for the Electronics Show with space for over 100 exhibit booths. Adjoining wings will be fitted and fixtured to provide an appropriate atmosphere for presentation of the technical program. At the Skirvin Tower Hotel space and facilities are being arranged for special meetings and gatherings. The Persian Room has been reserved for the banquet which will feature the social side of the conference. This hotel and others in the vicinity will be holding a large number of rooms open for reservation by out-of-town guests.

This event, representative of the Southwest's interest in the field of electronics, now goes into its eighth consecutive year. Instituted in 1949 by the Dallas-Fort Worth Section, it has since gained greater regional import through a policy of rotating showings among major cities of the Southwest.

Technical papers will be presented Thursday afternoon, Friday morning and afternoon, and Saturday morning and afternoon. Paper subjects will be grouped according to the technical group divisions, and papers have been received to give a comparatively complete coverage. A partial list of titles and authors of papers which have been accepted follows.

Characteristics of Reflex Klystrons in Communications Systems, Marion P. Hobgood, Philco Corporation; *Multi-Megawatt Klystron Radar Transmitters*, John Bushy, Sperry Gyroscope Company; *Color Telecasting*, J. L. Hathaway, National Broadcasting Company; *High Stability LC Oscillator for Use with a Capacitive Sensing Element*, A. J. Eldridge, Sandia Corporation; *Precision Voltage Calibrator Circuit*, R. E. McCallum, Sandia Corporation; *The Omnidirectional Antenna: an Omnidirectional Waveguide Array for UHF-TV Broadcasting*, O. M. Woodward, Jr. and James Gibson, RCA Laboratories; *The Use of Transmission Line Charts in Circuit Analysis*, H. F. Mathis, Goodyear Aircraft Corporation; *A Directional Glide Path System*, Lawrence Spinner, CAA; *Use of Finite Difference Operators to Determine the Poles and Zeros of a Network*, J. P. Lind-

sey, Phillips Petroleum Company; *Semiconductors Devices*, K. D. Smith, Bell Telephone Laboratories; *Forward Scattering, TACAN Air Navigation System*, Federal Telecommunication Laboratories; *Engineers and Computers*, W. B. Lewis, Boeing Airplane Company; *Application of Flying Spot Scanners in Television*, by R. Deichert, DuMont Laboratories; *Correlation and Power Spectrum Analysis Techniques*, F. E. Brooks, Jr. and H. W. Smith, University of Texas; *Electronics Logistics*, Col. D. B. Yount, Tinker Air Force Base; *Technique for the Simple Measurement of Extremely Small Amounts of FM on a Microwave Signal*, Hewlett-Packard Company.

Thursday morning sessions will be devoted to opening procedures and introductions, with registration desks operating continuously during the three days. A special address has been planned for Friday, entitled "Current Status of Color Television," by William B. Logde of CBS Television, New York. Mr. Logde will present, in connection with his address, a colored movie on television at CBS. The University of Oklahoma AIEE-IRE Joint Student Branch, under the leadership of Fritz Villines, plans to have one complete half day in which student papers may be presented by student branches in the region.

PGA COMMITTEE MEETS

The mid-year meeting of the Administrative Committee of the Professional Group on Audio was held coincidentally with the National Electronics Conference in Chicago, on October 4, 1955. Considerable attention was given to the question of increasing interest in Audio among IRE student members. A. B. Bereskin, of the University of Cincinnati, Editor of the *IRE Transactions on Audio*, was asked to study the various proposals made in this connection and to make recommendations to the Administrative Committee. The matter of establishing a PGA Student Award for outstanding papers on Audio by IRE student members was also discussed. This proposal was assigned for study to D. W. Martin, of Baldwin Piano Company, Chairman of the PGA Awards Committee.

Considerable attention was given to the question of standardization of systems and concepts dealing with "high fidelity" reproduction systems. After much discussion, the Administrative Committee agreed that the PGA is not in a position to promote standardization in this field. However, it was pointed out that a number of IRE standards exist which deal with measurement, terminology, and techniques of audio and these may be useful in the measurement of performance of various audio systems.

The Administrative Committee heard and approved the reports of A. B. Jacobsen, Motorola, Tapescripts Committee Chairman; Marvin Camras, Armour Research Foundation, Nominating Committee Chairman; D. W. Martin, Baldwin Piano Company, Awards Committee Chairman; and P. B. Williams, Jensen Mfg. Co., Program Committee Chairman. Committee budgets were approved.

Consideration was given to the participation of the PGA on the contemplated Acoustical Standards Board.

KANSAS CITY SECTION PLAYS HOST TO IRE BOARD OF DIRECTORS AT ANNUAL ELECTRONICS CONFERENCE

Right—(left to right): D. J. Tucker, Director of Region Six, G. W. Bailey, IRE Executive Secretary, and A. W. Graf, former Director of Region Five, were among those attending a reception for the IRE Board of Directors at the Kansas City Section IRE Conference.



Below—Incoming IRE President, A. V. Loughren (left) and his predecessor, J. D. Ryder (right) are shown chatting with Arthur B. Eisenhower, Kansas City bank official and brother of President Eisenhower, during the Kansas City Section IRE Conference.



Below—Toastmaster R. W. Fetter, Aeromotive Equipment Corp., and Chairman of the IRE Kansas City Section, was host to IRE officers and directors at the banquet. Seated with Mr. Fetter are (left to right): Mrs. R. W. Fetter, Mrs. V. M. Mathews, and V. M. Mathews, chairman of the conference.



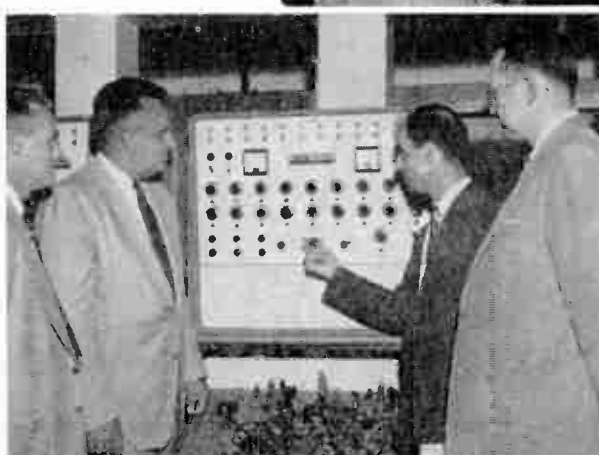
Below—High point of the conference was a banquet held at the Towne House Hotel in Kansas City, Kansas. Shown at the banquet head table are (left to right): Conference Vice-Chairman W. H. Ashley, Jr., Wilcox Electric Co.; Mrs. W. H. Ashley, Jr.; 1956 IRE President, A. V. Loughren, Hazeltine Corp.; 1955 IRE President, J. D. Ryder, Michigan State University; and the guest speaker, H. W. Wells, Carnegie Institution of Washington, D. C., whose address to the conference was entitled "Radio Astronomy."



ACTIVITIES OF IRE SECTIONS AND PROFESSIONAL GROUPS



Above—PGAP co-sponsored a recent Symposium on Radio Astronomy at Chicago. Participants in the panel discussion "Radio Astronomy Enlarges the Observable Universe," at the National Electronics Conference, Chicago, were (left to right): H. J. Ewen, Harvard University; R. C. Spencer, Air Force Cambridge Research Center; L. Berkner, Chairman, Associated Universities, Inc.; H. W. Dodson, McMath-Hulbert Observatory, Univ. of Michigan, and F. T. Haddock, Jr., Naval Research Laboratory.



Above—On a recent visit to Akron, Ohio, to address the local IRE Section, J. D. Ryder (second from left), past president of the IRE, examines L-3 GEDA computer at Good-year Aircraft as C. O. Lambert (left), H. L. Flowers (second from right), and H. F. Lanier (right) of the Akron Section watch.

(Above, left)—Lt. Col. H. C. Williams (left), Program Chairman, and R. O. Burns (right), Chairman of the Fort Huachuca Subsection, chat with T. L. Martin, Jr., University of Arizona, after he addressed the subsection at a fall meeting on the effects of cosmic rays and atmospheric electricity upon the human body.

This is the first of a new series of picture pages in our new program of reporting more fully the activities of the Professional Groups and Sections. With this expansion of the IRE NEWS AND RADIO NOTES section comes an opportunity for all Professional Groups and Sections to publicize activities of special national interest. News of IRE officers' visits, conferences, banquets, award ceremonies, and publications serve to keep the general membership informed of current activities.

Below—A. V. Loughren (right), 1954 award winner, congratulates L. M. Clement, 1955 recipient of the RETMA Radio Fall Meeting plaque "for his effective initiation and conduct of important activities in the field of reliability of electronic equipment and for his long time contributions to the work of the RETMA Engineering Department."



Below—At a recent dinner the North Carolina-Virginia Section installed Piedmont Subsection Officers. (left to right) E. W. Johnson, Subsection Secretary-Treasurer; C. M. Smith, Jr., Subsection Vice-Chairman; W. A. Welsh, Subsection Chairman; M. J. Minor, Section Vice-Chairman; G. B. Hoadley, Past Section Chairman, and A. L. Com-



OVER 1000 ATTEND PGANE ANNUAL CONFERENCE

The Second Annual East Coast Conference on Aeronautical and Navigational Electronics, sponsored jointly by the Baltimore Section of the IRE and the Professional Group on Aeronautical and Navigational Electronics, was held at the Lord Baltimore Hotel, Baltimore, Maryland, October 31 and November 1.

A highlight of the conference was a panel discussion of the design features required for military and civilian airborne equipment. Panel members were: Norman Caplan, Bendix Radio Division, Bendix Aviation Corporation; J. C. McElroy, Collins Radio Corporation; A. R. Applegarth, National Aeronautical Corporation; W. F. Carnes, Jr., Aeronautical Radio, Inc.; Ludlow Hallman, Wright Air Development Center; Max Karant, Aircraft Owners and Pilots Association; A. B. Winick, Bureau of Aero-

nautics; G. W. Church, Bendix Radio Division, Bendix Aviation Corporation; and Lt. Col. J. L. Wilson, Jr., Signal Corps.

F. W. Godsey, manager of the Baltimore Division of Westinghouse Electric Corporation, served as toastmaster at the conference banquet. Gustave Eckstein, physiologist and author, gave an address entitled "At Arm's Length," on the importance and significance of the human hand.

Responsible for the success of the Second Annual East Coast Conference on Aeronautical and Navigational Electronics were C. F. Miller, Chairman of the Baltimore Section; E. A. Post, Chairman of the Professional Group on Aeronautical and Navigational Electronics; C. D. Pierson, Conference Chairman; J. General, Conference Vice-Chairman; and S. Hershfield, Publicity Chairman.



Above: A modern exhibit. More than a thousand engineers and scientists registered at the conference. Thirty-eight papers covering a variety of subjects were presented and forty-two exhibitors showed their products.



Above—Scientists and engineers from military and civil organizations appearing as panel members were (left to right): Norman Caplan, Moderator, J. C. McElroy, G. W. Church, Max Karant, A. Rufus Applegarth, William F. Carnes, Jr., Ludlow Hallman, Alexander E. Winick, and Lt. Col. John L. Wilson.



At conference banquet were (below, left to right): C. F. Miller, Chairman of Baltimore Section; J. General, Conference Vice-Chairman; Capt. A. C. Packard, Bureau of Aeronautes; K. C. Black; C. D. Pierson; G. Eckstein, Speaker; F. W. Godsey, Jr., Westing-

house Electric Corp., Toastmaster; Col. G. J. Urban, Signal Corps; E. A. Post; Lt. C. T. K. Trigg, Signal Corps; N. Caplan; Lt. Col. J. L. Wilson, Jr., Signal Corps; and Hallman, Wright Air Development Center, Wright-Patterson Air Force Base.



1955 IRE PRESIDENT TOURS COUNTRY



Above: Dr. Ryder was the principal speaker at a recent meeting of the Lubbock Section. *Left to right:* D. J. Tucker, Director of Region Six, Dr. Ryder, and H. A. Spuhler, Lubbock Section Chairman.



Below: Dr. Ryder is shown chatting with R. C. Webb (*left*), Vice-Chairman of the IRE, and Arlie Paige, Chairman of the A.I.E.E. Section, at the joint dinner meeting of the Denver Sections of IRE and A.I.E.E.



Above: San Jose Mission was pointed out to J. D. Ryder, 1955 IRE President, on his visit to the San Antonio Section by Paul Tarrodaychik (*left*), Section Chairman.



Right: Dr. Ryder (*second from left*) journeyed on an experimental radar vessel from Montreal to Ottawa with (*left to right*) G. Glinski, Ottawa Section Chairman; B. G. Ballard, Director of the Radio and Electrical Engineering Division of the National Research Council; J. T. Henderson, Canadian IRE Regional Director; H. R. Smyth, captain of the vessel; and S. Bonneville, Montreal Section Chairman. Upon disembarking, Dr. Ryder addressed the Ottawa Section on the subject "Automatic Electronic Production."

NEWFOUNDLAND-LABRADOR SECTION GREETS RYDER

The Newfoundland-Labrador Section, which was officially recognized by the IRE on September 8, 1955, was visited by J. D. Ryder, former president of the IRE, on September 26, 1955. The Section has grown from a nucleus of Canadian and American engineers in September, 1953, when the first meeting was held, into a full Section.

When Dr. Ryder arrived by plane, he was met by E. D. Witherstone, Section Chairman, and Colonel J. A. MacDavid, Northeast Air Command. The following morning Dr. Ryder took part in a round table discussion at Armed Forces Radio Station VOUS which was recorded for later release on September 29. The formation of the new Section, the problem of the lack of engineers, and the impact of the IRE on the military were topics discussed. A luncheon followed, attended by members of the Executive Committee of the new Section. An informal discussion of the aims, structure, and organization of the IRE was held.

Dr. Ryder then visited Signal Hill, site of Marconi's first transatlantic radio communication.

He was guest of honor at a dinner in the Officers' Mess at Pepperrell Air Force Base on the evening of September 27. Civil and military officials attended the dinner, and the Newfoundland Minister of Mines and Resources brought greetings to the new Section from the Premier. Immediately after the dinner, Dr. Ryder presented the Charter of the Newfoundland-Labrador Section to its chairman, E. D. Witherstone. He also gave a short talk called "Automation in Printed Circuitry," and showed slides of IRE headquarters.

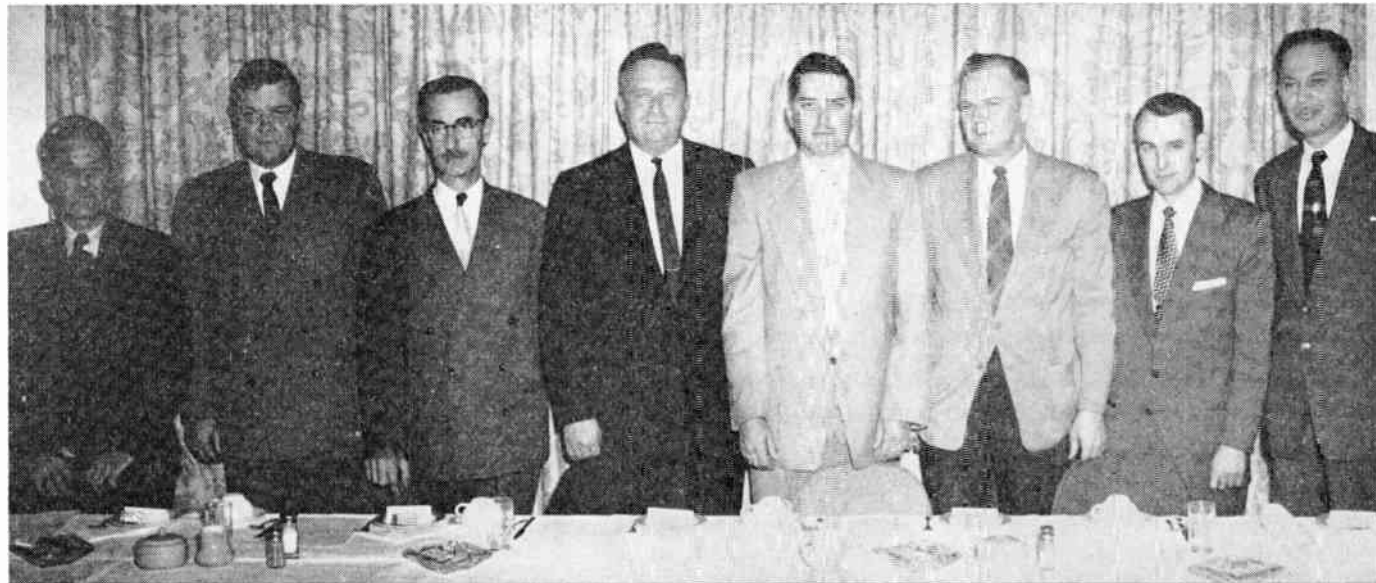


Above: J. D. Ryder (left), former president of the IRE, J. A. MacDavid (center), Northeast Air Command, and F. J. Schryer (right), Section Secretary, take part in a round table forum at Armed Forces Radio Station VOUS.



Above: D. B. Nowakoski (left), Section Vice-Chairman, and E. D. Witherstone (right), Section Chairman, are presented with the Charter of the Newfoundland-Labrador Section by 1955 IRE President J. D. Ryder.

Officers of the Newfoundland-Labrador Section honor Dr. Ryder at a dinner. Shown are (left to right): R. H. Bunt, Publicity; E. H. Schwarze, Meetings and Papers; E. D. Witherstone, Chairman; Dr. Ryder; D. B. Nowakoski, Vice-Chairman; J. B. Austin, Membership; F. J. Schryer, Secretary, and A. Jarrette, Meetings and Papers.



GUEST SPEAKERS ADDRESS PGED TECHNICAL MEETING AT WASHINGTON



Above: The luncheon speaker was D. G. Fink, who assessed the role of transistors and vacuum tubes today.



Right: L. M. Field described what has been done and what may come in the development of microwave tubes.



Below: (L.) Another speaker was J. A. Morton, whose topic was semiconductor devices. (R.) L. S. Nergaard gave an address on thermionic cathodes.



The Professional Group on Electron Devices held its first annual Technical Meeting at the Shoreham Hotel, Washington, D. C., October 24-25. Nearly nine hundred engineers attended the meeting at which more than fifty technical papers were presented, covering developments in microwave tubes, semiconductor devices, and non-microwave tubes.

The first day's program began with a general survey of trends in the development of electron devices. Three invited speakers, J. A. Morton of Bell Telephone Laboratories, L. S. Nergaard of RCA Laboratories, and L. M. Field of Hughes Aircraft Company presented papers on semiconductor devices, thermionic cathodes, and microwave tubes, respectively. At the luncheon which followed, D. G. Fink, Director of Research, Philco Corporation, spoke on the subject "Transistors vs. Vacuum Tubes," and told of the promise of a million-hour transistor. For the rest of the meeting, the engineers separated to hold simultaneous sessions on microwave tubes, semiconductor devices, and non-microwave tubes.

Chairman of the General Committee was G. D. O'Neill. The rest of the committee was composed of G. A. Esperson, Vice-Chairman; R. R. Law, Technical Program; H. L. Thorson, Secretary; G. W. Griffin, Jr., Public Relations; and J. S. Saby, Publication. The Local Arrangements Committee was headed by T. M. Liimatainen. Others on his committee were J. H. Wright, Vice-Chairman; R. I. Cole, Treasurer; A. L. Milk, Publicity; C. R. Knight, Hotel; H. D. Arnett, Registration; R. R. Grantham, Local Program; and H. J. Peake, Audio-Visual.

Papers presented at this meeting and available for publication will be published in a forthcoming issue of *Transactions of the IRE*, Professional Group on Electron Devices.



Below: Scientists and engineers gathered for luncheon at Shoreham Hotel, Washington, D. C., during the two-day Technical Meeting of the Professional Group on Electron Devices



7500 ATTEND 1955 NATIONAL ELECTRONICS CONFERENCE

Approximately 7,500 registrants participated in the eleventh National Electronics Conference held recently in Chicago, Illinois.

The conference was sponsored by the American Institute of Electrical Engineers, Illinois Institute of Technology, the IRE, Northwestern University and University of Illinois, with Michigan State University, Purdue University, University of Michigan, University of Wisconsin, Radio-Electronics-Television-Manufacturers Association, and Society of Motion Picture and Television Engineers participating.

The conference presented a diversified technical program with over 100 papers and 186 exhibit booths. All papers presented at the conference are being published in Volume 11 of the *Proceedings of the National Electronics Conference*.

A. V. Astin, Director, National Bureau of Standards, Washington, D. C. was the speaker at the first day's luncheon with his talk "Standards for Electronics." At this luncheon the second National Electronics Conference Award was made to A. W. Friend for his contribution to the electronics field through his comprehensive paper "The Use of Powered Iron in Television Deflecting Circuits" presented at the 1946 conference. At the second day's luncheon J. M. Robson, Research Physicist, Atomic Energy of Canada, Ltd., Chalk River, Ontario, Canada discussed "The Canadian Nuclear Reactor Accident." The last day's luncheon address "Uniform Confusion or Diverse Regimentation" was given by Ernst Weber, Director, Microwave Research Institute, Polytechnic Institute of Brooklyn, Brooklyn, N. Y. Another feature of this luncheon was the honoring of H. H. Beverage, Director of Radio Research of the RCA Laboratories, and L. N. McClellan, Assistant Commissioner, and Chief Engineer of U. S. Bureau of Reclamation as Eminent Members of Eta Kappa Nu.

Officers of the 1955 National Electron-

Below: H. H. Beverage, Director of Radio Research at RCA, was honored as an Eminent Member of Eta Kappa Nu, an honorary engineering organization.



ics Conference were: *President*, O. I. Thompson, DeVry Technical Institute; *Executive Vice-President*, R. R. Jenness, Northwestern University; *Chairman of the Board of Directors*, G. E. Aner, University of Illinois; *Executive Secretary*, J. S. Powers, Bell and Howell Company; *Secretary*, C. G. Miller, Weston Electrical Instrument Company; *Treasurer*, J. H. Enenbach, Illinois Bell Telephone Company; *Assistant Treasurer*, H. H. Brauer, Bell and Howell Company; *Arrangements Committee Chairman*, J. J. Walovich, General Transformer Company; *Awards Committee Chairman*, J. D. Ryder, Michigan State University; *Exhibits Committee Chairman*, G. J. Argall, DeVry Technical Institute; *Housing Committee Chairman*, A. J. Hoehn, Armour Research Foundation; *Party Committee Chairman*, W. R. Brock, Columbia Broadcasting System; *Procedures Committee Chairman*, G. T. Flesher, Illinois Institute of Technology; *"Proceedings" Committee Chairman*, G. E. Happell, Purdue University; *Program Committee Chairman*, G. Hok, University of Michigan; and *Publicity Committee Chairman*, J. Kocik, Illinois Bell Telephone Co.

Directors of the conference were: *Chairman*, G. E. Aner, University of Illinois, Urbana, Ill.; A. D. Bailey, University of Illinois, Urbana, Ill.; C. E. Barthel, Jr., Armour Research Foundation, Chicago, Ill.; R. R. Batcher, Hudson Wire Company, New York, N. Y.; H. H. Brauer, Bell and Howell Company, Chicago, Ill.; J. M. Cage, Purdue University, Lafayette, Ind.; M. H. Crothers, University of Illinois, Urbana, Ill.; J. H. Enenbach, Illinois Bell Telephone Co., Chicago, Ill.; G. T. Flesher, Illinois Institute of Technology, Chicago, Ill.; G. W. Goelz, Northwestern University, Evanston, Ill.; A. W. Graf, Patent Lawyer, Chicago, Ill.; A. J. Hoehn, Armour Research Foundation, Chicago, Ill.; Gunnar Hok, University of Michigan, Ann Arbor, Mich.; R. R. Jenness, Northwestern University, Evanston,



Above: O. I. Thompson of DeVry Technical Institute, Chicago, Illinois, presided over the 1955 National Electronics Conference.

Ill.; C. W. McMullen, Northwestern University, Evanston, Ill.; H. L. Messerschmidt, Western Electric Co., Inc., Chicago, Ill.; C. G. Miller, Weston Electrical Instrument Co., Chicago, Ill.; J. S. Powers, Bell and Howell Company, Chicago, Ill.; E. A. Roberts, Armour Research Foundation, Chicago, Ill.; K. E. Rollefson, The Muter Company, Chicago, Ill.; J. D. Ryder, Michigan State University, East Lansing, Mich.; E. H. Scheibe, University of Wisconsin, Madison, Wis.; J. C. Schuder, Purdue University, Lafayette, Ind.; R. M. Soria, American Phenolic Corporation, Chicago, Ill.; G. W. Swenson, Jr., Michigan State University, East Lansing, Mich.; O. I. Thompson, DeVry Technical Institute, Chicago, Ill.

Below: The second National Electronics Conference award went to A. W. Friend for his contribution to the electronics field through a paper presented at a previous conference.

Below: L. N. McClellan, Assistant Commissioner and Chief Engineer of the U. S. Bureau of Reclamation, was also honored as an Eminent Member of Eta Kappa Nu.





Left to right: W. D. Lewis, Bell Tel. Labs., Treasurer; J. G. Brainerd, Univ. of Penna., General Committee Chairman; J. Forrester, Digital Computation Lab., M.I.T.; and F. M. Verzuh, M.I.T., Local Arrangements Committee Chairman.

HOTEL STATLER, BOSTON WAS SCENE OF FIFTH EASTERN JOINT COMPUTERS CONFERENCE

The theme of the Fifth Eastern Joint Computers Conference, held November 7-9, was "Computers in Business and Industrial Systems." *Computers in Basic Business Applications* by F. J. Porter, *Operations Control with an Electronic Computer* by B. F. Butler, *The Place of the Special Purpose Electronic Data Processing Systems* by R. E. Sprague, *Electronics in Financial Accounting* by B. J. Bennett, K. E. Eldridge, T. H. Morris, J. D. Noe, and O. W. Whitby, *Manual Use of Automatic Records* by Anthony Oettinger, *Evaluation of Sorting Methods* by J. C. Hosken, *Document Processing* by R. H. Gregory, *Original Documents in Retail Accounts Receivable* by V. H. Roman, *The Computer and Its Peripheral Equipment* by N. Rochester, *Computers with Remote Data Input* by E. L. Fitzgerald, *Developments in Programming Research* by C. W. Adams, *Storage and Retrieval of Information* by L. N. Ridenour, *The Role of Communications Networks in Digital Data Systems* by R. C. Matlack, and *Standardization of Computer Intercommunication* by H. R. J. Grosch were presented at the conference.

Guided inspection trips were made to see the Mark I and Mark IV computers at Harvard Computation Laboratory, the Whirlwind Computer at M.I.T. Computation Laboratory, and several high speed printers at ANelex Corporation.

On the general committee in charge of the conference were J. G. Brainerd, Chairman; H. Mitchell, Jr., Secretary; W. D. Lewis, Treasurer; Irven Travis, Program; and N. P. Edwards, Publications. Members of the local arrangements committee include F. M. Verzuh, Chairman and Secretary; R. H. Gregory, and W. J. Oliphant, Finance; W. A. Johnson and Carl Reynolds, Registration; F. E. Heart and P. R. Bagley, Hotel Arrangements; R. C. Kelner and A. Oettinger, Inspection Trips; H. I. Cohen, and M. A. Meyer, Exhibits; J. C. Hosken and Laurence Rosenfeld, Publicity; and D. T. Ross, Robert Kramer and Robert Leonard, Printing.

Copies of the proceedings of the confer-

ence are being sent to full-fee registrants. Non-registrants may obtain copies of the proceedings from the headquarters of the IRE, the American Institute of Electrical Engineers, or the Association for Computing Machinery.

SECOND SYMPOSIUM ON RELIABILITY & QUALITY CONTROL WAS HELD EARLY THIS MONTH

The Second National Symposium on Reliability and Quality Control in Electronics was held at the Hotel Statler, Washington, D. C., January 9-10.

The symposium was sponsored by the Professional Group on Reliability and Quality Control. The Electronics Division of the American Society for Quality Control and the Staff Committee on Acceptance Procedures of the Radio-Electronics-Television Manufacturers' Association were co-sponsors.

A feature of the symposium was the luncheon on January 10th, at which Trevor Gardner, Assistant Secretary of the Air Force, spoke on "Security and Progress in National Defense."

Seventeen papers were presented. A joint Symposium on Precision Resistors was held with the Washington, D. C. Section. A movie entitled "The Priceless Component" was also shown. On the following day there was a panel discussion, sponsored by the RETMA Quality Acceptance Procedures Committee, on "Acceptance Procedures—The Design, Specifications, and Standards Problem Facing the Industry." Participants in the discussion were: L. J. Jacobson, Chairman of the Quality Acceptance Procedures Committee; G. Bowler, Chairman of the Inspection Bulletin Subcommittee; A. Warsher, Chairman of the Inspection and Acceptance Practices Subcommittee; and E. Torkleson, Chairman of the Technical Liaison Subcommittee.

On the last day of the symposium a tour

World Radio History

was made of the wind tunnels, magnetic research area, and technical shop at the Naval Ordnance Laboratory, White Oaks, Maryland.

PGCT INVITES PAPERS ON SIGNAL THEORY

The IRE Professional Group on Circuit Theory is planning to devote the September, 1956 issue of its *Transactions* to the subject of signal theory. Papers on this subject, as outlined below, are invited for consideration.

Signal theory is defined as being concerned with developing useful descriptions for (a) dynamical observables (such as signals, messages, noise and disturbances) in physical systems, and (b) the transforming effects of system elements on the significant characteristics of observables.

The purpose of the issue is to explore the suggestion that signal theory provides (a) a unifying basis for the analysis and design of diverse physical systems found in communications, process control and other fields of modern technology, and (b) an extended content for circuit theory.

Contributions are invited which present new theoretical results in any branch of signal theory or examples of the application of any branch of signal theory to the solution of a specific practical problem. Manuscripts giving new theoretical results should identify clearly the underlying problem of signal theory that is being attacked. Manuscripts giving specific applications of signal theory should but briefly identify the underlying theoretical problem before describing the practical application.

Authors planning to submit manuscripts should contact the guest editor, Professor J. M. Ham, Department of Electrical Engineering, University of Toronto, Toronto 5, Ontario, Canada. The deadline for all manuscripts is June 1.

CONVENTION MARKS THIRTIETH ANNIVERSARY OF IRE IN CANADA

The Canadian IRE Convention and Exposition will be held October 1-3, 1956, in the Automotive Building, Canadian National Exhibition Park, Toronto. The building is equipped with all facilities for convention and exhibition purposes and has unlimited parking space. A brochure giving complete details including floor plans and space rates will be mailed to prospective exhibitors. Copies are available from the convention manager, Grant Smedmor, 745 Mt. Pleasant Road, Toronto, Canada.

The exhibition will include a variety of products of industry and of allied fields such as instrumentation, laboratory apparatus, materials, and packaging. There will be displays of electronic equipment as used by all branches of the Canadian Armed Forces, and it is also expected that equipment relating to the industrial applications of atomic energy will be shown.

George Sinclair of the Department of Electrical Engineering, University of Toronto, Chairman of the Technical Papers Committee, has invited authors to submit titles and abstracts of 100-200 words on papers offered for presentation. The deadline for receiving titles and abstracts is May 31, 1956. The papers may be on any subject pertaining to radio or any allied field of interest to members of the IRE.

PARIS, FRANCE IS SITE OF INTERNATIONAL CONGRESS ON MICROWAVE TUBES

The International Congress on Microwave Tubes, organized by the Societe des Radioelectriens and the Societe Francaise des Ingenieurs Techniciens du Vide, will be held at the Conservatoire National des Arts et Metiers, Paris, May 29-June 2.

The purpose of this congress is to examine and discuss recent results in the field of microwave tubes. The term "microwave tubes" referred to here is used to mean radio tubes operating at frequencies above 500 mc; however, problems of special interest relating to tubes operating at lower frequencies may also be discussed. Due to the close analogy existing between certain particle accelerators and microwave tubes, questions concerning accelerators operating on frequencies above 500 mc will also be open to discussion. Papers presented will consist either of expository reports concerning developments, or of original work on specific problems. Each paper will be open to discussion.

Persons wishing to attend or to present papers should inform the Congres International Tubes Hyperfrequencies, S.F.I.T.V., 44 rue de Rennes, Paris 6, France, of their intention at an early date. Prospective authors should provide a summary, to be typewritten in either French or English and limited to thirty lines, containing the main points of the paper.

OBITUARY

Alva B. Clark (SM'46-F'56) died recently. He had retired last February as vice-president of Bell Telephone Laboratories after more than forty-three years with the Bell System. Since then he had been director of research and development in a sector of the United States Department of Defense.

During his career, Mr. Clark received forty-four patents for telephone devices and was an early leader in the development of basic communications systems, such as long-distance transmission of telephone, television and radio.

He directed the planning and engineering of the transcontinental coaxial cable and microwave radio relay systems for telephone and television transmission and earlier systems using the carrier principle of moving many messages simultaneously over one electrical pathway.



A. B. CLARK

More recently he directed the development of the direct dialing system for long-distance calls. He also guided the development of the automatic message accounting system, now used throughout the Bell system.

During World War II, he served as consultant or member of various divisions of the Office of Scientific Research and Development. In 1944, he was named consultant to the Secretary of War and made several trips to the Mediterranean and European zones of operation.

After graduation from the University of Michigan, he joined the American Telephone and Telegraph Company in 1911.

He worked in the engineering and then the development and research departments until 1934 when the latter division was consolidated with Bell Laboratories. With Bell, he was toll transmission development director and then director of transmission development.

In 1940, he assumed general direction of the laboratory work in telephone switching transmission and equipment development.

He became vice-president in 1944. From 1951 until his retirement, he was in charge of coordinating research between the laboratories, the American Telephone and Telegraph Company and Western Electric Co.

From 1938 to 1955, Mr. Clark was Bell System chairman of the Joint Subcommittee on Development and Research of the Edison Electric Institute and the Bell System.

He was a Fellow of A.I.E.E. and Acoustical Society of America, and a member of the American Association for Advancement of Science.

❖

Arnot P. Foster (A'41-M'45), President of the Foster Transformer Company in Cincinnati, Ohio, died recently after several months' illness at his home. Mr. Foster had attended Bethany College and the University of Cincinnati Evening College, receiving a degree in electrical engineering. After working briefly for the government, he joined the Crosley Radio Corporation in 1930 as a transformer design engineer. He continued at Crosley until 1940, when the transformer business which he had started in 1938 began to occupy his full attention.

Mr. Foster was an active supporter of the Spring Technical Conference on Television, sponsored by the Cincinnati Section of the IRE, from its beginning. He was also an active member of the Engineering Society of Cincinnati.

TECHNICAL COMMITTEE NOTES

The Navigation Aids Committee met at IRE Headquarters on October 21 with Chairman H. R. Minno presiding. The committee continued a discussion led by F. Moskowitz on the Proposed Standards on VHF Omni-Directional Radio Range (VOR). Discussion was directed primarily toward clarification of the purpose and recommended procedures. Numerous notes on the discussion were made for the guidance of an editorial group.

Chairman R. Serrell presided at a meeting of the Electronic Computers Committee on October 19. The major part of the meeting was devoted to discussing and amending the Proposed Standards on Electronic Computers: Definitions of Electronic Computers Terms. Following approval by Committee 8 of the Proposed Standards, a consolidated

list of the approved definitions to be designated as 55 IRE 8. PS1 will be prepared by L. C. Hobbs as soon as possible and submitted to the Definitions Coordinator of the Standards Committee.

Two new subcommittees were appointed. One of these subcommittees will be designated as "Subcommittee 8.7 on Computer Block Diagrams and Logical Symbols;" the other subcommittee, 8.8, will handle analog computer definitions and symbols.

The Circuits Committee convened on October 28 under the chairmanship of W. R. Bennett. The chairman conveyed word from T. R. Finch and V. G. Linville that the technical discussion held at the University of Connecticut, October 20 and 21 had been highly successful. However, some difficulties over terminology as applied to transistor circuits had appeared.

W. A. Lynch prepared a proposal for standardizing terminology and definitions on linear signal flow graphs. This field has become very important in feedback systems. The committee endorsed Prof. Lynch's suggestion that he ask E. J. Angelo to formulate a list of defined terms in this field with the help of W. A. Lynch, R. M. Foster and J. G. Truxal.

A revised list of feedback terms, 55 IRE 4.7 PS2, was presented by Chairman Lynch of Subcommittee 4.7, Linear Active Circuits and the remainder of the meeting was devoted to discussion of these terms.

The Radio Frequency Interference Committee met at IRE Headquarters on October 10 with Chairman R. M. Showers presiding. The chairman announced that RETMA Proposal S. P. 437 "Limits of Radiation from TV Broadcast Receivers between the Frequencies of 15 KC and 50 MC" was approved by the RETMA Standards Committee. M. S. Corrington, Chairman of Subcommittee 27.1, reported that the subcommittee, as requested by the main committee, reviewed the ASA C63.4 document informally. There are a number of items which require further consideration, and the subcommittee did not feel it was in a position to comment at the present time. The subcommittee is still working on the manual of good engineering practices. Dr. Showers requested Mr. Corrington to discuss the manual of good engineering practice with E. O. Johnson, chairman of the task force, and report to the committee a tentative date on which a draft of the document would be available. It was suggested that an outline of the manual be submitted as soon as possible. A. B. Glenn, Chairman of Subcommittee 27.3, reported that there is a task force of Subcommittee 27.3 investigating the problem of extending the range of measurement to 25 megacycles and rewriting where necessary the 1954 Standards. This task was assigned to Subcommittee 27.3. J. Minter, Chairman of Subcommittee 27.10, reported that there has been no activity on the part of his subcommittee. Dr. Showers suggested that a major item for the consideration of this subcommittee was the review of the ASA C63.4 proposal. This will be undertaken. H. E. Dinger, Chairman of Subcommittee 27.11, reported that there has been no activity in his subcommittee. The remainder of the meeting was devoted to a review of the revision of Standards on Television: Methods of Testing Television Receivers prepared by the Radio Receivers Committee.

Professional Groups^t

Aeronautical & Navigational Electronics—James L. Dennis, General Technical Films, 3005 Shroyer, Dayton, Ohio.

Antennas & Propagation—Delmer C. Ports, Jansky & Bailey, 1339 Wisconsin Ave., N.W., Washington 7, D.C.

Audio—W. E. Kock, Bell Tel. Labs., Murray Hill, N. J.

Automatic Control—Robert B. Wilcox, Raytheon Manufacturing Co., 148 California St., Newton 58, Mass.

Broadcast & Television Receivers—L. R. Fink, Research Lab., General Electric Company, Schenectady, N.Y.

Broadcast Transmission Systems—O. W. B. Reed, Jr., Jansky & Bailey, 1735 DeSales St., N.W., Washington, D.C.

Circuit Theory—H. J. Carlin, Microwave Res. Inst., Polytechnic Inst. of Brooklyn, 55 Johnson St., Brooklyn 1, N.Y.

^t Names listed are Group Chairmen.

Communications Systems—A. C. Peterson, Jr., Bell Labs., 463 West St., New York 14, N.Y.

Component Parts—A. W. Rogers, Comp. & Materials Branch, Squier Signal Lab., Ft. Monmouth, N.J.

Electron Devices—J. S. Saby, Electronics Laboratory, G.E. Co., Syracuse, N.Y.

Electronic Computers—J. H. Felker, Bell Labs., Whippny, N.J.

Engineering Management—Max Batsel, Engineering Products Dept., RCA Victor Div. Bldg. 10-7, Camden, N.J.

Industrial Electronics—George P. Bosomworth, Engrg. Lab., Firestone Tire & Rubber Co., Akron 17, Ohio

Information Theory—Louis A. DeRosa, Federal Telecommunications Lab., Inc., 500 Washington Avenue, Nutley, N.J.

Instrumentation—F. G. Marble, Boonton Radio Corporation, Intervale Road, Boonton, N.J.

Medical Electronics—V. K. Zworykin, RCA Labs., Princeton, N.J.

Microwave Theory and Techniques—A. C. Beck, Box 107, Red Bank, N.J.

Military Electronics—C. L. Engleman, 2480 16 St., N.W., Washington 9, D.C.

Nuclear Science—M. A. Schultz, Westinghouse Elec. Corp., Commercial Air Power, P.O. Box 355, Pittsburgh 30, Pa.

Reliability and Quality Control—Victor Wouk, Beta Electric Corp., 333 E. 103rd St., New York 29, N.Y.

Production Techniques—R. R. Batcher, 240-02—42nd Ave., Douglaston, L.I., N.Y.

Telemetry and Remote Control—C. H. Hoeppner, Stavid Engineering, Plainfield, N.J.

Ultrasonics Engineering—M. D. Fagen, Bell Labs., Whippny, N.J.

Vehicular Communication—Newton Monk, Bell Labs., 463 West St., N.Y., N.Y.

Sections*

Akron (4)—H. L. Flowers, 2029—19 St., Cuyahoga Falls, Ohio; H. F. Lanier, 49 West Lowell Ave., Akron, Ohio.

Alberta (8)—J. W. Porteous, Alberta Univ., Edmonton, Alta., Canada; J. G. Leitch, 13024—123A Ave., Edmonton, Alta., Canada.

Albuquerque-Los Alamos (7)—T. G. Banks, Jr., 1124 Monroe St., S.E., Albuquerque, N. Mex.; G. A. Fowler, 3333—49 Loop, Sandia Base, Albuquerque, N. Mex.

Atlanta (3)—D. L. Finn, School of Elec. Engr'g., Georgia Inst. of Tech., Atlanta, Ga.; P. C. Toole, 605 Morningside Dr., Marietta, Ga.

Baltimore (3)—C. F. Miller, Johns Hopkins University, 307 Ames Hall, Baltimore 18, Md.; H. R. Hyder, 3rd, Route 2, Owings Mills, Md.

Bay of Quinte (8)—J. C. R. Punchard, Elec. Div., Northern Elec. Co. Ltd., Sydney St., Belleville, Ont., Canada; M. J. Waller, R.R. 1, Foxboro, Ont., Canada

Beaumont-Port Arthur (6)—W. W. Eckles, Jr., Sun Oil Company, Prod. Laboratory, 1096 Calder Ave., Beaumont, Tex.; E. D. Coburn, Box 1527, Beaumont, Tex.

Binghamton (4)—O. T. Ling, 100 Henry Street, Binghamton, N.Y.; Arthur Hamburger, 926 Glendale Dr., Endicott, N.Y.

Boston (1)—T. P. Cheatham, Jr., Hosmer St., Marlborough, Mass.; R. A. Waters, IRE Boston Section Office, 73 Tremont St., Room 1006, Boston 8, Mass.

Buenos Aires—J. M. Rubio, Ayachucio 1147, Buenos Aires, Argentina; J. L. Blon, Transradio Internacional, San Martin 379, Buenos Aires, Argentina.

Buffalo-Niagara (1)—D. P. Welch, 859 Highland Ave., Buffalo 23, N.Y.; W. S. Holmes, 1961 Ellicot Rd., West Falls, N.Y.

Cedar Rapids (5)—Ernest Pappenfus, 1101

—20 St., S.E., Cedar Rapids, Iowa; E. L. Martin, 3821 Vine Ave., S.E., Cedar Rapids, Iowa.

Central Florida (3)—Hans Scharla-Nielsen, Radiation Inc., P.O. Drawer 'Q', Melbourne, Fla.; G. F. Anderson, Radiation Inc., P.O. Box 'Q', Melbourne, Fla.

Chicago (5)—J. S. Brown, 9829 S. Hoyne Ave., Chicago 43, Ill.; D. G. Haines, 17 West 121 Oak Lane, Bensenville, Ill.

China Lake (7)—G. D. Warr, 213-A Wasp Rd., China Lake, Calif.; B. B. Jackson, 54-B Rowe St., China Lake, Calif.

Cincinnati (4)—D. W. Martin, The Baldwin Company, 1801 Gilbert, Cincinnati 2, Ohio; F. L. Wedig, Jr., 3819 Davenant Ave., Cincinnati 13, Ohio.

Cleveland (4)—R. H. DeLany, 5000 Euclid Ave., Cleveland 3, Ohio; J. F. Keithley, 22775 Douglas Rd., Shaker Heights 22, Ohio.

Columbus (4)—W. E. Rife, 6762 Rings Rd., Amlin, Ohio; R. L. Cosgriff, 2200 Homestead Dr., Columbus, Ohio.

Connecticut Valley (1)—P. F. Ordung, Dunham Laboratory, Yale University, New Haven, Conn.; H. M. Lical, Box U-37, University of Connecticut, Storrs, Conn.

Dallas-Fort Worth (6)—M. W. Bullock, 6805 Northwood Rd., Dallas 25, Texas; C. F. Seay, Jr., Collins Radio Company, 1930 Hi-Line Dr., Dallas, Texas

Dayton (5)—W. W. McLennan, 304 Schenck Ave., Dayton 9, Ohio; N. A. Nelson, 310 Lewiston Rd., Dayton 9, Ohio.

Denver (6)—J. W. Herbstreit, 2000 E. Ninth Ave., Boulder, Colo.; R. S. Kirby, 455 Hawthorne Ave., Boulder, Colo.

Des-Moines-Ames (5)—A. D. Parrott, Northwestern Bell Telephone Company, Des Moines, Iowa; W. L. Hughes, E.E. Department, Iowa State College, Ames, Iowa

Detroit (4)—N. D. Saigon, 611 Nightingale, Dearborn, Michigan; A. L. Coates, 1022 E. Sixth St., Royal Oak, Mich.

Egypt—H. M. Mahmoud, 24 Falaki St.,

Cairo, Egypt; E. I. Elkashlan, Egyptian State Broadcasting, Cairo, Egypt

Elmira-Corning (1)—R. A. White, 920 Grand Central Ave., Horseheads, N.Y.; R. G. Larson, 220 Lynhurst Ave., Windsor Gardens, Horseheads, N.Y.

El Paso (6)—J. C. Nook, 1126 Cimarron St., El Paso, Texas; J. H. Maury, 3519 Fort Blvd., El Paso, Texas.

Emporium (4)—E. H. Boden, R.D. 1, Emporium, Pa.; H. S. Hench, Jr., R.D. 2, Emporium, Pa.

Evansville-Owensboro (5)—E. C. Gregory, 1120 S.E. First St., Apt. B-2, Evansville, Ind.; A. K. Mieg, 904 Kelsey Ave., Evansville, Ind.

Fort Wayne (5)—C. L. Hardwick, 2905 Chestnut St., Fort Wayne 4, Ind.; Paul Rudnick, Farnsworth Electronics Company, Fort Wayne 1, Ind.

Hamilton (8)—G. F. Beaumont, 6 Tallman Ave., Burlington, Ont., Canada; C. N. Chapman, 40 Dundas St., Waterdown, Ont., Canada.

Hawaii (7)—H. E. Turner, 44-271 Mikiola Dr., Kaneohe, Hawaii; G. H. Hunter, Box 265, Lanikai, Oahu, T.H.

Houston (6)—L. W. Erath, 2831 Post Oak Rd., Houston, Texas; R. W. Olson, Box 6027, Houston 6, Texas.

Huntsville (3)—A. L. Bratcher, 308 E. Holmes St., Huntsville, Ala.; W. O. Frost, Box 694, Huntsville, Ala.

Indianapolis (5)—A. J. Schultz, 908 E. Michigan St., Indianapolis, Ind.; H. L. Wisner, 5418 Rosslyn Ave., Indianapolis 20, Ind.

Israel—Franz Ollendorf, Box 910, Hebrew Inst. of Tech., Haifa, Israel; J. H. Halberstein, P.O.B. 1, Kiriath Mozkin, Israel

Ithaca (1)—Benjamin Nichols, School of Electrical Engineering, Cornell University, Ithaca, N.Y.; H. L. Heydt, General Electric Advanced Electronics Center, Cornell University Airport, Ithaca, N.Y.

* Numerals in parentheses following Section designation indicate Region number. First name designates Chairman, second name Secretary.

(Sections cont'd)

- Kansas City (6)**—Richard W. Fetter, 8111 W. 87 St., Overland Park, Kan.; Mrs. G. L. Curtis, Radio Industries, Inc., 1307 Central Ave., Kansas City 2, Kan.
- Little Rock (6)**—J. E. Wylie, 2701 N. Pierce, Little Rock, Ark.; Jim Spilman, A. R. & T. Electronics, P.O. Box 370, North Little Rock, Ark.
- London (8)**—C. F. MacDonald, 328 St. James St., London, Ont., Canada; J. D. B. Moore, 27 McClary Ave., London, Ont., Canada.
- Long Island (2)**—Paul G. Hansel, Addison Lane, Greenvale, L. I., N. Y.; W. P. Frantz, Sperry Gyroscope Co., Great Neck, L. I., N. Y.
- Los Angeles (7)**—Walter E. Peterson, 4016 Via Cardelina, Palos Verdes Estates, Calif.; John K. Gossland, 318 E. Calaveras St., Altadena, Calif.
- Louisville (5)**—O. W. Towner, WIIAS Inc., 525 W. Broadway, Louisville 2, Ky.; L. A. Miller, 314 Republic Bldg., Louisville 2, Ky.
- Lubbock (6)**—H. A. Spuhler, Electrical Engineering Department, Texas Technological College, Lubbock, Texas; J. W. Dean, 1903—49 St., Lubbock, Texas.
- Miami (3)**—C. S. Clemans, Station WSWN, Belle Glad, Fla.; H. F. Bernard, 1641 S.W. 82 Place, Miami, Fla.
- Milwaukee (5)**—Alex Paalu, 1334 N. 29 St., Milwaukee 8, Wis.; J. E. Jacobs, 6230 S. 116 St., Hales Corner, Wis.
- Montreal (8)**—Sydney Bonneville, Room 1427, 1050 Beaver Hall Hill, Montreal, Que., Canada; R. E. Penton, 2090 Claremont Ave., N.D.G., Montreal, Que., Canada.
- Newfoundland (8)**—E. D. Witherstone, 6 Cornell Heights, St. John's, Newfoundland, Canada; R. H. Bunt, Box H-182, St. John's, Newfoundland, Canada.
- New Orleans (6)**—J. A. Cronvich, Dept. of Electrical Engineering, Tulane University, New Orleans 18, La.; N. R. Landry, 620 Carol Dr., New Orleans 21, La.
- New York (2)**—A. C. Beck, Box 107, Red Bank, N. J.; J. S. Smith, 506 East 24 St., Brooklyn 10, N. Y.
- North-Carolina-Virginia (3)**—J. C. Mace, 1616 Jefferson Park Ave., Charlottes-
- ville, Va.; Allen L. Comstock, 1404 Hampton Drive, Newport News, Va.
- Northern New Jersey (2)**—P. S. Christaldi, Box 111, Clifton, N. J.; W. Cullen Moore, 130 Laurel Hill Rd., Mountain Lakes, N. J.
- Northwest Florida (3)**—B. H. Overton, Box 115, Shalimar, Fla.; G. C. Flening, 579 E. Gardner Dr., Ft. Walton Beach, Fla.
- Oklahoma City (6)**—A. P. Challenner, University of Oklahoma, Norman, Oklahoma; Frank Herrmann, 1913 N.W. 21 St., Oklahoma City, Okla.
- Omaha-Lincoln (5)**—M. L. McGowan, 5544 Mason St., Omaha 6, Neb.; C. W. Rook, Dept. of Electrical Engineering, University of Nebraska, Lincoln 8, Neb.
- Ottawa (8)**—George Glinski, 36 Granville Ave., Ottawa, Ont., Canada; C. F. Patterson, 3 Braemar, Ottawa 2, Ont., Canada.
- Philadelphia (3)**—C. R. Kraus, Bell Telephone Co. of Pa., 1835 Arch St., 16 Floor, Philadelphia 3, Pa.; Nels Johnson, Philco Corp., 4700 Wissahickon Ave., Philadelphia 44, Pa.
- Phoenix (7)**—William R. Saxon, 641 E. Missouri, Phoenix, Ariz.; G. L. McClanahan, 509 East San Juan Cove, Phoenix, Ariz.
- Pittsburgh (4)**—J. N. Grace, 112 Heather Dr., Pittsburgh 34, Pa.; J. B. Woodford, Jr., Box 369, Carnegie Tech. P.O., Pittsburgh 13, Pa.
- Portland (7)**—J. M. Roberts, 4325 N.E. 77, Portland 13, Ore.; D. C. Strain, 7325 S. W. 35 Ave., Portland 19, Ore.
- Princeton (2)**—G. C. Sziklai, Box 3, Princeton, N. J.; L. L. Burns, Jr., R.C.A. Labs., Princeton, N. J.
- Rochester (1)**—G. H. Haupt, 48 Van Voorhis Ave., Rochester 17, N. Y.; B. L. McArdle, Box 54, Brighton Sta., Rochester 10, N. Y.
- Rome-Utica (1)**—H. F. Mayer, 60 Fountain St., Clinton, N. Y.; R. S. Grisetti, 67 Root St., New Hartford, N. Y.
- Sacramento (7)**—R. C. Bennett, 3401 Chenowith Ave., Sacramento 21, Calif.; R. A. Poucher, Jr., 3021 Mountain View Ave., Sacramento 21, Calif.
- St. Louis (6)**—F. A. Fillmore, 5758 Itasca St., St. Louis 9, Mo.; Christopher Ethim, 1016 Louisville Ave., St. Louis 10, Mo.
- Salt Lake City (7)**—A. L. Gunderson, 3906 Parkview Dr., Salt Lake City, Utah; S. B. Hammond, Engineering Hall, Univ. of Utah, Salt Lake City 1, Utah.
- San Antonio (6)**—Paul Tarrodaychik, 215 Christine Dr., San Antonio 10, Texas; J. B. Porter, 647 McIlvaine St., San Antonio 1, Texas.
- San Diego (7)**—F. X. Brynes, 1759 Beryl St., San Diego 9, Calif.; R. T. Silberman, 4274 Middlesex Dr., San Diego, Calif.
- San Francisco (7)**—B. M. Oliver, 275 Page Mill Rd., Palo Alto, Calif.; Wilson Pritchett, Div. of Electrical Engineering, University of California, Berkeley 4, Calif.
- Schenectady (1)**—C. C. Allen, 2064 Baker Ave., Schenectady 9, N. Y.; A. E. Rankin, 833 Whitney Dr., Schenectady, N. Y.
- Seattle (7)**—W. C. Galloway, 5215 Pritchard St., Seattle 6, Wash.; J. M. Scovill, 7347—58 Ave., N.E., Seattle 15, Wash.
- Syracuse (1)**—G. M. Glasford, Electrical Engineering Dept., Syracuse University, Syracuse 10, N. Y. (Secretary).
- Toledo (4)**—L. R. Klopfenstein, Portage, Ohio; D. F. Cameron, 1619 Milburn Ave., Toledo 6, Ohio.
- Toronto (8)**—A. P. H. Barclay, 2 Pine Ridge Dr., Toronto 13, Ont., Canada; H. W. Jackson, 352 Laird Dr., Toronto 17, Ont., Canada.
- Tulsa (6)**—Glen Peterson, 502 S. 83 East Ave., Tulsa, Okla.; D. G. Egan, Research Laboratory, Carter Oil Company, Box 801, Tulsa 2, Okla.
- Twin Cities (5)**—N. B. Coil, 1664 Thomas Ave., St. Paul 4, Minn.; A. W. Sear, 5801 York Ave. S., Minneapolis 10, Minn.
- Vancouver (8)**—J. E. Breeze, 5591 Toronto Rd., Vancouver 8, B. C., Canada; R. A. Marsh, 3873 W. 23 Ave., Vancouver, B. C., Canada.
- Washington (3)**—H. I. Metz, U. S. Government Dept. of Commerce, CAA, Room 2076, T-4 Bldg., Washington 25, D. C.; A. H. Schooley, 3940 First St., S.W., Washington 24, D. C.
- Williamsport (4)**—G. B. Aney, 968 N. Market St., Williamsport, Pa.; W. H. Bresee, 818 Park Ave., Williamsport, Pa.
- Winnipeg (8)**—R. M. Simister, 179 Renfrew St., Winnipeg, Man., Canada; G. R. Wallace, 400 Smithfield Ave., Winnipeg, Man., Canada

Subsections

- Berkshire (1)**—Gilbert Devey, Sprague Electric Company, Marshall St., Bldg. 1, North Adams, Mass.; R. P. Sheehan, Ballou Lane, Williamstown, Mass.
- Buenaventura (7)**—W. O. Bradford, 301 East Elm St., Oxnard, Calif.; M. H. Fields, 430 Roderick St., Oxnard, Calif.
- Centre County (4)**—W. L. Baker, 1184 Omeida St., State College, Pa.; W. J. Leiss, 1173 S. Atherton St., State College, Pa.
- Charleston (3)**—W. L. Schachte, 152 Grove St., Charleston 22, S. C.; Arthur Jonas, 21 Madden Dr., Dorchester Terr., Charleston Heights, S. C.
- East Bay (7)**—J. M. Rosenberg, 1134 Norwood Ave., Oakland 10, Cal.; C. W. Park, 6035 Chabotyn Terrace, Oakland, Cal.
- Erie (1)**—R. S. Page, 1224 Idaho Ave., Erie 10, Pa.; R. H. Tuznik, 905 E. 25 St., Erie, Pa.
- Fort Huachuca (7)**—R. O. Burns, Army Electronic Proving Ground, Ft. Huachuca, Ariz.; J. H. Homsy, Box 123, San Jose Branch, Bisbee, Ariz.
- Lancaster (3)**—R. B. Janes, Radio Corporation of America, Tube Dept., Lancaster, Pa.; H. F. Kazanowski, 108 Mackin Ave., Lancaster, Pa.
- Mid-Hudson (2)**—R. E. Merwin, 13 S. Randolph Ave., Poughkeepsie, N. Y.; P. A. Bunyar, 10 Morris St., Saugerties, N. Y.
- Monmouth (2)**—G. F. Senn, Orchard Rd.-River Plaza, Red Bank, N. J.; C. A. Borgeson, 82 Garden Rd., Little Silver, N. J.
- Orange Belt (7)**—F. D. Craig, 215 San Rafael, Pomona, Calif.; W. F. Meggers, Jr., 6844 De Anza Ave., Riverside, Calif.
- Palo Alto (7)**—W. W. Harman, Electronics Research Laboratory, Stanford University, Stanford, Calif.; W. G. Abraham, 611 Hansen Way, c/o Varian Associates, Palo Alto, Calif.
- Pasadena (7)**—Jennings David, 585 Rim Rd., Pasadena 8, Calif. (Secretary).
- Piedmont**—Officers to be elected.
- Quebec (8)**—Officers to be elected.
- Richland (7)**—R. G. Clark, 1732 Howell Richland, Washington; R. E. Connally, 515 Cottonwood Dr., Richland, Wis.
- Tucson (7)**—R. C. Eddy, 1511 E. 20 St., Tucson, Ariz.; P. E. Russell, Elect. Eng. Dept., Univ. Ariz., Tucson, Ariz.
- USAFIT (5)**—J. J. Gallagher, Box 3482 USAFIT, Wright-Patterson AFB, Ohio (Secretary).
- Westchester County (2)**—Joseph Reed, 52 Hillcrest Ave., New Rochelle, N. Y.; D. S. Kellogg, 9 Bradley Farms, Chappaqua, N. Y.
- Wichita (6)**—M. E. Dunlap, 548 S. Lorraine Ave., Wichita 16, Kan.; English Piper, 1838 S. Parkwood Lane, Wichita, Kan.

NATIONAL SIMULATION CONFERENCE

TENTATIVE PROGRAM DALLAS, TEXAS JANUARY 19-21

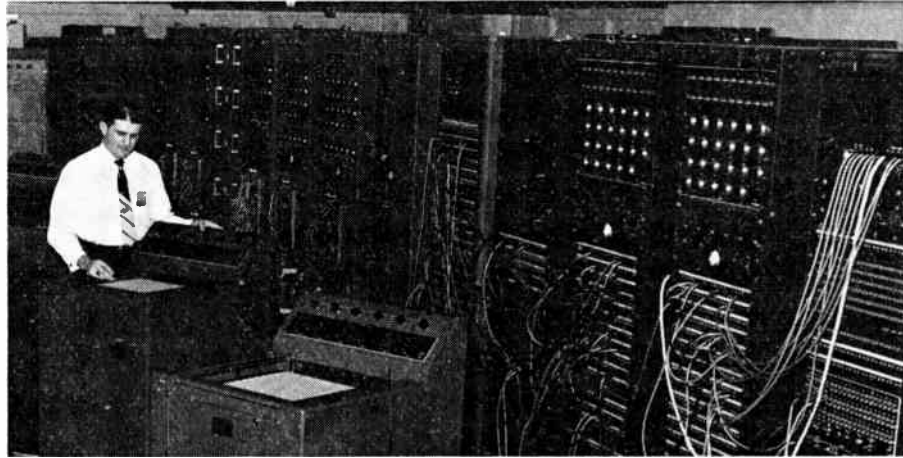
The National Simulation Conference, sponsored by the Dallas-Fort Worth Chapter of the IRE and the Professional Group on Electronic Computers, will be devoted to all types of simulation and associated computing techniques. Other groups participating in this conference will be the Dallas-Fort Worth Section of the IRE, the North Texas Section of the American Institute of Electrical Engineers, and the Dallas-Fort Worth Chapter of the Association for Computing Machinery.

Persons planning to attend may make hotel reservations at the conference headquarters, Baker Hotel, Dallas. Registration will begin Thursday morning, January 19, at 7:45 A.M., and registration facilities will be available before and during all sessions adjacent to the meeting room. The registration fee is \$5.00; registrants will also receive a free copy of the proceedings containing all technical papers by mail afterward. Students may choose to register for \$1.00, but they will not receive the proceedings. All registrants will receive abstracts of all papers upon registration.

All technical papers will be published in the proceedings of the conference. Copies of the proceedings may be ordered now at \$5.00 per copy from F. W. Tatum, Electrical Engineering Department, Southern Methodist University, Dallas, Texas. Make checks payable to the Institute of Radio Engineers.

An informal women's program will be available for wives accompanying their husbands to the conference. Complete details may be obtained at the registration desk.

Conference officers include: L. B. Wadel, Chance Vought Aircraft, Inc., *General Chairman*; J. R. Forester, Chance Vought Aircraft, Inc., and H. E. Blanton, Hycon Eastern, Inc., *Technical Program Co-Chairmen*; C. C. Calvin, Chance Vought Aircraft, Inc., *Secretary*; F. W. Tatum, Southern Methodist University, *Treasurer*; B. B. Mackey, Chance Vought Aircraft, Inc., *Proceedings Chairman*.



One of the facilities to be visited during the National Simulation Conference in January will be the electronic analog computer installation at Chance Vought Aircraft, Inc. in Dallas, a portion of which is shown here.

Thursday Morning

CHAIRMAN: J. A. GREEN, JOHN A. GREEN CO.

Simulation of Military Vehicle Suspension Systems, I. J. Sattinger and E. B. Therkelsen, Willow Run Research Center, Univ. of Michigan.

Analog Computer Computation of Propellant Linear Burning Rate, A. I. Rubin, Electronic Associates, Inc., Princeton, N. J.
Electric Analogy to Transient Heat Conduction in a Medium with Variable Thermal Properties, D. R. Otis, Convair.

Application of GEDA Analog Computers to Study Temperature Transients in a Plastic Windshield, P. J. Hermann, Goodyear Aircraft Corp.

Thursday Afternoon

CHAIRMAN: J. W. LUDWIG, CHANCE VOUGHT AIRCRAFT, INC.

Performance Requirements for Flight Tables, H. E. Blanton, Hycon Eastern, Inc.

The Use of the Bendix Flight Table, E. J. McGlinn, Bendix Aviation Corp.

The Design of a High Performance Hydraulic Servo, M. S. Feder and K. V. Bailey, Bendix Aviation Corp.

Flight Simulator for Acoustic Homing Torpedoes, C. G. Beatty, USNOTS.

Laboratory Evaluation of Systems Incorporating Scanning Reticles, H. H. Kantner and S. H. Cameron, Illinois Inst. of Tech.

Optical Simulation of Radar, W. Blitzstein and T. Levine, Moore School of Elec. Engrg., Univ. of Pennsylvania.

High Accuracy Operational Digital Simulation, Julius Tou, Moore School of Elec. Engrg., Univ. of Pennsylvania.

Friday Morning

CHAIRMAN: W. L. EVANS, CONVAIR

Dynamic Tester Tape Preparation on ORDVAC, G. A. Beck, Ballistic Research Labs.

A Comparative Evaluation of Several Methods for Achieving Greater Angular Accuracy

in Search Radars Using Simulation Techniques, C. M. Walter, Air Force Cambridge Research Center.

The Derivation of Simulators of Gas Turbine and Other Physical Systems from Experimental Data, L. Wolin, Naval Air Experimental Station.

The Uses of Post-Flight Simulation in Missile Flight Analysis, R. G. Davis, U. S. Naval Ordnance Lab.

Substitution Methods for the Verification of Analog Computer Solutions, H. F. Meissinger, Hughes Aircraft Co.

Analog Computer Prepatch Logic Using Subroutines, W. J. Wachter, Univ. of Pennsylvania.

Friday Afternoon

CHAIRMAN: W. W. KOESEL, SOUTHERN METHODIST UNIV.

An Approach to Digital Simulation, Max Palevsky, Bendix Aviation Corp.

The Simulation of a Digital Differential Analyzer on the IBM 701, B. M. Tostanoski, C. J. Hoppel, and M. M. Dickinson, IBM.

The Simulation of a Proposed Airborne Digital Computer on the IBM 701, J. R. Belford and M. E. Maron, IBM.

A Simulator for Analysis of Sampled Data Control Systems, P. K. Giloth, Bell Tel. Labs.

General Evaluation of a Linear Time-Variant System, J. M. Gallagher, Jr., Mass. Inst. of Tech.

Design of a Nonlinear Control System with Random Disturbances, K. B. Tuttle, Northrop Aircraft, Inc.

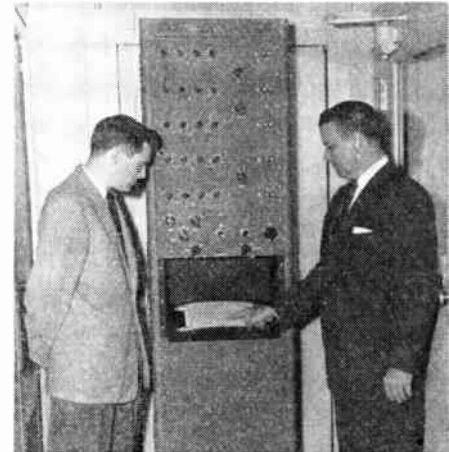
Friday Evening

Tours to local computer installations.

Saturday Morning

CHAIRMAN: C. F. SEAY, COLLINS RADIO CO.

Time Domain Network Synthesis for an Analog Computer Setup, J. Otterman, Univ. of Michigan.



J. R. Macdonald (left) is shown with an exponential-process analyzer and synthesizer. At right is E. Perry.

Simulation of Dead Time, N. L. Irvine, Aeroflight-General Corp.

A Simulation System for the Study of Human Dynamics, J. M. Stroud, U. S. Navy Electronics Lab.

The Applied Systems Development and Evaluation Center at the Navy Electronics Laboratory, R. Coburn, U. S. Navy Electronics Lab.

An Analog Computer for Radioactive Fallout Prediction, H. K. Skramstad and J. H. Wright, National Bureau of Standards.

An Exponential-Process Analyzer and Syn-

thesizer, J. R. Macdonald, Texas Instruments, Inc.

Saturday Afternoon

CHAIRMAN: J. R. MACDONALD,
TEXAS INSTRUMENTS, INC.

The Gated Amplifier Computer Technique, Sidney Godet, Reeves Instrument Corp.

A Wide-Band Direct-Coupled Operational Amplifier, C. S. Deering, Convair.

An Improved Diode Function Generator for

Analog Computers, R. A. Bruns, Calif. Inst. of Tech.

Use of Semi-Conducting Surfaces in Analog Function Generation, V. L. Larrowe and M. Spencer, Willow Run Research Center, Univ. of Michigan.

Repeatable Generation of Noise with a Masked Cathode Ray Tube, L. B. Wadel, C. C. Calvin, and J. W. Atkins, Jr., Chance Vought Aircraft, Inc.

A Comparison of Diode Switching Methods for Analog Function Generators, O. L. Updike and J. H. McLeod, Jr., USNAMTC

NATIONAL SYMPOSIUM ON MICROWAVE TECHNIQUES

UNIVERSITY OF PENNSYLVANIA
PHILADELPHIA, PENNSYLVANIA
FEBRUARY 2-3

A National Symposium on Microwave Techniques will be held at the University of Pennsylvania, Philadelphia, Pennsylvania, on Thursday and Friday, February 2 and 3. The Moore School of Electrical Engineering, University of Pennsylvania, is host to this symposium. The symposium is sponsored jointly by the Professional Group on Antennas and Propagation, the Professional Group on Microwave Theory and Techniques, and the Philadelphia Section of the IRE.

The technical program arranged for this symposium has been designed to present the most significant advances in the field of microwave engineering. Sessions will be devoted to microwave components, antennas, guided microwave transmission, scatter propagation and radiation, and ferrite theory and devices. Inspection of several laboratories and facilities of the new Physical Sciences building on the campus of the University of Pennsylvania will be possible during the symposium.

The symposium will be held in the new Physical Sciences building of the University of Pennsylvania. The registration fee is \$2.50 for advance registrants and \$3.50 for those registering at the door. Advance registrations should be sent by January 15 to Charles Polk, Chairman of the Arrangements Committee, Moore School of Electrical Engineering, University of Pennsylvania, Philadelphia 4, Pennsylvania. Checks should be made payable to I. L. Auerbach, Treasurer.

A cocktail party for those attending the symposium will be held at the Penn-Sherwood Hotel, 39th and Chestnut Streets, Philadelphia, February 2 at 5:30 p.m. Tickets at \$2.00 apiece will be required for admission.

Of interest to those attending the Symposium on Microwave Techniques is the regularly scheduled meeting of the Philadelphia Section of the IRE, Wednesday

evening, February 1, 8:00 p.m., at the Franklin Institute. D. G. Fink will speak on the topic "Danger! The Radio Spectrum is Bursting at the Seams." Those arriving in Philadelphia in time are invited to attend.

The Symposium on Microwave Techniques has been planned and organized by the Steering Committee under the chairmanship of R. F. Schwartz. Members of the Steering Committee are: R. F. Schwartz, *Chairman*, Moore School of Electrical Engineering, University of Pennsylvania; S. M. King, *Secretary and Publicity*, I-T-E Circuit Breaker Company; J. B. Williams, *Finance*, Philco Corporation; D. R. Crosby, *Technical Program*, Radio Corporation of America; Charles Polk, *Arrangements*, Moore School of Electrical Engineering, University of Pennsylvania; D. D. King, Johns Hopkins University; W. M. Sharpless, Bell Telephone Laboratories, Inc.; Ben Warriner, IV, General Electric Company; Sanford Hershfield, Glenn L. Martin Company; and N. I. Korman, Radio Corporation of America.

The Technical Program Committee who assembled the program for this symposium consists of the following members: D. R. Crosby, *Chairman*, Radio Corporation of America; S. E. Benson, Philco Corporation; Sanford Hershfield, Glenn L. Martin Company; R. W. Klopfenstein, Radio Corporation of America; P. P. Lombardini, Moore School of Electrical Engineering, University of Pennsylvania; Milton Nussbaum, American Electronic Laboratories, Inc.; A. A. Oliner, Polytechnic Institute of Brooklyn; T. S. Saad, Sage Laboratories, Inc.; and W. M. Sharpless, Bell Telephone Laboratories, Inc.

The Local Arrangements Committee responsible for the nontechnical phase of this symposium is composed of the following members: Charles Polk, *Chairman*, Moore School of Electrical Engineering, University of Pennsylvania; Robert Scudder, Radio Corporation of America; Ernest Jacobs, American Electronic Laboratories, Inc.; Sterling Wright, Philco Corporation; and P. J. Kelly, Moore School of Electrical Engineering, University of Pennsylvania.

Thursday, February 2

9:30 a.m.

Auditorium A

MICROWAVE COMPONENTS

Session Chairman: B. F. Wheeler, R.C.A.
"Recent Advances in Waveguide Hybrid Junctions," P. A. Loth, Wheeler Lab.

"A Traveling-Wave Ring Filter," F. S. Coale, Stanford Research Institute.

"Printed Microwave Bandpass Filters with an Application in the X-Band," J. H. Wenzel, Philco Corporation.

"Miniatrization of Microwave Assemblies," L. Lewin, Standard Telecommunication Laboratories Limited, England.

"Very Narrow Passband Waveguide Filters in Toll-Ticket Waveguide," David Proctor and G. W. Wolfe, Convair.

Auditorium B

ANTENNAS

Session Chairman: L. H. Hendrixson, Bell Telephone Company of Pennsylvania.

"A Broadband Receiving Antenna for Horizontal and Vertical Polarization," W. H. Clark and Werner Koppl, Radio Frequency and Antenna Consultants.

"Techniques for Controlling the Radiation from a Dielectric Rod Waveguide," J. W. Duncan and R. H. DuHamel, U. of Ill.

"Microwave Interferometer Studies in Dielectric Media and Parallel Wire Grids in Free Space and Waveguide," D. B. Medved and F. M. Millican, Convair.

"The Excitation of Surface Waveguides and Radiating Slots by Strip-Circuit Transmission Lines," A. D. Frost, C. R. McGeoch, and C. R. Mingins, Tufts University.

"New Method of Antenna Array Synthesis Applied to Generation of Double-step Patterns," C. J. Sletten, Air Force Cambridge Research Center.

2:00 p.m.

University Museum Auditorium

"Welcoming Remarks," C. C. Chambers, Vice-Pres. Engineering Affairs, U. of Penna.

PANEL ON GUIDED MICROWAVE TRANSMISSION

Moderator: Dr. W. L. Barrow, Sperry Gyroscope Company.

Members: R. W. Klopfenstein, Coaxial, Spiral and Dielectric Guides, RCA; George Goubau, Open Wire Lines, U.S.A. Signal Corps consultant; E. G. Fubini, Strip Lines, Airborne Instruments Laboratory, Inc.; T. N. Anderson, Rectangular and Ridge Waveguide, Airtron Inc.; S. E. Miller, Round Guide, Multimode Guide, Bell Telephone Laboratories, Inc.

Thursday evening, February 2

Cocktail party

Friday, February 3

9:30 a.m.

Auditorium A

SCATTER PROPAGATION AND RADIATION

Session Chairman: J. B. Williams, Philco Corporation.

"Summary of Scatter Propagation," W. E. Gordon, Cornell University.

"A Scatter Propagation Test at 400, 2250 and 2820 MC," S. P. Brown, Signal Corps, and H. R. Mathwich, RCA.

"On the Simulation of Fraunhofer Radiation Patterns in the Fresnel Region," D. K. Cheng, Syracuse University.

"Near-Zone Gain of Rectangular Aper-

tures," Charles Polk, Moore School of Electrical Engineering, University of Pa.

"Diffraction Zone SHF Antenna Pattern Range," J. O. Stenoien, Boeing Airplane Company.

Auditorium B

FERRITE THEORY

Session Chairman: N. C. Colby, Radio Corporation of America.

"Ferrites in the Region Below 3,000 MC," C. L. Hogan, Harvard University.

"Representation of Non-Reciprocal Two-Parts via the Modified Wheeler Network," H. M. Altschuler and W. K. Kahn, Polytechnic Institute of Brooklyn.

"Non-Linear Propagation in Ferrite-Loaded Waveguide," N. G. Sakiots, H. N. Chait and M. L. Kales, Naval Research Laboratory.

"Evaluation of Non-Reciprocal Microwave Circuits for Radar Applications," D. A. Caswell, Cascade Research Corp.

"Power Conservation in Waveguide Systems," A. G. Fox, Bell Telephone Laboratories, Inc.

2:00 p.m.

Auditorium A

MICROWAVE COMPONENTS

Session Chairman: E. I. Hawthorne, Moore School of Electrical Engineering, University of Pennsylvania.

"Criteria for Design of Loop Type Directional Couplers for the L-Band," P. P.

Lombardini, R. F. Schwartz and P. J. Kelly, Moore School of Electrical Engineering, University of Pennsylvania.

"Recent Advances in Finline Circuits," S. D. Robertson, Bell Telephone Laboratories, Inc.

"Broadband Waveguide Series Switching T," J. W. E. Griemann and G. S. Kasai, Polytechnic Institute of Brooklyn.

"A Coaxial Balanced Duplexer," John Reed and Gershon Wheeler, Raytheon Manufacturing Company.

"Image Rejection Converter," W. H. Horton, and F. Schnurer, General Electric Company.

Auditorium B

FERRITE DEVICES

Session Chairman: A. A. Oliner, Polytechnic Institute of Brooklyn.

"The Turnstile Circulator," P. J. Allen, Naval Research Laboratory.

"A Broad-Band Microwave Circulator," E. A. Ohm, Bell Telephone Laboratories, Inc.

"Optimum Design Parameters for Ferromagnetic Resonance Absorption Isolators," L. A. Blasberg, L. J. Lader and R. A. Young, Hughes Weapon Systems Development Laboratories.

"Improved Rectangular Waveguide Resonance Isolators," M. T. Weiss, Bell Telephone Laboratories, Inc.

"An Automatic Gain Control System for Microwaves," J. P. Vindling, Cascade Research Corporation.

Abstracts of IRE Transactions

The following issues of "Transactions" have recently been published, and are now available from the Institute of Radio Engineers, Inc., 1 East 79th Street, New York 21, N. Y. at the following prices. The contents of each issue and, where available, abstracts of technical papers are given below.

Sponsoring Group	Publication	Group Members	IRE Members	Non- Members*
Information Theory	Vol. IT-1, No. 2	\$1.90	\$2.85	\$5.70
Instrumentation	Vol. PGI-4	\$2.70	\$4.05	\$8.10
Medical Electronics	PGME-2	\$0.85	\$1.25	\$2.55
Telemetry and Remote Control	Vol. TRC-1, No. 3	\$0.70	\$1.05	\$2.10

* Public libraries and colleges may purchase copies at IRE Member rates.

Information Theory

Vol. IT-1, No. 2, SEPTEMBER, 1955

On Optimum Multiple-Alternative Detection of Signals in Noise—D. Middleton and D. Van Meter

The problem of the optimum detection signals in noise, when a possible signal can arise from more than one class of signal types, is considered from the point of view of decision theory. Specifically, optimization here consists of minimizing the average risk for preassigned costs appropriate to the possible correct and

incorrect decisions, when only a single signal, of class k, may occur out of $N+1$ mutually exclusive signal classes. The analysis is a generalization of the authors' earlier work on binary, or single alternative detection systems. The present treatment outlines the optimization procedure for additive signals and noise, indicates the general structure of the detector, and gives expressions for the probabilities of error and minimum average (or Bayes) risk. Some explicit results for normal statistics are included, and an example—coherent detection of similar signals, differing only in amplitude—illustrates the general approach.

A Note on the Envelope and Phase-Modulated Components of Narrow-Band Gaussian Noise—Robert Price

The autocorrelation function and power spectrum of the phase-modulated portion of narrow-band gaussian noise is studied and specific computations are carried out for the case of a rectangular noise spectrum. Related results are given for the noise envelope. General asymptotic expressions for the spectra are obtained, together with experimental verification.

Error Bounds in Noisy Channels Without Memory—Amiel Feinstein

It is shown that for any noisy channel without memory having only a finite number of received signals, the error in transmitting information at a rate $H < C$ and using uniformly

good codes of length n is bounded by an expression $F e^{-Bn(C-H)}$, where F and B are constants depending upon the channel parameters but not upon H or n .

A Bibliography on Noise—P. L. Chessin
Supplement to A Bibliography of Information Theory (Communication Theory—Cybernetics)—F. L. Stumpers
Correspondence
PGIT News

Instrumentation

VOL. PG1-4, OCTOBER, 1955

(Fourth Conference on High Frequency Measurements—IRE, AIEE, NBS, and URSI, Washington, D. C., January 17-19, 1955)

Measurements and Components for Rectangular Multimode Waveguides—D. J. Angelakos

This paper is divided into four sections: (1) measurement techniques as applied to rectangular guides in which TE_{10} , TE_{20} , and combinations of these modes may exist, (2) scattering by, and field distributions in, slots cut in multimode guides, (3) directional couplers used as mode selectors for guides containing both TE_{10} and TE_{20} , and (4) multimode guides partially filled with dielectrics (propagation constants and measurement techniques).

A Comparison Method for Tuning Wideband TR Tubes—H. H. Rickert

The method consists of comparing each production TR tube with a specially constructed and adjusted standard, in a microwave circuit which yields the differences in reflection and transmission. The test signal is swept continuously across the X-band at a rapid rate, while the difference outputs are displayed on an oscilloscope. The production tubes are tuned to best agreement with the standard; limit lines drawn on the scope face indicate whether the tuned tube is acceptable. The method has made it possible to maintain unusual tolerance of uniformity among TR tubes.

Radio Interference Measurement Techniques—L. W. Thomas

The importance of using proper techniques for the measurement of radio interference cannot be overemphasized. The amount of radio interference produced by many commercial items determines to a great extent the acceptability of that item to the user. Manufacturers of many items have formulated voluntary codes recommending minimum interference values which current manufacturers attempt to meet. The desired technique for the assessment of radio interference is one that will produce significant and uniform indications of the interference potentialities of the item in question. It has been found, however, that meter indications of interference can vary by factors of as much as one hundred to one when variations are made in the measurement technique. Many technical groups are actively prosecuting the development of standards for radio interference measurements.

Pattern Measurements of Large Fixed Antennas—J. P. Shanklin

The measurement of the pattern of large fixed antennas poses many problems if good quantitative results are desired. A method has been devised for obtaining the pattern and power gain of large antennas in the vhf range using an airborne receiver. A discussion of the problems involved in making such tests is given, followed by a description of the details of tests recently performed on some very large rhombic antennas. The lecture is illustrated with slides showing various aspects of the technique together with samples of the recorded data. Comparisons with theoretical characteristics of the antenna are made wherein it is shown that good agreement with theory is obtained.

Accurate Radar Attenuation Measurements Achieved by In-Flight Calibration—F. J. Janza and R. E. West

To achieve accurate inflight loop attenuation measurements with a pulse radar, instabilities inherent in the active networks (mixers, IF amplifiers, etc.) necessitate obtaining complete input-output calibration curves in flight at frequent intervals. By this technique, receiver calibration accuracy can be held within ± 1 db. Slightly less accurate results may be obtained by calibrating in the air at only one point on the input-output curve, provided that laboratory calibrations are made immediately before and after each flight. Comparisons shown between laboratory and various inflight calibrations demonstrate beyond question the need for the latter. Variations recorded in environmental testing on the ground were much less than those found in the air, even though the vibration, pressure, and temperature variations were nominally more severe in the testing laboratory on the ground.

Use of Distribution Curves in Evaluating Microwave Path Clearance—B. F. Wheeler and H. R. Mathwich

It has been found that distribution curves of the fading experienced on paths in a microwave relay system can assist in evaluating whether or not the paths have adequate clearance above intervening obstacles. Several months' propagation data must be taken on each path, recording the depth of each fade and its duration at each of several chosen reference signal levels. These data are then plotted in two fashions. The first is to plot as the abscissa "the per cent of fades for which the duration is equal to or exceeds the ordinate" and as the ordinate "the fade duration in minutes." The second type curve is to plot as the abscissa "the per cent of total outage time contributed by fades of duration equal to or exceeding the ordinate" and again the ordinate is "the fade duration in minutes." The shape of these curves has been found to differ significantly between paths whose clearance is adequate and those whose clearance is not adequate. Data from a number of paths of various lengths, clearances, and frequencies will be used to illustrate these points.

6 KMC Sweep Oscillator—D. A. Alsberg

An external cavity klystron sweep oscillator has been developed for use in the 6 kmc common carrier band. The oscillator has a useful output over the frequency range of 5.4-7.2 kmc. A power output of more than 300 mw can be realized constant over more than 650 mc within our ability to measure (.2 db). The sweep width may be adjusted continuously from 10-800 mc. The center of the sweep frequency may be set conveniently anywhere in the band and may be read directly on a calibrated dial. The oscillator is frequency modulated mechanically at a rate of 53 cycles per second with almost complete suppression of external vibration. Oscilloscope sweep voltage, optional blanking and measure-reference switching are provided. Discussed in some detail are microwave cavity, tuner and iris design, mechanical vibration and fatigue problems and electromechanical considerations. The design practices developed for the 6 kmc oscillator have been found applicable in other microwave frequency ranges with comparable results.

Data on Temperature Dependence of X-Band Fluorescent Lamp Noise Sources—W. W. Mumford and R. L. Schaefersman

This paper is concerned primarily with the performance of fluorescent lamps as microwave noise sources at 9,000 mc. In particular, it deals with the temperature dependence of the excess noise ratio of an eight-watt lamp running at a lamp current of 150 millamps in a 10 degree E plane holder. It was found that (a) the bulb temperature is much higher than that with a lamp of 75 millamps encountered in the 90 degree H plane circuit investigated previously at 4,000 mc—hence, the temperature

coefficient of excess noise waveguide temperature obtained in the 4,000 mc circuit does not apply; (b) anomalous and unrepeatable inversions in the temperature coefficient at these higher bulb temperatures have been observed; and (c) these anomalies can be avoided by operating the bulb at lower temperatures, 40 to 50 degrees C, where the lamps appear to be just as uniform and stable and probably just as noisy as they are at 4,000 mc.

Broadband UHF and VHF Noise Generators—W. H. Spencer and P. D. Strum

This paper discusses the application of slow-wave structures to noise generator design and describes in detail the design of a uhf and a vhf generator. The uhf generator has a uniform spectrum from 200 to 3,000 mc. The vhf generator has a uniform spectrum from 80 to 300 mc. Reduced output can be obtained from either at lower frequencies with the aid of a calibrated chart. The UHF generator utilizes a helical transmission line to provide coupling to a gas-discharge tube, while the vhf generator utilizes a lumped-constant transmission line. The output impedance of the uhf generator is 50 ohms and that of the vhf generator is 350 ohms. Design criteria and families of design curves will be presented. Limitations on the upper and lower frequencies will be discussed. A brief discussion of measurement precautions is given.

A Noise Figure Meter Having Large Dynamic Range—P. D. Strum

This paper describes a continuous-reading noise figure meter having a range of 0 to 35 db. The meter incorporates a gas-discharge tube as a standard source of noise power. To provide continuous reading over a large dynamic range, the noise generator is modulated and a coherent detector is used to compare noise outputs during the on and off periods. The output reading is presented on a direct-reading meter in such a manner that an accuracy of ± 0.3 db is obtained over most of the range. It is possible to use a wide variety of gas-discharge noise sources covering continuously the frequency band from tens of megacycles to tens of thousands of megacycles.

Precise Insertion Loss Measurements Using Imperfect Square Law Detectors and Accuracy Limitations Due to Noise—G. Sorger and B. O. Weinschel

The theory showing inaccuracies of insertion loss measurements as a function of the deviation of the square law detector from square law and as a function of the insertion loss is discussed. Experimental data are given showing good agreement with the theory. Insertion loss test sets are described which measure 10 db with an accuracy of 0.02 db. General precautions are mentioned necessary for precise loss measurements. This principle has been reduced to practice in the range of 30 to 10,000 mc; however, it can be used wherever a transmission system can be properly terminated in a bolometer. The behavior of square law and synchronous detectors in the presence of noise is reviewed. Graphs are given showing the rms meter fluctuation as a function of the ratio of input to output bandwidth with signal to noise at the input as a parameter.

Microwave Peak Power Measurement Techniques—R. E. Henning

The theory, advantages, and disadvantages of several peak power measurement techniques will be discussed. These include the barretter integration-differentiation, "notch," and average power measurement techniques. The extreme simplicity and, therefore, field and production testing application of the barretter integration-differentiation technique will be covered in detail. An analysis of error sources and magnitudes is included.

Application of UHF Impedance Measuring Techniques in Biophysics—H. P. Schwan

A summary is presented of important applications of uhf impedance measuring techniques in biophysics and medicine. These ap-

plications are partly of fundamental interest and partly of practical importance. Of practical importance is the knowledge of the dielectric data of various body tissues up to 10,000 mc in order to evaluate the potential health hazards associated with the use of powerful radar equipment. Furthermore, of practical use is the understanding of the mechanism of absorption of electromagnetic energy in tissue in order to promote better equipment in the field of diathermy. These applications are demonstrated by results which show how such quantities as the complex reflection coefficient of the body surface varies with parameters such as skin, amount of subcutaneous fat, and muscular tissue. Standards for good performance of radiation diathermy equipment can be formulated now and lead to proposals for more advanced equipment than presently available. From a basic point of view, the relationship of observed dielectric data from such tissue components as water, salt content, and protein material is of interest. Techniques are proposed for measuring the amount of "bound" water, absorbed by protein molecules, by the determination of dielectric parameters of protein solutions at uhf. Recent advances with regard to this important contribution to uhf-measuring techniques are discussed. Finally, technical requirements for impedance measuring equipment, useful for biophysical work, are formulated, and presently-used equipment which fulfills these requirements is described.

Representation and Measurement of a Dissipative Four-Pole by Means of a Modified Wheeler Network—H. M. Altschuler

A specific network representation (of a passive, reciprocal, but otherwise general four-pole), consisting of only lossless transmission lines, ideal transformers, and a single dissipative attenuator element, is described. The net work is derived from a prototype given by H. A. Wheeler, and the manner in which it transforms the reflection coefficient locus is indicated. Several desirable features and some limitations of the network are pointed out. The modified Wheeler network is particularly suited for application in the measurement of symmetric dissipative four-poles. A semi-precision measurement method to be followed in such cases is sketched.

The Use of Concentric-Line Transformers in UHF Measurements—W. A. Harris and J. J. Thompson

Concentric lines fitted with movable, adjustable stubs have been designed for use in measurements within the range from 500 to 1,000 megacycles per second. The lines are used as calibrated transformers connected to the input and output terminals of a tube. The design and calibration of the lines are discussed, and the results of measurements on several tube types are presented. The data obtained with calibrated lines and associated equipment are used to determine input, output, forward, and feedback admittance, and for the analysis of triode noise.

Figure of Merit of Probes as Standing Wave Detectors—S. W. Rubin

In the measurement of standing-wave ratio and phase, errors arise due to the interaction of the detector probe with the terminations of the line. Present knowledge of these effects suffers in some important cases from gaps in information and, in other cases, from discouraging mathematical complexities. Equally important, the need exists for a systematic correlation and interpretation of such knowledge. This paper partly fills the gap in error formulae and correlates a group of existing formulae which apply to the bulk of practical cases. Further, a simple consistency is observed which permits defining a figure of merit of probes which is inversely proportional to the error in the particular types of measurement, and which may be measured readily for a given

probe. This viewpoint is developed analytically to yield a concise figure of merit for the entire measuring system showing the effect of the probe parameters of tuning, efficiency, and reflection coefficient, and the external parameters of available source power and minimum detectable signal. For comparing two given probes, the formula simplifies to just the probe parameters. Application of these results permits the prediction of maximum measurement error, the rating of the merits of given probes, and partial design criteria for probes. Some experimental verifications are included.

Characteristics of Microwave Comparators—E. W. Matthews

An analysis is made of the characteristics of hybrid junctions with regard to their use as microwave comparators. The effects of such factors as unbalance, asymmetry, cross-coupling, and condition of match on the performance of comparators are discussed. These quantities are represented analytically in terms of the scattering coefficients of the junction. An attempt is made to determine the origin of these factors, and techniques are outlined for the measurement of their magnitudes.

A Comparison Method for Measuring Cavity Q—E. B. Mullen and P. M. Pan

To facilitate measuring the microwave permeability tensor of ferrites, a bridge has been built whereby the "Q" and resonant frequency of a cavity containing the ferrite can be found by comparison with those of a cavity with calibrated controls. The reflections from the two cavities are combined in the difference arm of a magic T and the resulting signal displayed on an oscilloscope. A teflon plunger in the cavity provides sensitive tuning from 9,100 to 9,375 mcps. Changes in "Q" are obtained through the variable loading presented to the fixed TE₁₁₁ mode pattern of the cavity by a rotatable coupling arm containing a resistive termination. In this way, the "Q" of the comparator cavity can be varied in the range from 750 to 5,000.

A Portable Frequency Standard for Navigation—P. Antonucci, J. O. Israel, E. B. Mechling, and F. G. Merrill

Precision in a modern, single site, long distance, navigation system, called Navarho, requires an extremely accurate and stable reference frequency standard that can be carried in a plane. The oscillator described in this paper will provide such a standard stable to one part per billion under extreme changes of ambient conditions such as temperature, humidity, vibration, and supply voltage. This precision compares favorably with that of the best ground stations and makes possible the measurement of distance with an accuracy better than one per cent during flight periods as long as eight hours. This paper describes the use of the oscillator as part of a navigational distance measuring instrument, together with a description of three important phases of the oscillator development: the oscillator circuit with high phase stability, the crystal oven maintaining the crystal temperature to ± 0.01 degree C, and the method of comparing the oscillator frequency with the Bell System Standard of Frequency to one part per ten billion.

Locked Oscillators in Frequency Standards and Frequency Measurements—J. K. Clapp

Locked oscillators can be used as frequency multipliers, dividers, and selectors. Different methods of locking an oscillator are briefly described with representative applications. An oscillator of extreme frequency stability and of precisely variable frequency is described. Such an oscillator is useful in studying very sharply resonant systems such as quartz crystal filters. A standard frequency multiplier, multiplying 0.1 mc to 1,000 mc, is described.

Measurement of the Carrier Frequency of RF Pulses—A. Bagley and D. Hartke

The problem of accurate determination of carrier frequency during short rf pulses is discussed. Several methods are described for making measurements from uhf to X-band, and typical results are given. By one method, a carrier frequency in the vicinity of 1,000 mc, which is modulated by 2.5 microsecond pulses at a 30-cycle repetition rate, is measured with an accuracy of ± 10 kc.

An Instrument for Precision Range Measurements—D. H. Beck

A calibrator for time delays, such as radar range, with a precision not heretofore obtained is described. The spacing accuracy of the generated reference pulse pairs is of the order of 10^{-8} seconds, over a range to 10,000 microseconds. A crystal oscillator provides several marker chains and synchronizes the repetition frequency generator. Gating circuits select a fixed and a variable pulse from the 10 microsecond chain. A three-decade electronic counter indicates the selected course delay in multiples of 10 microseconds. A vernier delay of up to 10 microseconds may be added which is produced by a directly calibrated phantastron. The device operates with triggered fast-writing oscilloscopes. Other applications are listed.

6 KMC Phase Measurement System for Traveling Wave Tubes—C. F. Augustine and A. Slocum

A method is presented for measuring phase shift at a frequency of six kilomegacycles with a precision of one-tenth degree. The technique of measurement is based on comparing the unknown phase shift with a precisely calibrated phase shifter. The talk covers the problems solved in designing the phase comparator and the calibrated adjustable phase standard. An application is presented which incorporates this method of measuring phase shift to detect level to phase conversion of traveling-wave tubes.

A New Precision X-Band Phase Shifter—E. F. Barnett

This paper describes a waveguide phase shifter of the rotary type which operates over the entire X-band guide range from 8,200 to 12,400 mc with a maximum error of about ± 2 degrees. The 90 and 180 degree differential phase sections consist of dielectric slabs together with cavities and grooves in the guide wall. Strips of resistive material are used to suppress resonances due to higher-order waveguide modes. The method used to calibrate this instrument is discussed, and curves showing the overall performance are given.

A Molecular Microwave Spectrometer, Oscillator and Amplifier—J. P. Gordon

An experimental device has been developed which can be used as a very high resolution microwave spectrometer, a microwave amplifier, or a very stable oscillator. It utilizes a beam of molecules, electrostatic focussing of certain states of these molecules, and a cavity in which radiation can occur and can be detected. The device amplifies microwaves as a result of interaction between radiation and the beam of molecules. As an amplifier, it has very narrow bandwidth and can give noise figures very close to unity. Sustained oscillations powered by induced emission from the molecules may be produced when the beam is sufficiently intense. Comparison of two such oscillators shows that they have a spectral purity of better than one part in 10^{11} and that frequency stabilities on the order of one part in 10^9 or 10^{10} can be fairly readily achieved.

Insertion Loss Test Sets Using Square Law Detectors—B. O. Weinschel

This paper discusses theory and errors, when measuring radio frequency attenuation, using imperfect square law detectors. The audio modulation of a radio frequency source is detected by the resistance modulation of a bolometer producing an audio frequency voltage. For ideal square law detectors, the varia-

tion of the audio frequency level in decibels, using a constant current source, is twice the decibel change of the radio frequency level. A theoretical analysis of the error due to deviation from square law is given. Experimental data regarding this error based on the static characteristic and independent experimental data relying upon differential rf measurements are furnished and are in agreement with the theory. Applying this error analysis to typical barretters, accuracies of .01 db are feasible for a measurement of a 20 db loss. A simple test set which has been reduced to practice is discussed. It permits rf loss measurements of 30 db with an accuracy of .1 db.

The Thermal Time Constant of a Bolometer
—G. U. Sorger

A convenient method for measuring r-f power ratios with audio frequency techniques is the following: r-f power is modulated with audio frequency and dissipated in a bolometer. The resistance of the bolometer changes then with the audio frequency and by feeding the bolometer with a constant dc current an ac

voltage across the bolometer is produced which is amplified and detected. The bolometer must be able to change its resistance sufficiently fast so it can follow the modulated power. This ability is limited by the thermal time constant of the bolometer. The first part of this paper deals with the theory of the time constant of bolometers, the second part discusses two methods of measurement and the third part treats a theory of multiple time constants including their distribution.

Medical Electronics

VOL. PGME-2, OCTOBER, 1955

Panel Discussion on Medical Electronics, Session XLI at the 1955 IRE National Convention

Telemetry and Remote Control

VOL. TRC-1, No. 3, AUGUST, 1955

A Message from the Chairman—C. H. Hoepner

Problems in Ultra-High-Speed Flight—H. L. Dryden

An Automatic Self-Verifying, Self-Correcting Data Transmission System—Ivan Flores
Function Generation on the Differential Analyzer Extended to the Analog Computer—D. F. Rearick

This paper discusses the technique of "generating" certain analytically-defined mathematical functions by continuously solving a differential equation having the desired function as solution. This principle was first applied to the mechanical differential analyzer, described in the first section. The characteristics of the differential analyzer and the electrical analog computer are compared, and extension of this function generating scheme to the latter machine is discussed. Methods are described for determining a differential equation yielding a given function as its solution. Finally, experimental results obtained on an analog computer are described.



Abstracts and References

Compiled by the Radio Research Organization of the Department of Scientific and Industrial Research,
London, England, and Published by Arrangement with that Department and the
Wireless Engineer, London, England

NOTE: The Institute of Radio Engineers does not have available copies of the publications mentioned in these pages, nor does it have reprints of the articles abstracted. Correspondence regarding these articles and requests for their procurement should be addressed to the individual publications, not to the IRE.

Acoustics and Audio Frequencies	134
Antennas and Transmission Lines	134
Automatic Computers	135
Circuits and Circuit Elements	135
General Physics	137
Geophysical and Extraterrestrial Phenomena	139
Location and Aids to Navigation	140
Materials and Subsidiary Techniques	140
Mathematics	142
Measurements and Test Gear	143
Other Applications of Radio and Electronics	144
Propagation of Waves	144
Reception	145
Stations and Communication Systems	145
Subsidiary Apparatus	145
Television and Phototelegraphy	145
Transmission	146
Tubes and Thermionics	146
Miscellaneous	148

The number in heavy type at the upper left of each Abstract is its Universal Decimal Classification number and is not to be confused with the Decimal Classification used by the United States National Bureau of Standards. The number in heavy type at the top right is the serial number of the Abstract. DC numbers marked with a dagger (†) must be regarded as provisional.

ACOUSTICS AND AUDIO FREQUENCIES

- 534.2 + [538.566:535.43] 3464
On the Scattering of Spherical Waves by a
Cylindrical Object—Wait. (See 3582.)

- 534.2** Sound Scattering and Transmission by Thin Elastic Rectangular Plates—J. Martinek and G. C. K. Yeh. (*Quart. J. Mech. appl. Math.*, vol. 8, Part 2, pp. 179-190; June, 1955.) Analysis is given for the case where the plate separates two fluid media and is excited to forced vibrations by the incident wave. The pressure in the scattered and transmitted waves is determined in terms of the characteristic parameters of the plate and of the two media.

- 534.2 The Attenuation of Sound in a Turbulent Atmosphere over a Desert Terrain—M. Mokhtar and M. A. Mahrous. (*Acustica*, vol. 5, pp. 179–181; 1955.)

- 534.213.4** **3467**
Attenuation of the (1, 0) and (2, 0) Modes
in Rectangular Ducts—A. M. Ghabrial.
(Acustica, vol. 5, pp. 187-192; 1955.) Report of
an experimental investigation using sound in
the frequency range 1.18-3.4 kc. The values
found for the attenuation constants are in
agreement with values deduced from Beatty's
theory (1045 of 1951).

- 534.23-14-8 3468
Sound Absorption in Liquids in Relation to their Specific Heats—S. Parthasarathy and D. S. Guruswamy. (*Ann. Phys., Lpz.*, vol. 16, pp. 31-42; June 15, 1955. In English.) A formula is derived relating the absorption to the specific heats for a frequency of 3 mcs.

The Index to the Abstracts and References published in the PROC. IRE from February, 1954 through January, 1955 is published by the PROC. IRE, April, 1955, Part II. It is also published by *Wireless Engineer* and included in the March, 1955 issue of that journal. Included with the Index is a selected list of journals scanned for abstracting with publishers' addresses.

- 534.232** 3469
Directivity and Mechanical-Impedance Characteristics of Cylindrical Acoustic Sources—M. Federici. (*Ricerca sci.*, vol. 25, pp. 1423–1430; June, 1955.) Analysis is given for a cylinder executing radial vibrations. The directivity characteristic is expressed as the product of a trigonometric function of cylinder height and a Bessel function of the radius. For cylinders long with respect to λ the mechanical impedance is expressed as the ratio between two Bessel functions of the radius. Results are shown graphically.

534.232-8:621.318.134 3470
Use of Ferrites in Ultrasonic Generators—U. Enz. (*Tech. Mitt. schweiz. Teleph.-Verw.*, vol. 33, pp. 209–212; June 1, 1955. In German.) The suitability of various ferrites as magnetostrictive generators is discussed in relation to measurements of their magnetic properties. Generators of various shapes are illustrated; the highest efficiency attained is 94 per cent. A radiated output as high as 1 kw/cm² is attainable in theory; in practice, limitations arise due to the inadequate mechanical strength of the ferrite and other causes. The strength can be increased by addition of PbO during preparation, or by pre-stressing. Possible applications are discussed.

534.3/4 3471
The Physical Structure of the Musical Signal—A. Moles. (*Rev. sci., Paris*, vol. 91, pp. 277–303; July/December, 1953.)

534.32:621.395.625 3472
The Subjective Discrimination of Pitch and Amplitude Fluctuations in Recording Systems—A. Stott and P. E. Axon. (*Proc. Instn. elect. Engrs.*, Part B, vol. 102, pp. 643–656; September, 1955.) Technique and equipment developed by the B.B.C. are described for making controlled tests of the threshold of perception of pitch and amplitude fluctuations, using musical or other program signals. The results enable frequency weighting characteristics to be defined which can be incorporated into instruments for measuring the magnitude of unwanted fluctuations in any kind of recording equipment.

534.613 3473
Use of a Bifilar Device as a Balance for measuring Acoustic Radiation Pressure—G. Laville. (*C. R. Acad. Sci., Paris*, vol. 241, pp. 465–467; August 1, 1955.)

534.84:534.6 3474
Measurements of the Reflection of Flexural Waves at Sudden Changes of Cross-Section of Rods—Mugiono. (*Acustica*, vol. 5, pp. 182–186; 1955. In German.) Report of a theoretical and practical investigation relevant to the propagation of flexural waves in building structures.

534.844 3475
Normal Modes and Reverberation—N. B. Bhatt. (*J. Instn. Telecommun. Engrs., India*, vol. 1, pp. 61–68; June, 1955.) Analysis is presented for reverberation in rooms with nonuniform distribution of absorption over the walls. For a room with one absorbing wall and the other walls perfectly reflecting, there exist two reverberation times corresponding respectively to sound propagated normal to and parallel to the absorbing wall, giving rise to a discontinuity in the decay characteristic.

534.86:621.396.712.3:621.395.625.3 3476
Artificial Reverberation—P. E. Axon, C. L. S. Gilford, and D. E. L. Shorter. (*Proc. Instn. elect. Engrs.*, Part B, vol. 102, pp. 624–640; September, 1955. Discussion, pp. 640–642.) The characteristics of artificial-reverberation apparatus using delay channels with overall feedback are discussed and illustrated by the results of early experiments with acoustic-delay tubes. Details are given of a magnetic-recording delay system used by the B.B.C.; the effective number of delay paths is greatly increased by use of a double recording track. Flutter effects associated with impulsive signals are reduced by use of a small auxiliary reverberation chamber.

621.395.616 3477
Stable Laboratory-Standard Capacitor Microphone—J. F. Houdek, Jr. (*Elect. Commun.*, vol. 32, pp. 75–81; June, 1955; *J. audio Engng. Soc.*, vol. 2, pp. 234–238; October, 1954.) A detailed description is given of a precision microphone of rugged construction, with a spring-loaded rear-electrode assembly, providing constant diaphragm tension.

621.395.616 3478
The Electrostatic Microphone—(*TSF et TV*, vol. 31, pp. 194–197; July/August, 1955.) Description of the French Type-515C high-quality capacitor microphone.

621.395.625.3:771.53 3479
Recent Developments in Magnetic Striping by the Lamination Process—R. F. Dubbe. (*J. Soc. Mot. Pict. Telev. Engrs.*, vol. 64, pp. 378–379; July, 1955.) Commercial equipment suitable for 8-mm and 16-mm films and operating at film speeds up to 125 ft/min is briefly described.

ANTENNAS AND TRANSMISSION LINES

621.315.21:621.372.2 3480
Scattering of Electrical Waves in Slightly Nonuniform Transmission Lines—M. Didlaukis. (*Arch. elekt. Übertragung*, vol. 9, pp. 269–271; June, 1955.) The form of the correlation function of the random deviations of the characteristic impedance is discussed and a Fourier-transformation method is developed.

for deducing the function from the measurable spectrum of the mean-square deviations of the input impedance.

621.315.212.1:621.372.21 3481

Comparative Study of Pulse Echoes due to Irregularities in Coaxial Cables—G. Comte, F. de Carfort, and A. Ponthus. (*Câbles & Transm.*, vol. 9, pp. 202–227; July, 1955.) An expression is given for the waveforms of echoes caused by sudden and by gradual impedance changes along the line. Testing equipment and typical test results are discussed; the importance of the test-pulse shape is indicated.

621.315.28:621.395.44 3482

A Transatlantic Telephone Cable—M. J. Kelly, G. Radley, G. W. Gilman and R. J. Halsey. (*Proc. Instn. elect. Engrs.*, Part B, vol. 102, pp. 717–719; September, 1955.) Discussion on 1547 of June.

621.372:621.317.336 3483

Transmission-Line Termination—J. M. C. Dukes. (*Wireless Engr.*, vol. 32, pp. 266–271; October, 1955.) The concepts presented previously (1255 of May) are extended and applied to the determination of the impedance of a line termination when measured through a mismatched junction between two dissimilar transmission lines.

621.372.8+621.372.413 3484

Theory of Imperfect Waveguides: the Effect of Wall Impedance—A. E. Karbowiak. (*Proc. Instn. elect. Engrs.*, Part B, vol. 102, pp. 698–708; September, 1955.) Analysis shows that although with circular waveguides all *E* and *H* modes are stable, with rectangular guides all *E* modes and higher-order *H* modes are unstable, only *H_o* modes propagating without change of form. Formulas are derived for calculating the propagation coefficients of waveguides with wall impedance and the bandwidth and resonance frequency of cavities with wall impedance.

621.372.8 3485

Irregular Waveguides with Slowly Varying Parameters—B. Z. Katsenelenbaum. (*C. R. Acad. Sci. U.R.S.S.*, vol. 102, pp. 711–714; June 1, 1955. In Russian.) The irregular waveguide is considered as a stepped waveguide made up of short sections of regular waveguides of different constant cross sections. The coefficients of the functions describing the field are connected by a system of linear differential equations of the first order. A method of solving the problem is developed for the simple case when *H* waves only are propagated, as in a conical junction in a circular waveguide.

621.372.8 3486

On the Theory of Disc-Loaded Waveguide—H. Derfler. (*Z. angew. Math. Phys.*, vol. 6, pp. 190–206; May 25, 1955. In English.) Theory based on the difference equation discussed previously (3438 of November) is presented.

621.372.8 3487

Note on the Properties of Two Functions appearing in the Theory of TM Wave Propagation through Periodically Iris-Loaded Guides—C. C. Grosjean. (*Nuovo Cim.*, vol. 1, pp. 1264–1266; June 1, 1955. In English.) Functions introduced previously (2832 of October) are discussed in detail.

621.372.8(083.74) 3488

IRE Standards on Antennas and Waveguides: Definitions for Waveguide Components, 1955—(PROC. IRE, vol. 43, pp. 1073–1074; September, 1955.) Standard 55 IRE 2.S1.

621.372.8:621.318.134 3489

Unusual Waveguide Characteristics associated with the Apparent Negative Permeability obtainable in Ferrites—G. H. B. Thompson.

(*Nature, London*, vol. 175, pp. 1135–1136; June 25, 1955.) With the ferrite magnetized in the same direction as that in which a right-handed circularly polarized plane wave of frequency 10 kmc is propagated, the effective permeability associated with the transverse field components may be negative, the wave then being evanescent. In a waveguide, this effect occurs for guide dimensions above a critical value; below this value the wave is propagated, but with negative group velocity. Experimental results are shown graphically for two circular waveguides with diameters respectively above and below the critical value.

621.372.8:621.318.134:538.6 3490

Figure of Merit for Microwave Ferrites at Low and High Frequencies—B. Lax. (*J. appl. Phys.*, vol. 26, p. 919; July, 1955.) The figure of merit for Faraday rotators comprising waveguides containing ferrites is defined as the ratio of rotation to attenuation and is equal to ωT , where *T* is the relaxation time constant of the ferrite. Theoretical estimates are made of losses at frequencies below about 3 kmc, and the figure of merit and low-frequency limits of operation are hence deduced. For a device with an insertion loss of 0.5 db this limit is about 1 kmc, and for a 1-db insertion loss about 500 mc. At 9 kmc the figure of merit of 120 for single crystals may define the upper limit.

621.396.67 3491

Multipoles and Schelkunoff Waves. The General Case—I. Ferrari. (*R.C. Accad. naz. Lincei*, vol. 18, pp. 623–630; June, 1955.) The analysis presented previously (27 of January and 2838 of October) is extended to deal with systems with more marked asymmetry.

621.396.67:621.317.3 3492

Measurements on Receiving Aerials: Part 1—I. Grosskopf. (*Arch. tech. Messen.*, no. 233, pp. 121–124; June, 1955.)

621.396.67:621.396.712 3493

F.M. Antenna Inside the A.M. Tower—M. W. Scheldorf and G. Klink, Jr. (*Electronics*, vol. 28, pp. 130–131; August, 1955.) A note describing the antenna arrangements at station WTOP.

621.396.67:621.396.81 3494

The Limits of Communication Reception using Antennas with Losses—M. Didlaukis. (*FernmeldeTech. Z.*, vol. 8, pp. 384–386; July, 1955.) An evaluation is made of the lowest value of field strength capable of being received in some telegraphy and df systems.

621.396.674.3:621.397.6 3495

V.H.F. Antennas for Television Broadcasting—G. J. Phillips. (*Proc. Instn. elect. Engrs.*, Part B, vol. 102, pp. 687–688; September, 1955.) Antennas have been designed by the B.B.C. using batwing elements in conjunction with masts of thickness comparable with λ ; arrangements suitable for (a) horizontal and (b) vertical polarization are described, for bands I and III. Antennas using systems split into an upper and lower half are also mentioned; the two halves are fed separately, thus avoiding the need for a reserve antenna.

621.396.677.3.029.63 3496

Metal-Foil "Fir-Tree" Antenna [dipole array] for Decimeter Wavelengths—H. Schneider. (*FernmeldeTech. Z.*, vol. 8, pp. 312–315; June, 1955.) Microstrip construction is used, the dipoles, feeders and reflectors being of copper foil stuck between two insulating sheets. For an array area 120×90 cm including 144 dipoles, half-power beam widths of 6 degrees and 9 degrees have been obtained at 13.6 cm λ . Dipole arrays produced by such methods may be economically comparable with mirror- and lens-type antennas.

621.396.677.43 3497

Radiation Resistance and Gain of Rhombic

Antennas, with Damping due to Radiation taken into Account Approximately—H. Zuhrt. (*Arch. elekt. Übertragung*, vol. 9, pp. 255–258; June, 1955.) The formulas derived are sufficiently accurate for most practical applications. Design curves are also given.

621.396.677.85 3498

Dielectric Lens for Microwaves—K. S. Kelleher and C. Goatley. (*Electronics*, vol. 28, pp. 142–145; August, 1955.) By varying the size and spacing of holes in laminated disks of dielectric material, a controlled variation of refractive index is obtained across the lens thus built up.

AUTOMATIC COMPUTERS

681.142

High-Speed Electronic-Analogue Computing Techniques—D. M. MacKay. (*Proc. Instn. elect. Engrs.*, Part B, vol. 102, pp. 609–620; September, 1955. Discussion, pp. 620–623.) An investigation has been made of the upper limits of speed conveniently attainable in various basic operations performed with a particular differential analyzer. With multidimensional displays and electronic programming a very large increase in information capacity is attainable in problems requiring systematic search processes for their solution.

681.142

A Mercury Delay Line Storage Unit—R. D. Ryan. (*J. Brit. Instn. Radio Engrs.*, vol. 15, pp. 419–427; August, 1955.) Reprint. See 2578 of 1954.

681.142

Magnetic Memory Device for Business Machines—S. J. Begun. (*Elect. Engng., N.Y.*, vol. 74, pp. 466–468; June, 1955.) Description of a device combining the short access time of a magnetic drum and the large storage capacity of the tape record.

681.142

Synchronizing Magnetic Drum Storage Speed—E. W. Bivans. (*Electronics*, vol. 28, pp. 140–141; August, 1955.) Synchronization to an acoustic delay line is obtained by a time-difference discriminator which controls the drum speed. An accuracy within $\pm 0.5 \mu s$ is achieved with a 10 per cent line-voltage variation.

681.142

Square-Law Circuit—K. S. Lion and R. H. Davis. (*Electronics*, vol. 28, pp. 192, 202; September, 1955.) A device for use as a multiplier in analog computers consists of a source producing a negative-going triangular waveform which is superposed on a positive-going input signal applied to a diode. The average value of the output voltage is proportional to the square of the input voltage.

681.142:621.383.2

Photoelectric Transformation of Mathematical Functions. Solution of Equations—G. Biet. (*Bull. Soc. franç. Élect.*, vol. 5, pp. 341–344; June, 1955.) An arrangement comprising a mirror galvanometer in combination with an appropriately shaped diaphragm and a photocell is used to generate a current $f(x)$ when the current x flows through the galvanometer. Elaboration of the arrangement to generate complex functions is discussed.

681.142:621.385.5

Binary Adder Tube for High-Speed Computers—Maynard. (See 3805.)

CIRCUITS AND CIRCUIT ELEMENTS

621.3:061.4

Interesting New Developments in the Components Industry at the Hanover Exhibition—(*Funk-Technik, Berlin*, vol. 10, pp. 294–297; June, 1955.)

- 621.314.22.011.23 3507
Stray Reactances in Power and Instrument Transformers—W. Knaack. (*Electrotech. u. Maschinensb.*, vol. 72, pp. 269–279, 291–298; June 15, and July 1, 1955.)
- 621.318.435:621.373.443 3508
Saturating Reactor Magnetic Pulser Design—E. M. Williams and R. A. Mathias. (*Elect. Engng., N.Y.*, vol. 74, p. 525; June, 1955.) Digest of paper to be published in *Trans. Amer. IEE*, Part I, *Communication and Electronics*, vol. 74, pp. 185–207; 1955. See also 2362 of 1951 (Melville).
- 621.318.57:621.3.042 3509
The Transfluxor—a Magnetic Gate with Stored Variable Setting—J. A. Rajchman and A. W. Lo. (*RCA Rev.*, vol. 16, pp. 303–311; June, 1955.) The transfluxor is a device comprising a magnetic core with two or more apertures, the core material having a nearly rectangular hysteresis loop. Switching and storage operations are performed by controlled transfer of the flux from leg to leg of the core. The operation of a two-aperture device is described in detail.
- 621.318.57:621.374.3:621.314.7 3510
[Junction-] Transistor Binary-Number Store for Pulse Operations—E. Munk and P. Batz. (*FernmeldeTech. Z.*, vol. 8, pp. 379–381; July, 1955.)
- 621.318.57:621.374.32 3511
The Design of Hard-Valve Binary Counters—D. M. Taub. (*Electronic Engng.*, vol. 27, pp. 386–392; September, 1955.) The method of design takes account of tolerances on component values, tube characteristics and supply voltages, and indicates modifications necessary when Se diodes are used in place of hot-cathode diodes for interstage coupling; it is valid at counting speeds up to several kc.
- 621.37 3512
The Relation between Standing-Wave Ratio and Bandwidth in Wide-Band Compensation of a Reactance—R. Merten. (*FernmeldeTech. Z.*, vol. 8, pp. 387–393; July, 1955.) Calculations are made for two different equivalent circuits representing a resistance accompanied by inherent reactance. The swr obtained when the compensated resistance is connected to a loss-free line with purely resistive characteristic impedance is used as a criterion of the compensation. The results are expressed as irrational algebraic functions which are presented as bandwidth curves. Simple relations are derived between the permissible swr and the bandwidth.
- 621.37:621.318.57 3513
The Folded Tree—A. W. Burks, R. McNaughton, C. H. Pollmar, D. W. Warren, and J. B. Wright. (*J. Franklin Inst.*, vol. 260, pp. 9–24, 115–126; July/August, 1955.) The problem of constructing circuits to perform certain functions, such as switching functions, is treated by representing the circuits by "vertex diagrams," of which the "folded tree" is a particular form.
- 621.372.029.64:538.569.4 3514
Revolutionary New Oscillator-Amplifier—Shunaman. (See 3583.)
- 621.372.412:549.514.51 3515
Effects of Impurities on Resonator Properties of Quartz—A. R. Chi, D. L. Hammond and E. A. Gerber. (*PROC. IRE*, vol. 43, pp. 1137; September, 1955.)
- 621.372.412:621.314.7 3516
Calculation of the Oscillation Frequency of a Quartz Crystal maintained by a Transistor—G. Briffod. (*C. R. Acad. Sci. (Paris)*, vol. 241, pp. 159–161, 458–459; July 11/August 1, 1955.) The calculation presented previously (1895 of July) is extended to the general case where it is required to determine both the influence of the maintaining system on the frequency and the possibility of aligning this frequency with a given reference frequency. Formulas are derived based on the use of capacitors in series and in parallel with the crystal.
- 621.372.413+621.372.8 3517
Theory of Imperfect Waveguides: the Effect of Wall Impedance—Karbowski. (See 3484.)
- 621.372.413 3518
Wide-Range Electronic Tuning of Microwave Cavities—F. R. Arams and H. K. Jenny. (*PROC. IRE*, vol. 43, pp. 1102–1110; September, 1955.) Analysis is presented for tuning by introducing into the cavity an electron beam with its direction parallel to the magnetic field, so that spiralling of the beam is produced. Measurements are reported indicating that the tuning range is much greater for a cavity containing a gas at low pressure than for an evacuated cavity.
- 621.372.44 3519
Series Resonance with Nonlinear Capacitor—J. C. Hoffmann. (*C.R. Acad. Sci. (Paris)*, vol. 241, pp. 180–182; July 11, 1955.) A graphical method is used to explain multiple resonance and hysteresis in a circuit tuned by a capacitor with a BaTiO₃ dielectric.
- 621.372.5 3520
Unambiguous Choice of Arrow Direction for Currents and Voltages in Quadrupoles with Applications to Directional Quadrupoles and Gyrators—M. J. O. Strutt. (*Arch. Elektrotech.*, vol. 42, pp. 1–5; June 20, 1955.) It is recommended that the positive direction of the voltage arrow should always point from positive to negative charge; with quadrupole diagrams, the output-current arrow should point away from the quadrupole. Simplifications of network analysis resulting from adoption of this convention are indicated.
- 621.372.5 3521
Conditions for Aperiodicity in Linear Systems—A. T. Fuller. (*Brit. J. appl. Phys.*, vol. 6, pp. 195–198; June, 1955.) The necessary and sufficient conditions are derived; when expressed in terms of the coefficients of the characteristic equation they take the form of a number of simple determinantal inequalities which are closely analogous to the Routh-Hurwitz stability criteria.
- 621.372.5 3522
Definition of the Ideal Transformer and the Ideal Gyrator by their Impedance-Transforming Properties—F. A. Fischer. (*FernmeldeTech. Z.*, vol. 8, pp. 309–311; June, 1955.) The fundamental difference between the two networks is that the input impedance of the ideal transformer is directly proportional to the load impedance, while for the ideal gyrator the proportionality is inverse. The ideal gyrator can be completely defined as a passive linear loss-free quadrupole with frequency-independent transforming properties.
- 621.372.5 3523
A New Method for investigating Linear Quadrupoles: Part 2—J. de Buij. (*FernmeldeTech. Z.*, vol. 8, pp. 335–340; June, 1955.) Continuation of work abstracted in 2864 of October. A distinction is made between elliptic, hyperbolic, parabolic and loxodromic quadrupoles.
- 621.372.5 3524
Two Network Theorems for Analytical Determination of Optimum-Response Physically Realizable Network Characteristics—S. S. L. Chang. (*PROC. IRE*, vol. 43, pp. 1128–1135; September, 1955.)
- 621.372.512.3:621.314.7 3525
How to Design I.F. Transistor Transformers—R. R. Webster. (*Electronics*, vol. 28, pp. 156–158, 160; August, 1955.) Design curves are given for single- and double-tuned units providing matching of collector and base impedances while meeting bandwidth and minimum-insertion-loss requirements.
- 621.372.54 3526
Symmetrical Lattice Filters—J. Oswald and J. Dubos. (*Câbles & Transm.*, vol. 9, pp. 177–201; July, 1955.) The calculation and field of utility of standard types of lattice filter are discussed and permissible approximations are indicated. Classification based on image parameters is proposed, on the lines of the system used in a previous paper on ladder filters [1710 of 1954 (Oswald)].
- 621.372.54 3527
Note on Antimetrical Lattice Filters with Successive Reactances of Alternate Sign—R. Leroy. (*Câbles & Transm.*, vol. 9, pp. 246–247; July, 1955.) A simplification of the treatment given by Oswald (64 of January).
- 621.372.543.3 3528
Notch Network Design—C. J. Savant, Jr., and C. A. Savant. (*Electronics*, vol. 28, p. 172; September, 1955.) Curves are given facilitating the design of bridged-T band-stop filters operating between equal impedances.
- 621.373 3529
The Period and Amplitude of the van der Pol Limit Cycle—E. Fisher. (*J. appl. Phys.*, vol. 25, pp. 273–274; March, 1954.) "The amplitude and period of the limit cycle of the van der Pol equation, $y + y = vy(1 - y^2)$, are found for all values of v by joining graphically the results of solutions about $v = 0$ and $v = \infty$."
- 621.373 3530
Limit-Cycle Period of Nonlinear Oscillation—J. Groszkowski. (*Bull. Acad. polon. Sci., Classe 4*, vol. 3, pp. 85–91; 1955. In English.) The problem is discussed with reference to previous work on the solution of the van der Pol equation $\ddot{x} + v(1 - x^2)\dot{x} + x = 0$. A formula is derived for the limit-cycle period which is applicable both for small and large values of v , corresponding respectively to quasi-sinusoidal and relaxation oscillations. Results obtained from various formulas are compared in a table.
- 621.373.42.029.42 3531
The Design and Performance of a Simple V.L.F. Oscillator—R. A. Seymour and J. S. Smith. (*Electronic Engng.*, vol. 27, pp. 380–384; September, 1955.) Using a Wien RC network for frequency control, the oscillator covers the range 0.01–100 c/s in finite steps, with a maximum output of 6 v rms into a 6-kΩ load.
- 621.373.43:621.385.15 3532
Secondary-Emission-Valve Pulse Generator with Cathode Output—R. Favre. (*Helv. phys. Acta*, vol. 28, pp. 167–171; May 31, 1955. In French.) A positive-feedback circuit giving a very low output impedance is used, capable of producing pulses of amplitude 50–60 v with rise time about 20 μs. By using a pentode as cathode load it is possible to obtain a wide variety of pulse waveforms. The arrangement gives a better performance than the ordinary blocking oscillator.
- 621.373.431.1:621.373.44 3533
Investigation of the Time Delay in the Triggering of a Pulse in a Monostable Multivibrator—G. Haas. (*Arch. elekt. Übertragung*, vol. 9, pp. 272–276; June, 1955.) Results of experiments indicate that a monostable multivibrator may be used as a pulse amplifier in applications where waveform distortion is unimportant. With pulse voltages above 100 mv the multivibrator used showed time delays of less than 10^{-8} sec and these were independ-

ent of pulse width over a wide range. The gain obtainable is about 500. Time delays in a free-running multivibrator are of the order of 10^{-8} to 10^{-6} seconds; this is shown theoretically to be due to the stray capacitances present.

621.373.444 3534
Triggered Microsecond Sweep Generators—D. P. C. Thackeray. (*Electronic Engng.*, vol. 27, pp. 397–401; September, 1955.) Hard-tube balanced-output and single-ended sweep generators are described using Miller integrator feedback for linearization; both are capable of providing a 450-v sweep in 1 μ s. Applications in high-speed photography are indicated.

621.374.3:621.314.7:621.318.57 3535
A Time-Delay Device using Transistors—G. F. Pittman, Jr. (*Elect. Engng., N.Y.*, vol. 74, pp. 498–501; June, 1955.) Pulse shaping and counting circuits are described in which junction transistors are used for switching, in conjunction with magnetic cores with rectangular hysteresis loops. The number of pulses required to saturate the core is such that long time delays can be produced. Published also in *Trans. Amer. IEE, Part I, Communication and Electronics*, vol. 74, pp. 54–58; March, 1955.

621.374.32 3536
High-Frequency Pulse Counter—R. Favre. (*Helv. phys. Acta*, vol. 28, pp. 179–184; May 31, 1955. In French.) A circuit based on the secondary-emission-tube pulse generator described in 3532 above.

621.374.4:621.375.3.029.3:621.395.2 3537
All-Magnetic Audio Amplifier—J. J. Suozzi and E. T. Hooper. (*Electronics*, vol. 28, pp. 122–125; September, 1955.) Three cascaded magnetic frequency triplers are used to provide a 10.8-kc carrier from a 400-c/line frequency. Used with a carbon microphone and a two-stage magnetic amplifier, the system gives an audio output power of 2.5 w, with linear operation over the range 90–3,000 c/s.

621.374.44:621.385.15 3538
Wide-Band Frequency Divider—R. Favre. (*Helv. phys. Acta*, vol. 28, pp. 172–178; May 31, 1955. In French. Addendum, *ibid.*, vol. 28, pp. 343–344; August 31, 1955.) A circuit for operation at frequencies up to 25 mc, based on the secondary-emission-tube pulse generator described in 3532 above.

621.375.121:621.372.542.2 3539
Design of Low-Pass Amplifiers for Fast Transients—G. Thirup. (*Phillips Res. Rep.*, vol. 10, pp. 216–230; June, 1955.) The proposed synthesis of an interstage coupling network for wide-band low-pass amplifiers is based on Darlington's design method (2742 of 1952). Some practical details are given of a 50-mc amplifier; experimentally determined phase and amplitude characteristics are presented graphically; oscillograms of the transient response are shown. Details are also given of the design of a phase-correction network.

621.375.13.018.3 3540
The Mechanism of Subharmonic Generation in a Feedback System—J. C. West and J. L. Douce. (*Proc. IEE, Part B*, vol. 102, pp. 569–574; September, 1955. Discussion, pp. 594–595.) Analysis is given for nonlinear feedback systems, using the description-function method. Subharmonics are produced as a result of modification of the response of the nonlinear element by the input signal. Conditions are derived for the absence of subharmonic oscillations. Theoretical and experimental results for a particular unit with an approximately cubic characteristic are in agreement.

621.375.2+621.373.4+621.317.3].029.6 3541
Disc-Seal Circuit Techniques—J. Swift. (*Proc. IRE (Australia)*, vol. 16, pp. 205–217,

247–260, 295–307; July/September, 1955.) A survey of amplifiers and oscillators using disk-seal tubes, and of associated microwave measurement methods.

621.375.221.2 3542

On Distributed Amplification—D. G. Sarmia. (*Proc. IEE, Part B*, vol. 102, pp. 689–697; September, 1955.) The response characteristics of a distributed amplifier can be improved by making the delay characteristics of the anode and grid lines different, this technique being termed "staggering." The improvement is illustrated by photographic records of the responses of experimental amplifiers.

621.375.223:621.372.543.2 3543

Filters with Very Narrow Pass Band variable on the Principle of the Fabry-Pérot Interferometer—G. Raoult and J. C. Pecker. (*C. R. Acad. Sci. (Paris)*, vol. 241, pp. 25–27; July 4, 1955.) Analysis is given for a narrow-band rf amplifier with n equal stages each comprising a tube and a three-mesh CR phase-shift network. Maximum gain is obtained at a frequency slightly different from that for which the phase shift is $2\pi n$. A relative bandwidth of 2×10^{-4} is attainable with 10 stages.

621.375.232 3544

Note on the Design of Wide-Band Low-Noise Amplifiers—D. Weighton. (*PROC. IRE*, vol. 43, pp. 1096–1101; September, 1955.) Methods of reconciling the design requirements for minimum noise factor and those for adequate bandwidth are discussed. The problem can be solved by equalization using either feedback or complementary networks. Some measurements on an experimental grounded-cathode amplifier with feedback are reported; satisfactory performance with bandwidths up to about 20 mc appears possible.

621.375.3 3545

Figure of Merit in Magnetic Amplifiers—J. T. Carleton and W. F. Horton. (*Tele-Tech & Electronic Ind.*, vol. 14, pp. 96–97, 170; June, 1955.) The figure of merit discussed is the ratio of power amplification to amplifier response time. It is useful as a basis for the comparison of amplifiers which are linear over the working range and have equal rated output powers.

621.375.4:621.314.7 3546

Transistor Operating Points—R. E. Skipper. (*Tele-Tech & Electronic Ind.*, vol. 14, pp. 104–105, 182; June, 1955.) A theoretical and experimental investigation is reported of the relation between the junction-transistor noise and gain and the collector-to-base voltage; the results are used in the design of a high-gain low-noise amplifier.

621.375.4:621.314.7 3547

Automatic Gain Control of Transistor Amplifiers—W. F. Chow and A. P. Stern. (*PROC. IRE*, vol. 43, pp. 1119–1127; September, 1955.) Satisfactory agc circuits can be designed based on variation of either emitter current I_e or collector voltage V_c . The required control power is very low if the variation of I_e or V_c is produced by varying the base current. Distortion may become a serious problem.

621.375.4:621.314.7 3548

Transistor Equivalent Circuits—Cocking. (See 3780.)

621.375.4.029.3 3549

Transistor-Equipped Light-Weight Programme-Input Amplifier Type V79—H. H. Lammers. (*Tech. Hausmitt. Nordw. Dtsch. Rdsfunks*, vol. 7, pp. 94–100; 1955.) An amplifier for a portable sound recorder is described. In the pre-amplifier the microphone is matched to the first transistor via a transformer. By use of current feedback in the first stage it is possible to connect without attenuation capacitance

microphones with terminal resistance $>1k\Omega$. The second stage includes a feedback circuit providing equalization up to 15 kc. The final stage is designed for an output of 32 mw. Shifting of the working point due to internal heating is reduced by use of a special stabilizing circuit.

621.374.3 3550

Millimicrosecond Pulse Techniques [Book Review]—I. A. D. Lewis and F. H. Wells. Publishers: McGraw-Hill, New York, and Pergamon Press, London, 1954, 310 pp., 40s. (*Science*, vol. 121, p. 826; June 10, 1955.) A survey with an excellent bibliography.

GENERAL PHYSICS

53.05

Note on Carpet Graphs—J. R. Ellis. (*Engineer*, (London), vol. 199, pp. 869–870; June 24, 1955.) Description of a method developed at the National Physical Laboratory for presenting information concerning three variables in a single combined graph.

535.376

Theory of Electroluminescence—W. W. Piper and F. E. Williams. (*Phys. Rev.*, vol. 98, pp. 1809–1813; June 15, 1955.) On the basis of the threshold value of the field necessary to excite luminescence, the following three possible mechanisms are discussed: (a) direct ionization of impurity systems by the field; (b) acceleration of conduction electrons or valence-band holes to velocities sufficient to produce excitation by inelastic collisions; (c) injection of charge carriers.

535.6

Empirical Relationships with the Munsell Value Scale—J. H. Ladd and J. E. Pinney. (*PROC. IRE*, vol. 43, p. 1137; September, 1955.) A discussion relevant to the establishment in color television of an equal-step grey scale.

535.6.08

The Specification of Colours based on Measurements with the Trichromatic Colorimeter—F. Blottiau. (*Cah. Phys.*, No. 54, pp. 37–52; February, 1955.)

537.22

A General Mathematical Treatment applicable to certain Electrode Systems—G. Power. (*Brit. J. appl. Phys.*, vol. 6, pp. 245–247; July, 1955.) Formulas are developed for a basic system of two coaxial dielectric cylinders of different homogeneous and isotropic media containing an embedded line charge. These are applied to determine the fields in a circular-cylinder electrode system, the results being expressed as series converging reasonably rapidly. Other electrode systems considered are a semi-infinite strip, an elliptic cylinder, and a parabolic cylinder.

537.311.1

On the Theory of Plasma Oscillations in Metals—H. Kanazawa. (*Progr. theor. Phys.*, Osaka, vol. 13, pp. 227–242; March, 1955.) The effect of the crystal lattice on plasma oscillations is investigated on the basis of quantum mechanics. See also 1023 of 1954 (Wolff) and 1613 of June (Hubbard).

537.311.33:535.35

Application of the Method of Generating Function to Radiative and Nonradiative Transitions of a Trapped Electron in a Crystal—R. Kubo and Y. Toyozawa. (*Progr. theor. Phys.*, Osaka, vol. 13, pp. 160–182; February, 1955.) See also 3449 of 1952 (Kubo).

537.52

Measurement of the Statistical Time Lag of Breakdown in Gases and Liquids—R. F. Saxe and T. J. Lewis. (*Brit. J. appl. Phys.*, vol. 6, pp. 211–216; June, 1955.)

- 537.525:538.56.029.6** 3559
The Direct Current associated with Micro-wave Gas Discharge between Coaxial Cylinders: Part 4 —K. Mitani. (*J. phys. Soc. (Japan)*, vol. 10, pp. 391-397; May, 1955.) Measurements made by a double-probe method give results in good agreement with theory. Part 3: *ibid.*, vol. 8, pp. 642-645; September/October, 1953.
- 537.525:538.56.029.6** 3560
Investigation of High-Frequency Discharge by Method of Probes—Kh. A. Dzherpetov and G. M. Pateyuk. (*Zh. eksp. teor. Fiz.*, vol. 28, pp. 343-351; March, 1955.) The methods used by Banerji and Ganguli (*Phil. Mag.*, vol. 11, pp. 410-422; February, 1931) and by Beck (*Z. Phys.*, pp. 355-375; October 18, 1935) were compared experimentally; the results obtained in the two cases were similar. A study was also made of the temperature, concentration of electrons and potential along the axis of the discharge tube at various pressures between about 0.1 and 1 mm Hg of H₂, Ar, and Ne at frequencies of the order of 100 mc; the distribution was found to depend on the gas pressure, the diameter of the tube and the hf field strength. Results are presented graphically.
- 537.525.5** 3561
Retrograde Motion in Gas Discharge Plasmas—K. G. Hernqvist and E. O. Johnson. (*Phys. Rev.*, vol. 98, pp. 1576-1583; June 15, 1955.) A phenomenon observed in cylindrical diodes operating in the ball-of-fire mode [959 of 1952 (Malter et al.)] is discussed.
- 537.525.8** 3562
Diffusion in Moving Striations—V. D. Farris. (*Proc. phys. Soc.*, vol. 68, pp. 383-385; June 1, 1955.) A digest is presented of a thesis developing a diffusion theory of striations and testing the theory with experimental results reported by Pupp (*Phys. Z.*, vol. 36, pp. 61-69; January 15, 1935.)
- 537.525.8** 3563
Field Measurements in Glow Discharges with a Refined Electron-Beam Probe and Automatic Recording—R. Warren. (*Phys. Rev.*, vol. 98, pp. 1650-1658; June 15, 1955.)
- 537.525.8** 3564
Interpretation of Field Measurements in the Cathode Region of Glow Discharges—R. Warren. (*Phys. Rev.*, vol. 98, pp. 1658-1664; June 15, 1955.)
- 537.533/.534** 3565
Self-Focusing Streams—W. H. Bennett. (*Phys. Rev.*, vol. 98, pp. 1584-1593; June 15, 1955.) A restatement of the theory of magnetic self-focusing of streams comprising a mixture of ions and electrons. See also 126 of January (Bennett and Hulbert).
- 537.533/.534:538.691** 3566
The Theoretical Possibility of separating Beams of Charged Particles having Different Polarizations in a Magnetic Field—V. V. Vladimirska. (*C.R. Acad. Sci. U.R.S.S.*, vol. 102, pp. 1099-1100; June 21, 1955. In Russian.) It is shown that a separation of beams such as is obtained in the Stern-Gerlach experiment can theoretically be obtained also in the case of charged particles.
- 537.533:539.211** 3567
Electron Emission and Other Phenomena on Freshly Disturbed Metal Surfaces—L. Grunberg. (*Research*, (London), vol. 8, pp. 210-214; June, 1955.) A general account of the effects and methods of observing them using an open-ended Geiger counter or a photographic plate. See also 2301 of 1953 (Kramer).
- 537.533.7** 3568
A Note on the Diffusion in a Gas of Electrons from a Small Source—L. G. H. Huxley and R. W. Crompton. (*Proc. phys. Soc.*, vol. 68, pp. 381-383; June 1, 1955.)
- 537.533.7:538.63** 3569
Experimental Investigation of the Motions of Electrons in a Gas in the Presence of a Magnetic Field—B. I. H. Hall. (*Proc. phys. Soc.*, vol. 68, pp. 334-341; June 1, 1955.) The aim of this investigation was to verify the theory given by Huxley and Zaazou (*Proc. roy. Soc. A*, vol. 196, pp. 402-426; April 7, 1949.)
- 537.533.8** 3570
Secondary Electron Emission—S. Rodda. (*Nature*, (London), vol. 175, pp. 1112-1114; June 25, 1955.) Report of colloquium held at the Institute of Physics in March, 1955.
- 537.533.8** 3571
Secondary Electron Emission by Primary Electrons in the Energy Range of 20 keV to 1.3 MeV—B. L. Miller and W. C. Porter. (*J. Franklin Inst.*, vol. 260, pp. 31-39; July, 1955.) Experiments were made using a primary beam from a small linear accelerator, after passage through a magnetic analyzer, and targets of various metals. The secondaries comprised two groups, one with energy mainly <30 ev and the other, possibly elastically scattered, with high energies. Curves show both the total secondary emission and the high-energy component as functions of primary voltage for various target metals; for a gold target the energy spectrum of the low-velocity secondaries is investigated. Another graph shows the high-energy components plotted against the atomic number of the target metal. Some experiments with insulator targets are briefly reported.
- 537.533.8:621.38.032.11** 3572
A Demountable Vacuum System for Secondary-Emission Studies—A. Lempicki. (*J. sci. Instrum.*, vol. 32, pp. 221-223; June, 1955.)
- 537.56** 3573
The Growth of an Electron Avalanche retarded by its Own Space Charge—G. Francis. (*Proc. phys. Soc.*, vol. 68, pp. 369-380; June 1, 1955.) The calculation presented shows how the ionization coefficient α and the total multiplication in the avalanche vary with the distance traveled when the positive ions formed have an appreciable effect. The time taken for an avalanche to develop is also calculated. The cases of (a) constant field at electrodes, and (b) constant potential between them are considered, assuming plane parallel geometry.
- 537.56** 3574
Passage of Charged Particles through Plasma—J. Neufeld and R. H. Ritchie. (*Phys. Rev.*, vol. 98, pp. 1632-1642; June 15, 1955.) A phenomenological approach is used to examine the behavior of a dispersive plasma and determine its response to an external disturbance, in particular that created by a moving point charge. The validity of this approach is discussed. An analysis is made of the field and the polarization charge density produced by an incident particle and the effectiveness of the plasma in stopping the particle.
- 537.56** 3575
Microwave Study of Positive-Ion Collection by Probes—G. J. Schulz and S. C. Brown. (*Phys. Rev.*, vol. 98, pp. 1642-1649; June 15, 1955.) The electron density in a plasma is determined from the shift in resonance frequency of a cavity in which a discharge is maintained. The results are used to verify theory of positive-ion collection by negatively biased or double probes. Experiments were performed in H, Ar and He at pressures from 0.05 to 6 mm Hg. Agreement between experimental and theoretical results is good at the lower pressures; at high pressures the probe collected about twice the current predicted by theory.
- 538.3** 3576
A Short Modern Review of Fundamental Electromagnetic Theory—P. Hammon. (*Proc. IEE, Part B*, vol. 102, pp. 716-717; September, 1955.) Further discussion on 97 of January.
- 538.3:52** 3577
Magneto-Hydrodynamics—V. C. A. Ferraro. (*Nature*, (London), vol. 176, pp. 234-237; August 6, 1955.) Report of a Royal Society discussion held in May, 1955.
- 538.3:538.6** 3578
Electromagnetic Field Equations for a Moving Medium with Hall Conductivity—J. H. Piddington. (*Mon. Not. R. astr. Soc.*, vol. 114, pp. 638-650; 1954.) The well known equation representing the electromagnetic field in a moving isotropic conductor is adapted to treat the case of an anisotropic conductor, such as an ionized gas moving in a strong magnetic field, by introducing a tensor conductivity. The modified equation is used to analyze astrophysical problems, including the propagation of magnetohydrodynamic waves.
- 538.56:538.6** 3579
The Motion of Ionized Gas in Combined Magnetic, Electric and Mechanical Fields of Force—J. H. Piddington. (*Mon. Not. R. astr. Soc.*, vol. 114, pp. 651-663; 1954.) "Transient electric and mechanical forces uniform in space are applied to a gas in the presence of a steady magnetic field. The current transport equation for the anisotropically conducting medium is used to determine the subsequent motion of the gas, the internal electric field and the current density. These are damped oscillatory functions leading to a steady state. There is a close connection between the effects of the electric and mechanical forces: a steady internal electric field perpendicular to the magnetic field cannot exist unless accompanied by a mechanical force. The relationship between the two is examined."
- 538.56.029.6** 3580
Cerenkov Radiation and its Applications—J. V. Jelley. (*Brit. J. appl. Phys.*, vol. 6, pp. 227-232; July, 1955.)
- 538.566** 3581
Reflection at Arbitrary Incidence from a Parallel Wire Grid—J. R. Wait. (*Appl. sci. Res.*, vol. B4, pp. 393-400; 1955.) The analysis presented is valid for any direction of polarization, angle of incidence or value of wire conductivity.
- 538.566:535.43]+534.2** 3582
On the Scattering of Spherical Waves by a Cylindrical Object—J. R. Wait. (*Appl. sci. Res.*, vol. B4, pp. 464-468; 1955.) Analysis indicates that the ratio of the amplitude of the scattered field for a spherical incident wave to that for a plane wave is equal to $[p_0/(p_0 + p)]^2$, where p_0 is the distance of the source and p that of the observer from the cylinder axis.
- 538.569.4:621.372.029.64** 3583
Revolutionary New Oscillator-Amplifier—F. Shunaman. (*Radio-Electronics*, vol. 26, pp. 56-57; June, 1955.) Short simplified description of the "maser" (name derived from "microwave amplification by stimulated emission of radiation"). See also 100 of January (Gordon et al.).
- 538.569.4.029.6:535.33.08** 3584
A Microwave Spectrometer and its Applications to some Organic Molecules—G. Erlandsson. (*Ark. Fys.*, vol. 9, pp. 399-434; May 13, 1955.) A Stark-modulated microwave spectrometer operating in the frequency range 12-25 kmc is described in detail; circuit diagrams are given. Spectra of several asymmetric-top molecules have been investigated.
- 538.569.4.029.6:538.61** 3585
Some Magneto-optical Phenomena connected with the Molecular Resonance of Gases

at Microwave Frequencies—A. Gozzini. (*J. Phys. Radium*, vol. 16, pp. 357-359; May, 1955.) The production of birefringence and Faraday rotation is discussed quantitatively with particular reference to NH₃.

GEOPHYSICAL AND EXTRATERRESTRIAL PHENOMENA

52:538.3 3586
Magneto-Hydrodynamics—Ferraro. (See 3577.)

523.16 3587
New Science of Radio Astronomy—B. J. Bok. (*Sci. Mon.*, vol. 80, pp. 333-345; June, 1955.) A review of research methods and results, based on an address delivered to the American Association for the Advancement of Science.

523.16 3588
The Spatial Distribution and the Nature of Radio Stars—M. Ryle and P. A. G. Scheuer. (*Proc. roy. Soc. A*, vol. 230, pp. 448-462; July 12, 1955.) Data obtained from a survey of radio stars by Shakeshaft et al. (to be published in *Mem. R. astr. Soc.*) are analyzed. The results indicate an apparent increase in the spatial distribution density with distance in all directions. A reasonable interpretation of the results cannot be provided unless most of the stars are assumed to be outside the galaxy.

523.16 3589
An Alternative Identification of the Radio Source in the Direction of the Galactic Centre—R. D. Davies and D. R. W. Williams. (*Nature, Lond.*, vol. 175, pp. 1079-1081; June 18, 1955.) An attempt has been made to determine the distance of the radio source observed e.g., by McGee and Bolton (2932 of 1954) from the absorption by interstellar hydrogen at 1.42 kmc. The results suggest that this source is considerably closer than the galactic nucleus.

523.16 3590
Radio Emission from Jupiter—(*Nature, Lond.*, vol. 175, p. 1074; June 18, 1955.) Brief report of reception at Seneca, Maryland, of radiation on 22 mc; a large cross antenna was used of the type developed by Mills [see e.g., 633 of 1954 (Mills and Little)]. The effect in a broadcast receiver was similar to that with thunderstorm interference. See also 2933 of October (Burke and Franklin).

523.16 3591
Radio Waves from the Planet Jupiter and a Cosmogenic Hypothesis—Q. Majorana. (*R.C. Accad. naz. Lincei*, vol. 18, pp. 577-580; June, 1955.) The reported observation of radiation at about 22 mc [2933 of October (Burke and Franklin)] is discussed in relation to theories concerning physical conditions on Jupiter. It is suggested that Saturn may also emit radio waves, but with lower intensity. Theoretical considerations indicate that astral heat and light may be a direct effect of the gravitational force.

523.5:537.56 3592
Meteor Radiation, Ionization and Atomic Luminous Efficiency—E. J. Öpik. (*Proc. roy. Soc. A*, vol. 230, pp. 463-501; July 12, 1955.) A theoretical paper; empirically constructed tables are presented for calculating the radiation from meteors.

523.72:550.385 3593
Corpuscular Streams—R. C. Jennison. (*Observatory*, vol. 75, pp. 125-126; June, 1955.) Solar emission of particles giving rise to variations of the geomagnetic field [2494 of 1952 (Kiepenheuer)] is discussed. If the stream of particles is borne in the wake of a shock wave with a velocity of the order of 1500 km, complete transport of material from the sun to the

earth need not be postulated. The steep nature of the shock front is consistent with the sudden commencement of magnetic storms.

523.746 3594
Provisional Determination of the Mean Length of the 80-Year Sunspot Cycle—W. Gleissberg. (*Naturwiss.*, vol. 42, p. 410; July, 1955.) Analysis of available data shows that during the past 16 centuries the duration of the 80-year cycle has fluctuated between five and eleven 11-year cycles, the mean being (7.1 ± 0.3) 11-year cycles; taking the mean duration of the 11-year cycle as 11.1 years, this corresponds to a range 75.5-82.1 and a mean value 78.8 years.

523.75:550.385:537.591 3595
Solar Flare and Magnetic Storm Effects in Cosmic-Ray Intensity near the Geomagnetic N Pole—J. W. Graham and S. E. Forbush. (*Phys. Rev.*, vol. 98, pp. 1348-1349; June 1, 1955.) Phenomena observed during and following the solar flare of July 25, 1946 are discussed. If the observed increase in cosmic-ray intensity was due to charged particles from the sun, the trajectories must have been strongly affected by factors other than the geomagnetic field.

550.372 3596
Measurement of Soil Conductivity by the Wave-Tilt Method—S. C. Mazumdar. (*J. Instn. Telecommun. Engrs., India*, vol. 1, pp. 76-83; June, 1955.) Description of the experimental arrangement and report of results obtained in the vicinity of Delhi.

550.38 3597
Geomagnetism—(*Indian J. Met. Geophys.*, vol. 5, Special Number, pp. 1-242; December, 1954.) This special number commemorates the golden jubilee of the Alibag observatory. The 30 papers presented include the following:
The Contrast between Geomagnetic S and L at Huancayo—J. Bartels (pp. 69-74).
Characteristics of Polar Magnetic Storms—T. Nagata and N. Fukushima (pp. 75-88).
Ionospheric Magnetic Fields during Marked Decreases in Cosmic Rays—S. E. Forbush and E. H. Vestine (pp. 113-116).
Magnetohydrodynamic Waves and Solar Prominences—H. Alfvén (pp. 133-136).
Auroral Activity at Medium Latitudes—A. Vassy and E. Vassy (pp. 137-140). In French.
Solar Radiation in the Far Ultraviolet and some Related Geophysical Phenomena—A. K. Das (pp. 141-152).
On the Emission of Electric Currents from the Sun—V. C. A. Ferraro (pp. 157-160).
Sunspots and Geomagnetic Variation—S. K. Pramanik and M. K. Ganguli (pp. 161-178).
Magnetic Storms and Solar M Regions—P. K. Sen Gupta (pp. 179-188).
The Dynamo Action of the Diurnal Atmospheric Oscillation—R. Pratap. (pp. 189-194).
Recurrence Tendency of Geomagnetic Activity during the Current Sunspot Minimum—A. M. Naqvi and B. N. Bhargava (pp. 195-202).
Some Remarks on the Equatorial Electrojet, as revealed by the Analysis of Solar Flare Effects—J. Veldkamp and J. G. Scholte (pp. 203-212).
Geomagnetic Records at Colaba and Alibag on Days of Solar Eclipse—S. L. Malurkar. (pp. 213-220).

Some others are abstracted individually.

550.380.8 3598
Apparatus for Measurement of the Intensity of the Terrestrial Magnetic Field—R. Birebent. (*C.R. Acad. Sci., Paris*, vol. 241, pp. 368-369; July 25, 1955.) An adaptation of the device described previously (2367 of August).

550.385

Notes on the Theory of Magnetic Storms—S. Chapman. (*Indian J. Met. Geophys.*, vol. 5, Special Number, pp. 33-40; December, 1954.) "A non-mathematical account is given of the model problems and their solutions, by which Chapman and Ferraro have sought to illustrate some aspects of the theory of magnetic storms. These problems are here used to develop a qualitative solution of the motion of an infinite neutral ionized plane sheet of gas (or of a succession of such sheets) towards a unidirectional magnetic field whose intensity decreases as an inverse power of the distance from an axis to which the sheet is parallel. The gas in the center approaches to a minimum distance from the axis and then recedes again. The gas far to either side moves onward with little distortion. Between these central and outer parts there are two strips of the sheet whose ions and electrons separate from each other, under the influence of the magnetic field; partly because these strips become much extended and reduced to low density. Some charges are deviated away to infinity, others are captured by the field and build up a 'westward' electric current to which is ascribed the main phase of a magnetic storm."

550.385:551.510.535

The Relation between the Geomagnetic Field and Range Disturbance in Various Latitudes—R. P. W. Lewis and D. H. McIntosh. (*Indian J. Met. Geophys.*, vol. 5, Special Number, pp. 51-62; December, 1954.) Analysis of observations leads to a theory of the mechanism of magnetic disturbances intermediate between the classical theory and that advanced by Nikolsky (3897 of 1947). The true storm-time effect is greatest at the equator; an additional effect comprising instantaneous response to and recovery from the disturbance is greatest in the auroral zone. The effect on the ionosphere at high latitudes is briefly considered.

551.51:061.3

Assembly of the International Union for Geodesy and Geophysics, Rome 1954—(*Ann. Geophys.*, vol. 11, pp. 115-248; April/June, 1955.) The text is given of 11 papers, most of them in English, dealing with the structure of the atmosphere and especially with research by means of rockets since 1946.

551.510.53

Dissociation of Oxygen in the Upper Atmosphere—E. T. Byram, T. A. Chubb, and H. Friedman. (*Phys. Rev.*, vol. 98, pp. 1594-1597; June 15, 1955.) The O₂ content of the atmosphere at heights between 110 and 130 km was determined by measuring the transmission of solar radiation in the wavelength band from 1425 to 1500 Å, using an ultraviolet photon counter in a rocket. At 130 km the O₂ concentration was 10%/cm³, indicating that 12 per cent of the atmospheric oxygen was still undissociated.

551.510.535

Determination of the True Distribution of Electron Density in the Ionosphere: Part 1—W. Becker. (*Arch. elekt. Übertragung*, vol. 9, pp. 277-284; June, 1955.) A survey leads to the conclusion that existing methods of investigating the electron-density distribution are either too inaccurate or too complicated for routine use. 51 references.

551.510.535

Resonance Absorption of Sunlight in Twilight Layers—T. M. Donahue and R. Resnick. (*Phys. Rev.*, vol. 98, pp. 1622-1625; June 15, 1955.) Calculations are made relevant to the determination of the thickness of the atmospheric sodium layer, which appears to be located at a height between 70 and 115 km.

- 551.510.535** 3605
New Representation of the Longitude Effect in the Ionosphere F₂ Layer—F. Deloboue. (*C.R. Acad. Sci., Paris*, vol. 241, pp. 439–441; July 25, 1955.) The representation is based on a chart with geographic latitude as abscissa and magnetic latitude as ordinate. On plotting the positions of existing ionospheric stations the need for stations in certain regions is demonstrated, particularly for stations with south geographic and north magnetic latitude.
- 551.510.535** 3606
Simultaneous Fluctuations of the F₂-Layer Ionization at Two Widely Spaced Observation Stations—O. Burkard. (*Öst. Z. Telegr. Teleph. Funk Fernsehtech.*, vol. 9, pp. 57–59; May /June, 1955.) Observations of short-term variations of f_0F_2 at Graz in Austria and at Cape-town in S. Africa during January, 1953 are compared. Correlation factors up to 0.725 were obtained for values observed at the same universal time, but the correlation decreases rapidly as the time difference between the measurements increases. The results support the view that the ionizing radiation itself undergoes short-term fluctuations.
- 551.510.535** 3607
The Ionospheric F₂ Layer over India in Minimum Sunspot Year 1953—K. R. Ramanathan and K. M. Kotadia. (*Indian J. Met. Geophys.*, vol. 5, Special Number, pp. 117–122; December, 1954.) A summary of observations made at various stations in India.
- 551.510.535** 3608
A Singular Echo Trace observed in Ionograms from the Kerguelen Islands Station—R. Busch and A. Luchet. (*C.R. Acad. Sci., Paris*, vol. 241, pp. 507–509; August 1, 1955.) Traces have been obtained indicating reflections from a layer at a height of 48–55 km in summer and 55–65 km in winter, corresponding to the temperature-maximum region at the upper boundary of the ozone layer. The results are in agreement with those of Major (3252 of November).
- 551.510.535:621.396.812.3.029.55** 3609
Investigation of Vertical Movements of the F₂ Layer—N. V. G. Sarnia. (*Curr. Sci.*, vol. 24, pp. 190–191; June, 1955.) Calculations based on observations of the rate of fading of 4.92-mc signals and simultaneous independent determinations of E layer vertical movements confirm that the vertical drift velocity of the F₂ layer at morning and evening is greater than that of the E layer.
- 551.594.5** 3610
Diurnal Variation in Auroral Activity—N. C. Gerson. (*Proc. phys. Soc.*, vol. 68, pp. 408–414; July 1, 1955.) An analysis of amateur-radio contacts during the period 1949–1951, using vhf transmissions incident obliquely to the ionized aurora, is compared with results obtained by radio soundings at normal incidence. Auroral activity shows a strong maximum at 2100 hours local time, with 86 per cent of the total occurrences between 1700 and 2400 hours.
- 523.16** 3611
Radio Astronomy. [Book Review]—J. L. Pawsey and R. N. Bracewell. Publishers: Geoffrey Cumberlege, Clarendon Press, Oxford, 1955, 354 pp., 55s. (*J. Brit. Instn. Radio Engrs.*, vol. 15, p. 11; August, 1955.) Intended primarily for physicists and astronomers.
- 523.5:621.396.96** 3612
Meteor Astronomy. [Book Review]—A. C. B. Lovell. Publishers: Clarendon Press, Oxford; Oxford University Press, London, 1954, 463 pp., 60s. (*Nature* (London), vol. 176, pp. 135–136; July 23, 1955.) A comprehensive up-to-date survey indicating the importance of radio techniques.
- 523.7** 3613
The Sun (The Solar System—Vol. 1). [Book Review]—G. P. Kuiper (Ed.). Publishers: University of Chicago Press, Chicago, and Cambridge University Press, London, 1953, 745 pp., 94 s. (*Nature* (London), vol. 176, p. 5; July 2, 1955.) Chapters on the various aspects of the subject are contributed by acknowledged leaders in the field, to produce a reference book for the specialist and a useful survey for the nonspecialist.
- 551.510.535:621.396.11** 3614
The Physics of the Ionosphere. [Book Notice]—Publishers: The Physical Society, London, 1955, 406 pp., 40s. (*J. Brit. I.R.E.*, vol. 15, p. 11; August, 1955.) A collection of 50 papers presented at the Physical Society Conference held at Cambridge, England, in September, 1954.
- LOCATION AND AIDS TO NAVIGATION**
- 621.396.96:535.37:551.46** 3615
Radar and Phosphorescence at Sea—B. Hilder. (*Nature* (London), vol. 176, pp. 174–175; July 23, 1955.) Mariners' observations of phosphorescence apparently stimulated by radar are reported and discussed.
- 621.396.96:621.374.3** 3616
Target Discriminator for Countermeasures—M. Weiss and S. R. Sixbey. (*Electronics*, vol. 28, pp. 118–120; August, 1955.) A voltage-difference discriminator driven by the output from a logarithmic amplifier provides a device capable of discriminating between input voltage pulses of amplitudes in the ratio of 5 to 4, and independent of pulse width, repetition rate and absolute pulse amplitude.
- 621.396.96.029.65:551.578** 3617
Measurements of the Effect of Rain, Snow and Fogs on 8.6-mm Radar Echoes—N. P. Robinson. (*Proc. IEE, Part B*, vol. 102, pp. 709–714; September, 1955.) Measurements of the attenuation caused by rain and of the back-scattered radiation agreed well with predictions from theory. The echo intensity from fog was too low to be detected, but measurements of the attenuation of echoes from a corner reflector in fogs of different thicknesses were of the same order as the predicted values. The attenuation caused by moist snow was $\frac{1}{2}$ times that caused by rain with a similar precipitation rate. The echo intensity from the "radar bright band" composed of melting snow was 14–19 db greater than that from the dry snow above and 2–8 db greater than that from the rain below.
- MATERIALS AND SUBSIDIARY TECHNIQUES**
- 533.56** 3618
The Final Vacua of Oil Diffusion Pumps—R. F. Coe and L. Riddiford. (*J. sci. Instrum.*, vol. 32, pp. 207–213; June, 1955.) Measurements of the vapor pressures of apiezon C, octoil S, DC 703 and some other oils by various methods are compared with final pressures measured with both ionization and Knudsen gauges. The residual molecules are decomposition products of the oil and vary with the type of oil; their average molecular weight is less than that of the oil.
- 535.215:546.482.21:539.231** 3619
Production of Light-Sensitive Cadmium-Sulphide Films by Cathode Sputtering—G. Helwig and H. König. (*Z. angew. Phys.*, vol. 7, pp. 323–325; July, 1955.) The deposition of photoconductive CdS films on glass by sputtering Cd in an atmosphere of H₂S and an inert gas is described. The ratio of current at an illumination of 1000 lux to the dark current is of the order of 10^4 to 10^5 .
- 535.37:546.472.21** 3620
Laws of Decay of Afterglow in Zinc-
- Sulphide Phosphors in Region of Temperature Quenching**—F. I. Vergunas and N. L. Gasting. (*Zh. eksp. teor. Fiz.*, vol. 28, pp. 352–360; March, 1955.) An experimental investigation is reported on ZnS-Cu, ZnS-(Cu, Co), and ZnS-Zn phosphors. In all cases the decay of afterglow varied with temperature up to quenching temperature and with the intensity of the exciting light. As the temperature increased, the hyperbolic curve representing the early stages of the characteristic changed into an exponential curve; simultaneously, the hyperbolic curve representing the later stages of the decay shrank, so that at high temperatures the whole of the decay curve was approximately exponential. Corresponding results were obtained for the effect of intensity and duration of excitation. Results are presented graphically.
- 535.376** 3621
Alternative Explanation of the Weymouth-Bitter Experiments—L. Burns. (*Phys. Rev.*, vol. 98, p. 1863; June 15, 1955.) An alternative explanation is advanced of electroluminescence observations reported by Weymouth and Bitter (441 of February).
- 535.376:546.472.21** 3622
Light Patterns in Electroluminescent ZnS Single Crystals activated by Diffusion of Cu—G. Diemer. (*Philips Res. Rep.*, vol. 10, pp. 194–204; June, 1955.)
- 535.376:546.472.21** 3623
Some Aspects of the Voltage and Frequency Dependence of Electroluminescent Zinc Sulphide—P. Zalm, G. Diemer, and H. A. Klasens. (*Philips Res. Rep.*, vol. 10, pp. 205–215; June, 1955.) "Experiment shows that the relation between the luminous emittance H of an electroluminescent cell and the applied r.m.s. voltage V is given by $H = H_0 \exp(-c/V)$. A mechanism is proposed that may explain both the well-known linear frequency dependence at a constant rms voltage of the emittance and the observed voltage dependence."
- 537.221:546.48** 3624
Work Function of Cadmium—P. A. Anderson. (*Phys. Rev.*, vol. 98, pp. 1739–1740; June 15, 1955.) Continuation of work reported previously (993 of 1953).
- 537.226:538.221** 3625
Model for Magnetization Process in Ferroelectrics—M. N. Grigorev and I. M. Kirko. (*C. R. Acad. Sci. U.R.S.S.*, vol. 102, pp. 733–736; June 1, 1955. In Russian.) The magnetic properties of materials composed of steel spheres embedded in a quartz-sand insulating medium were investigated experimentally; results were compared with theory. Conclusions indicate that the effective permeability in a constant field and the dispersion in an alternating field can be determined if the following are known: (a) the permeability and dispersion of the steel, (b) its conductivity, and (c) the permeability of the ferroelectric at one frequency in the dispersion region.
- 537.226:621.315.6** 3626
Physics, Chemistry and Insulation—C. G. Garton. (*J. Instn. elect. Engrs.*, vol. 1, pp. 576–580; September, 1955.) A short review with particular reference to von Hippel's two books, *Dielectrics and Waves* (2045 of July) and *Dielectric Materials and Applications* (3030 of October).
- 537.226.2:537.224** 3627
Abnormal Increase in the Dielectric Constant of an Electret-Forming Material—S. D. Chatterjee and T. C. Bhadra. (*Phys. Rev.*, vol. 98, pp. 1728–1729; June 15, 1955.) "An electret with its two surfaces covered by plates which are connected together presents a situation in which the average (zero) field between the plates is composed of two equal and opposite parts, one due to the polarization and the

other due to the charges on or adjacent to the plates. These opposing fields can be very large ($\sim 10^6$ volts/cm) and as a result, large fluctuations may be expected in the vicinities of individual molecules. For these reasons it is surmised that the dielectric constant of the material of an electret may show an abnormal value, depending upon "strength" of the electret. The experiments described verify the existence of such an abnormality."

537.227 3628
A Neutron-Diffraction Study of the Ferroelectric Transition of Potassium Dihydrogen Phosphate—G. E. Bacon and R. S. Pease. (*Proc. roy. Soc. A*, vol. 230, pp. 359–381; June 21, 1955.)

537.227:546.431.824-31:621.396.822 3629
Noise Generation in Crystals and in Ceramic Forms of Barium Titanate when Subjected to Electric Stress—A. C. Kibblewhite. (*Proc. IEE, Part B*, vol. 102, pp. 683–684; September, 1955.) Discussion on 1347 of May.

537.311.3:546.73.281 3630
The Crystal Structure of CO_2Si —S. Geller and V. M. Wolontis. (*Acta Cryst.*, vol. 8, pp. 83–87; February, 1955.)

537.311.3:546.97.289 3631
The Rhodium-Germanium System: Part 1—The Crystal Structures of Rh_2Ge , Rh_5Ge_3 and RhGe —S. Geller. (*Acta Cryst.*, vol. 8, pp. 15–21; January 10, 1955.)

537.311.31:546.87:538.63 3632
Effect of Hydrostatic Pressure on the Galvanomagnetic Effects in Bi and its Alloys: Part 1—N. E. Alekscevski and N. B. Brandt. (*Zh. eksp. teor. Fiz.*, vol. 28, pp. 379–383; March, 1955.) Brief report of an experimental investigation at a pressure of 1500 atm and at temperatures in most cases equal to or not much above that of liquid He. Results are presented graphically.

537.311.33 3633
Semiconductors: No Man's Land between Metals and Insulators—R. W. Douglas. (*Nature, Lond.*, vol. 175, pp. 1059–1061; June 18, 1955.) A simple introduction to the subject.

537.311.33 3634
Intermetallic Semiconductors—I. M. Ross. (*Nature, Lond.*, vol. 176, pp. 341–343; August 20, 1955.) Report of a symposium held in April, 1955 at the Services Electronics Research Laboratory, Baldock, Herts. Emphasis was on compounds of the zinc-blende type, particularly InSb .

537.311.33 3635
Ionic and Homopolar Bonds in Semiconductors—I. M. Tsidil'kovski. (*C. R. Acad. Sci. U.R.S.S.*, vol. 102, pp. 737–740; June 1, 1955. In Russian.) A discussion relating to semiconductors such as oxides, sulphides, and selenides.

537.311.33:538.63 3636
Galvanomagnetic Effects in Semiconductors—O. Madelung. (*Naturwiss.*, vol. 42, pp. 406–410; July, 1955.) A survey with particular reference to Hall effect and resistance variation due to the magnetic field.

537.311.33:538.63 3637
Theory of the Hall and Nernst-Ettingshausen Effects in Semiconductors with Mixed Conductivity—F. G. Bass and I. M. Tsidil'kovski. (*Zh. eksp. teor. Fiz.*, vol. 28, pp. 312–320; March, 1955.) The theoretical discussion presented is based on the assumption of a law for the mean free path l of the form $l = \Phi(T)v^\nu$, where $\Phi(T)$ is a function of temperature, v is the velocity of the charge carriers and ν has the same value for electrons and holes.

537.311.33:539.15 3638
Overhauser Effect in Nonmetals—A. Abramo-

gam. (*Phys. Rev.*, vol. 98, pp. 1729–1735; June 15, 1955.) A survey is made of different ways in which nuclear spins can relax through their interaction with electronic spins. The case of a paramagnetic ion is examined in detail with reference to Honig's experiment on As-doped Si (753 of March).

537.311.33:54 3639
Chemical Aspects of Semiconductors—F. S. Stone. (*Nature, Lond.*, vol. 176, pp. 153–155; July 23, 1955.) Brief report of symposium held at Reading in March, 1955.

537.311.33:546.26-1 3640
Semiconductivity of a Type IIb Diamond—J. F. H. Custers. (*Nature, Lond.*, vol. 176, pp. 173–174; July 23, 1955.) The semiconductor properties of this class of diamond are thought to be due to crystal imperfections. The temperature variation of conductivity obeys an exponential law. In a particular specimen the energy gap was 0.70 ev. Rectification is obtainable. All blue diamonds are of this type, though not all of this type are blue.

537.311.33:[546.28+546.289] 3641
Optical and Impact Recombination in Impurity Photoconductivity in Germanium and Silicon—N. Sclar and E. Burstein. (*Phys. Rev.*, vol. 98, pp. 1757–1760; June 15, 1955.) Factors affecting the time taken to restore charge-carrier equilibrium are investigated by comparing the nonradiative, radiative and three-body recombination coefficients calculated on the basis of a simple model with hydrogen-like impurity centers. None of the mechanisms considered is consistent with time constants as short as those observed.

537.311.33:[546.28+546.289] 3642
Electron Voltaic Study of Electron Bombardment Damage and its Thresholds in Ge and Si—J. J. Loferski and P. Rapaport. (*Phys. Rev.*, vol. 98, pp. 1861–1863; June 15, 1955.)

537.311.33:546.28 3643
Solution of the Hartree-Fock-Slater Equations for Silicon Crystal by the Method of Orthogonalized Plane Waves—T. O. Woodruff. (*Phys. Rev.*, vol. 98, pp. 1741–1742; June 15, 1955.)

537.311.33:546.28 3644
Pressure Dependence of the Resistivity of Silicon—W. Paul and G. L. Pearson. (*Phys. Rev.*, vol. 98, pp. 1755–1757; June 15, 1955.) Measurements made on high-purity single crystals of Si in the intrinsic range indicate that the energy gap narrows as the applied pressure increases.

537.311.33:546.28 3645
Interpretation of Donor-State Absorption Lines in Silicon—W. Kohn. (*Phys. Rev.*, vol. 98, pp. 1856–1857; June 15, 1955.)

537.311.33:546.28 3646
Infrared Absorption of Silicon near the Lattice Edge—G. G. Macfarlane and V. Roberts. (*Phys. Rev.*, vol. 98, pp. 1865–1866; June 15, 1955.) Report of measurements over the temperature range 20–3330 degrees K.

537.311.33:546.289 3647
Fast-Neutron Bombardment of *n*-Type Ge—J. W. Cleland, J. H. Crawford, Jr., and J. C. Pigg. (*Phys. Rev.*, vol. 98, pp. 1742–1750; June 15, 1955.) Report of an extensive experimental study. The results indicate that the neutron bombardment produces two vacant states in the energy gap, one deep and one shallow. Mobility studies indicate that scattering associated with bombardment-induced lattice disorder is more complex than that due to charged impurities. Appreciable photoconductivity associated with minority-carrier trapping is produced.

537.311.33:546.289

3648

Microwave Determination of the Average Masses of Electrons and Holes in Germanium—J. M. Goldey and S. C. Brown. (*Phys. Rev.*, vol. 98, pp. 1761–1763; June 15, 1955.) A determination of the dielectric constant was made by measuring the complex transmission coefficient at 24.15 kmc through a thin slab of Ge at several temperatures. Values of the effective masses of electrons and holes thus determined are $(0.09 \pm 0.05)m_0$ and $(0.30 \pm 0.05)m_0$ respectively.

537.311.33:546.289

3649

Water-Vapor-Induced *n*-Type Surface Conductivity on *p*-Type Germanium—R. H. Kingston. (*Phys. Rev.*, vol. 98, pp. 1766–1775; June 15, 1955.) Measurements have been made of the *n*-type surface conductance of the *p*-type region in an *n-p-n* transistor, using a direct-reading instrument in contrast to the bridge measurements made by Brown (166 of 1954). From the results it is deduced that the density and type of carrier at the surface of an etched Ge crystal depend on the surface treatment and surrounding gas rather than on the carrier concentration in the bulk material. See also 1951 of 1954.

537.311.33:546.289

3650

Electrical Breakdown in Germanium at Low Temperatures—F. J. Darnell and S. A. Friedberg. (*Phys. Rev.*, vol. 98, pp. 1860–1861; June 15, 1955.) Report of an investigation of current/electric-field characteristics at different values of temperature and transverse magnetic field. Values of carrier mean free time and path are deduced.

537.311.33:546.289

3651

New Radiation resulting from Recombination of Holes and Electrons in Germanium—J. R. Haynes. (*Phys. Rev.*, vol. 98, pp. 1866–1868; June 15, 1955.) In addition to a previously reported radiation maximum at about 1.8 μ wavelength, evidence has been found for a second radiation maximum at about 1.5 μ .

537.311.33:546.289

3652

Surface Recombination in Germanium in the Presence of Strong Electric Fields—H. K. Henisch and W. N. Reynolds. (*Proc. phys. Soc.*, vol. 68, pp. 353–356; June 1, 1955.) The effect on the surface recombination velocity of a field normal to the crystal surface was investigated experimentally using Many's method (2129 of 1954) to determine the minority-carrier lifetime. The *n*- and *p*-type specimens were about 0.05 cm thick, 0.4 cm wide, and 1.5–3 cm long; the resistivities varied between 5 and 12 Ω . cm. The surface-recombination-velocity/applied-voltage curves obtained had similar slopes for both types of specimen. A possible theoretical explanation of the results is discussed.

537.311.33:546.289

3653

A Pulse Method for measuring the Injection Ratio of Metal-Semiconductor Contacts—G. G. E. Low. (*Proc. phys. Soc.*, vol. 68, pp. 447–452; July 1, 1955.) A tungsten point contact connected to a constant-current pulse generator divides a filamentary specimen of *n* or *p*-type Ge so as to form two arms of a bridge circuit. The change in conductance of the specimen with time after injection of a current pulse is measured. Curves of injection ratio against emitter current are given for various conditions.

537.311.33:546.289

3654

On the Behavior of Rapidly Diffusing Acceptors in Germanium—F. van der Maesen and J. A. Brenkman. (*J. electrochem. Soc.*, vol. 102, pp. 229–234; May, 1955.) Experiments on the acceptor activity and diffusion of Cu and Ni in Ge are reported. The results are interpreted as indicating that these impurities may occur both substitutionally and interstitially in

the lattice, different diffusion constants being appropriate for the two cases.

537.311.33:546.289 3655

Magnetic Susceptibility of Germanium—G. Busch and N. Helfer. (*Helv. phys. Acta*, vol. 27, pp. 201-204; June 30, 1954. In German.) Measurements on single crystals were made over the temperature range 56-1180 degrees K. The susceptibility passes through a maximum value at about 800 degrees K. The effect of thermally produced holes is discussed.

537.311.33:546.289 3656

Charge-Carrier Susceptibility and Cyclotron Resonance of Germanium—C. Enz. (*Helv. phys. Acta*, vol. 28, pp. 158-166; May 31, 1955.) In German.) On the basis of energy-band theory, the carrier susceptibility in the intrinsic range is calculated and compared with experimental results obtained by Busch and Helfer (3655 above). The agreement between theoretical and experimental results is much better if the number of families of ellipsoids in the conduction band is taken to be 4 rather than 8.

537.311.33:546.289 3657

Germanium in Some of the Waste-Products from Coal—K. V. Aubrey. (*Nature, Lond.*, vol. 176, pp. 128-129; July 16, 1955.) Experimental investigations are reported leading to conclusions differing in some respects from those of Forrest et al. (2659 of September). Possible reasons are discussed for the lower concentrations of Ge encountered in power-station boiler deposits as compared with deposits from the waste-gas flues of producer-gas plant.

537.311.33:546.289:539.32 3658

Elastic Constants of Germanium between 1.7° and 80°K—M. E. Fine. (*J. appl. Phys.*, vol. 26, pp. 862-863; July, 1955.)

537.311.33:621.314.632.1 3659

The Effect of Field-Dependent Mobilities on the Diffusion Theory of Rectification—P. T. Landsberg. (*Proc. phys. Soc.*, vol. 68, pp. 366-368; June 1, 1955.) A note on the theoretical part of Lees' work (462 of 1954) showing that if the mobility and diffusion coefficient of the current carriers are subjected to a much smaller fractional change, as a function of position in the barrier layer, than is the electric field, then many results of the general theory of barrier-layer rectifiers remain essentially unchanged.

537.311.33:621.314.7 3660

Semiconductors and Transistors: some Current Problems—J. R. Tillman. (*Nature, Lond.*, vol. 176, pp. 9-11; July 2, 1955.) A concise survey of the existing state of knowledge.

537.311.33:621.396.822 3661

Electronic Fluctuations in Semiconductors—R. E. Burgess. (*Brit. J. appl. Phys.*, vol. 6, pp. 185-190; June, 1955.) Various types of electrical fluctuations which occur in a semiconductor are compared with the corresponding processes in a vacuum tube. The types considered include thermal, shot, partition, avalanche, and modulation noise, the last-mentioned being conspicuous at low frequencies, especially when current-carrying contacts or barriers occur.

537.311.33:669.046.54 3662

Zone Melting Apparatus—(*Tech. News Bull. nat. Bur. Stand.*, vol. 39, p. 81; June, 1955.) Automatic apparatus for producing high-purity semiconductors uses a water-cooled rf heating coil concentric with a vycor tube which surrounds the boat holding a bar of the semiconductor. The coil is motor-driven along the tube.

537.311.33:669.046.54:546.289 3663

Zone Melting—W. G. Pfann and K. M. Olsen. (*Bell. Lab. Rec.*, vol. 33, pp. 201-205;

June, 1955.) A short illustrated description of the method of purifying Ge crystals, or producing a desired constituent distribution, by repeated crystallization, the Ge ingot in a graphite boat being traversed through a series of induction heating coils.

538.22 3664

Tentative Interpretation of the Magnetic Properties at High Temperature of the Rhombohedral Sesquioxides of Titanium, Vanadium, Chromium, and Iron (Ti_2O_3 , V_2O_3 , Cr_2O_3 , and Fe_2O_3)—J. Wucher. (*C.R. Acad. Sci., Paris*, vol. 241, pp. 288-290; July 18, 1955.)

538.22:621.318.134 3665

A Review of the Structure and some Magnetic Properties of Ferrites—L. C. F. Blackman. (*J. Electronics*, vol. 1, pp. 64-77; July, 1955.)

538.221 3666

Density of States of Conduction Electrons in Ferromagnetics—A. V. Sokolov and S. M. Tsipis. (*Zh. eksp. teor. Fiz.*, vol. 28, pp. 321-325; March, 1955.) The calculation presented is based on a model with *s-d* electron interaction.

538.221 3667

Some Magnetic Properties of Dilute Ferromagnetic Alloys: Part 1—G. Bate, D. Schofield, and W. Sucksmith. (*Phil. Mag.*, vol. 46, pp. 621-631; June, 1955.) An account is given of an investigation into the variation with heat treatment of the magnetic properties of Cu-Co and Cu-Fe alloys containing small percentages of ferromagnetic component. A maximum in the coercivity is found which is thought to be associated with single-domain precipitates; the characteristics of the hysteresis loops at this stage indicate coercivities >1,000 oersted.

538.221 3668

The Influence of Temperature on Magnetic Viscosity—J. H. Phillips, J. C. Woolley, and R. Street. (*Proc. phys. Soc.*, vol. 68, pp. 345-352; June 1, 1955.) Extension of earlier work (3272 of 1954). Measurements were made to demonstrate the influence of temperature on irreversible magnetic viscosity in different types of precipitation alloys: Pt-Co, Ni₃Au, and alnico in an undeveloped state.

538.221 3669

The Absence of Block Walls in Certain Ferromagnetic Materials—P. M. Prache. (*Cables & Transm.*, vol. 9, p. 228; July, 1955.) Corrections to paper abstracted in 3018 of October.

538.221 3670

Low-Temperature Evolution of the Coercive Force of Finely Divided Nickel—L. Weil. (*C.R. Acad. Sci., Paris*, vol. 241, pp. 470-472; August 1, 1955.) Measurements of the coercive force were made at progressively lower temperatures on Ni powders prepared by reduction. The results are not affected by applied magnetic fields, but are strongly affected by the thermal history of the specimens. Transformations effected at low temperature persist on reheating.

538.221:539.23 3671

Magnetization Reversal in Thin Films—R. L. Conger. (*Phys. Rev.*, vol. 98, pp. 1752-1754; June 15, 1955.) An experiment has been performed which indicates that magnetization reversal in evaporated films of 80 per cent Ni, 20 per cent Fe, 2×10^{-6} cm thick takes place by domain rotation rather than by the motion of 180 degree domain walls."

538.221:669.24 3672

Nickel Alloys made by Powder Metallurgy Techniques—(*Metallurgia, Manchr.*, vol. 51, pp. 215-217; May 1955.) The close control

in the production of Ni and Ni alloys by the technique described resulted in high-purity materials particularly suitable for use in tubes. A magnetic alloy of composition Ni 77 per cent, Fe 14 per cent, Mo 4 per cent, Cu 5 per cent, was also developed; this can be annealed in pure or wet hydrogen without detriment to its magnetic properties. Initial permeabilities >25,000 have been obtained in strip material of thickness down to 0.0005 inch; by suitable heat treatment, the details of which are not given, this may be increased to 60,000-100,000. Tables are given of the electrical resistivity of various samples of high-purity Ni, of the mean coefficient of expansion of Ni-Fe alloys, and of the chemical composition of the materials discussed.

539.23:537.311.3

3673

Experimental Investigation of the Electrical Conductivity of Complex Metal/Dielectric Films produced by Evaporation—C. Feldman. (*Ann. Phys., Paris*, vol. 10, pp. 435-478; May/June, 1955.) A study was made of films produced by (a) evaporating metal on to a previously deposited salt film, (b) evaporating metal and salt simultaneously, and (c) evaporating a salt on to a previously deposited metal film. The variation of conductivity with temperature and electric field is expressed by a formula of the same type as that for simple metal films, with different values of the constants. Theoretical discussion is based on the presence of very low potential barriers due to extremely close spacing between the grains. Complex films can be produced with either linear or nonlinear resistance characteristics. 49 references.

546.681

3674

Magnetic Susceptibilities of Crystal and of Liquid Gallium—A. Marchand. (*C. R. Acad. Sci., Paris*, vol. 241, pp. 468-470; August 1, 1955.) Experimental results are reported.

548.5

3675

On the Distribution of Impurity in Crystals Grown from Impure Unstirred Melts—K. F. Hulme. (*Proc. phys. Soc.*, vol. 68, pp. 393-399; July 1, 1955.)

621.315.61:546.287

3676

Silicones as Engineering Materials—L. P. Smith. (*Engineering, Lond.*, vol. 179, pp. 789-792; June 24, 1955.) The physical and chemical properties of silicones are briefly described and various applications are indicated.

621.318.2

3677

Impulse Magnetizer for Permanent Magnets—G. M. Moore. (*Electronics*, vol. 28, pp. 121-123; August, 1955.) A 200-ka pulse is obtained by discharging a capacitor through a current step-up transformer. Reversal of the magnetizing pulse is prevented by use of a thyratron-controlled ignitron shunting the magnetizing loop. Application is to magnetron magnets.

666.1/2

3678

The Devitrification Behaviour of Glasses Used in Vacuum Techniques—O. Knapp. (*Acta tech. Acad. Sci. hungaricae*, vol. 8, pp. 67-78; 1954. *Glass Ind.*, vol. 36, pp. 262-264, 285; May, 1955.) Experimental results indicate lower liquidus temperatures and higher rates of crystal growth for lime and lead glasses than were reported by Kalsing et al. (*Glastechn. Ber.*, vol. 21, p. 66; 1943.) The liquidus temperatures for both types is about 825-830 degrees C.

MATHEMATICS

512

3679

A Direct Iterative Method for the Hurwitz Expansion of a Polynomial—F. L. Bauer. (*Arch. elekt. Übertragung*, vol. 9, pp. 285-290; June, 1955.)

- 517 3680 The Evaluation of Integrals containing a Parameter—R. B. Dingle. (*Appl. sci. Res.*, vol. B4, pp. 401–410; 1955.) The problem considered is that of finding suitable expressions for the integral (a) for small and (b) for large values of a parameter. Methods based on (a) the Taylor expansion, (b) integration by parts, (c) Mellin transforms, and (d) the differential equation are expounded by evaluating the same function, $E_{i_n}(x) = \int_1^{\infty} u^{-n} e^{-xu} du$. The various expansions developed for $E_{i_n}(x)$ are used in two following papers (not abstracted) on the functions $C_{i_n}(x)$, $S_{i_n}(x)$, $CI_{i_n}(x)$ and $SI_{i_n}(x)$.
- 519.2 3681 A Sequential Two-Sample Life Test—B. Epstein. (*J. Franklin Inst.*, vol. 260, pp. 25–29; July, 1955.) Analysis is presented relevant to the problem of determining, from tests on samples, which of two lots of components has the greater mean life.
- 519.2 3682 An Introduction to Stochastic Processes, with Special Reference to Methods and Applications. [Book Review]—M. S. Bartlett. Publishers: University Press, Cambridge, 1955, 312 pp., 35s. (*Nature, Lond.*, vol. 176, p. 275; August 13, 1955.) Has application to communication theory.
- MEASUREMENTS AND TEST GEAR**
- 529.7 3683 Precision Measurement of Time—H. M. Smith. (*J. sci. Instrum.*, vol. 32, pp. 199–204; June, 1955.) A brief survey is given of methods and instruments used; the construction of chronometers is described and the application of standard-frequency transmissions is discussed.
- 53.082.7:535.22:538.56.029.6 3684 The Velocity of Propagation of Electromagnetic Waves—J. T. Henderson and A. G. Mungall. (*Canad. J. Phys.*, vol. 33, pp. 265–274; June, 1955.) Measurements were made by a coaxial-cavity-resonator method using a frequency of 400 mc which is close to that used for geodetic surveying in Canada. Consistent results were obtained giving a value of 299 780 km for c . This value is believed to be low owing to an indeterminate systematic error introduced by discontinuities at junctions in the cavity; coaxial-cavity methods are not considered capable of giving the desired degree of accuracy at this frequency.
- 53.082.7:535.22:621.396.11.029.62 3685 A Measurement of the Velocity of Propagation of Very-High-Frequency Radio Waves at the Surface of the Earth—E. F. Florman. (*J. Res. nat. Bur. Stand.*, vol. 54, pp. 335–345; June, 1955.) An interferometer method was used, operating at a frequency of 172.8 mc to avoid skywave interference and ground effects and to keep the size of the measuring system within convenient limits. The value derived for the free-space velocity was 299795.1 ± 3.1 km; this uncertainty includes a 95 per cent confidence interval for the mean and an estimated limit of ± 0.7 km for the systematic error. The accuracy of the result is limited by the accuracy with which the refractive index of the air path is known. (See also *Tech. News. Bull. Nat. Bur. Stand.*, vol. 39, pp. 1–3; January, 1955.)
- 621.3.018.41(083.74)+529.786 3686 An Atomic Standard of Frequency and Time Interval—L. Essen and J. V. L. Parry; E. C. Bullard. (*Nature, Lond.*, vol. 176, pp. 280–282; August 13, 1955.) Description of a frequency standard constructed at the National Physical Laboratory, based on a natural resonance of the Cs atom and using the atomic-beam magnetic-resonance technique. Using this standard, quartz clocks can be calibrated with an accuracy within ± 1 part in 10^9 , corresponding to 0.0001 sec/day. The value of the frequency standardized is 9192632050 ± 10 c/s. A note by Bullard is appended, discussing the desirability of abandoning the astronomical second in favor of a physically defined second.
- 621.3.018.41(083.74)+529.786 3687 Frequency and Time Standards—F. D. Lewis. (*PROC. IRE.*, vol. 43, pp. 1046–1068; September, 1955.) A review paper. Quartz-crystal resonators and stable oscillators including them are described. A discussion of the present status of atomic and molecular frequency standards includes the ammonia absorption cell and the ammonia- and caesium-beam oscillators. Instrumentation for precision frequency measurement is outlined and a current list of standard-frequency broadcasting stations is given.
- 621.317.3:621.385.2/.3].029.63 3688 Conductance and Slope Measurements on Transit-Time Diodes and Triodes—F. W. Gundlach and H. Lonsdorfer. (*FernmeldeTech. Z.*, vol. 8, pp. 305–309; June, 1955.) Theory is given and methods are described for measuring the conductance of disk-seal diodes and the input conductance and transconductance of disk-seal triodes at about 50 cm and 12 cm λ . Some results are reported.
- 621.317.3+621.375.2+621.373.4].029.6 3689 Disc-Seal Circuit Techniques—Swift. (See 3541.)
- 621.317.3.029.6 3690 Microwave Measurements—G. Pircher. (*Rev. gén. Élect.*, vol. 64, pp. 301–311; June, 1955.) A survey of up-to-date methods and equipment including standing-wave detectors, wavemeters, bolometers, attenuators and turntable apparatus for measurements on antennae.
- 621.317.335(083.7) 3691 The Measurement of the Dielectric Constant of Standard Liquids—L. Hartshorn, J. V. L. Parry, and L. Essen. (*Proc. phys. Soc.*, vol. 68, pp. 422–446; July 1, 1955.) Methods are described and results are presented for measurements on benzene, cyclohexane, dichlorethane and nitrobenzene, made with the object of providing dielectric-constant values of improved accuracy. Both audio and microwave frequencies were used.
- 621.317.336 3692 Rapid Measurement of Impedance and Admittance—B. Salzberg and J. W. Marini. (*Electr. Engng., N.Y.*, vol. 74, p. 503; June, 1955.) Digest of paper to be published in *Trans. Amer. IEE, Part I, Communication and Electronics*, vol. 74, 1955. A method of determining the driving-point impedance of linear networks over the frequency range 50 kc–5mc involves measuring the resistive and reactive components by means of mixers whose local-oscillator voltage is derived from the current through the impedance while the voltage across the impedance is used as the signal voltage.
- 621.317.336:621.372 3693 Transmission-Line Termination—Dukes. (See 3483.)
- 621.317.341:621.372.56 3694 Resistance Attenuator Circuits for Attenuation Measurements up to 20 Nepers—R. Dallemande. (*Câbles & Transm.*, vol. 9, pp. 229–245; July, 1955.) Details are given of the construction and use of equipment for measurement of attenuation and crosstalk over the frequency band 5–800 kc. Correction of the effects of parasitic impedances due to wiring etc., in the attenuator used is simplified by representing them as T , Π , or lattice networks.
- 621.317.36:621.373.1.029.64 3695 Ammonia Absorption Line (3, 3) as Standard for Measurement of Frequencies in the 5–20-Mc/s Band with Accuracy of 10^{-6} —B. D. Osipov and A. M. Prokhorov. (*C.R. Acad. Sci. U.R.S.S.*, voi. 102, pp. 933–934; June 11, 1955. In Russian.) Equipment using a Stark-modulated microwave spectrometer was used, the signal being suitably frequency-multiplied, to bring it into the 24-kmc band. A block diagram of the equipment is given.
- 621.317.382:621.396.61.029.62 3696 Measurement of Transmitter Power of the order of Tens of Watts at Metre Wavelengths—R. Bryssinck and A. G. Tellier. (*Rev. HF, Brussels*, vol. 3, pp. 71–82; 1955.) Calorimetric, directional-coupler, peak-voltmeter and photometric methods of measurement are discussed and some results are reported. With these four methods the attainable accuracies are respectively within 2 per cent, 5 per cent, 8 per cent and 10 per cent, or 30 per cent in the last case for low powers. With correctly designed loads the last three methods can be used satisfactorily.
- 621.317.44:537.311.33:546.682.86:538.632 3697 Indium Antimonide as a Fluxmeter Material—E. W. Saker, F. A. Cunnell, and J. T. Edmond. (*Brit. J. appl. Phys.*, vol. 6, pp. 217–220; June, 1955.) The principles of measurement of magnetic fields by use of the Hall effect are considered. The efficiency of Hall-voltage generators is proportional to the square of the carrier mobility in the material used. The mobility for InSb is 60,000 cm/s per v/cm, compared with 3600 cm/s per v/cm for Ge; the theoretically attainable output power of an InSb generator is therefore about 280 times that of a Ge generator. The construction of suitable probes is described and sensitivity, linearity, and temperature compensation are discussed.
- 621.317.7 3698 The Damping of Moving-Coil Vibrating Systems by means of Quadrupole Resonant Circuits—E. G. Schlosser. (*Arch. Elektrotech.*, vol. 42, pp. 47–47; June 20, 1955.) An arrangement of two resonant circuits is described, capable of providing optimum damping for recording instruments.
- 621.317.7.029.53/.55 3699 Broad-Band Reflectometers at High Frequencies—R. T. Adams and A. Horvath. (*Elect. Commun.*, vol. 32, pp. 118–125; June, 1955.) A directional coupler using resistive rather than reactive coupling elements has constant sensitivity over the frequency range 300 kc–30 mc.
- 621.317.725.029.42:621.383.2 3700 A Photoelectric Relay for measuring Voltages of Low Frequency—J. M. W. Milatz, H. J. J. van Boort, J. van Laar, and C. T. J. Alkemade. (*Appl. sci. Res.*, vol. B4, pp. 447–456; 1955.) The instrument described is designed for amplifying and measuring signals such as bolometer outputs varying at a frequency of the order of 1 c/s, and comprises primary dc galvanometer, rotating-disk light chopper, and photo-cell coupled to 50-c/s amplifier, with ac galvanometer as indicator. The sensitivity is limited only by the Johnson noise of the input circuit; drift effects are very low.
- 621.317.729 3701 A Microwave Phase Contour Plotter—J. S. Ajioka. (*PROC. IRE*, vol. 43, pp. 1088–1090; September, 1955.) A simple arrangement is described, using two field-sampling probes, one of which provides the reference signal.
- 621.317.733 3702 Measurement of Inductances, Capacitances and Frequencies—W. Herzog and E. Frisch.

(*Fernmeldetech. Z.*, vol. 8, pp. 325-328; June, 1955.) Descriptions are given of a bridge connected as oscillator, for measurement of inductances, and a passive bridge for measurement of capacitances and frequencies. Adjustment of a capacitance over a range 1:10 enables capacitances and inductances over a range 1:1000 and frequencies over a range 1:30 to be measured. See also 1117 of April (Herzog).

621.317.755 3703

Towards the Universal Oscilloscope—J. Crozier. (*Électronique, Paris*, pp. 48-51; July/August, 1955.) Design principles are discussed for equipment for studying phenomena over a wide frequency range, having interchangeable timebase units together with a common unit comprising er tube, output amplifiers and calibrating voltage.

621.317.755 3704

A Rapid and Simple Method for obtaining Permanent Records from Cathode-Ray Oscilloscopes—H. D. Rathgeber. (*J. sci. Instrum.*, vol. 32, pp. 232; June, 1955.) The cro image is traced with a ball-point pen on a removable strip of transparent plastic tape stuck on the screen.

621.317.755:778.6 3705

Colour Photography of Oscillograms—G. H. Hille. (*Elektronik*, vol. 4, pp. 129-130; June, 1955.) Technique is described for photographing in different colors curves displayed simultaneously on the cro screen.

621.317.784.029.6 3706

A Milliwattmeter for Centimetre Wavelengths—A. C. Gordon-Smith. (*Proc. IEE, Part B*, vol. 102, pp. 685-686; September, 1955.) "The instrument is in the form of a differential air thermometer, and consists of two similar glass cells connected by a glass capillary tube. A carbon-coated strip is placed in each of the two cells; one of these strips absorbs the radio-frequency power to be measured and the other is heated by direct current. A liquit pellet in the capillary tube is displaced as a result of the differential expansion of the air in the two cells arising from the heat dissipated in the carbon-coated strips. After balancing the system by adjustment of the dc cell the radio-frequency power is finally determined by the measurement of the dc power which must be substituted for the radio-frequency power in the saine cell in order to maintain the state of balance. The instrument has been used to measure powers of 10 to 100 mw at a wavelength of 3 cm with a discrimination of about 0.2 mw."

621.317.794.029.64 3707

An Improved Method of measuring Efficiencies of Ultra-high-Frequency and Microwave Bolometer Mounts—R. W. Beatty and F. Reggia. (*J. Res. nat. Bur. Stand.*, vol. 54, pp. 321-327; June, 1955.) A method is described based on that of Kerns (3471 of 1949) but modified so as to avoid direct measurement of impedance.

621.396.62.001.4(083.7) 3708

IRE Standards on Radio Receivers: Method of Testing Receivers employing Ferrite Core Loop Antennas, 1955—(*Proc. IRE*, vol. 43, pp. 1086-1088; September, 1955.) Standard 55 IRE 17.S1.

621.397.6.001.4:535.623 3709

Differential Gain tests TV Color—Schroeder. (See 3758.)

621.397.8.001.4 3710

Method for the Assessment and Characterization of the Distortion of the Sawtooth Test Signal in Tests on Television Transmission Lines—Bödeker. (See 3767.)

OTHER APPLICATIONS OF RADIO AND ELECTRONICS

621.317.39:534.13 3711

Use of $\lambda/4$ Coaxial Line for Measurement of Mechanical Oscillations—E. Löb. (*Arch. Elektrotech.*, vol. 42, pp. 5-13; June 20, 1955.) The amplitude of vibration is determined by arranging the vibrating object near the open end of the line, so as to vary its electrical length periodically, and observing the corresponding periodic variations of tuning. Vibrations of nonmetallic as well as metallic objects can be investigated.

621.365.5(083.74) 3712

IRE Standards on Industrial Electronics: Definitions of Industrial Electronics Terms, 1955—(*PROC. IRE*, vol. 43, pp. 1069-1072; September, 1955.) Standard 55 IRE 10.S1 on induction and dielectric heating.

621.384.6 3713

Strong Focusing in [particle] Accelerators—W. Dällenbach. (*Z. angew. Phys.*, vol. 7, pp. 344-360; July, 1955.) Full text of paper abstracted in 3059 of October.

621.384.611/.612 3714

The 156-in. Cyclotron at Liverpool—M. J. Moore. (*Nature, Lond.*, vol. 175, pp. 1012-1015; June 11, 1955.) The machine described is a synchro-cyclotron producing protons of energy about 400 mev.

621.384.611 3715

General Purpose X-Band Laboratory Microtron with Facilities for Electron Extraction—H. F. Kaiser and W. T. Mayes. (*Rev. sci. Instrum.*, vol. 26, pp. 565-567; June, 1955.)

621.384.612 3716

The Synchrotron and Problems relating to it—E. Persico. (*J. Phys. Radium*, vol. 16, pp. 360-365; May, 1955.) A short survey.

621.384.612 3717

Betatron Oscillations in the Synchrotron—C. L. Hammer, R. W. Pidd, and K. M. Terwilliger. (*Rev. sci. Instrum.*, vol. 26, pp. 555-556; June, 1955.) Experimental results indicate that a transverse rf electric field will excite the betatron oscillations at several frequencies, the spacing of which is equal to the synchrotron-frequency. The effect is believed to be due to frequency modulation of the betatron oscillations by the synchrotron oscillations.

621.384.612 3718

Experimental Characteristics of the Proton Synchrotron—P. B. Moon, L. Riddiford, and J. L. Symonds. (*Proc. roy. Soc. A*, vol. 230, pp. 204-215; June 21, 1955.) Features of the Birmingham proton synchrotron which are important in relation to the experimental use of the machine are described.

621.384.612 3719

Some Proton Synchrotron Beam Studies with the Induction Electrode—L. Riddiford, H. B. van der Raay, and R. F. Coe. (*Proc. phys. Soc.*, vol. 68, pp. 489-502; June 1, 1955.)

621.384.622.2 3720

The Linear Accelerator—(*Elect. Rev., Lond.*, vol. 156, pp. 1144-1146; June 24, 1955.) A simplified explanation of the mode of operation.

621.385.833 3721

Third-Order Aberrations of a Typical Electrostatic Unipotential Lens—W. Glaser and P. Schiske. (*Optik, Stuttgart*, vol. 12, pp. 233-245; 1955.)

621.387.424 3722

Sensitive Volume of External-Cathode Geiger-Müller Counters—D. Blanc. (*Nuovo Cim.*, vol. 1, pp. 1280-1281; June 1, 1955. In French.)

621.389:539.155.082.7

3723

Recent Research with an Experimental Mass Spectrometer—G. P. Barnard. (*J. Electronics*, vol. 1, pp. 78-102; July, 1955.) Description of a precision all-metal instrument constructed at the National Physical Laboratory; it is a 60 degree sector type, first-order, single-focusing, with 4 inch radius of curvature in the magnetic analyzer.

PROPAGATION OF WAVES

538.566.2

3724

Reflection of a Plane Electromagnetic Wave by an Ionized Medium—P. Poincelot. (*C.R. Acad. Sci., Paris*, vol. 241, pp. 186-188; July 11, 1955.) Expressions involving Hankel functions are derived for the strength of the electric and magnetic fields in a medium where the refractive index varies with altitude according to a stated law.

538.566.2

3725

Reflection of a Plane Electromagnetic Wave by an Ionized Gas with a Given Distribution Law—P. Poincelot. (*C. R. Acad. Sci., Paris*, vol. 241, pp. 290-292; July 18, 1955.) Continuation of 3724 above. See also note of correction *ibid.*, vol. 241, pp. 649-651; August 29, 1955.

621.396.11:551.510.535

3726

Ionospheric-Absorption Equivalence Theorems—É. Argence, K. Rawer, and K. Suchy. (*C.R. Acad. Sci., Paris*, vol. 241, pp. 505-507; August 1, 1955.) A more general analysis is presented than that of Appleton and Beynon (2400 of August); partial reflections and electron collisions are taken into account. The case of strong absorption is investigated using theory of dispersive media and metallic reflection.

621.396.11.029.55

3727

Simplification of the "Spanish Method" [for ionospheric prediction of m.u.f.]—R. Gea Sacasa. (*Rev. Telecommunicación, Madrid*, vol. 9, pp. 31-51; March, 1955. In Spanish and English.) The monthly predictions published by the Commonwealth Observatory of Australia for the months of December and June, 1953 and 1954, are compared with those computed by the author's method. The results are similar, but in nearly all cases, and particularly in summer, the Spanish method predicts higher mufs than the Australian. By the use of a set of abacs developed by the author, predictions for any period of the year and for any locality and range may be very simply obtained.

621.396.11.029.6

3728

V.H.F. and U.H.F. Signals in Central Canada—D. R. Hay and R. C. Langille. (*PROC. IRE*, vol. 43, p. 1136; September, 1955.) Measurements are reported of signals at frequencies of 49, 91, 173 and 495 mc, at ranges between 20 and 235 miles. The results are close to those predicted from theory of propagation round a smooth spherical earth [802 of 1948 (Bullington)] for ranges up to 30-40 miles. At ranges >80 miles the deviations from the predicted value increase with increasing frequency. Assuming that at ranges >80 miles the signals are propagated by scatter from atmospheric turbulence, the results are consistent with the scatter formula proposed by Gordon (1136 of April).

621.396.11.029.62/.63

3729

Factors affecting Radio Propagation in the TV and F. M. Bands—W. E. Utlaut. (*Tele-Tech & Electronic Ind.*, vol. 14, pp. 98-101, 378; June, 1955.) An account is presented of the effects at frequencies up to about 1 kmc of (a) diffraction by the earth and by obstacles, (b) atmospheric refraction, (c) atmospheric reflection, (d) scattering, and (e) the sporadic E layer, with particular reference to recent

theoretical and experimental work mainly by the Central Radio Propagation Laboratory.

621.396.11.029.62 3730
Long-Distance V.H.F. Fields: Part 1—Partial Reflections from a Standard Atmosphere. Part 2—Refractivity Profiles containing "Sharp Layers." Part 3—The Case of Two Elevated Layers—F. H. Northover. (*Canad. J. Phys.*, vol. 33, pp. 241–256, 316–349; May /June, 1955.) Various explanations are discussed for the high field strengths of vhf radio signals which have been consistently observed beyond the horizon. Detailed analysis indicates that the phenomenon cannot be explained solely in terms of partial internal reflections when the propagation takes place in a standard atmosphere, characterized by a continuous slow decrease of refractive index with height. While the phenomenon could be due to this cause when high-level inversion layers are present, scattering from atmospheric turbulence is considered a more probable cause. The general theory is used to derive an equation for the eigenvalues of the propagation for the case of two sharply defined atmospheric layers.

621.396.11.029.62:53.082.7:535.22 3731
A Measurement of the Velocity of Propagation of Very-High-Frequency Radio Waves at the Surface of the Earth—Florman. (See 3685.)

621.396.81.029.62 3732
Note on the Diurnal Variation of Field Strength in the U. S. W. Band—L. Klinker. (*Z. Met.*, vol. 9, pp. 178–191; June, 1955.) Diurnal variations are discussed associated with the night-time formation of low-level inversion and its disappearance during the day. For transmission distances up to twice the optical path length the effect can be accounted for by variations of atmospheric refraction. Using measurements of the vertical gradients of temperature and water vapor pressure, a calculation is made of the daily variation from the known formula for field strength. For average conditions, the calculated value is brought into agreement with observations by taking account of the temperature gradient only. For longer distances the observed and calculated values differ by an amount which increases with the path length, since the effect of refraction decreases relative to that of other factors notably scattering due to turbulence.

621.396.812.3 3733
Distribution-in-Speed of Fading of 150-kc/s Waves—R. B. Banerji. (*Nature, Lond.*, vol. 176, p. 131; July 16, 1955.) Fading observations were made at the Pennsylvania State University, using time intervals much longer than those used e.g., by Mitra at Cambridge working with frequencies of 2–6 mc (442 of 1950). No significant deviation from a Gaussian distribution of speed of fading was found; this supports the theoretical prediction that such a deviation should be less readily evident at low than at high frequencies.

551.510.535:621.396.11 3734
The Physics of the Ionosphere. [Book Notice]—(See 3614.)

RECEPTION

621.396.62 3735
Cross-Section of the Technical Novelties of [West German] 1955/56 Broadcast Receivers—W. W. Diefenbach. (*Funk-Technik, Berlin*, vol. 10, pp. 352–356; July, 1955.) The principal trends include developments in usw/fm and lf stages, use of rotatable ferrite-rod built-in antennas and use of several loudspeakers of both moving-coil and es types in the larger table models. Further details are given in a supplement and in subsequent issues of the journal.

621.396.62.001.4(083.74) 3736
IRE Standards on Radio Receivers: Method of Testing Receivers employing Ferrite Core Loop Antennas, 1955—(Proc. IRE, vol. 43, pp. 1086–1088; September, 1955.) Standard 55 IRE 17.S1.

621.396.621:621.396.822 3737
The Resolution of Signals in White, Gaussian Noise—C. W. Helstrom. (Proc. IRE, vol. 43, pp. 1111–1118; September, 1955.) "The resolution of two signals of known shapes $F_1(t)$ and $F_2(t)$ in white Gaussian noise is treated as a problem in statistical decision theory. The observer must decide which of the signals is present with a minimum probability of error. The optimum system for this decision is specified in terms of filters matched to the two signals, the outputs of which are compared. The error probability is exhibited as a function of the cross-correlation of the two signals and of the signal-to-noise ratio. If the phases of the two signals are unknown, as in radar, and if the signals are of equal strength and equal *a priori* probability, the optimum system consists of filters matched to each of the signals, each followed by a detector. The observer then bases his decision upon which of the detectors has the larger output. The probability of error is computed for this case also."

621.396.621.54:621.319.43:537.227 3738
The Application of Dielectric Tuning to Panoramic Receiver Design—T. W. Butler, Jr., W. J. Lindsay, and L. W. Orr. (Proc. IRE, vol. 43, pp. 1091–1096; September, 1955.) Continuous tuning over a 2:1 frequency band is obtained at frequencies up to 110 mc by using ferroelectric tuning capacitors with nonlinear characteristics.

621.396.81:621.396.67 3739
The Limits of Communication Reception using Aerials with Losses—Didlaukis. (See 3494.)

STATIONS AND COMMUNICATION SYSTEMS

621.376.5:621.39 3740
Quantitative Noise Reduction in Pulse Time Modulation—J. Das. (*Electronic Engng.*, vol. 27, pp. 406–409; September, 1955.) Rigorous analysis of typical systems, based on the principles proposed by Deloraine and Labin (1947 of 1945), gives results for improvement of signal/noise ratio in agreement with experiment.

621.39.001.11:519.2 3741
On the Average Uncertainty of a Continuous Probability Distribution—A. D. du Mosch. (*Appl. Sci. Res.*, vol. B4, pp. 469–473; 1955.) Discussion of importance in communication theory.

621.395.2:621.374.4:621.375.3.029.3 3742
All-Magnetic Audio Amplifier—Suozzi and Hooper. (See 3537.)

621.395.44:621.315.28 3743
A Transatlantic Telephone Cable—M. J. Kelly, G. Radley, G. W. Gillman, and R. J. Halsey. (Proc. IEE, Part B, vol. 102, pp. 717–719; September, 1955.) Discussion on 1547 of June.

621.396 3744
The Argentine Telecommunications Networks—H. B. R. Boosman. (*Tijdschr. ned. Radiogenoot.*, vol. 20, pp. 115–135; May, 1955. In English.) See 2745 of September.

621.396.3 3745
The T.O.R. [teletype on radio] Circuits for The Argentine Radio Links—W. Six. (*Commun. News*, vol. 15, pp. 108–119; August, 1955; *Tijdschr. ned. Radiogenoot*, vol. 20, pp. 137–159; May, 1955. In English.) Application of the error-reducing system described by van Duuren

(2837 of 1951) to the Argentine radiotelegraph system (3744 above). Most of the switching is performed by means of cold-cathode tubes Types Z500T and Z501T. A radio test on a circuit between Hilversum and Eindhoven showed that introduction of the TOR system reduced the number of mutilated characters by a factor of 2000.

621.396.65.029.64 3746
Radio Link Operating in 4000 Mc/s Band, for Television and Multichannel Telephony—H. C. B. Everts. (*Tijdschr. ned. Radiogenoot.*, vol. 20, pp. 183–193; May, 1955. In English.) Description of link equipment using Type-EC56 triodes for mixing and amplifying at frequencies in the 3.8–4.2-kmc band. Heterodyne repeater stations are used. Some details are given of the antenna system, which comprises a parabolic reflector illuminated by a square waveguide continued as a pair of rectangular waveguides, one leading to the transmitter and the other to the receiver and each containing a "uniline" control device operated by ferromagnetic resonance in a small sheet of ferrite.

SUBSIDIARY APPARATUS

621-526 3747
The Response of Remote-Position-Control Systems with Hard-Spring Nonlinear Characteristics to Step-Function and Random Inputs—J. C. West and P. N. Nikiforuk. (Proc. IEE, Part B, vol. 102, pp. 575–593; September, 1955. Discussion, pp. 594–595.)

621-526 3748
The Adjustment of Control Systems for Quick Transient Response—A. T. Fuller. (Proc. IEE, Part B, vol. 102, pp. 596–601; September, 1955.) A theoretical investigation indicates that for a large class of linear systems the error due to a transient disturbance is dependent on only one system parameter, the "settling time-constant," and that the quickest approach to correction is obtained when the system is adjusted so as to be quasicritically damped. The adoption of quasicritical damping as a design criterion for stability is recommended.

621-526 3749
The Integral-of-Error-Squared Criterion for Servo Mechanisms—H. H. Rosenbrock. (Proc. IEE, Part B, vol. 102, pp. 602–607; September, 1955.)

621.314.63:621.311.6 3750
Silicon Alloy Junction Diodes for Power Supply Applications—J. Shields. (*Engineer, Lond.*, vol. 199, pp. 801–803; June 10, 1955. *B.T.-H. Activ.*, vol. 26, pp. 102–107; July/August, 1955.) Characteristics of low-power and high-power Si diodes are presented and various applications indicated.

TELEVISION AND PHOTOTELEGRAPHY

621.397.24:621.397.6 3751
An Unconventional Wired Television Distribution System—E. J. Gargini. (*J. Telev. Soc.*, vol. 7, pp. 403–427; April/June, 1955.) The advantages and disadvantages of radio and wired television systems are compared. Tests of the suitability of various types of cable for multichannel operation are mentioned. Various distribution-network arrangements are considered; good area coverage is obtained by use of a network comprising spiral main feeder sections with short spurs. A detailed description is given of a wired system in which receiver design is simplified by transferring as much circuitry as possible to the sending end. See also 1173 of April.

621.397.26 3752
Long-Range Television Reception—(*Wireless World*, vol. 61, pp. 504–505; October, 1955. Correction, *ibid.*, vol. 61, p. 530; November, 1955.) Good reception has been recorded

in Sweden of television broadcasts on 48, 55 and 62 mc from Russia, Italy, etc.

621.397.26:621.396.65 3753

The Roving Eye—T. Worswick and G. W. H. Larkby. (*J. Telev. Soc.*, vol. 7, pp. 397-400; April/June, 1955.) Description of the B.B.C. mobile television-camera unit. A frequency of about 200 mc is used for the vision-signal radio link to base; four-element Yagi antenna arrays are used both on the vehicle and at the base; arrangements for keeping the vehicle antenna on the correct bearing are described. Positive modulation is used, the transmitter power being about 12 w on peak white. In open country the range is of the order of two miles, the limit being set by man-made interference. In built-up areas the range may be anything up to a mile, depending entirely on topography.

621.397.26:621.396.65.029.64 3754

The Manchester-Kirk o'Shotts Television Radio-Relay System—G. Dawson, L. L. Hall, K. G. Hodgson, R. A. Meers, and J. H. H. Merriman. (*Proc. IEE, Part B*, vol. 102, pp. 607-608; September, 1955.) Discussion on 2784 of 1954.

621.397.5 3755

Television Technique—A. Karolus. (*Tech. Mitt. schweiz. Telegr.-Teleph. Verw.*, vol. 33, pp. 169-186; May 1, 1955. In German.) An account, intended for nonspecialists, of the historical development of television.

621.397.5 3756

Limits of Quality with Intercarrier Sound Reception—H. J. Griese. (*Fernmeldetechn. Z.*, vol. 8, pp. 374-378; July, 1955.) Sources of noise on the intercarrier system are examined. Transmitter tests necessary for investigating interference phase modulation are discussed. Most of the audio interference observed originates in the receiver rather than the transmitter. The less stringent requirements as regards oscillator-frequency constancy and avoidance of microphony with the intercarrier system make this system greatly preferable for operation in bands III and IV.

621.397.6.001.4 3757

Determination of the Characteristic Parameters of a Television F.M. Link by Measurements between Video Input and Video Output—G. Brühl. (*Fernmeldetechn. Z.*, vol. 8, pp. 362-366; July, 1955.) Methods of measurement for both video and rf parts of the system are discussed. In order to ascertain which part is responsible for observed imperfections of reproduction, the amplitude and frequency of the test signals should be appropriately chosen, and the sequence of the operations should be: (a) linearity measurement of the video stages, using very low frequencies, and any necessary corrections; (b) measurement and adjustment of the frequency characteristic of the rf stages; (c) measurement of overall frequency and delay characteristics.

621.397.6.001.4:535.623 3758

Differential Gain tests TV Color—J. O. Schroeder. (*Electronics*, vol. 28, pp. 114-117; August, 1955.) A composite signal, consisting of a small-amplitude 3.5-mc sine wave mixed with a large-amplitude 120-c/s rectangular wave of variable duty cycle, is used to check the linearity of the transfer characteristic of video equipment.

621.397.61+[621.396.61:621.376.3 3759

General Outline of the Development of Transmitters for Television and Frequency Modulation [in the Netherlands]—P. W. L. v. Iterson and H. A. Teunissen. (*Tijdschr. ned. Radiogenoot.*, vol. 20, pp. 207-222; May, 1955. In English.)

621.397.61:621.372.55 3760

Application of Differential Equalization in Television—R. Theile. (*Arch. elekt. Übertragung*, vol. 9, pp. 247-254; June, 1955.) A development of Gouriet's equalization method (1936 or 1953) is described. A simple equalizer circuit is used; its performance is shown by oscillograms and photographs of a test pattern.

621.397.61:621.372.55 3761

Circuits for Aperture Compensation in Television Cameras—W. Dillenburger. (*Frequenz*, vol. 9, pp. 181-188; June, 1955.) Phase-linear amplitude equalizers permitting 100 per cent modulation of the video signal at frequencies up to 5 mc are discussed, including various differentiating equalizers and the "cosine" equalizer. Use of aperture compensation is scarcely worth while if the uncompensated camera gives a modulation depth of 50 per cent or more at 5 mc. See also 3104 of October.

621.397.611.2 3762

Limiting Resolution due to Charge Leakage in the Scenioscope, a New Television-Camera Tube—P. Schagen. (*Philips Res. Rep.*, vol. 10, pp. 231-238; June, 1955.) The loss of modulation depth in the picture signal due to charge leakage is calculated as a function of the resistivity and thickness of the glass target. Estimates show that for practical applications the resistivity should be $> 2.3 \times 10^4 \Omega \text{ cm}$. In a 625-line system the diameter of a picture element is about 75μ with a scanned target area of $45 \times 60 \text{ mm}^2$; in order to obtain satisfactory resolution the target thickness must not exceed 100μ .

621.397.62(94) 3763

Television Channels, Standard Intermediate Frequencies and Standards for Limits of Radiation from Receivers—*Proc. IRE Aust.*, vol. 16, pp. 173-175; June, 1955.) A statement prepared by the Australian Broadcasting Control Board for the information of television-receiver manufacturers. Ten vhf and 50 uhf channels, each of 7 mc, have been allocated. Sound if should be $30.5 \text{ mc} \pm 0.25 \text{ mc}$, vision if should be $36 \text{ mc} \pm 0.25 \text{ mc}$. Limits are stated for radiation due to beat oscillators; it has not yet been found practicable to recommend limits for radiation due to sweep circuits.

621.397.62+778.5]:535.6 3764

Color Television vs. Color Motion Pictures—D. G. Fink. (*J. Soc. Mot. Pict. Telev. Engrs.*, vol. 64, pp. 281-290; June, 1955.) The technical capabilities and limitations of the two systems are compared under five headings: (a) the viewing situation, (b) image photometry, (c) colorimetry, (d) structure, and (e) continuity. The results of a survey of 8-mm, 16-mm, and 35-mm film practice are tabulated and compared with the contemporary performance of 21-inch color television receivers. The conclusions are also tabulated.

621.397.62:621.385.3.029.62/.63 3765

A U.H.F.-V.H.F. Television Tuner using Pencil Tubes—W. A. Harris and J. J. Thompson. (*RCA Rev.*, vol. 16, pp. 281-292; June, 1955.) The resonance frequencies of the experimental pencil-type triodes used are high enough to permit use of shunt-tuned circuits, and the feedback inductance is low enough to ensure stability. Advantages of shunt-tuning are the small overall dimensions and the moderate number of switching components required.

621.397.62.029.62 3766

A Survey of Tuner Designs for Multi-channel Television Reception—D. J. Fewings and S. L. Fife. (*J. Brit. IRE*, vol. 15, pp. 379-404; August, 1955.) The survey includes designs of British, U.S., and European origin; a rotary-coil-turret design developed in the U.S. appears to be most generally suitable. Noise considerations are discussed; calculations indicate that optimum conditions are obtained with

a receiver noise factor of 22 db at 40 mc decreasing to 3 db at 220 mc; the importance of these considerations for fringe-area reception is emphasized. Arrangements enabling existing single-channel receivers to operate for multi-channel reception without use of double heterodyning are described. Future requirements for uhf reception in the U.K. are discussed and tuner designs incorporating lumped and distributed tuning elements are examined.

621.397.8.001.4 3767

Method for the Assessment and Characterization of the Distortion of the Sawtooth Test Signal in Tests on Television Transmission Lines—H. Bödeker. (*FernmeldeTech. Z.*, vol. 8, pp. 323-324; June, 1955.) The fidelity with which the sawtooth level-setting signal is transmitted is tested by comparing the received sawtooth signal as displayed on a cro screen with engraved markings on a transparent template arranged just in front of the screen.

TRANSMISSION

621.396.61:621.376.3]+621.397.61 3768

General Outline of the Development of Transmitters for Television and Frequency Modulation [in the Netherlands]—P. W. L. v. Iterson and H. A. Teunissen. (*Tijdschr. ned. Radiogenoot.*, vol. 20, pp. 207-222; May, 1955. In English.)

621.396.61:621.396.662 3769

Automatic Tuning of Transmitters—W. L. Vervest. (*Tijdschr. ned. Radiogenoot.*, vol. 20, pp. 195-206; May, 1955. In English.) Description of the instantuner system. Automatic changing from one pre-set frequency to another is accomplished in 1-3 seconds for small transmitters and in 2-10 seconds for large transmitters.

621.396.61.029.63:621.385.4 3770

A Novel Ultra-high-Frequency High-Power-Amplifier System—L. L. Koros. (*RCA Rev.*, vol. 16, pp. 251-280; June, 1955.) The amplifier was developed for television transmitters and uses grid-driven 15-kw beam power tetrodes Type 6448 described by Bennett in *TRANS. IRE*, pp. 11-17; March, 1955, developed from the Type 6181 described previously by Bennett and Kazanowski (1206 of 1953). The anode cavity resonator is of transmission-line type, consisting essentially of one high-impedance and one low-impedance $\lambda/4$ section; it acts as a step-down transformer between tube and load.

TUBES AND THERMIONICS

621.314.63 3771

The Determination of the Dynamic Properties of Crystal Diodes—G. Stuart-Montieith. (*Brit. J. appl. Phys.*, vol. 6, pp. 254-256; July, 1955.) The ac characteristics of a forward-biased crystal diode depend on the frequency and the amplitude of the applied voltage. A method is given for determining the dynamic resistance for low values of bias current.

621.314.632:546.289:621.374 3772

Germanium Positive-Gap Diode: New Tool for Pulse Techniques—A. H. Reeves and R. B. W. Cooke. (*Elect. Commun.*, vol. 32, pp. 112-117; June, 1955.) English version of 2257 of 1954 (Reeves).

621.314.7 3773

A Simple Explanation of Transistor "h" Parameters—L. B. Johnson. (*Mullard Tech. Commun.*, vol. 2, pp. 58-63; July, 1955.) The small-signal performance of transistors can be calculated from hybrid or "h" parameters which are given by the slopes of the characteristic curves at the working point. This mode of assessment is likely to be used extensively in manufacturers' published data. An indication is given of the use of these parameters for calculations on complex circuits.

621.314.7 **3774**
High-Frequency Power Gain of Junction Transistors—R. L. Pritchard. (*PROC. IRE*, vol. 43, pp. 1075–1085; September, 1955.) Different ways of defining power gain at high frequencies are discussed. An equation is presented for calculating the gain in terms of the quadrupole parameters of the transistor driven by a generator with purely resistive impedance. Secondly, an expression is derived relating the gain to the fundamental device parameters for transistors in which the base impedance is frequency dependent, as in grown-junction transistors. Measurements on about 60 grown-junction transistors on the whole confirm the theory. Thirdly, the gain of an idealized model of a grown-junction transistor is calculated from the physical parameters. The results indicate that it should be possible to obtain a gain of 30 db at 5 mc and that these transistors should oscillate at frequencies up to several hundred mc.

621.314.7 **3775**
Emitter Efficiency of Junction Transistor—T. Misawa. (*J. phys. Soc. Japan*, vol. 10, pp. 362–367; May, 1955.) The efficiency is calculated on the basis of the quasi-Fermi-level concept, by introducing modified boundary conditions appropriate to the case of moderately high injection level. The results are compared with those of Webster (2798 of 1954) and of Rittner (3390 of 1954).

621.314.7 **3776**
A Germanium Point-Contact Transistor to operate at High Ambient Temperatures—A. F. Gibson, J. W. Granville, and W. Bardsley. (*Brit. J. appl. Phys.*, vol. 6, pp. 251–254; July, 1955.) The process of carrier exclusion, previously termed "carrier extraction" [2017 of July (Arthur et al.)], is applied in specially constructed transistors to suppress the normal increase of minority carriers with temperature, thereby increasing the upper temperature limit of the transistor by about 30 degrees C and improving the speed of operation. The sweep current required has no effect on the noise factor. The technique may be applied to junction diodes, but not to junction transistors.

621.314.7(47) **3777**
Technical Data on Russian Transistors—(*Radio Moscow*, p. 30, June, 1955.) Data are tabulated for eight point-contact and seven junction-type transistors.

621.314.7:537.311.33 **3778**
Semiconductors and Transistors: Some Current Problems—J. R. Tillman. (*Nature, Lond.*, vol. 176, pp. 9–11; July 2, 1955.) A concise survey of the existing stage of knowledge.

621.314.7:546.28 **3779**
Forming Procedures for Silicon Point-Contact Transistors—J. W. Granville, W. Bardsley, and A. F. Gibson. (*Brit. J. appl. Phys.*, vol. 6, pp. 206–210; June, 1955.) Suitable whisker materials for use as emitters and collectors on *n*- and *p*-type Si and the pulsing techniques used in forming are described. Si transistors have been made with power gains not markedly inferior to those of Ge point-contact transistors. Experimentally determined characteristics are given. For a different method of forming, see 1195 of April (Jacobs et al.).

621.314.7:621.375.4 **3780**
Transistor Equivalent Circuits—W. T. Cocking. (*Wireless World*, vol. 61, pp. 331–334, 388–392, 444–448, and 499–502; July/October, 1955.) The principles for developing equivalent circuits of the thermionic tube are described and applied to the directly analogous *n-p-n* transistor with earthed emitter, leading on to the case of the earthed-base transistor. Equivalent circuits for transistor amplifiers are

discussed, and formulas defining performance are deduced.

621.314.7:621.396.822 **3781**
Experimental Investigation and Separation of Noise Sources in Junction Transistors—W. Guggenbühl and M. J. O. Strutt. (*Arch. elekt. Übertragung*, vol. 9, pp. 259–269; June, 1955.) Analysis of equivalent quadrupoles shows that in the frequency-independent range the noise of a *p-n-p* transistor can be completely accounted for by (a) emitter-junction shot noise, (b) base-resistance noise, (c) collector saturation noise, and (d) current partition noise. The noise factors for the three basic transistor circuits are nearly equal. Results show that the noise factors of modern junction transistors are of the same order as those in good triode tubes operating under comparable conditions. The noise factors of transistors Type 0C70, 0C71, and 0C601, determined experimentally by a method described previously (2778 of September) are presented graphically as a function of frequency.

621.385:621.317.723 **3782**
Receiving Tubes with Very Small Grid Current—H. Takayama and K. Shimoda. (*J. phys. Soc. Japan*, vol. 10, pp. 387–391; May, 1955.) The use of miniature tubes for electrometer purposes is discussed. Types 6AK5 and 3S4 are found to be appropriate. The grid current of the latter has been reduced to about 10^{-16} A by appropriate silicone treatment, a voltage gain of 20–40 being obtained.

621.385.002.2 **3783**
Materials for Radio Valves—R. L. Smith-Rose. (*Nature, Lond.*, vol. 175, pp. 1029–1030; June 11, 1955.) Report of a discussion at the Institution of Electrical Engineers.

621.385.013.78.71 **3784**
The Thermally Conducting Valve Screen—N. G. Webb. (*Marconi Instrumentation*, vol. 5, pp. 38–41; June, 1955.) A toroidal coil spring is fitted inside a screening can so that it encircles and makes contact with the hottest part of the tube envelope. The can screws on to a threaded metal bush on the tube holder or a metal screening box. A helical compression spring in the top of the can retains the tube in its holder. A bulb temperature of 220 degrees C in free air was reduced to 130 degrees C by this means.

621.385.029.6 **3785**
On the Initial Space-Charge Distribution in a Cylindrical Magnetron Diode—R. Q. Twiss. (*J. Electronics*, vol. 1, pp. 1–7; July, 1955.) Calculations are made taking account of thermal emission velocities but neglecting electron-electron interactions. The space-charge distribution is of double-stream type even when the ratio of the radius of the space-charge cloud to the cathode radius is less than 2. Comparison of the results with experimental data (3786 below) indicates that the stream theory does not describe the steady-state distribution.

621.385.029.6 **3786**
The Space Charge Distribution in the Pre-oscillation Magnetron—L. E. S. Mathias. (*J. Electronics*, vol. 1, pp. 8–24; July, 1955.) An experimental study has been made of smooth-anode cylindrical magnetrons with anode-radius/cathode-radius ratios of 2–2.5, using molecular-beam technique. The space-charge density falls off with increasing distance from the cathode, at first smoothly and then in a series of small steps beyond the cloud radius predicted by stream theories. The space charge has no definite edge. Increasing the anode voltage increases the radius of the cloud and the density at each point in the space charge. Discrepancies between these results and those given by theory are discussed by Twiss (3785 above).

621.385.029.6

Theory of the Pre-oscillating Magnetron: **3787**
Part 1—D. Gabor and G. D. Sims. (*J. Electronics*, vol. 1, pp. 25–34; July, 1955.) A discussion is presented which may be of interest for a general understanding though not necessarily for a quantitative explanation of pre-oscillations in the cylindrical magnetron.

621.385.029.6 **3788**
The Effect of Initial Noise Current and Velocity Correlation on the Noise Figure of Traveling-Wave Tubes—S. Bloom. (*RCA Rev.*, vol. 16, pp. 179–196; June, 1955.) The effect of correlation between fluctuation due to shot noise and that due to electron-velocity distribution is to introduce a further noise-current space-charge wave. Neither the degree of initial correlation nor the individual values of the shot-noise and velocity-distribution fluctuations affect the conditions for minimizing the noise figure of the tube, which depends only on the standing-wave ratio of the resultant noise-current wave and the position of the helix with respect to this wave.

621.385.029.6 **3789**
The 4-cm-λ Travelling-Wave Valve developed at the Centre National d'Études des Télécommunications—Bobenrieth, Cahen, Lestel, and Picquendat. (*Électronique, Paris*, pp. 15–23; May, 1955.) Details are given of the Type-S47 tube developed by the French Post Office for use in radio links branching from the main 8-cm-λ links. Output is >1w and practically independent of frequency over the band 6–8.5 kmc; gain is of the order of 40 db, and operating voltage is 1350 ± 30 v.

621.385.029.6:537.533 **3790**
Some Experiments on a Cylindrical Electron Beam Constrained by a Magnetic Field—J. D. Lawson. (*J. Electronics*, vol. 1, pp. 43–52; July, 1955.) Measurements were made of longitudinal variations of beam cross section and radial current distribution, using a movable intercepting screen. The influence of angle of entry into the constraining axial magnetic field was studied. Operating parameters giving the smallest beam-diameter variations were: beam voltage 500 v, beam current 12 ma, beam radius about 1.2 mm, magnetic field 140 oersted. Discrepancies between the results and predictions from theory are discussed.

621.385.029.63 **3791**
Factors in the Design of Power Amplifiers for Ultra-high Frequencies—J. Dain. (*J. Electronics*, vol. 1, pp. 35–42; July, 1955.) Amplifier tubes for the frequency range 400–900 mc with outputs >10 kw and power gains not much less than 10 are discussed. The relative merits of triodes, tetrodes, klystrons and traveling-wave tubes are compared.

621.385.029.64 **3792**
High-Grain Travelling-Wave Output Valve with Permanent Magnet—W. Eichin, P. Meyerer, W. Veith, and O. Zinke. (*Fernmelde-techn. Z.*, vol. 8, pp. 369–373; July, 1955.) Description of the Type-V503 tube, which gives linear operation with gain >30 db at a power output >3 w over the frequency range 3.6–4.2 kmc. The reflection factor at the input is <10 per cent and at the output <5 per cent over a 30-mc band. Helix voltage is 1.3 kv and beam current about 35 ma. The cathode has a diameter of 8 mm, and the gun focusing is assisted by a permanent magnet, the resulting concentration being such that <1 ma is intercepted by the helix.

621.385.032.213.2 **3793**
The Bolt Cathode: an Indirectly Heated Tungsten Cathode for Electron Guns—E. B. Bas. (*Z. angew. Phys.*, vol. 7, pp. 337–344; July, 1955.) The heavy-duty cathode described comprises a tungsten rod with a coaxial external

helical heater. One of the end faces of the rod is the emitter surface. Additional heating of the rod is obtained by electron bombardment from the heater. A magnetically stabilized heating circuit is used. Operating conditions were investigated experimentally. Results are presented graphically and discussed.

621.385.032.216 3794

The Resistance of the Oxide-Coated Cathode at Ultra-high Frequencies—L. J. Herbst and J. E. Houldin. (*Brit. J. appl. Phys.*, vol. 6, pp. 236-238; July, 1955.) Measurements were made on disk-seal triodes over the frequency range 730 mc-2.360 kmc with cathode temperatures from 1250 to 1400 degrees K. The cathode behavior can be represented by the equivalent circuit comprising the grid-cathode capacitance in series with the coating resistance. Accurate determination of the dc coating resistance is not possible; the results agree approximately with those at rf. Determinations correspond to specific conductivities between 0.3 and 0.4 $\Omega^{-1}m^{-1}$, at a temperature of 1250 degrees K. Heater resistance decreases with increasing cathode temperature and this effect can be used to measure power loss in the coating under oscillatory conditions.

621.385.032.216 3795

Mass-Spectrometer Investigation of Gases in Electronic Apparatus with Oxide Cathodes—N. D. Morgulis and G. Ya. Plikus. (*C.R. Acad. Sci. U.R.S.S.*, vol. 102, pp. 1103-1106; June 21, 1955. In Russian.) The gas in an evacuated tube containing a heated oxide cathode was analyzed at intervals up to 300 hours, and at the end of the subsequent period of about 330 hours. The latter analysis showed a large increase in the H₂ and He content. This was probably due to a diffusion of these gases through the molybdenum-glass envelope. Other gases observed were H₂O, O, O₂ and N₂+CO. Results are presented graphically.

621.385.032.216 3796

A Study of the Long-Term Emission Behaviour of an Oxide-Cathode Valve—G. H. Metson. (*Proc. IEE, Part B*, vol. 102, pp. 657-675; September, 1955. Discussion, pp. 675-677.) Conditions for maintaining emission over a long period are discussed; it is assumed that emission is maintained as long as there is a sufficiency of metallic Ba in the oxide matrix. Factors causing loss or gain of the Ba metal are examined. The tentative conclusion is that a cathode working under a current load in gas-free surroundings will continue to emit until the BaO matrix is exhausted by electrolysis and evaporation.

621.385.032.216:621.315.612.8 3797

Some Experiments on the Breakdown of Heater-Cathode Insulation in Oxide-Cathode Receiving Valves—G. H. Metson, E. F. Rickard, and F. M. Hewlett. (*Proc. IEE, Part B*, vol. 102, pp. 678-683; September, 1955.) The sintered alumina used for insulating the tungsten-wire heater is more liable to failure when the heater is run positive with respect to the cathode than when it is run negative, due to enhanced transfer of the tungsten across the alumina. The effect is attributed to production of positive tungsten ions under electron bombardment from the cathode, and is retarded when the alumina contains a pore-free layer.

621.385.032.24.002.2 3798

Frame-Grid Technique and its Significance in the Construction of Modern Amplifier Valves

—O. Pfetscher. (*Elektronik*, vol. 4, pp. 139-143; June, 1955.)

621.385.15 3799

Anode-Dynode Beam Deflection Amplifier—H. J. Wolkstein and A. W. Kaiser. (*Electronics*, vol. 28, pp. 132-136; August, 1955.)

The tube described has a composite output element such that in the absence of an applied signal the anode and dynode currents are out of phase and cancel. Signal variations produce currents in each element which are in phase, resulting in a linear input-voltage/output-current characteristic. Linear negative or positive transconductance can be produced. Applications to gating circuits, difference amplifiers, binary storage circuits etc., are described.

621.385.15:621.373.4.029.6 3800

Transit-Time Functions of a Dynatron Oscillator—G. Dieiner. (*Appl. sci. Res.*, vol. B4, pp. 457-463; 1955.) A new type of dynatron tube is discussed in which the primary electrons are directed obliquely towards the secondary-emission electrode. High values of the negative dynode admittance are attained by using a primary-electron voltage such that the secondary-emission factor has its maximum value. Analysis of high-frequency operation shows that oscillations can be produced at cm λ .

621.385.2.[3].029.63:621.317.3 3801

Conductance and Slope Measurements on Transient-Time Diodes and Triodes—Gundlach and Lonsdorfer. (See 3688.)

621.385.3.029.62/.63:621.397.62 3802

A U.H.F.-V.H.F. Television Tuner using Pencil Tubes—Harris and Thompson. (See 3765.)

621.385.3.029.63 3803

Development of the Premium Ultra-high-Frequency Triode 6J4-WA—G. W. Barclay. (*RCA Rev.*, vol. 16, pp. 293-302; June, 1955.) This tube is a version of the Type-6J4 for military applications. Modifications leading to improvement of interelectrode insulation, reduction of heater-to-cathode leakage and reduction of grid-to-cathode shorts are indicated, and the manufacture of the close-wound grid is described. The importance of quality control is emphasized.

621.385.4:621.396.61.029.63 3804

A Novel Ultra-high-Frequency High-Power-Amplifier System—Koros. (See 3770.)

621.385.5:681.142 3805

Binary Adder Tube for High-Speed Computers—F. B. Maynard. (*Electronics*, vol. 28, pp. 161-163; September, 1955.) The composite tube described replaces a typical binary adder circuit employing eleven tubes. It may also be used as a coincidence detector etc.

621.385.83 3806

Electrode Shapes for a Cylindrical Electron Beam—P. N. Daykin. (*Brit. J. appl. Phys.*, vol. 6, pp. 248-250; July, 1955.) A new approximate analytical solution of Laplace's equation for the es potential outside the space-charge region is derived and numerical tables are developed for applying the appropriate boundary conditions to give the required electrode shapes. A plot of the electrode shapes, applicable to both solid and hollow beams, is presented.

621.385.832

A New Method for magnifying Electron Beam Images—W. R. Beam. (*RCA Rev.*, vol. 16, pp. 242-250; June, 1955.) A magnified spot is obtained in a cr tube by deflecting the beam across a small aperture and again deflecting the transmitted beam and tracing the image on a fluorescent screen. The procedure is useful in electron-gun design work.

MISCELLANEOUS

061.4:621.39

Radio Show Review—(*Wireless World*, vol. 61, pp. 476-491; October, 1955.) A trend towards basic circuit standardization in television receivers was noted; more sets were fitted with agc in the vision channel, the majority making use of the mean bias voltage developed on the grid of the synchronizing-signal separator; true gated agc systems were rare. On the sound channel agc was practically universal. For station selection many sets had turret tuners with separate coils for each channel. Incremental-inductance tuning was also common. Convertors were available for most band I sets to enable them to be used on band III. Antennas for television reception were very varied. Printed circuits were common for filters and crossover networks. In vhf fm sound receivers precautions were taken to prevent oscillator radiation. Progress in transistor design is shown both for af and hf amplification and for power rectification. For dc conversion, efficiencies as high as 80 per cent are attained. For another account see *Wireless Engr.*, vol. 32, pp. 280-285; October, 1955.

061.4:621.39

British Aircraft Radio—(*Wireless World*, vol. 61, pp. 491-494; October, 1955.) Apparatus shown at Farnborough in 1955 reflected the continuous progress in reducing the size and weight of airborn gear. Navigational aids included new direction-finding and position-finding systems. Other exhibits included communication equipment for use on the 225-400-mc band and sets with tubes entirely replaced by transistors.

061.4:621.39

German Radio Show—(*Wireless World*, vol. 61, pp. 468-470; October, 1955.) In German vhf receivers emphasis is placed on freedom from radiation likely to cause interference. Television receivers for bands I and III have in many cases provision for conversion to band IV. Test and measuring gear was shown by several manufacturers.

621.3.002.2

Mechanized Production of Electronic Equipment—J. Markus. (*Electronics*, vol. 28, pp. 137-160; September, 1955.) Present and projected practice in the U.S.A. involves mechanical preparation of components for insertion in etched wiring circuits, followed by automatic assembly, dip soldering, and automatic testing of completed circuits. Illustrations of the various processes are given.

413.164:621.396/.397

Elsevier's Dictionary of Television, Radar and Antennas in Six Languages. [Book Review]—W. E. Clason. Publishers: Elsevier, London and New York etc., 1955, 760 pp., 120s. (*J. Brit. Instn. Radio Engrs.*, vol. 15, p. 11; August, 1955.) The languages included are English, French, Spanish, Italian, Dutch, and German.